THE

LONDON, EDINBURGH, AND DUBLIN

PHILOSOPHICAL MAGAZINE

AND

JOURNAL OF SCIENCE.

[SEVENTH SERIES.]

APRIL 1928.

LXXII. *The Stream-line Motion of Fluid in a Curved Pipe.* (Second Paper.)

By W. R. DEAN, *M.A., Imperial College of Science* *.

IN a previous paper † a first approximation has been found to the steady motion of incompressible fluid through a pipe of circular cross-section (radius a) coiled in a circle of radius R. The first approximation gives a motion in qualitative agreement with that found experimentally, but is valid only in a limited field, and fails to show that the relation between pressure gradient and rate of flow through a curved pipe is dependent on the curvature ; the present paper is the outcome of an attempt to extend the analysis so as to find this dependence theoretically.

This extension, so far as it has been carried, represents a fourth approximation to the problem ; it is given in §§ 2–9. It leads to no important quantitative result ; it shows that the rate of flow is slightly reduced by curvature, even in the limited range of velocities to which it applies, and makes possible an estimate of the velocity at which in a given case the reduction is first likely to be measurable. The difficulty of making the successive approximations increases so rapidly that no further extension on the same lines is worth while.

It appears, however, in the course of the work that the reduction in the rate of flow due to curvature depends on a single variable K, equal to $2n^2a/\mathrm{R}$ when the motion is slow,

* Communicated by Prof. S. Chapman, F.R.S.

† Phil. Mag. iv. p. 208 (1927).

n being the Reynolds' number, and always of this order of magnitude. The problem of determining the relation between flux and pressure gradient in any curved pipe (the motion being, of course, supposed stream-line) therefore reduces to that of finding a single function $f(\mathrm{K})$. This result is not exact: in § 3 the assumption that a/R is small is made, but it is shown in § 7 by consideration of an analogous assumption that the error, nominally of order a^2/R^2, is not likely to be serious.

The function $f(\mathrm{K})$ can be determined by experiment on a single curved pipe, and it is therefore possible to correlate experimental results for pipes of different curvatures. In §§ 12–18 the theory is applied to observations due to Prof. J. Eustice of the rate of flow of water through pipes of various radii of curvature, R. In these experiments a single flexible tube was used, and wound on cylinders of different radii in order to vary R; there was in consequence distortion, considerable in some cases, of the tube. The tube was found to be sinuous when free, and may have remained in this condition when coiled. It therefore appeared better to correlate several pairs of results than to attempt to determine $f(\mathrm{K})$ absolutely. The agreement found when the motion is stream-line (by this is meant, when $n < 2000$) is good, except in one case, wherein the distortion of the tube due to coiling was exceptionally large.

All calculations have been extended to velocities above the assumed critical velocity. Though the errors that result are not in certain conditions large, it is clear that the theory applies only to stream-line motion; it can, however, probably be modified so as to apply to all velocities by substituting a coefficient of eddy viscosity for the ordinary coefficient μ.

2. Fig. 1 shows the system of coordinates that has been used. The surface of a pipe of circular section, coiled in a circle, is an anchor ring; the figure shows OZ, the axis of the anchor ring, and a section of it by an axial plane that makes an angle θ with a fixed axial plane. The position of any point P is specified by the orthogonal coordinates r, ψ, θ. The components of the velocity of the fluid corresponding to these coordinates are U, V, W; U is therefore in the direction CP, V perpendicular to U and in the plane of the cross-section, and W perpendicular to this plane. The radius of any cross-section is a, while R is the radius of the circle in which the pipe is coiled.

It is assumed that the motion of the fluid is steady, and,

further, that U, V, and W (but not P, the pressure) are independent of θ.

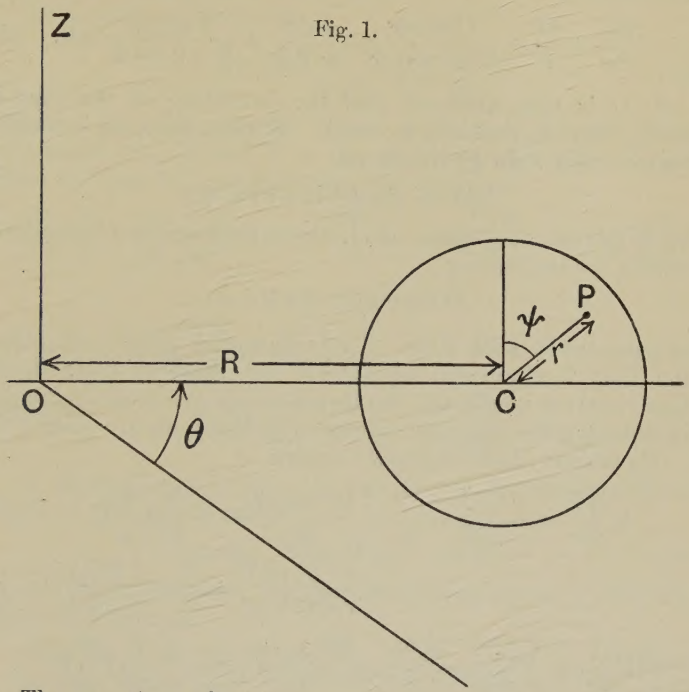

Fig. 1.

The equations of motion are then

$$U\frac{\partial U}{\partial r}+\frac{V}{r}\frac{\partial U}{\partial \psi}-\frac{V^2}{r}-\frac{W^2\sin\psi}{R+r\sin\psi}=-\frac{\partial}{\partial r}\left(\frac{P}{\rho}\right)$$
$$-\nu\left(\frac{1}{r}\frac{\partial}{\partial\psi}+\frac{\cos\psi}{R+r\sin\psi}\right)\left(\frac{\partial V}{\partial r}+\frac{V}{r}-\frac{1}{r}\frac{\partial U}{\partial\psi}\right), \quad . \quad (1)$$

$$U\frac{\partial V}{\partial r}+\frac{V}{r}\frac{\partial V}{\partial\psi}+\frac{UV}{r}-\frac{W^2\cos\psi}{R+r\sin\psi}=-\frac{1}{r}\frac{\partial}{\partial\psi}\left(\frac{P}{\rho}\right)$$
$$+\nu\left(\frac{\partial}{\partial r}+\frac{\sin\psi}{R+r\sin\psi}\right)\left(\frac{\partial V}{\partial r}+\frac{V}{r}-\frac{1}{r}\frac{\partial U}{\partial\psi}\right), \quad . \quad (2)$$

and

$$U\frac{\partial W}{\partial r}+\frac{V}{r}\frac{\partial W}{\partial\psi}+\frac{UW\sin\psi}{R+r\sin\psi}+\frac{VW\cos\psi}{R+r\sin\psi}$$
$$=-\frac{1}{R+r\sin\psi}\frac{\partial}{\partial\theta}\left(\frac{P}{\rho}\right)+\nu\left[\left(\frac{\partial}{\partial r}+\frac{1}{r}\right)\left(\frac{\partial W}{\partial r}+\frac{W\sin\psi}{R+r\sin\psi}\right)\right.$$
$$\left.+\frac{1}{r}\frac{\partial}{\partial\psi}\left(\frac{1}{r}\frac{\partial W}{\partial\psi}+\frac{W\cos\psi}{R+r\sin\psi}\right)\right]. \quad . \quad (3)$$

The fluid is assumed incompressible; then the equation of continuity is

$$\frac{\partial U}{\partial r}+\frac{U}{r}+\frac{U\sin\psi}{R+r\sin\psi}+\frac{1}{r}\frac{\partial V}{\partial\psi}+\frac{V\cos\psi}{R+r\sin\psi}=0. \quad (4)$$

3. It is now assumed that the curvature of the pipe is small: that is, that a/R is small. We can then, for example, replace $(R+r\sin\psi)$ by R, and

$$\partial/\partial r+\sin\psi/(R+r\sin\psi)$$

by $\partial/\partial r$; on the other hand, there is clearly no immediate reason for neglecting

$$W^2\sin\psi/(R+r\sin\psi)$$

in comparison with V^2/r. This assumption greatly simplifies the four fundamental equations, but there is little doubt that it leaves unaffected the terms which are most important in deciding the effect of curvature on the motion. (See § 7.)

Equations (1) to (4) now become

$$U\frac{\partial U}{\partial r}+\frac{V}{r}\frac{\partial U}{\partial\psi}-\frac{V^2}{r}-\frac{W^2\sin\psi}{R}=-\frac{\partial}{\partial r}\left(\frac{P}{\rho}\right)-\frac{\nu}{r}\frac{\partial}{\partial\psi}\left(\frac{\partial V}{\partial r}+\frac{V}{r}-\frac{1}{r}\frac{\partial U}{\partial\psi}\right), \quad (5)$$

$$U\frac{\partial V}{\partial r}+\frac{V}{r}\frac{\partial V}{\partial\psi}+\frac{UV}{r}-\frac{W^2\cos\psi}{R}=-\frac{1}{r}\frac{\partial}{\partial\psi}\left(\frac{P}{\rho}\right)+\nu\frac{\partial}{\partial r}\left(\frac{\partial V}{\partial r}+\frac{V}{r}-\frac{1}{r}\frac{\partial U}{\partial\psi}\right), \quad (6)$$

$$U\frac{\partial W}{\partial r}+\frac{V}{r}\frac{\partial W}{\partial\psi}=-\frac{1}{R}\frac{\partial}{\partial\theta}\left(\frac{P}{\rho}\right)+\nu\left(\frac{\partial^2 W}{\partial r^2}+\frac{1}{r}\frac{\partial W}{\partial r}+\frac{1}{r^2}\frac{\partial^2 W}{\partial\psi^2}\right), \quad (7)$$

and

$$\frac{\partial U}{\partial r}+\frac{U}{r}+\frac{1}{r}\frac{\partial V}{\partial\psi}=0. \quad (8)$$

As U, V, and W are assumed independent of θ, it follows from (7) that P/ρ must be of the form $\theta f_1(r,\psi)+f_2(r,\psi)$, and then from (5) and (6) that $f_1(r,\psi)$ must be a constant. We can therefore write

$$-\frac{1}{R}\frac{\partial}{\partial\theta}\left(\frac{P}{\rho}\right)=\frac{G}{\rho}, \quad (9)$$

where G is a constant which may be termed the mean

pressure gradient; it is equal to the space-rate of decrease in pressure along the central line *.

From (8) we can write

$$rU = -\frac{\partial f}{\partial \psi}, \quad V = \frac{\partial f}{\partial r}, \quad . \quad . \quad . \quad . \quad (10)$$

where f is a function of r and ψ only. Inserting these expressions for U and V in the equations and eliminating P from (5) and (6), we have the two equations

$$\left(\frac{\partial f}{\partial \psi}\frac{\partial}{\partial r} - \frac{\partial f}{\partial r}\frac{\partial}{\partial \psi}\right)\nabla_1^2 f + \frac{2W}{R}\left(r\cos\psi\frac{\partial W}{\partial r} - \sin\psi\frac{\partial W}{\partial \psi}\right) = -\nu r\nabla_1^4 f, \quad . \quad . \quad . \quad . \quad . \quad (11)$$

and

$$\frac{1}{r}\left(\frac{\partial f}{\partial r}\frac{\partial W}{\partial \psi} - \frac{\partial f}{\partial \psi}\frac{\partial W}{\partial r}\right) = G/\rho + \nu\nabla_1^2 W, \quad . \quad (12)$$

where

$$\nabla_1^2 \equiv \frac{\partial^2}{\partial r^2} + \frac{1}{r}\frac{\partial}{\partial r} + \frac{1}{r^2}\frac{\partial^2}{\partial \psi^2}. \quad . \quad . \quad . \quad (13)$$

4. Equations (11) and (12) can be put in non-dimensional form by the substitutions

$$f = \nu\phi, \quad W = W_0 w, \quad r = ar', \quad . \quad . \quad . \quad (14)$$

where W_0 is assumed to have the dimensions of a velocity; they then become

$$\left(\frac{\partial \phi}{\partial \psi}\frac{\partial}{\partial r'} - \frac{\partial \phi}{\partial r'}\frac{\partial}{\partial \psi}\right)\nabla_1^2\phi + Kw\left(r'\cos\psi\frac{\partial w}{\partial r'} - \sin\psi\frac{\partial w}{\partial \psi}\right) = -r'\nabla_1^4\phi, \quad (15)$$

and

$$\frac{1}{r'}\left(\frac{\partial \phi}{\partial r'}\frac{\partial w}{\partial \psi} - \frac{\partial \phi}{\partial \psi}\frac{\partial w}{\partial r'}\right) = C + \nabla_1^2 w. \quad . \quad . \quad (16)$$

In these equations

$$K = 2W_0^2 a^3/\nu^2 R, \quad . \quad . \quad . \quad . \quad . \quad (17)$$

and

$$C = Ga^2/\mu W_0; \quad . \quad . \quad . \quad . \quad . \quad . \quad (18)$$

∇_1^2 now stands for the operator derived from expression (13) by replacing r by r': there is no need to alter the notation. As to the constant K: if the motion is slow, W_0 can be taken to be the "θ" component of the velocity of the fluid at any point of the central line, and the distribution of this component approximates to that in a straight pipe, and is nearly parabolic. Consequently aW_0/ν is roughly

* The circle traced out by C, fig. 1.

equal to the Reynolds' number n, which is $\bar{v}d/\nu$, where $\bar{v}$ is the mean velocity and d the diameter of the pipe. Thus for slow motion, $K=2n^2a/R$.

The problem is now to find solutions of equations (15) and (16) that will satisfy the boundary conditions ; these require that the velocity (U, V, W) should vanish at the surface of the pipe, $r=a$, so that we must have

$$\frac{\partial\phi}{\partial r'}=\frac{\partial\phi}{\partial\psi}=w=0, \quad . \quad . \quad . \quad . \quad . \quad (19)$$

when $r'=1$.

5. Very little progress has at present been made analytically. No method has so far been found other than that of successive approximation, which is effectively equivalent to expanding ϕ and w in ascending powers of K. The difficulty is, that K is not small in most cases. Suppose that $a/R=0{\cdot}01$; this must be considered a small value of a/R, though pipes of smaller curvature have certainly been used in experiment. Suppose, further, that the critical velocity in this pipe is the same as if the pipe were straight ; it is then such that $n=2000$. Although K is not always equal to $2n^2a/R$, it is always of this order of magnitude, and consequently for a complete discussion of stream-line motion we must have a solution of the equations that holds for values of K up to perhaps 10^5. It is certain that such solutions cannot be obtained by successive approximation ; four approximations have been found, and give a result probably not valid when K exceeds 400. Some account of the method is given in the following paragraphs.

It follows immediately that there is no theoretical ground for supposing that if a/R is small the motion in a curved pipe must approximate to that in a straight pipe ; the far more stringent condition that K must be small has to be fulfilled.

6. If the pipe is straight, a/R, and therefore K, are zero, and equations (15) and (16) can be satisfied by

$$w=1-r'^2, \quad \phi=0,$$

provided $C=4$. No arbitrary constant is required in the expression for w ; W_0 is the only constant needed.

If K is not zero, let

$$\left.\begin{aligned} w&=w_0+Kw_1+K^2w_2+\ldots,\\ \phi&=\quad K\phi_1+K^2\phi_2+\ldots,\end{aligned}\right\} \quad . \quad . \quad . \quad . \quad (20)$$

where w_0, w_1, ϕ_1, w_2, ϕ_2, ... are functions of r' and ψ only.

Substituting these expressions in the equations and equating coefficients of powers of K, we have a series of relations from which w_0, w_1, ϕ_1 ... can successively be found.

The first equation from (16) is

$$\nabla_1^2 w_0 + C = 0; \quad . \quad . \quad . \quad . \quad (21)$$

this and the boundary condition $w=0$, $r'=1$ are satisfied by

$$w_0 = 1 - r'^2, \quad C = 4. \quad . \quad . \quad . \quad . \quad . \quad . \quad (22)$$

The first equation from (15) is

$$r' \nabla_1^4 \phi_1 = -r' \cos\psi w_0 \frac{\partial w_0}{\partial r},$$

$$= 2r'^2(1-r'^2)\cos\psi; \quad . \quad . \quad . \quad (23)$$

to satisfy this and the boundary conditions $\frac{\partial \phi}{\partial r'} = \frac{\partial \phi}{\partial \psi} = 0$, $r'=1$, we must take

$$\phi_1 = \frac{\cos\psi}{144} r'(1-r'^2)^2(1-r'^2/4). \quad . \quad . \quad . \quad (24)$$

The second equation from (16) is

$$\nabla_1^2 w_1 = -\frac{1}{r'} \frac{\partial \phi_1}{\partial \psi} \frac{\partial w_0}{\partial r'}, \quad . \quad . \quad . \quad . \quad (25)$$

whence

$$w_1 = \frac{\sin\psi}{576}\left(\frac{19r'}{40} - r'^3 + \frac{3r'^5}{4} - \frac{r'^7}{4} + \frac{r'^9}{40}\right). \quad . \quad (26)$$

7. At this stage it is convenient to consider the probable effect of the assumption made in § 3. In the first paper * the functions ϕ_1 and w_1 were calculated exactly, so that the errors in expressions (24) and (26) can be found. In (24) there is no error, while to get the correct expression for w_1 there must be added to (26)

$$-3ar'(1-r'^2)\sin\psi/4\mathrm{RK}.$$

K can certainly exceed 10^4, and only cases in which K is large are of interest; it can be concluded that, at least in the early stages, the important parts of the terms are unaffected. The assumption can, however, be examined from a more general point of view. It is purely geometrical; by a sufficient decrease in a/R the error due to it can be reduced to within any given limit; but if at the same time the mean velocity is sufficiently increased, K will not be small, and the motion will be quite different from that in a

* Phil. Mag. iv. p. 214 (1927), equations (23) to (25).

straight pipe. What is of most interest is the effect of curvature on the relation between pressure gradient and rate of flow. The reason why the pressure required to maintain a given rate of flow is greater in a curved pipe than in a straight one is mainly that in a curved pipe part of the fluid is continually oscillating between the central part of the pipe, where the velocity is high, and the neighbourhood of the boundary, where the velocity is low. This movement is due to the centrifugal tendency of the fluid, and implies a loss of energy which has no counterpart in stream-line motion in a straight pipe. It is clear from equations (5) and (6), wherein two terms equivalent to an inward acceleration of W^2/R appear, that the lateral motion of the fluid is not eliminated by the assumption made; we can say, then, that it ignores in the equations of motion the geometrical terms due to curvature, but leaves the dynamical terms unaffected.

In the similar problem of flow in a curved channel (bounded by two coaxial circular cylinders) there is no lateral motion of the fluid. Hence the effect of curvature is, in the sense defined, purely geometrical, and as its magnitude is known, we can get an idea of the error likely to result from the assumption made in the other problem.

The ratio of the flux due to given pressure gradient * in a channel whose boundaries are cylinders of radii $R \pm a$, to that due to the same gradient in a channel bounded by parallel plane walls a distance $2a$ apart, is

$$\frac{3}{16a^4}\left[4R^2a^2-(R^2-a^2)^2\left\{\log\frac{R+a}{R-a}\right\}^2\right].$$

When a/R is small this expression is approximately

$$1-2a^2/15R^2; \quad \ldots\ldots \quad (27)$$

when a/R has its maximum value unity (the inner cylinder being then a line) the ratio has its minimum value 3/4. Hence in this case the geometrical effect of curvature cannot in any circumstances reduce the rate of flow by more than 1/4, and from expression (27) we can perhaps infer that the error due to the assumption made in the other problem, nominally of order a^2/R^2, is not likely to be really greater on account of large coefficients.

8. The rate of flow is proportional to

$$\int_0^1 dr' \int_0^{2\pi} r' w \, d\psi,$$

* This is a mean pressure gradient defined as in § 3.

and is therefore determined by the part of w that is independent of ψ. Consequently w_1 makes no contribution, so that at the present stage of the approximation the relation between flux and pressure is the same as if the pipe were straight. The next approximation does modify this relation, and can be found without difficulty.

From equation (15)

$$-r'\nabla_1^4\phi_2=\left(\frac{\partial\phi_1}{\partial\psi}\frac{\partial}{\partial r'}-\frac{\partial\phi_1}{\partial r'}\frac{\partial}{\partial\psi}\right)\nabla_1^2\phi_1 + w_0\left(r'\cos\psi\frac{\partial w_1}{\partial r'}-\sin\psi\frac{\partial w_1}{\partial\psi}\right) + w_1 r'\cos\psi\frac{\partial w_0}{\partial r'},$$

and ϕ_2 is therefore proportional to $\sin 2\psi$. Again,

$$r'\nabla_1^2 w_2=\left(\frac{\partial\phi_1}{\partial r'}\frac{\partial w_1}{\partial\psi}-\frac{\partial\phi_1}{\partial\psi}\frac{\partial w_1}{\partial r'}\right)-\frac{\partial\phi_2}{\partial\psi}\frac{\partial w_0}{\partial r'},$$

and it follows that w_2 is of the form $f_2(r')+\mathrm{F}_2(r')\cos 2\psi$. The second of these terms need not be calculated, as it does not affect the flux to order K^2 *. Consequently ϕ_2 need not be evaluated. We then have, to determine that part of w_2 which is a function of r' only,

$$r'f_2''(r')+f_2'(r')=\tfrac{1}{2}(\chi_1'f_1+\chi_1 f_1'),$$

where dashes denote differentiations with respect to r', $\phi_1=\chi_1\cos\psi$, and $w_1=f_1\sin\psi$. On integrating this equation we have

$$r'f_2'(r')=\tfrac{1}{2}f_1\chi_1,$$

the arbitrary constant vanishing ; thence by using (24) and (26), and integrating again,

$$f_2(r')=\frac{1}{32(144)^2}\left[-\cdot1839+\cdot95r'^2-2\cdot0687r'^4+2\cdot4750r'^6 -1\cdot7781r'^8+\cdot7850r'^{10}-\cdot2062r'^{12} +\cdot0286r'^{14}-\cdot0016r'^{16}\right].$$

* It must be calculated for a closer approximation : w_4 cannot be found until $\mathrm{F}_2(r')$ is known.

The corresponding approximation to the flux is given by

$$\int_0^a 2\pi r \mathrm{W}\, dr = 2\pi \mathrm{W}_0 a^2 \int_0^1 r' w\, dr'$$

$$= 2\pi \mathrm{W}_0 a^2 \int_0^1 r'[1 - r'^2 + \mathrm{K}^2 f_2(r')]\, dr'$$

$$= \frac{\pi \mathrm{W}_0 a^2}{2}\left[1 - \left(\frac{\mathrm{K}}{576}\right)^2 (\cdot 03058)\right].$$

If the pipe were straight the flux would be $\pi \mathrm{W}_0 a^2/2$. The factor in square brackets, and similar factors below, will be denoted $\mathrm{F}_c/\mathrm{F}_s$. Then

$$\mathrm{F}_c/\mathrm{F}_s = 1 - \left(\frac{\mathrm{K}}{576}\right)^2 (\cdot 03058) \quad . \quad . \quad . \quad (28)$$

represents the decrease in flux due to the curvature; it is the ratio of the rates of flow due to a given pressure gradient in two pipes of the same cross-section which are respectively curved and straight.

9. It is possible to find the limits within which equation (28) is reliable only by carrying the process of approximation to a further stage. The difficulty of successively finding the functions ϕ and w becomes rapidly greater, and only the third term has been found of the series whose first two terms are given by (28) ; even this calculation is rather long, and no numerical details will be given. The resulting expression for the ratio is

$$\mathrm{F}_c/\mathrm{F}_s = 1 - \left(\frac{\mathrm{K}}{576}\right)^2 (\cdot 03058) + \left(\frac{\mathrm{K}}{576}\right)^4 (\cdot 01195). \quad (29)$$

A rough estimate of the range of validity of equation (29) can be made. It can certainly be assumed that if the curvature of a pipe of given cross-section is increased, the flux due to a given pressure gradient will diminish. Hence $\mathrm{F}_c/\mathrm{F}_s$ must decrease as a/R increases ; it must therefore decrease as K increases. Expression (29) for $\mathrm{F}_c/\mathrm{F}_s$ has a minimum value when K is roughly 650, so that the result cannot in any case be used if K exceeds this value. The error of (29) when $\mathrm{K} = 576$ is not likely to be serious*. For this value of K, $\mathrm{F}_c/\mathrm{F}_s$ is 0·981, so that the flux is reduced in consequence of the curvature by about 1·9 per cent. The reduction will be greater if K is increased, by increasing either the curvature or the mean velocity.

* This is clear from the expressions for ϕ_3, w_3, w_4, not given here.

This is the only numerical result that can be obtained from the preceding work at its present stage, and any extension of it on the same lines is not likely to lead to anything of much greater value. Suppose, for instance, that K is 1000, a value which, as we have seen, must be considered relatively small. Equation (29) gives a value of F_c/F_s greater than unity, so that the fourth term of this series must be calculated, and even if the value of F_c/F_s is then less than unity, at least one more term must be found to see to what extent the result given by the first four terms is reliable. In the most favourable case eight more of the functions ϕ and w must be evaluated, and each of these evaluations will be lengthier than the one before.

10. Some information of a more general character can, however, be deduced from the preceding work. In the first place we can roughly estimate the velocity at which the relation between pressure gradient and flux in a given curved pipe begins to differ appreciably from that for a straight pipe of the same cross-section. To take a numerical example, suppose that pressure and flux can be measured to an accuracy of one per cent. We see that $F_c/F_s=0{\cdot}99$ when K is roughly 350, using equation (29), which is valid for such a small value of K. For this value of K, again, the velocity at points of the central line will not differ much from W_0, and K will be approximately $2n^2a/R$. Consequently $F_c/F_s=0{\cdot}99$ when $2n^2a/R=350$, and the effect of curvature should be first measurable when the values of n and a/R are roughly such that the last equation is true.

Some experimental work by J. H. Grindley and A. H. Gibson * bears upon this. In these experiments air was forced under pressure through a circular pipe of radius 0·16 cm. coiled in a circle of radius † 18 cm.; the value of a/R was accordingly 1/112. Values of μ, the coefficient of viscosity, were calculated from observed pressure and flux on the assumption that these quantities were related as if the pipe were straight. Coefficients of viscosity so calculated were found to increase with the flux, and it was determined that the increase first became sensible when the mean velocity was about 2 feet per second. The value of the corresponding Reynolds' number is given ‡ as 130. Accordingly $2n^2a/R$ is about 300.

* Proc. Roy. Soc. A, vol. lxxx. p. 114 (1908).

† This value is taken from one of the articles by Prof. Gibson in 'Mechanical Properties of Fluids,' p. 163.

‡ *Op. cit.* p. 164.

Now, the value of a/R in these experiments is certainly small enough for the error due to the assumption of § 3 to be negligible, so that it can be stated with confidence that when $a/R = 1/112$ and $2n^2a/R = 350$, the flux in the curved pipe is one per cent. less than that in a straight one, and hence that the value of μ calculated as explained above should exceed by one per cent. its proper value. If, then, the experimental determinations had been accurate to one per cent., the increase in measured values of μ would not have been appreciable till K was 350. The increase in μ was, in fact, found sensible when K had the smaller value 300; this suggests that the measurements were more accurate than has been assumed in the numerical illustration. As it was estimated * that the results were accurate to $\frac{1}{2}$ per cent., some confirmation of the theory is provided by this comparison.

The velocity corresponding to the Reynolds' number 130 has been called † the critical velocity. But there is, I think, no conclusive evidence that this velocity is what is usually called a critical velocity; there is no evidence, that is to say, that at this velocity any change in the type of motion takes place. There is no need to assume a change in the motion to account for the increased values of μ; they can be attributed to the fact that the effect of curvature increases with the mean velocity, and the rough numerical agreement just found suggests that this alternative explanation is the correct one. There is, however, more direct evidence. In experiments by Prof. Eustice ‡ it has been shown directly (by observation of colour bands) that the motion of water in curved pipes can be stream-line when the Reynolds' number is greater than 1000, and a/R much greater than 1/100.

11. Another general result which is of some importance can be deduced. The ratio of the rate of flow due to a given pressure gradient in a curved pipe to that caused by the same gradient in a straight pipe of equal area depends only on the value of K. This can be expressed

$$F_c/F_s = (K). \quad . \quad . \quad . \quad . \quad . \quad . \quad (30)$$

The problem of determining the relation between flux and gradient in any curved pipe (the motion being, of course, supposed stream-line) therefore reduces to that of finding

* *Loc. cit.* p. 118.

† 'Mechanical Properties of Fluids,' p. 163; also p. 130 of the paper.

‡ Proc. Roy. Soc. A, vol. lxxxv. p. 119 (1911).

the single function $f(\mathrm{K})$. Equation (30) is not exactly true because of the assumption of § 3, but the error will in most cases be of little consequence.

Very little progress has been made with the analytical determination of $f(\mathrm{K})$, but there remains the possibility of deducing it from experiment; it can obviously be found from experiments on a single curved pipe, provided only the range of values of K is large enough. It is therefore possible to correlate experimental results for pipes of different curvatures.

It is convenient to write (30) in a different form. The analysis is most simply done in terms of K, but except when the motion is relatively slow, the quantity so denoted is not of much direct significance.

From equation (22) the constant C of (16) is equal to 4. Hence from equation (18)

$$\mathrm{G}a^2/\mu\,\mathrm{W}_0=\mathrm{C}=4,$$

where G is the pressure gradient. From (17)

$$\begin{aligned}\mathrm{K}&=2\,\mathrm{W}_0{}^2a^3/\nu^2\mathrm{R}\\&=\mathrm{G}^2a^7/8\mu^2\nu^2\mathrm{R}.\end{aligned}$$

We can therefore replace (30) by

$$\mathrm{F}_c/\mathrm{F}_s=f\left[\frac{\mathrm{G}^2a^7}{\mu^2\nu^2\mathrm{R}}\right]. \quad . \quad . \quad . \quad . \quad . \quad . \quad (31)$$

This result is used below in the following form. Suppose that fluid flows under gradient G through a pipe of radius a coiled in a circle of radius R, and that the ratio of the flux to $\pi a^4\mathrm{G}/8\mu$ * is known; then the ratio of the flux due to gradient G′ in a pipe of radii a' and R′ to $\pi a'^4\mathrm{G}'/8\mu'$ is the same, provided that

$$\frac{\mathrm{G}^2a^7}{\mu^2\nu^2\mathrm{R}}=\frac{\mathrm{G}'^2a'^7}{\mu'^2\nu'^2\mathrm{R}'}. \quad . \quad . \quad . \quad . \quad . \quad . \quad (32)$$

12. In the rest of this paper an attempt is made to use equation (32) of the preceding paragraph to correlate results obtained by Prof. Eustice † by observation of the flow of water through pipes of various radii of curvature.

* The flux through a straight pipe of radius a due to gradient G. Lamb, 'Hydrodynamics,' § 331.

† Proc. Roy. Soc. A. vol. lxxxiv. p. 107 (1910). In the numerical work that follows observed values were in the first instance got by measurement of the curves in fig. 5 of this paper, and some errors necessarily resulted; the values given below are taken from copies of tables of results not given in full in the paper. I am much indebted to Prof. Eustice for these copies, and also for references to papers which he has written on this subject, among them that now quoted.

There are some difficulties in the way of the application of the theory to these experiments. A single flexible tube of rubber and canvas was used, and the radius of curvature, R, was varied by winding a given length of the tube on circular cylinders of various diameters. When the tube was free and the motion stream-line, it was found that the pressure gradient was roughly proportional to $\overline{v}^{1\cdot2}$, because the tube in this condition was sinuous; in a straight tube the gradient is, of course, proportional to the first power of the mean velocity. It seems possible that some influence due to this unstrained configuration of the tube may have persisted when the tube was coiled, particularly when the number of coils was small.

The second point is that the coiling was accompanied in every case by a decrease (in one instance of more than 30 per cent.) in the area of the cross-section. From (32) it is evidently possible to allow for an alteration in the radius of the section, but it is not possible to allow for the effect of the alteration in the form of the section that the diminution in area implies. It must therefore be assumed that the cross-section of the tube when coiled is circular. (See § 17.)

Consequently the function $f(K)$ has not been calculated absolutely. It appeared better to use the result stated in equation (32). The method is then to start from the observed (F, G) relation for one value of R, deduce the relation for a different value of R, and compare this with experiment. The first source of error indicated above will then be of less consequence.

13. Three such comparisons are given below. In the first we take the experimental (F, G) relation when the given length (81·5 cm.) of tube is wound into a single coil, and deduce from it the relation when the length is wound in 5 coils. Table I. shows the method of calculation. In the first two columns, F_1* and g_1* give the observed relation for the single coil: F_1 is the flux at 14° C. in c.c. per second; the formula

$$F \propto (1 + 0{\cdot}03368\,T + 0{\cdot}000221\,T^2),$$

where T is temperature centigrade †, was used to deduce the flux at temperature 14° C. from the observed value. In the second column g_1 denotes the decrease in pressure,

* The suffix denotes here and subsequently the number of coils.

† It follows from (31) that a different temperature correction is required for a curved pipe, but as the temperatures were all near 14° C. the difference is probably small; no allowance has been made for this.

measured in cm. of water, in the length 81·5 cm. of the coiled tube. The corresponding pressure gradient G_1 in C.G.S. units is very approximately given by

$$G_1 = \frac{981}{81{\cdot}5} g_1,$$

but as we are concerned only with ratios of pressure gradients it is more convenient to work with g_1, for instance, than with G_1.

The area of cross-section, which is assumed a circle of radius a_1, is given as 0·1065 cm.^{2} Then

$$\pi a_1^2 = 0{\cdot}1065,$$

and for $(F_s)_1$, the rate of flow of water at 14° C. through a straight pipe of radius a_1 due to pressure gradient G_1, we have

$$(F_s)_1 = \pi a_1^4 G_1 / 8\mu_{14}$$

$$= \frac{(\cdot 1065)^2(981)}{8\pi(\cdot 01174)(81{\cdot}5)} g_1 = 0{\cdot}4627 g_1.$$

$(F_s)_1$ is given in the third column, and $(F_s)_1/F_1$ in the fourth.

The ratio $(F_s)_5/F_5$ is the same as $(F_s)_1/F_1$ when the pressure difference g_5 is such that

$$g_1^2 a_1^7 / R_1 = g_5^2 a_5^7 / R_5.$$

When the tube was wound in 5 coils the area of the section diminished to 0·0996 cm.^{2}, so that $\pi a_5^2 = 0{\cdot}0996$ and $R_1 = 5R_5$. Hence corresponding values of g_1 and g_5 must be such that

$$g_5 = 0{\cdot}5028 g_1.$$

In the sixth column $(F_s)_5$, the flux in a straight pipe of radius a_5 due to pressure difference g_5, is tabulated; then dividing each value by the value $(F_s)_1/F_1$ in the same row, we have finally values of the flux F_5 in the coiled tube due to pressure difference g_5. Not all the values that have been calculated are given in Table I.; a selection has been made such that consecutive values of F_5 differ by about 0·5.

In the same way the $(F_{1/2}, g_{1/2})$ relation has been calculated from the observed (F_1, g_1) relation. The calculated and observed relations in both cases are compared in Tables II. and III., and shown graphically in fig. 2.

TABLE I.

Calculation of (F_5, g_5) from observed (F_1, g_1).

Observed values.		$(F_s)_1$.	$(F_s)_1/F_1$.	g_5.	$(F_s)_5$.	F_5.
g_1. cm.	F_1. c.c./sec.					
3·37	1·02	1·56	1·53	1·69	·684	·45
8·64	2·15	4·00	1·86	4·34	1·76	·95
17·6	3·65	8·14	2·23	8·85	3·58	1·61
26·5	4·87	12·3	2·53	13·3	5·38	2·13
35·4	5·94	16·4	2·76	17·8	7·20	2·61
43·8	6·93	20·3	2·93	22·0	8·90	3·04
52·6	7·86	24·3	3·09	26·4	10·7	3·46
63·9	9·22	29·6	3·21	32·1	13·0	4·05
75·8	10·6	35·1	3·32	38·1	15·4	4·64
83·9	11·2	38·8	3·45	42·2	17·1	4·96
125	14·3	57·8	4·05	62·9	25·5	6·30

TABLE II. (F_5, g_5).

Calc.		Obs.	
g_5.	F_5.	g_5.	F_5.
1·69	·45	3·99	·94
4·34	·95	6·89	1·41
8·85	1·61	9·13	1·76
13·3	2·13	13·5	2·30
17·8	2·61	22·8	3·32
22·0	3·04	41·3	5·02
26·4	3·46	63·2	6·90
32·1	4·05		
38·1	4·64		
42·2	4·96		
62·9	6·30		

TABLE III. $(F_{1/2}, g_{1/2})$.

Calc.		Obs.	
$\frac{1}{2}g$.	$F_{1/2}$.	$g_{1/2}$.	$F_{1/2}$.
1·18	·48	1·70	·63
2·46	·86	3·40	1·11
4·76	1·44	6·74	1·94
8·54	2·30	11·2	2·68
11·2	2·79	17·8	3·90
18·4	4·10	21·9	4·58
24·8	5·16	26·1	5·20
31·3	6·22	29·5	6·02

14. It must be noticed that in calculating part of the (F_5, g_5) relation from the observed (F_1, g_1) relation, the theory is used outside the limits within which it is necessarily valid, because the result stated in equation (32) is applicable only to the correlation of two steady motions. Let it be assumed that the critical velocity in a slightly curved pipe is the same as if the pipe were straight ; it is then such that $\bar{v}d/\nu = 2000$.

Fig. 2.

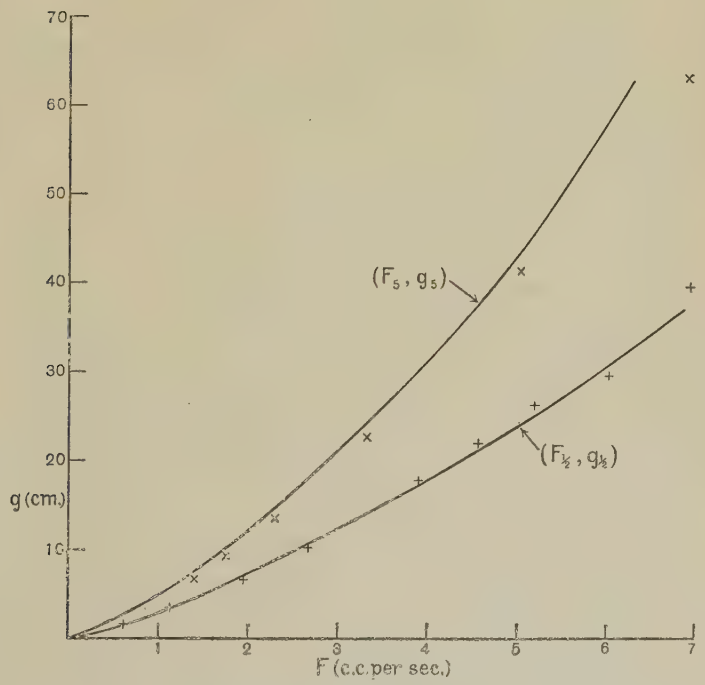

(F_5, g_5); calculated from (F_1, g_1), (—), and observed (×).
$(F_{1/2}, g_{1/2})$; calculated from (F_1, g_1), (—), and observed (+).

At temperature 14° C. the value of ν for water is 0·01174, and if it is assumed that the tubes with which we are concerned have a circular section of area 0·1 cm.², $d = 0{\cdot}357$ cm. Consequently the critical velocity is such that

$$\bar{v} = 65{\cdot}8 \text{ cm./sec.},$$

the corresponding flux being 6·6 c.c./sec. When the flux is greater than this we may suppose that the motion is turbulent.

In finding part of the (F_5, g_5) relation given in Table I., the (F_1, g_1) relation is used at velocities above the critical. Thus the pair of values, $F_5 = 3{\cdot}04$, $g_5 = 22{\cdot}0$, is calculated from the pressure observed when the flux in the tube in one coil was 6·93, and the motion presumably turbulent. All pairs of values in which F_5 is greater than 3·04 are calculated under the same condition. The reason is simply that the corresponding pressure differences in the two tubes are not equal, so that one pressure may cause stream-line motion in one pipe while the corresponding pressure causes turbulent motion in the other. The difficulty can be avoided by starting from the observed values in the pipe of greater curvature; thus in the calculation of $(F_{1/2}, g_{1/2})$ from (F_1, g_1), corresponding pressures are such that

$$g_1/g_{1/2} = 0{\cdot}708,$$

so that if $g_{1/2}$ is small enough to produce steady motion the corresponding value of g_1 will certainly do so.

The agreement between the theoretical and calculated (F_5, g_5) relations is, however, little worse in a certain range above the flux 3·04 than it is below. This suggested that the theory might be of some value as a rough means of calculation, or might even hold good without modification, above the critical velocity; both the calculations above have therefore been extended so as to include values of the flux greater than 6. The agreement gets steadily, but not rapidly, worse. (See § 18.)

15. As a more severe test of the theory the (F_1, g_1) relation has been calculated from the observed (F_{10}, g_{10}) for values of the flux up to about 30, and is compared with observation in Table IV. and fig. 3. When the flexible tube was wound into ten coils the area of its section diminished to 0·0735 cm.^{2}; it has been assumed, as in the other calculations, that the section is a circle of this area.

This comparison differs from the previous two in that calculated values of the flux are consistently less than the observed at low pressures, but consistently greater at high pressures; in the second case above, with only a few exceptions, the calculated values are greater than the observed, while in the first case they are, without exception, less.

16. If the flux does not exceed 6·6, in which range the motion of the water may be supposed stream-line, only in the calculation of (F_1, g_1) from (F_{10}, g_{10}) is there a discrepancy of any importance between calculated and observed values.

TABLE IV.

(F_1, g_1); calculated from (F_{10}, g_{10}), and observed.

Calc.	g_1	2·31	3·80	9·39	12·6	26·4	47·4
	F_1	·54	·83	1·81	2·30	4·18	6·58
	g_1	76·4	115	150	193	299	379
	F_1	9·37	12·7	15·2	18·0	24·6	28·8

Obs.	g_1 ...	1·74	3·37	6·05	8·64	13·0	17·6	22·2	31·0
	F_1 ...	·61	1·02	1·63	2·15	2·90	3·65	4·42	5·41
	g_1 ...	39·8	52·6	63·9	125	166	250	340	420
	F_1 ...	6·45	7·86	9·22	14·3	16·8	20·8	24·1	27·0

Fig. 3.

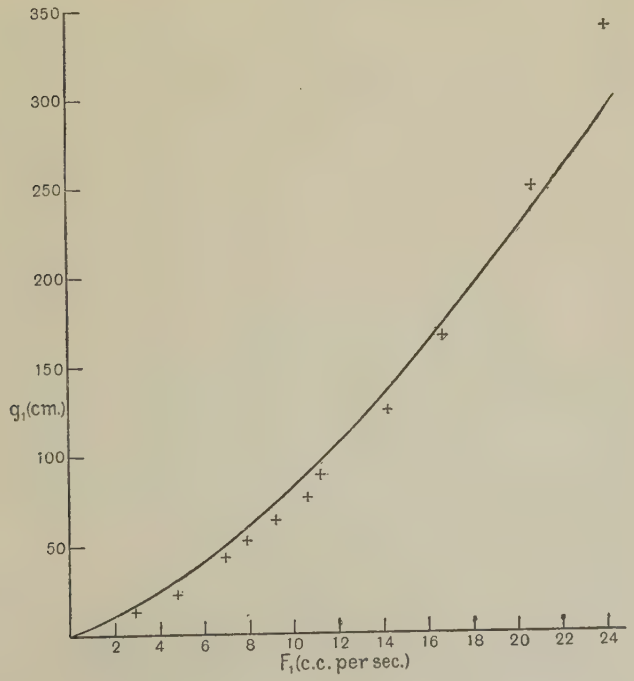

(F_1, g_1); calculated from (F_{10}, g_{10}), (—), and observed (+).

In the calculation of (F_5, g_5) from (F_1, g_1) the differences between calculated and observed rates of flow are all of the same sign, and all except one are less than 0·2 ; in the exceptional case the difference is less than 0·6, and the observed rate of flow 6·90. In the calculation of $(F_{1/2}, g_{1/2})$ from (F_1, g_1) the agreement is still better ; the differences are not all of the same sign and do not exceed 0·2 until the observed flux is 6·94, in which case the difference is less than 0·3. In a part of the first of these calculations the theory has, as stated, been used when it is not necessarily valid, but it appears that the accuracy is not immediately affected.

In the calculation of (F_1, g_1) from (F_{10}, g_{10}) the agreement in stream-line motion is poor. The maximum difference between calculated and observed rates of flow lies between 0·7 and 0·8 ; for the small value 1·02 of the observed rate of flow the fractional error is about 1/4, but it decreases as the flux increases, and is about 1/10 at the critical velocity. But there are several sources of error which together may account for this discrepancy.

17. It has been assumed that the cross-section of the tube when in ten coils was circular, while in fact it was oval. Allowance for this, if it could be made *, would improve the agreement ; this is easily seen from the method of calculation shown in Table I. Assume that the section is circular when the tube is in one coil, but elliptical when it is in ten ; then the theory would give the (F_1, g_1) relation correctly if for the observed values of F_{10} are substituted the larger values of the flux through a circular pipe of the same sectional area. For given g_{10}, F_{10} must be increased. $(F_s)_{10}$ depends on g_{10} and a_{10}, and will be unaltered ; so will g_1 and hence $(F_s)_1$, but the ratio $(F_s)_{10}/F_{10}$ will be decreased, and thus finally F_1 will be increased. As the calculated values are too small, this correction will improve the agreement. It must, however, be pointed out that a considerable distortion due to coiling would have to be assumed to account for the whole of the difference that has been found above. The ratio of the rates of flow through two straight pipes of the same area, one circular and the other elliptical, is †

$$2ab/(a^2+b^2),$$

if a, b are the semi-axes of the ellipse. This ratio is 0·9

* The dimensions (apart from the area) of the section of the tube when coiled are not given, and would probably be difficult to find with accuracy.

† Lamb, *op. cit.* § 332.

when $b/a=0{\cdot}63$, and if the rate of flow is not more sensitive to form of section in a curved pipe than in a straight one, a distortion of at least this magnitude must be assumed.

A correction for form of section is needed only in this case, as in the other two the alterations in area were much smaller. The area of the section, 0·1066 cm.^{2} when the tube was free, decreased by only 0·0070 cm.^{2} when it was in five coils ; the correction for the small change of form that may have accompanied this decrease is certainly negligible.

It may be noted that the theory applies, in certain conditions, to tubes of elliptical cross-section. Suppose that the sections are elliptical when the tube is in 1 and 1/2 coils. As the areas are almost the same (the difference is given as 10^{-4} cm.^{2}), the ellipses can be assumed geometrically similar. In such a case as this no alteration in the calculation above is required. The only reference to the form of the section in the fundamental equations of § 4 is contained in the boundary condition in which the boundary is given as $r'=1$. If we are to compare two tubes whose sections are similar ellipses, the boundary is $r'=f(\psi)$, the function f being the same for both. The quantity a may now stand for the mean radius. The standard of comparison is not now a straight pipe of circular section, but a straight pipe whose section is a similar ellipse. Hence in what corresponds to Table I. for this calculation the numbers in the columns $(F_s)_1$ and $(F_s)_{1/2}$ have to be multiplied by the same constant, and the final result is unaffected.

There are other corrections that should strictly be made, but none likely to be important. The error due to the assumption of § 3 is, of course, greatest when the tube is in ten coils ; the external and internal diameters of the coil are then 3·2 cm. and 1·9 cm. respectively, and taking a to be 0·153 cm., we have $a/R=0{\cdot}12$. The fractional error, nominally of order a^2/R^2, would be only 0·002 if equation (27) were correct, and in any case can hardly result in a final error of much importance. If a correction were to be made its effect would be to improve agreement.

Another point is that no allowance can be made for the effect of the sudden change in curvature at the ends of the coiled tube. It is likely that the flow will be more disturbed when the tube is in ten coils than when it is in one, so that, although the method of calculation eliminates some of the end effect, a correction may be required which again would improve agreement.

Although the differences between calculated and observed

values are in this case large, they do not therefore necessarily imply that the theory is at fault, especially as any calculated value of F_1 is more than three times the observed value of F_{10} from which it is derived, so that errors of observation (likely to be greatest when the flux is small) are magnified.

18. In all three cases the calculations have been extended to values of the flux greater than 6·6, the assumed limit of stream-line motion, in order to see what errors resulted from the use of the theory outside its proper scope. Some of the results in the calculation of (F_1, g_1) from (F_{10}, g_{10}) are shown in fig. 3. For all observed values of F_1 between 6·6 and 24·1, the difference between observed and calculated values of F_1 does not exceed 10 per cent. ; in this range the Reynolds' number varies from about 2000 to over 7000. However, in the last paragraph the need has been shown for corrections which will certainly decrease the range in which the theory is correct to within 10 per cent. In the calculation of $(F_{1/2}, g_{1/2})$ from (F_1, g_1), observed and calculated values of $F_{1/2}$ differ by less than 5 per cent. for all observed values of $F_{1/2}$ up to 10·7, which corresponds to a Reynolds' number of over 3000.

The agreement in the calculation of (F_5, g_5) from (F_1, g_1) is much worse. The difference between the two values of F_5 is 10 per cent. when the observed value of F_5 is 8·6, increases steadily, and is 24 per cent. when the observed value is 17·5.

It can be concluded that if an attempt is to be made to correlate results in which the critical velocity is exceeded, it is better to start from the observed values for the pipe of greater curvature, and that then the errors will not be very serious if the Reynolds' number does not exceed perhaps 4000. The reason why it is better to correlate in one way rather than in the other is partly that it is better to make a crude interpolation than an equally crude extrapolation ; but there is also the fact that in finding, for instance, the calculated value $F_5 = 16{\cdot}5$, the observed value $F_1 = 37{\cdot}6$, to which, corresponds a Reynolds' number of more than 10^4, is used.

19. The theory can probably be extended so as to apply to all velocities by substituting a coefficient of eddy viscosity for the ordinary coefficient μ. For this, however, the absolute determination of the function $f(K)$, by experiment or otherwise, is almost a necessity ; the method of comparison used in this paper would be unsuitable, as it would be much more difficult to find the corresponding motions in the two

pipes compared. It is clear from some of the results above that at velocities just above the critical the coefficient of eddy viscosity must differ only slightly from the ordinary coefficient if there is to be agreement: this follows immediately from the statement of Prof. Eustice * that there is no marked critical velocity in the coiled tubes. The reason for this difference between straight and curved pipes appears clear. That the pressure gradient required to maintain a given rate of flow increases more or less suddenly when the critical velocity is exceeded is a consequence of the sudden change in the type of motion: turbulence is accompanied by a lateral movement of the fluid, which implies a loss of energy that has no counterpart in steady motion. In a curved pipe, on the other hand, lateral movement is already taking place before the critical velocity is reached; it is probably increased when turbulence sets in, but there is clearly less reason in this case to expect a rapid increase in the resistance to flow.

LXXIII. *Electrical Properties of Monatomic Gases.* By J. S. Townsend, *F.R.S., Wykeham Professor of Physics, Oxford, and* S. P. MacCallum, *Fellow of New College, Oxford* †.

1. In the course of an investigation of the electrical properties of monatomic gases we made several experiments to determine the best method of purifying the gases, and we observed that small traces of an impurity are removed in a few seconds by the action of a high-frequency discharge. This effect of the discharge, which may be obtained with external electrodes, was observed in the process of filling a quartz tube with neon.

The tube was heated to a temperature of about 600° C., and washed out with pure neon in order to remove the gas given off from the surface. This operation was repeated until a stage was reached at which no effect of impurities was seen in the colour of the discharge, and there were no lines in the spectrum except those due to neon.

A constriction in a narrow quartz side-tube through which the gas was admitted was then sealed in order to disconnect the electrodeless tube containing neon. Immediately after

* *Loc. cit.* p. 114; see also fig. 4.

† Communicated by the Authors.

sealing off the tube a high-frequency discharge was produced in the gas, and at first it appeared to be very impure, but after a few seconds the impurity disappeared and the colour of the discharge and the lines in the spectrum became exactly as they were before the constriction was sealed. The impurity was probably hydrogen which got into the gas when the constriction was heated to the very high temperature required for sealing, and the high-frequency discharge, which ionized the gas, caused the hydrogen to be rapidly absorbed by the quartz.

In other experiments we have observed that the effect of an impurity is more noticeable in a wide tube where the force required to maintain the discharge is comparatively small, than in a narrow tube where a larger force is required.

From measurements of the currents in these discharges, and the potentials at the external electrodes, it has been found that the positive ions and the electrons do not recombine to any appreciable extent in the gas *.

The disappearance of ions from the gas is due primarily to the electrons which diffuse rapidly to the sides of the vessel, leaving a positive charge in the gas. The positive ions are repelled to the sides by this charge, and in the stable distribution which is established almost instantaneously the positive ions reach the sides at the same rate as the electrons. These losses are balanced by the process of ionization by collisions of electrons with molecules, and a constant steady state is maintained. Thus molecules of diatomic gases which are easily ionized are driven by the force on their positive charges into contact with the sides of the quartz, where they remain for a considerable time.

We have found this property of the electrodeless discharge to be very useful in cases where it is necessary to remove small traces of impurities.

2. In order to obtain accurate measurements of sparking potentials and photo-electric currents, an apparatus comprising parallel plates was made up with quartz insulation and fitted into one end of a quartz cylinder 23 cm. long and 5·8 cm. in diameter. The free space at the other end of the cylinder, about 10 cm. long, was used for obtaining a high-frequency discharge with external electrodes. One of the plates of the measuring instrument was mounted on a micrometer screw to which a rod of soft iron was attached. By

* J. S. Townsend and R. H. Donaldson, Phil. Mag. p. 179 (Jan. 1928). J. S. Townsend, *Comptes Rendus*, p. 55 (Jan. 1928).

this means it was possible to adjust the distance between the plates with a magnet.

Each specimen of gas used in the experiments was purified by passing it slowly along a tube containing copper oxide at a high temperature, to remove traces of hydrogen, and thence into a tube containing charcoal which was cooled by liquid air. The gas was kept for sixteen hours in the charcoal tube before it was admitted into the quartz cylinder.

The apparatus was heated to a temperature of about 300° C. to 400° C. for several hours and washed out with pure neon. This operation was repeated until there was no visible change in the colour of the high-frequency discharge when the gas was left in the cylinder for twenty-four hours. A point was thus reached at which the sparking potential, as found by the parallel plate electrodes with a battery of small accumulators, was constant for a given value of the product of the pressure and distance between the plates, and remained at that value for some hours after the gas was admitted to the cylinder. Very small traces of impurities have a comparatively large effect on the sparking potential, and a considerable change was obtained when the gas was left in the quartz cylinder for twenty-four hours ; but the impurity accumulated in the gas in that time is immediately removed by the high-frequency discharge, and the sparking potential regains the same value observed in a fresh sample of pure gas.

3. As an example of these experiments the sparking potentials observed in neon at a pressure of 37·2 mm. are given in Table I., the potentials being in volts and the distance S between the plates in millimetres. The sparking potentials obtained a few hours after the gas had been in the apparatus are given in column A_1. At this stage there is no change in the potentials of more than one volt, due to the passage of the high-frequency discharge through gas. The potentials obtained after the gas had been in the apparatus for twenty-four hours are given in columns B_1 and C_1, the latter being the potentials after the high-frequency discharge had been maintained in the gas for one or two minutes.

These methods of purifying the gas are very reliable, and constant results are obtained on repeating the experiments. Thus, after the gas at 37·2 mm. pressure had been in the apparatus for a week, the quartz cylinder was heated and the gas was pumped out. After washing out the apparatus with pure gas, a fresh quantity at 37·4 mm. was admitted and the experiments were repeated. The sparking potentials obtained

shortly after admitting the gas are given in column A_2, and those obtained after twenty-four hours in columns B_2 and C_2, the change from B_2 to C_2 being effected by means of the high-frequency discharge, as in the experiments with the gas at 37·2 mm. pressure.

Table I.—Sparking Potentials in Neon.

S.	p=37·2 mm.			p=37·4 mm.		
	A_1.	B_1.	C_1.	A_2.	B_2.	C_2.
4.....	263	251	263	264	254	264
5.....	292	278	292	294	277	294
6.....	317	300	318	319	298	320
7.....	342	320	344	344	312	344

Small traces of impurities which are not easily observed in a direct-vision spectroscope are easily detected by a measurement of the sparking potential.

The agreement between the figures in columns A and C indicates the degree of accuracy which may be obtained.

4. The photo-electric currents obtained with a constant electric force and a constant gas-pressure were also determined with different distances x between the plates. The current n in terms of the distance was found to be in accordance with the formula

$$n = n_0 \frac{(\alpha - \beta)\epsilon^{(\alpha-\beta)(x-\delta)}}{\alpha - \beta\epsilon^{(\alpha-\beta)(x-\delta)}}$$

for a range of distances from a certain small distance δ to the sparking distance S. The sparking distance is the value of x obtained by equating to zero the denominator of the term on the right of the equation. The effect of small traces of impurities on the constants α and β is easily observed, but the experimental error involved in the determination of these coefficients is much greater than in the determination of a sparking potential. As an example of the determinations of these coefficients, the results of experiments made with the sample of gas at 37·2 mm. pressure are given in Table II. The figures in column A give the results obtained after the gas was in the quartz cylinder for a few hours,

those in columns B and C after twenty-four hours, the change from B to C being produced by the action of a high-frequency discharge. A slightly different value of the electric force was taken in the three sets of experiments as indicated by the values of X in the first line of figures, which are the forces in volts per centimetre.

TABLE II.—Neon, $p=37{\cdot}2$.

	A.	B.	C.
X	483	476	487
α	4·2	4·76	4·3
β	·32	·24	·31

Thus there are two completely different methods of removing small traces of impurities from a monatomic gas—that involving the use of charcoal cooled with liquid air and that of the high-frequency discharge. It may be concluded that the gas taken from the charcoal tube contains no impurities which alter the electrical properties of the gas, as the gas is not affected by the high-frequency discharge until after it has been in the quartz cylinder containing the parallel-plate apparatus for several hours.

These experiments therefore lead to the conclusion that the atoms of monatomic gases are ionized by the collisions of electrons, and that the development of large currents in gases is principally due to this process. This conclusion applies even in cases where ratio X/p is small, as in the experiments with the gas at 37·2 mm. pressure, where $X/p=13$, or in an electrodeless discharge where the ratio X/p may be as low as 2·5.

5. These conclusions are not in accordance with other theories which have been adopted without taking into consideration the general properties of electric discharges. These theories have appeared in different forms, and there is at present a tendency to attribute predominating effects to impurities which some time ago were attributed to electrons set free from the electrodes by radiation from the gas. They all involve the hypothesis that an electron loses all or most of its energy in a collision with a molecule when the kinetic energy is equal to, or slightly greater than, the energy corresponding to the first resonance potential of the gas. Thus, when electrons move in a gas at a high pressure under

the action of a small electric force, they will never attain sufficient energy to ionize molecules.

It would be interesting to know the order of the electric force as well as the pressure of a monatomic gas in a discharge-tube when the energy of the electrons is thus limited. An example of the application of this hypothesis is suggested by Merton and Pilley * in the case of a tube containing helium at about 30 mm. pressure and a very small quantity of nitrogen. It is stated that a large excess of helium atoms in the discharge must act as "safety valves" which blow off when they are struck by 20·4-volt electrons, and which, therefore, set a superior limit to the energy which there is any significant probability that an electron will acquire. The intensity of the electric force is not mentioned, and it is not stated whether any helium lines were observed in the visible spectrum of the discharge in the experiments in which the energy of the electron is thus limited.

The "safety-valve" action would presumably be a predominant factor in determining the energy of the electron whether the gas is pure or impure, so that electrons would never acquire sufficient energy to ionize atoms of a monatamic gas under the action of small forces. The electrons under the above circumstances would not acquire even as much energy as that represented by the second or third resonance potential, so that the line corresponding to the first resonance potential, which is in the ultra-violet, would be the only helium line in the spectrum of a discharge.

With regard to impurities, it is quite plain there must be processes by which impurities have been successfully removed to such an extent that they have no predominant effect on the discharge. In the well-known neon lights used for commercial purposes, there is a long column of luminous gas where the current is maintained by a small electric force. In order to maintain the current a continuous rate of supply of ions and electrons must be maintained throughout the luminous column, as positive ions are being continually removed towards the negative electrode. A simple calculation shows that, in order to maintain the current, it would be necessary according to this theory to suppose that no small amount of diatomic material is conveyed along the luminous column, and that this process is maintained indefinitely while the light in the visible spectrum of the gas may be almost completely free from lines corresponding to the material from which the positive ions are derived.

* T. R. Merton and J. G. Pilley, Proc. Roy. Soc. A, vol. cvii. p. 411 (1925).

LXXIV. *Some Problems in the Conduction of Heat. By* George Green, *D.Sc., Lecturer in Physics in the Applied Physics Department of the University of Glasgow* *.

THE present paper contains a continuation of the work published in a former paper to the Philosophical Magazine under the same title †. In the paper referred to the method of solution of problems in heat-conduction employed is such that each problem in heat-conduction is treated as a problem in wave-motion. For the solution of two-dimensional problems in heat-conduction it is shown that there are two fundamental wave-trains travelling in the positive direction and two corresponding wave-trains travelling in the negative direction, and that the solution of any problem can be expressed in terms of these four wave-trains. Similarly, in the case of cylindrical and spherical waves there are two positive wave-trains and two negative wave-trains, and the solution of any problem can be expressed in terms of these four wave-trains. The former paper dealt with several fundamental problems involving plane and spherical waves, and it is intended in the present paper to deal with some of the fundamental problems involving cylindrical waves by the method employing positive and negative wave-trains, and to investigate the nature of the special solutions usually employed in cylindrical heat problems, and the relation of these solutions to the four fundamental wave-trains. An interesting feature of the investigations is the comparison which they enable us to make between different methods of arriving at equivalent solutions of the same problem.

We proceed first to obtain the four fundamental wave-trains referred to above. The equation of conduction of heat in a uniform medium, in its simplest form for cylindrical conduction, is

$$\frac{\partial v}{\partial t} = \kappa\left(\frac{\partial^2 v}{\partial \rho} + \frac{1}{\rho}\frac{\partial v}{\partial \rho}\right), \quad . \quad . \quad . \quad . \quad . \quad (1)$$

and the solutions which we require are those for which the temperature v at radius ρ from the axis of coordinates varies with the time t according to the factor e^{ikt}, where k represents the frequency of a periodic vibration. The equation to determine v as a function of ρ then becomes

$$\frac{\partial^2 v}{\partial \rho^2} + \frac{1}{\rho}\frac{\partial v}{\partial \rho} - \frac{ik}{\kappa}v = 0, \quad . \quad . \quad . \quad . \quad (2)$$

* Communicated by the Author.

† Phil. Mag. vol. iii. Suppl. April 1927, pp. 784–800.

of which the general solution is

$$v = \mathrm{A}\mathrm{I}_0\left(\sqrt{\frac{ik}{\kappa}}\cdot\rho\right) + \mathrm{B}\mathrm{K}_0\left(\sqrt{\frac{ik}{\kappa}}\rho\right),$$

where A and B are arbitrary constants, and $\mathrm{I}_0\left(\sqrt{\frac{ik}{\kappa}}\rho\right)$ and $\mathrm{K}_0\left(\sqrt{\frac{ik}{\kappa}}\rho\right)$ are functions of ρ defined by

$$\mathrm{I}_0(z) = 1 + \frac{z^2}{2^2} + \frac{z^4}{2^2\cdot 4^2} + \frac{z^6}{2^2\cdot 4^2\cdot 6^2} + \text{ etc.}, \quad . \quad . \quad , \quad (3)$$

$$\mathrm{K}_0(z) = \alpha\mathrm{I}_0(z) - \log z\,\mathrm{I}_0(z) + \frac{z^2}{2^2} + \left(1+\frac{1}{2}\right)\frac{z^4}{2^2\cdot 4^2} + \text{ etc.}, \quad (4)$$

where $\alpha = \log -\gamma$, γ being Euler's constant.

By employing Stokes's method to obtain the solutions of equation (1), we find asymptotic expansions for these functions when ρ is large. These expansions are given by

$$\mathrm{I}_0(z) = \frac{e^z}{\sqrt{2\pi z}}\left\{1 + \frac{1^2}{(8z)} + \frac{1^2\cdot 3^2}{2\,!\,(8z)^2} + \text{ etc.}\right\}, \quad (5)$$

$$\mathrm{K}_0(z) = \pi\frac{e^{-z}}{\sqrt{2\pi z}}\left\{1 - \frac{1^2}{(8z)} + \frac{1^2\cdot 3^2}{2\,!\,(8z)^2} - \text{ etc.}\right\}. \quad (6)$$

The function $\mathrm{K}_0(z)$ becomes infinite as $\log z$ as z tends to zero, and as z tends to infinity its value tends to zero. The $\mathrm{I}_0(z)$ function is finite at the origin and becomes infinite in value as z increases indefinitely. The two fundamental positive or diverging wave-trains are accordingly represented by the real and imaginary parts of $e^{ikt}\mathrm{K}_0\left(\sqrt{\frac{ik}{\kappa}}\rho\right)$ respectively: the two fundamental negative wave-trains are represented by the real and imaginary parts of $e^{ikt}\mathrm{I}_0\left(\sqrt{\frac{ik}{\kappa}}\rho\right)$ respectively.

We can now find the solution representing a line source at which there is a periodic heat supply of amount $q\cos kt$ or $q\sin kt$ per unit length. It involves only the diverging waves; hence we may take

$$v = \mathrm{A}e^{ikt}\mathrm{K}_0\left(\sqrt{\frac{ik}{\kappa}}\rho\right),$$

and determine the constant A from the condition

$$\operatorname*{Lt}_{\rho\to 0}\left(-2\pi\mathrm{K}\rho\frac{\partial v}{\partial\rho}\right) = qe^{ikt}. \quad . \quad . \quad . \quad . \quad (7)$$

In this way we find that the periodic line source is represented by

$$v = \frac{q}{2\pi \mathrm{K}} e^{ikt} \mathrm{K}_0\left(\sqrt{\frac{ik}{\kappa}}\rho\right). \quad . \quad . \quad . \quad . \quad (8)$$

This result may also be obtained as follows. Take the solution given in equation (39) of the former paper, representing a periodic heat supply $q \cos kt$ or $q \sin kt$ at a point which is origin of the coordinate r,

$$v = \frac{q}{4\pi \mathrm{K} r} e^{-r\sqrt{\frac{k}{2\kappa}}} \left\{ \cos\left(kt - r\sqrt{\frac{k}{2\kappa}}\right) + i \sin\left(kt - r\sqrt{\frac{k}{2\kappa}}\right)\right\}. \quad (9)$$

In this replace q by $q\,dz$ and integrate along the axis of z from $-\infty$ to $+\infty$. The periodic line source solution is thus obtained in the form

$$v = \frac{q}{4\pi \mathrm{K}} \int_{-\infty}^{+\infty} \frac{dz}{r} e^{ikt - \sqrt{\frac{ik}{\kappa}} r}; \qquad r^2 = \rho^2 + z^2, \quad . \quad (10)$$

and by substituting $\rho \sinh \theta$ for z in this, it becomes

$$\begin{aligned} v &= \frac{q e^{ikt}}{2\pi \mathrm{K}} \int_0^\infty d\theta\, e^{-\rho \cosh\theta \sqrt{\frac{ik}{\kappa}}} \\ &= \frac{q}{2\pi \mathrm{K}} \int_0^\infty d\theta\, e^{-\rho \cosh\theta \sqrt{\frac{k}{2\kappa}}} \left\{ \cos\left(kt - \rho \cosh\theta \sqrt{\frac{k}{2\kappa}}\right) \right. \\ &\qquad \left. + i \sin\left(kt - \rho \cosh\theta \sqrt{\frac{k}{2\kappa}}\right)\right\}, \quad (11) \end{aligned}$$

which is an equivalent form of equation (8) above.

To verify that the periodic line source solution given above leads by integration to the well-known plane source solution, replace q in the above expression by $q\,dz$, and ρ by $\sqrt{z^2 + x^2}$, and integrate with respect to z from $-\infty$ to $+\infty$. Thus we find that

$$v = \frac{q e^{ikt}}{2\pi \mathrm{K}} \int_{-\infty}^{+\infty} dz\, \mathrm{K}_0\left(\sqrt{\frac{ik}{\kappa}}\sqrt{z^2 + x^2}\right), \quad . \quad (12)$$

and by using the evaluation of this integral given in

Watson's 'Theory of Bessel Functions,' p. 417, we obtain the solution

$$v = \frac{qe^{ikt}}{2\pi K} \cdot \frac{\pi}{\sqrt{\frac{ik}{\kappa}}} e^{-z\sqrt{\frac{ik}{\kappa}}}, \quad . \quad . \quad . \quad . \quad (13)$$

which represents a periodic plane source supplying qe^{kt} per unit area.

Proceed now to determine the solution representing a surface source at which there is a periodic heat supply of amount $q\cos kt$ or $q\sin kt$ per unit area. Let $\rho = a$ be the surface at which the heat is supplied; then outside this surface the solution involves only the diverging wave, and inside this surface it involves only the inward travelling wave. Hence we take

$$v_i = Ae^{ikt} I_0\left(\sqrt{\frac{ik}{\kappa}}\rho\right) \quad . \quad . \quad \rho < a, \quad . \quad (14)$$

$$v_0 = Be^{ikt} K_0\left(\sqrt{\frac{ik}{\kappa}}\rho\right) \quad . \quad . \quad \rho > a, \quad . \quad (14')$$

and determine the two constants A and B from the conditions which hold at the surface $\rho = a$; namely,

$$v_i = v_0, \quad \text{and} \quad -K\left(\frac{\partial v_0}{\partial \rho} - \frac{\partial v_i}{\partial \rho}\right) = qe^{ikt}. \quad . \quad (15)$$

In this way we find that a periodic surface source of strength qe^{ikt} at $\rho = a$ is represented by

$$v_i = \frac{qa}{K} e^{ikt} K_0\left(\sqrt{\frac{ik}{\kappa}}a\right) I_0\left(\sqrt{\frac{ik}{\kappa}}\rho\right) \quad . \quad . \quad \rho < a, \quad (16)$$

$$v_0 = \frac{qa}{K} e^{ikt} I_0\left(\sqrt{\frac{ik}{\kappa}}a\right) K_0\left(\sqrt{\frac{ik}{\kappa}}\rho\right) \quad . \quad . \quad \rho > a. \quad (16')$$

Verify that

$$\begin{aligned} &-K\left(\frac{\partial v_0}{\partial \rho} - \frac{\partial v_i}{\partial \rho}\right)_{\rho=a} \\ &= qe^{ikt}\sqrt{\frac{ik}{\kappa}}a \left\{ K_0\left(\sqrt{\frac{ik}{\kappa}}a\right) I_1\left(\sqrt{\frac{ik}{\kappa}}a\right) \right. \\ &\qquad \left. + K_1\left(\sqrt{\frac{ik}{\kappa}}a\right) I_0\left(\sqrt{\frac{ik}{\kappa}}a\right) \right\} \\ &= qe^{ikt} \quad . \quad . \quad . \quad . \quad . \quad . \quad . \quad . \quad . \quad . \quad . \quad . \quad . \quad (17) \end{aligned}$$

as required.

An alternative method by which this result may be arrived at is to take the periodic line solution given in equation (8), replace the q in it by $qa\,d\theta'$ and ρ by r, and integrate with respect to θ' from $-\pi$ to $+\pi$. The solution obtained for a periodic cylindrical surface source of strength qe^{ikt} per unit area of the surface, $\rho=a$, is accordingly

$$v = \frac{qa}{2\pi \mathrm{K}} \int_{-\pi}^{+\pi} d\theta' e^{ikt}\, \mathrm{K}_0\left(\sqrt{\frac{ik}{\kappa}}\, r\right), \quad . \quad . \quad (18)$$

where $r^2 = a^2+\rho^2-2a\rho\cos\theta'$.

But by the addition theorem we have

$$\mathrm{K}_0\left(\sqrt{\frac{ik}{\kappa}}\, r\right) = \sum_{m=-\infty}^{m=+\infty} \mathrm{K}_m\left(\sqrt{\frac{ik}{\kappa}}\, a\right) \mathrm{I}_m\left(\sqrt{\frac{ik}{\kappa}}\, \rho\right) \cos m\theta'$$
$$\ldots a > \rho \quad . \quad . \quad (19)$$
$$= \sum_{m=-\infty}^{m=+\infty} \mathrm{K}_m\left(\sqrt{\frac{ik}{\kappa}}\, \rho\right) \mathrm{I}_m\left(\sqrt{\frac{ik}{\kappa}}\, a\right) \cos m\theta'$$
$$\ldots \rho > a; \quad . \quad . \quad (19')$$

hence, when these values are inserted in (18), and when the integration with respect to θ' is carried out, we reach again the result already given in equation (16) above.

From the above periodic solutions we can obtain others by integration. Thus, by taking the real part only of equation (8) which represents a periodic line source emitting $q\cos kt$ per unit length, and integrating with respect to k, we obtain the solution representing an instantaneous line source of strength q per unit length; that is,

$$v = \frac{q}{2\pi^2 \mathrm{K}} \int_0^{\infty} dk\, e^{ikt}\, \mathrm{K}_0\left(\sqrt{\frac{ik}{\kappa}}\, \rho\right)$$
$$= \frac{q}{2\pi^2 \mathrm{K}} \int_0^{\infty} d\theta \int_0^{\infty} dk\, e^{-\rho\cosh\theta\sqrt{\frac{k}{2\kappa}}}$$
$$\cos\left\{kt-\rho\cosh\theta\sqrt{\frac{k}{2\kappa}}\right\}. \quad (20)$$

The integration with respect to k has already been given in equation (13) of the former paper, and when the value there given is inserted in the above, we obtain the result in the form

$$v = \frac{q}{2\pi \mathrm{K}} \int_0^{\infty} d\theta\, \frac{\rho\cosh\theta}{2\sqrt{\pi\kappa t^3}}\, e^{-\frac{\rho^2\cosh^2\theta}{4\kappa t}}; \quad . \quad . \quad (21)$$

and as the integral that remains is easily transformed into a well-known integral, we obtain, finally, the evaluation indicated by

$$v = \frac{q}{2\pi^2 \mathrm{K}} \int_0^\infty dk\, e^{ikt}\, \mathrm{K}_0\left(\sqrt{\frac{ik}{\kappa}}\,\rho\right) = \frac{q}{4\pi \mathrm{K} t}\, e^{-\frac{\rho^2}{4\kappa t}}. \quad (22)$$

In this equation the real part of the integral only is equated to the well-known instantaneous line source solution corresponding to a generation of q heat units per unit of length of the line. When in the above process we take the imaginary part of equation (8), the evaluation given in equation (15) of the former paper becomes available, and we find as the equation corresponding to (22) for the imaginary part of the integral

$$v = \frac{q}{2\pi^2 \mathrm{K}} \int_0^\infty dk\, e^{ikt}\, \mathrm{K}_0\left(\sqrt{\frac{ik}{\kappa}}\,\rho\right)$$
$$= -\frac{q}{\pi^2 \mathrm{K} t}\left(\frac{(8\kappa t)}{(2\rho)^2} + \frac{2 \cdot 1 \cdot 3 \cdot (8\kappa t)^2}{3 \cdot (2\rho)^4}\right.$$
$$\left. + \frac{2 \cdot 4 \cdot 1 \cdot 3 \cdot 5 \cdot (8\kappa t)^3}{3 \cdot 5 \cdot (2\rho)^6} + \text{etc.}\right). \quad (23)$$

Similarly we may obtain by integration of (16) the solution representing an instantaneous cylindrical surface source at $\rho = a$, q being the amount instantaneously generated per unit area. The solution is given by

$$v_i = \frac{qa}{\pi \mathrm{K}} \int_0^\infty dk\, e^{ikt}\, \mathrm{K}_0\left(\sqrt{\frac{ik}{\kappa}}\,a\right) \mathrm{I}_0\left(\sqrt{\frac{ik}{\kappa}}\,\rho\right) \ldots a > \rho, \quad (24)$$

$$v_0 = \frac{qa}{\pi \mathrm{K}} \int_0^\infty dk\, e^{ikt}\, \mathrm{K}_0\left(\sqrt{\frac{ik}{\kappa}}\,\rho\right) \mathrm{I}_0\left(\sqrt{\frac{ik}{\kappa}}\,a\right) \ldots \rho > a. \quad (24')$$

Both these integrals can be evaluated by the same method; hence this need be indicated for the upper only. When we make use of the equation

$$e^{ikt}\, \mathrm{K}_0\left(\sqrt{\frac{ik}{\kappa}}\,a\right)$$
$$= \int_0^\infty d\theta\, e^{-\rho \cosh\theta \sqrt{\frac{k}{2\kappa}}} \left\{ \cos\left(kt - \rho \cosh\theta \sqrt{\frac{k}{2\kappa}}\right)\right.$$
$$\left. + i \sin\left(kt - \rho \cosh\theta \sqrt{\frac{k}{2\kappa}}\right)\right\}, \quad (25)$$

along with the expansion for $\mathrm{I}_0\left(\sqrt{\frac{ik}{\kappa}}\rho\right)$ given in (3) above, we obtain under the integral sign a series which can be integrated term by term. For the real terms in the integration with respect to k, the evaluation given in equation (13) of the former paper is again available, and the integration with respect to θ then follows easily, exactly as in the case of the instantaneous line source solution obtained immediately above. These two integrations lead to the result :

$$v_i = \frac{q}{2\mathrm{K}}\left\{1+\frac{1}{2^2}\cdot\frac{\rho^2}{\kappa}\frac{\partial}{\partial t}+\frac{1}{2^2.4^2}\cdot\frac{\rho^4}{\kappa^2}\cdot\frac{\partial^2}{\partial t^2}+\text{ etc.}\right\}\left(e^{-\frac{a^2}{4\kappa t}}\Big/t\right), \quad . \ . \ . \quad (26)$$

$$v_0 = \frac{q}{2\mathrm{K}}\left\{1+\frac{1}{2^2}\cdot\frac{a^2}{\kappa}\frac{\partial}{\partial t}+\frac{1}{2^2.4^2}\cdot\frac{a^4}{\kappa^2}\cdot\frac{\partial^2}{\partial t^2}+\text{ etc.}\right\}\left(e^{-\frac{\rho^2}{4\kappa t}}\Big/t\right), \quad . \ . \ . \quad (26')$$

each of which is converted into the other by the interchange of a and ρ. The reciprocal nature of these results is made clear by taking out the factor $e^{-\frac{\rho^2+a^2}{4\kappa t}}$ in both; in this way we find that

$$v_i = \frac{qa}{2\mathrm{K}t}e^{-\frac{a^2+\rho^2}{4\kappa t}}\mathrm{I}_0\left(\frac{a\rho}{2\kappa t}\right), \quad . \ . \ . \ . \quad (27)$$

$$v_0 = \frac{qa}{2\mathrm{K}t}e^{-\frac{a^2+\rho^2}{4\kappa t}}\mathrm{I}_0\left(\frac{a\rho}{2\kappa t}\right), \quad . \ . \ . \ . \quad (27')$$

represents an instantaneous cylindrical surface source of strength q per unit area of the cylinder $\rho=a$.

To obtain a solution representing a periodic cylindrical surface source of the type supplying $qe^{ikt}\cos n\theta$ per unit area, we have merely to follow the process adopted above. But in this case the differential equation to be solved is

$$\frac{\partial^2 v}{\partial\rho^2}+\frac{1}{\rho}\cdot\frac{\partial v}{\partial\rho}-\frac{ik}{\kappa}v-\frac{n^2}{\rho^2}v=0, \quad . \ . \ . \quad (28)$$

and the general solution is

$$\mathrm{AI}_n\left(\sqrt{\frac{ik}{\kappa}}\rho\right)+\mathrm{BK}_n\left(\sqrt{\frac{ik}{\kappa}}\rho\right),$$

where A and B are arbitrary constants and $\mathrm{I}_n(z)$ and $\mathrm{K}_n(z)$ are functions of z derivable from the functions $\mathrm{I}_0(z)$ and

$K_0(z)$ already defined. The required solution is given by

$$v_i = A\cos n\theta\, e^{ikt} I_n\left(\sqrt{\frac{ik}{\kappa}}\rho\right) \ldots a>\rho, \quad (29)$$

$$v_0 = B\cos n\theta\, e^{ikt} K_n\left(\sqrt{\frac{ik}{\kappa}}\rho\right) \ldots \rho>a, \quad (29')$$

where the constants A and B are to be determined by the conditions to be fulfilled at the surface $\rho=a$; namely,

$$v_i = v_0\,; \quad \text{and} \quad -K\left(\frac{\partial v_0}{\partial\rho}-\frac{\partial v_i}{\partial\rho}\right) = q\, e^{ikt}\cos n\theta. \quad (30)$$

These conditions lead to the result

$$v_i = \frac{qa}{K}\cos n\theta\, e^{ikt} K_n\left(\sqrt{\frac{ik}{\kappa}}a\right) I_n\left(\sqrt{\frac{ik}{\kappa}}\rho\right), \quad (31)$$

$$v_0 = \frac{qa}{K}\cos n\theta\, e^{ikt} K_n\left(\sqrt{\frac{ik}{\kappa}}\rho\right) I_n\left(\sqrt{\frac{ik}{\kappa}}a\right). \quad (31')$$

Verify that

$$-K\left(\frac{\partial v_0}{\partial\rho}-\frac{\partial v_i}{\partial\rho}\right)_{\rho=a} = q\, e^{ikt}\cos n\theta\sqrt{\frac{ik}{\kappa}}a$$
$$\left[-K'_n\left(\sqrt{\frac{ik}{\kappa}}a\right) I_n\left(\sqrt{\frac{ik}{\kappa}}a\right)\right.$$
$$\left.+K_n\left(\sqrt{\frac{ik}{\kappa}}a\right) I'_n\left(\sqrt{\frac{ik}{\kappa}}a\right)\right]$$
$$= q\, e^{ikt}\cos n\theta. \quad (32)$$

An alternative method of deriving this result is to take the periodic line source solution (8), replace q by $qa\,d\theta'\cos n\theta'$, and integrate round the cylindrical surface $\rho=a$. In this way we find

$$v = \frac{qa\, e^{ikt}}{2\pi K}\int_0^{2\pi} d\theta'\cos n\theta'\, K_0\left(\sqrt{\frac{ik}{\kappa}}r\right) \quad (33)$$

for all values of ρ,

where $r^2=a^2+\rho^2-2a\rho\cos(\theta'-\theta)$. The integration can be performed after using the addition theorem (19), when it is found that only those terms in the series for which m has the values $+n$ and $-n$ contribute to the final result. Thus for

$a > \rho$ the above integral reduces to

$$v_i = \frac{qa\, e^{ikt}}{2\pi \mathrm{K}} \int_0^{2\pi} d\theta' \cos n\theta' \cdot 2\mathrm{K}_n\left(\sqrt{\frac{ik}{\kappa}}\, a\right) \mathrm{I}_n\left(\sqrt{\frac{ik}{\kappa}}\, \rho\right) \cos n(\theta' - \theta), \quad (34)$$

which is readily seen to be in agreement with the results given above.

Alternative methods are again available to determine the solution representing a cylindrical surface source at which there is an instantaneous heat supply of amount $q \cos n\theta$ per unit area at $\rho = a$. We may start from the solution for an instantaneous line source q per unit of length, given in equation (22) above. Replace the q by $qa\, d\theta' \cos n\theta'$ and ρ by r, and integrate with respect to θ' round the cylindrical surface, $\rho = a$. The temperature at point (ρ, θ), due to the whole surface distribution, is represented by

$$v = \frac{qa}{4\pi \mathrm{K} t} \int_\theta^{2\pi} d\theta' \cos n\theta'\, e^{-\frac{r^2}{4\kappa t}}, \quad . \quad . \quad (35)$$

where $r^2 = \rho^2 + a^2 - 2a\rho \cos(\theta' - \theta)$.

If we alter the variable in this integration from θ' to ϕ, where $\theta' - \theta = \phi$, we can rewrite the above solution in the form:

$$v = \frac{qa\, e^{-\frac{\rho^2 + a^2}{4\kappa t}}}{4\pi \mathrm{K} t} \int_{-\theta}^{2\pi - \theta} d\theta \cos n(\theta + \phi)\, e^{\frac{a\rho}{2\kappa t} \cos \phi}, \quad . \quad (36)^*$$

which leads us finally to the solution represented by

$$v = \frac{qa \cos n\theta}{2\mathrm{K} t}\, e^{-\frac{\rho^2 + a^2}{4\kappa t}} \mathrm{I}_n\left(\frac{a\rho}{2\kappa t}\right), \text{ for } \rho > a \text{ and } \rho < a. \quad (37)$$

The alternative method open to us is to integrate with respect to k the solution representing a periodic cylindrical surface source of the type $q \cos n\theta\, e^{ikt}$ per unit area, which has been derived immediately above. This method gives

$$v_i = \frac{qa \cos n\theta}{\pi \mathrm{K}} \int_0^\infty dk\, e^{ikt} \mathrm{K}_n\left(\sqrt{\frac{ik}{\kappa}}\, a\right) \mathrm{I}_n\left(\sqrt{\frac{ik}{\kappa}}\, \rho\right) \quad . \quad \rho < a, \quad . \quad . \quad . \quad (38)$$

$$v_0 = \frac{qa \cos n\theta}{\pi \mathrm{K}} \int_0^\infty dk\, e^{ikt} \mathrm{K}_n\left(\sqrt{\frac{ik}{\kappa}}\, \rho\right) \mathrm{I}_n\left(\sqrt{\frac{ik}{\kappa}}\, a\right) \quad . \quad \rho > a. \quad . \quad . \quad . \quad (38')$$

* See Rayleigh, 'Scientific Papers,' vol. vi. p. 55.

A demonstration of the equivalence of the two solutions (37) and (38) could doubtless be obtained by applying the method already used to prove the equivalence of the two solutions in the case where $n=0$ given in (24) and (27) above.

In the cases which we have dealt with above, the initial conditions refer to heat supply. It is of interest to take up here some of the fundamental problems in which the initial conditions refer to temperature. Before we proceed to build up solutions from the two fundamental wave-trains, as we have done in the cases considered above, we shall find it worth while to examine the solution obtained from that representing an instantaneous supply of heat q per unit area at $\rho=a$.

If we differentiate with respect to a the solution given by equation (27) above, under the condition that the total heat supply of unit length of the cylinder is kept constant ($qa=$const.), we obtain the solution

$$v = -\frac{q}{2\mathrm{K}}\cdot\frac{a}{2\kappa t^2}\,e^{-\frac{a^2+\rho^2}{4\kappa t}}\left\{a\,\mathrm{I}_0\left(\frac{a\rho}{2\kappa t}\right)-\rho\,\mathrm{I}_1\left(\frac{a\rho}{2\kappa t}\right)\right\}, \quad (39)$$

which is equivalent to the doublet-solution for the surface $\rho=a$. When t tends to zero, $\frac{a\rho}{2\kappa t}$ tends to become infinite, and the two functions $\mathrm{I}_0\left(\frac{a\rho}{2\kappa t}\right)$ and $\mathrm{I}_1\left(\frac{a\rho}{2\kappa t}\right)$ may be represented with sufficient accuracy each by the first term only of its asymptotic expansion. Thus when $t\to 0$ (or $\rho\to\infty$) the above equation may be replaced by

$$v = -\frac{q}{2\mathrm{K}}\cdot\frac{a}{2\kappa t^2}\,e^{-\frac{a^2+\rho^2}{4\kappa t}}\left\{e^{\frac{a\rho}{2\kappa t}}\sqrt{\frac{\kappa t}{\pi a\rho}}(a-\rho)\right\} \quad (40)$$

$$= \frac{q}{2\mathrm{K}}\cdot\sqrt{\frac{a}{\rho}}\cdot\frac{(\rho-a)}{2\sqrt{\pi\kappa t^3}}\,e^{-\frac{(\rho-a)^2}{4\kappa t}}. \quad . \quad . \quad . \quad . \quad (40')$$

Now compare this result with equation (13) of the former paper, and it becomes evident that, in the limit $t\to 0$, the value of v is $(q/2\mathrm{K})$ for $\rho>a$, and it is $-(q/2\mathrm{K})$, for $\rho<a$. Thus the solution

$$v = -\frac{\theta a}{2\kappa t^2}\,e^{-\frac{a^2+\rho^2}{4\kappa t}}\left\{a\mathrm{I}_0\left(\frac{a\rho}{2\kappa t}\right)-\rho\mathrm{I}_1\left(\frac{a\rho}{2\kappa t}\right)\right\} \quad . \quad (41)$$

gives initially $v=\theta$ on the outer side, and $v=-\theta$ on the inner side of the surface, $\rho=a$. At the same time the

gradient of temperature on the two sides of the surface is continuous; that is, $\left(\frac{\partial v_i}{\partial \rho} = \frac{\partial v_0}{\partial \rho}\right)_{\rho=a}$. If we differentiate with respect to a, the solution given in equation (24) above, keeping (qa=constant) as before, we ought to obtain a solution equivalent exactly to that given in (39) above; namely,

$$v_i = -\frac{qa}{\pi K}\int_0^\infty dk\, e^{ikt}\sqrt{\frac{ik}{\kappa}}\cdot K_1\left(\sqrt{\frac{ik}{\kappa}}a\right) I_0\left(\sqrt{\frac{ik}{\kappa}}\rho\right) \quad \ldots\ a>\rho, \quad (42)$$

$$v_0 = \frac{qa}{\pi K}\int_0^\infty dk\, e^{ikt}\sqrt{\frac{ik}{\kappa}}\cdot K_0\left(\sqrt{\frac{ik}{\kappa}}\rho\right) I_1\left(\sqrt{\frac{ik}{\kappa}}a\right) \quad \ldots\ \rho>a. \quad (42')$$

Replace (q/K) by 2θ in this, and we obtain a solution satisfying all the conditions fulfilled by the solution (41); that is,

$$\text{at } t=0, \quad (v_0=+\theta,\ v_i=-\theta)_{\rho=a}: \quad \text{and} \quad \left(\frac{\partial v_i}{\partial \rho}=\frac{\partial v_0}{\partial \rho}\right)_{\rho=a}. \quad \ldots \quad (43)$$

Verify that

$$(v_0-v_i)_{\rho=a} = \frac{2\theta}{\pi}\int_0^\infty dk\, e^{ikt}\sqrt{\frac{ik}{\kappa}}a\left\{K_0\left(\sqrt{\frac{ik}{\kappa}}a\right) I_1\left(\sqrt{\frac{ik}{\kappa}}a\right) + K_1\left(\sqrt{\frac{ik}{\kappa}}a\right) I_0\left(\sqrt{\frac{ik}{\kappa}}a\right)\right\} \quad (44)$$

$$= \frac{2\theta}{\pi}\int_0^\infty dk\, e^{ikt} = 2\theta \text{ at } t=0 \text{ (real part)} \quad \text{and} \quad = 0 \quad \text{for } t>0$$

by Fourier's fundamental integral. Note also that when ρ and a both become infinite, while the difference between them ($\rho-a$) remains finite, the solution becomes identical with (13) of the former paper. The peculiar nature of these solutions, especially with reference to the initial space distributions of temperature which they represent, is a matter requiring further careful examination ; but we shall leave it to another occasion.

We may treat the problem dealt with above from a different standpoint, by starting out from the solutions of

equation (28), represented by

$$v_i = -\Theta \cos n\theta \,.\, e^{ikt}\, \mathrm{I}_n\left(\sqrt{\frac{ik}{\kappa}}\,\rho\right)\Big/ \mathrm{I}_n\left(\sqrt{\frac{ik}{\kappa}}\,a\right), \qquad (45)$$

$$v_0 = \quad \Theta \cos n\theta \,.\, e^{ikt}\, \mathrm{K}_n\left(\sqrt{\frac{ik}{\kappa}}\,\rho\right)\Big/ \mathrm{K}_n\left(\sqrt{\frac{ik}{\kappa}}\,a\right). \qquad (45')$$

These obviously fulfil the condition that at the surface $\rho = a$ the temperature is given by $\mp\, \Theta \cos n\theta \,.\, e^{ikt}$, but they also require that the heat-flow from the surface $\rho = a$ on the outward side is not equal to the heat-flow to the surface on the inward side, since

$$\left.\begin{aligned} &\frac{\partial v_0}{\partial \rho_{\rho=a}} \\ &\quad = \Theta \cos n\theta\, e^{ikt} \sqrt{\frac{ik}{\kappa}} \,.\, \mathrm{K}'_n\left(\sqrt{\frac{ik}{\kappa}}\,a\right)\Big/ \mathrm{K}_n\left(\sqrt{\frac{ik}{\kappa}}\,a\right) \\ &-\frac{\partial v_i}{\partial \rho_{\rho=a}} \\ &\quad = \Theta \cos n\theta\, e^{ikt} \sqrt{\frac{ik}{\kappa}}\, \mathrm{I}'_n\left(\sqrt{\frac{ik}{\kappa}}\,a\right)\Big/ \mathrm{I}_n\left(\sqrt{\frac{ik}{\kappa}}\,a\right). \end{aligned}\right\} \qquad (46)$$

If we take the periodic heat supply from the surface $\rho = a$, represented by these terms respectively, and deduct the corresponding solutions as given by (31) from the solution (45), we obtain a new solution :

$$v_i = -\Theta \cos n\theta\, e^{ikt} \frac{\mathrm{I}_n\left(\sqrt{\frac{ik}{\kappa}}\,\rho\right)}{\mathrm{I}_n\left(\sqrt{\frac{ik}{\kappa}}\,a\right)} \left\{1 - \sqrt{\frac{ik}{\kappa}}\, a\, \mathrm{K}_n\left(\sqrt{\frac{ik}{\kappa}}\,a\right) \mathrm{I}'_n\left(\sqrt{\frac{ik}{\kappa}}\,a\right)\right\}, \qquad (47)$$

$$v_0 = \quad \Theta \cos n\theta\, e^{ikt} \frac{\mathrm{K}_n\left(\sqrt{\frac{ik}{\kappa}}\,\rho\right)}{\mathrm{K}_n\left(\sqrt{\frac{ik}{\kappa}}\,a\right)} \left\{1 + \sqrt{\frac{ik}{\kappa}}\, a\, \mathrm{K}'_n\left(\sqrt{\frac{ik}{\kappa}}\,a\right) \mathrm{I}_n\left(\sqrt{\frac{ik}{\kappa}}\,a\right)\right\}, \qquad (47')$$

which satisfies the condition of equality in the flow of hea

outwards and inwards from the surface $\rho=a$; that is,

$$\left(\frac{\partial v_0}{\partial \rho}-\frac{\partial v_i}{\partial \rho}\right)_{\rho=a}$$
$$=\Theta\cos n\theta\, e^{ikt}\sqrt{\frac{ik}{\kappa}}\left[\frac{\mathrm{K'}_n}{\mathrm{K}_n}+\frac{\mathrm{I'}_n}{\mathrm{I}_n}\right.$$
$$\left.+\sqrt{\frac{ik}{\kappa}}a\left\{\frac{\mathrm{K'}_n{}^2\mathrm{I}_n{}^2-\mathrm{K}_n{}^2\mathrm{I'}_n{}^2}{\mathrm{K}_n\mathrm{I}_n}\right\}\right]=0. \quad (48)$$

Now proceed to the solution derived from this by an integration with respect to k, representing a temperature instantaneously generated at the surface $\rho=a$:—

$$v_i=\frac{\Theta a}{\pi}\cos n\theta\int_0^\infty dk\, e^{ikt}\sqrt{\frac{ik}{\kappa}}\,\mathrm{K'}_n\left(\sqrt{\frac{ik}{\kappa}}a\right)\mathrm{I}_n\left(\sqrt{\frac{ik}{\kappa}}\rho\right), \quad . \quad . \quad . \quad (49)$$

$$v_0=\frac{\Theta a}{\pi}\cos n\theta\int_0^\infty dk\, e^{ikt}\sqrt{\frac{ik}{\kappa}}\,\mathrm{K}_n\left(\sqrt{\frac{ik}{\kappa}}a\right)\mathrm{I'}_n\left(\sqrt{\frac{ik}{\kappa}}a\right), \quad . \quad . \quad . \quad (49')$$

and it will be seen that a solution exactly similar to (42) is obtained. The first terms of (47) and (47′) in this form of the solution, taken by themselves, evidently give after integration $\qquad -v=v_0=\Theta\cos n\theta$

at the surface $\rho=a$, and it follows that $(t>0)$

$$\int_0^\infty dk\, e_{ikt}\sqrt{\frac{ik}{\kappa}}\,\mathrm{K'}_n\left(\sqrt{\frac{ik}{\kappa}}a\right)\mathrm{I}_n\left(\sqrt{\frac{ik}{\kappa}}a\right)$$
$$=\int_0^\infty dk\, e^{ikt}\sqrt{\frac{ik}{\kappa}}\,\mathrm{K}_n\left(\sqrt{\frac{ik}{\kappa}}a\right)\mathrm{I'}_n\left(\sqrt{\frac{ik}{\kappa}}a\right). \quad (50)$$

A confirmation of this result by another method is desirable. The two equivalent solutions of the problem of finding the temperature due to the instantaneous generation of temperature $\Theta\cos n\theta$ at the surface $\rho=a$, derived by the methods indicated above, are given by

$$v=-\frac{\Theta a\cos n\theta}{2\kappa t^2}e^{-\frac{a^2+\rho^2}{4\kappa t}}\left\{a\,\mathrm{I}_n\left(\frac{a\rho}{2\kappa t}\right)-\rho\,\mathrm{I'}_n\left(\frac{a\rho}{2\kappa t}\right)\right\}, \quad . \quad (51)$$

$$v_i=\frac{2\Theta a\cos n\theta}{\pi}\int_0^\infty dk\, e^{ikt}\sqrt{\frac{ik}{\kappa}}\,\mathrm{K'}_n\left(\sqrt{\frac{ik}{\kappa}}a\right)\mathrm{I}_n\left(\sqrt{\frac{ik}{\kappa}}\rho\right), \quad . \quad . \quad . \quad (52)$$

$$v_0=\frac{2\Theta a\cos n\theta}{\pi}\int_0^\infty dk\, e^{ikt}\sqrt{\frac{ik}{\kappa}}\,\mathrm{K}_n\left(\sqrt{\frac{ik}{\kappa}}\rho\right)\mathrm{I'}_n\left(\sqrt{\frac{ik}{\kappa}}a\right),$$

respectively. $\quad . \quad . \quad . \quad (52')$

The solutions which we have obtained above may be regarded as fundamental solutions, in the sense that they form the basis from which we derive the solution of any problem for which the initial conditions include a given heat distribution throughout space, or a given temperature condition at particular surfaces. For example, starting from equation (27) we may obtain by integration the effect of a uniform instantaneous supply of heat q per unit volume of a cylinder of radius $\rho=a$. By replacing q by qda' and integrating with respect to a', we obtain

$$v=\frac{q}{2\mathrm{K}t}\int_0^a da'a'e^{-\frac{\rho^2+a'^2}{4\kappa t}}\mathrm{I}_0\left(\frac{a'\rho}{2\kappa t}\right). \quad . \quad . \quad (53)$$

In this connexion it is very important to investigate the special solutions usually employed in building up solutions for cylindrical heat conduction problems, and, in the first instance, to establish these special solutions from the fundamental wave-trains employed in the present paper. Consider the case of a heat distribution $q\cos n\theta\,\mathrm{J}_n(k'a)$ per unit volume, instantaneously generated throughout space. We have, again, alternative methods of proceeding. In the first method we start from the solution representing the effect of an instantaneous surface distribution $q\cos n\theta$ per unit area at the surface $\rho=a$, given in equation (37) above. Replace q by $q\mathrm{J}_n(k'a)$, and integrate with respect to a from 0 to ∞. This gives the solution which we require in the form :

$$v=\frac{q\cos n\theta}{2\mathrm{K}t}e^{-\frac{\rho^2}{4\kappa t}}\int_0^\infty da\,a\,e^{-\frac{a^2}{4\kappa t}}\mathrm{J}_n(k'a)\,\mathrm{I}_n\left(\frac{a\rho}{2\kappa t}\right). \quad (54)$$

By means of an evaluation given in Watson's 'Theory of Bessel Functions,' p. 395, this solution takes the form :

$$v=\frac{q\cos n\theta}{2\mathrm{K}t}e^{-\frac{\rho^2}{4\kappa t}}.2\kappa t\,e^{-k'^2\kappa t+\frac{\rho^2}{4\kappa t}}\mathrm{I}_n\left(\frac{ik'\rho}{2\kappa t}.2\kappa t\right). \quad (55)$$

$$=q\cos n\theta\,.\,\frac{\kappa}{\mathrm{K}}e^{-k'^2\kappa t}\mathrm{J}_n(k'\rho), \quad . \quad . \quad . \quad . \quad . \quad . \quad (56)$$

which is the well-known form of the solution of this problem. Now take, instead of (37), the equivalent solution in terms of K_n and I_n ; namely,

$$v_i=\frac{qa\cos n\theta}{\pi\mathrm{K}}\int_0^\infty dk\,e^{ik\kappa t}\mathrm{K}_n\left(\sqrt{\frac{ik}{\kappa}}a\right)\mathrm{I}_n\left(\sqrt{\frac{ik}{\kappa}}\rho\right). \quad . \quad . \quad \rho<a, \quad . \quad . \quad . \quad (57)$$

$$v_0 = \frac{qa\cos n\theta}{\pi \mathrm{K}} \int_0^\infty dk\, e^{ikt}\, \mathrm{K}_n\left(\sqrt{\frac{ik}{\kappa}}\rho\right) \mathrm{I}_n\left(\sqrt{\frac{ik}{\kappa}}a\right) \quad \rho > a. \quad (57')$$

To find the effect at (ρ, θ) of the heat distribution specified above, we repeat the process just employed. Replace q by $q\, da\, \mathrm{J}_n(k'a)$ and integrate from 0 to ∞. For values of a less than ρ we must use v_0 in this integration, and for values of a greater than ρ we must use v_i in the integration. Hence the solution equivalent to (54) is

$$v = \frac{q\cos n\theta}{\pi \mathrm{K}} \int_0^\infty dk\, e^{ikt}\, \mathrm{F}(k, a),$$

where

$$\mathrm{F}(k, a) = \mathrm{K}_n\left(\sqrt{\frac{ik}{\kappa}}\rho\right) \int_0^\rho da\, a\, \mathrm{I}_n\left(\sqrt{\frac{ik}{\kappa}}a\right) \mathrm{J}_n(k'a) + \mathrm{I}_n\left(\sqrt{\frac{ik}{\kappa}}\rho\right) \int_\rho^\infty da\, a\, \mathrm{K}_n\left(\sqrt{\frac{ik}{\kappa}}a\right) \mathrm{J}_n(k'a). \quad (58)$$

Each of the above integrations with respect to a can be performed by means of Lommel's method of integration (Gray, Mathews and MacRobert, 'Bessel Functions,' p. 69). By this method we find that

$$\left(k'^2 + \frac{ik}{\kappa}\right) \int_\rho^\infty da\, a\, \mathrm{J}_n(k'a)\, \mathrm{K}_n\left(\sqrt{\frac{ik}{\kappa}}a\right) = -\rho \left\{ \sqrt{\frac{ik}{\kappa}}\, \mathrm{J}_n(k'\rho)\, \mathrm{K}'_n\left(\sqrt{\frac{ik}{\kappa}}\rho\right) - k'\mathrm{J}'_n(k'\rho)\, \mathrm{K}_n\left(\sqrt{\frac{ik}{\kappa}}\rho\right) \right\}, \quad (59)$$

$$\left(k'^2 + \frac{ik}{\kappa}\right) \int_0^\rho da\, a\, \mathrm{J}_n(k'a)\, \mathrm{I}_n\left(\sqrt{\frac{ik}{\kappa}}a\right) = \rho \left\{ \sqrt{\frac{ik}{\kappa}}\, \mathrm{J}_n(k'\rho)\, \mathrm{I}'_n\left(\sqrt{\frac{ik}{\kappa}}\rho\right) - k'\mathrm{J}'_n(k'\rho)\, \mathrm{I}_n\left(\sqrt{\frac{ik}{\kappa}}\rho\right) \right\}, \quad (60)$$

and when we insert these results in the right-hand side of equation (58) we obtain

$$v = \frac{q\cos n\theta}{\pi \mathrm{K}} \mathrm{J}_n(k'\rho) \int_0^\infty dk\, \frac{e^{ikt}}{k'^2 + \frac{ik}{\kappa}} f\left(\sqrt{\frac{ik}{\kappa}}\rho\right), \quad (61)$$

where

$$f(z) = +z\{\mathrm{K}_n(z)\,\mathrm{I}'_n(z) - \mathrm{I}_n(z)\,\mathrm{K}'_n(z)\} = 1. \quad . \quad . \quad (62)$$

Hence

$$v = \frac{q\cos n\theta}{\pi \mathrm{K}} \mathrm{J}_n(k'\rho) \int_0^\infty dk\, \frac{e^{ika}}{k'^2 + \frac{ik}{\kappa}}, \quad . \quad . \quad (63)$$

in which form the solution depends upon a well-known integral. If we retain the real part only of the expression on the right-hand side, the result arrived at by integration is

$$v = q\cos n\theta \cdot \frac{\kappa}{\mathrm{K}} \mathrm{J}_n(k'\rho)\, e^{-k'^2\kappa t}, \quad . \quad . \quad . \quad (64)$$

as before. It is worthy of note, in connexion with this group of special solutions, that the initial heat distributions which they represent are distributions for which the total quantity of heat is zero. It is evident also from the above that we can deal with any arbitrary initial heat distribution by two distinct methods, and that the investigation of this general case should lead to the establishment of certain mathematical theorems.

Having obtained the above important confirmation of the method of solution by means of wave-trains, we can now employ this method to determine solutions in more general problems. One of the most important fundamental problems is that of determining the Green's Function in various special cases. As an example, we may consider the effect of an instantaneous line source emitting q units of heat per unit of length at (a', θ'), the cylindrical surface $\rho = a$ being kept at zero temperature, $(a > a')$. We may start from the solution representing a periodic line source $q\,e^{ikt}$ situated at (a', θ'),

$$v = \frac{q}{2\pi \mathrm{K}} e^{ikt}\, \mathrm{K}_0\left(\sqrt{\frac{ik}{\kappa}}\, r\right); \quad r^2 = \rho^2 + a'^2 - 2\rho a\cos(\theta - \theta') \quad . \quad . \quad . \quad (65)$$

$$= \frac{q}{2\pi \mathrm{K}} e^{ikt} \sum_{-\infty}^{+\infty} \mathrm{K}_m\left(\sqrt{\frac{ik}{\kappa}}\,\rho\right) \mathrm{I}_m\left(\sqrt{\frac{ik}{\kappa}}\,a'\right) \cos m(\theta - \theta'); \quad \rho > a'. \quad (66)$$

Each term of this expression indicates a periodic temperature at the surface $\rho = a$; and to reduce the temperature at a to zero, we have, therefore, to add a negative wave-train corresponding to each positive component in the above solution.

From equation (45) it appears that the solution determined by the above temperature condition at $\rho = a$ is

$$v = \frac{q}{2\pi \mathrm{K}} e^{ikt} \sum_{-\infty}^{+\infty} \mathrm{K}_m\left(\sqrt{\frac{ik}{\kappa}}\, a\right) \mathrm{I}_m\left(\sqrt{\frac{ik}{\kappa}}\, a'\right) \cos m(\theta - \theta') \cdot \frac{\mathrm{I}_m\left(\sqrt{\frac{ik}{\kappa}}\, \rho\right)}{\mathrm{I}_m\left(\sqrt{\frac{ik}{\kappa}}\, a\right)}. \quad (67)$$

To fulfil the condition stated at the surface $\rho = a$, this has to be deducted from the solution representing a line source at (a', θ'). Thus the periodic solution which represents a line source at (a', θ'), the boundary $\rho = a$ being kept at zero temperature, is

$$v = \frac{q}{2\pi \mathrm{K}} e^{ikt} \sum_{-\infty}^{+\infty} \cos m(\theta - \theta')\, \mathrm{F}_m(\rho, a, a'), \quad . \quad (68)$$

where

$$\mathrm{F}_m = \frac{\mathrm{I}_m\left(\sqrt{\frac{ik}{\kappa}}\, a'\right)}{\mathrm{I}_m\left(\sqrt{\frac{ik}{\kappa}}\, a\right)} \left\{ \mathrm{K}_m\left(\sqrt{\frac{ik}{\kappa}}\, \rho\right) \mathrm{I}_m\left(\sqrt{\frac{ik}{\kappa}}\, a\right) - \mathrm{I}_m\left(\sqrt{\frac{ik}{\kappa}}\, \rho\right) \mathrm{K}_m\left(\sqrt{\frac{ik}{\kappa}}\, a\right) \right\}, \quad (69)$$

and the corresponding solution, which represents an instantaneous line source q at (a', θ'), the boundary $\rho = a$ being kept at zero temperature, is

$$v = \frac{q}{2\pi^2 \mathrm{K}} \sum_{-\infty}^{+\infty} \cos m(\theta - \theta') \int_0^{\infty} dk\, e^{ikt}\, \mathrm{F}_m \quad . \quad . \quad (70)$$

By means of the substitutions

$$\sqrt{\frac{ik}{\kappa}} = i\lambda, \qquad ik = -\kappa\lambda^2,$$

this transforms into

$$v = \frac{q\kappa}{\pi^2 \mathrm{K} i} \sum_{-\infty}^{+\infty} \cos m(\theta - \theta') \int d\lambda\, \lambda\, e^{-\lambda^2 \kappa t} \frac{\mathrm{J}_m(\lambda a')}{\mathrm{J}_m(\lambda a)} \{ \mathrm{G}_m(\lambda\rho)\, \mathrm{J}_m(\lambda a) - \mathrm{J}_m(\lambda\rho)\, \mathrm{G}_m(\lambda a) \}. \quad (71)$$

If the expression under the integral sign be integrated round a contour consisting of the two lines inclined to the

real axis of λ at angle $\frac{\pi}{4}$ on each side and the circular arcs of infinite radius connecting them, we find by the theory of residues that

$$v = \frac{q\kappa}{\pi \mathrm{K} a} \sum_{-\infty}^{+\infty} \cos m(\theta - \theta') \sum_{s=1}^{s=\infty} \lambda_s e^{-\lambda_s^2 \kappa t} \frac{\mathrm{J}_m(\lambda a') \mathrm{G}_m(\lambda a)\, \mathrm{J}_m(\lambda \rho)}{\mathrm{J}'_m(\lambda a')}, \quad . \quad . \quad . \quad (72)$$

the summation with respect to s extending over the roots of $\mathrm{J}_m(\lambda a) = 0$. Further, since

$$\mathrm{G}_m(\lambda\rho)\, \mathrm{J}'_m(\lambda\rho) - \mathrm{J}_m(\lambda\rho)\, \mathrm{G}'_m(\lambda\rho) = \frac{1}{\lambda\rho}, \quad . \quad (73)$$

at each root of $\mathrm{J}_m(\lambda\rho) = 0$ we have

$$\mathrm{G}_m(\lambda_s a) = \frac{1}{\lambda_s a\, \mathrm{J}'_m(\lambda_s a)} \quad . \quad . \quad . \quad . \quad (74)$$

and

$$v = \frac{q\kappa}{\pi \mathrm{K} a^2} \sum_{m=-\infty}^{m=+\infty} \cos m(\theta - \theta') \sum_{s=1}^{s=\infty} e^{-\kappa \lambda_s^2 t} \frac{\mathrm{J}_m(\lambda_s a')\, \mathrm{J}_m(\lambda_s \rho)}{[\mathrm{J}'_m(\lambda_s a)]^2}, \quad (75)$$

which is identical with the result given in Carslaw, ' Fourier Series and Integrals,' p. 394.

The problem of determining the Green's Function in the corresponding case, where radiation takes place at the outer boundary $\rho = a$, can be dealt with in an exactly similar manner. We start again from (66). Each wave-train represented in this expression suffers reflexion at the surface $\rho = a$, under the condition

$$-\mathrm{K} \frac{\partial v}{\partial \rho} = hv,$$

and the reflected waves are all of the type

$$\mathrm{A}_m \cos m(\theta - \theta')\, e^{ikt}\, \mathrm{I}_m\left(\sqrt{\frac{ik}{\kappa}}\rho\right).$$

Hence the required solution, obtained by adding the reflected waves, may be written in the form :

$$v = \frac{q}{2\pi^2 \mathrm{K}} \sum_{-\infty}^{+\infty} \cos m(\theta - \theta') \int_0^\infty dk\, e^{ikt}$$
$$\left[\mathrm{K}_m\left(\sqrt{\frac{ik}{\kappa}}\rho\right) \mathrm{I}_m\left(\sqrt{\frac{ik}{\kappa}}a'\right) + \mathrm{A}_m \mathrm{I}_m\left(\sqrt{\frac{ik}{\kappa}}\rho\right)\right], \quad (76)$$

where A_m is a complex constant (to include both types of

inward travelling wave-trains) determined by the condition stated above. The value for A_m is

$$A_m = -\frac{K\sqrt{\frac{ik}{\kappa}}\,K'_m\left(\sqrt{\frac{ik}{\kappa}}a\right)I_m\left(\sqrt{\frac{ik}{\kappa}}a'\right) + h\,K_m\left(\sqrt{\frac{ik}{\kappa}}a\right)I_m\left(\sqrt{\frac{ik}{\kappa}}a'\right)}{K\sqrt{\frac{ik}{\kappa}}\,I'_m\left(\sqrt{\frac{ik}{\kappa}}a\right)+h\,I_m\left(\sqrt{\frac{ik}{\kappa}}a\right)}, \quad (77)$$

and the solution corresponding to an instantaneous line source at (a', θ'), the boundary condition being

$$-K\frac{\partial v}{\partial \rho} = hv \quad \text{at} \quad \rho = a,$$

is accordingly

$$v = \frac{q}{2\pi^2 K}\sum_{-\infty}^{+\infty}\cos m(\theta-\theta')\int_0^\infty dk\, e^{ikt} f(k,\rho), \quad . \quad (78)$$

where $f(k, \rho)$

$$= \frac{I_m\left(\sqrt{\frac{ik}{\kappa}}a'\right)}{I_m\sqrt{\frac{ik}{\kappa}}\,I'_m\left(\sqrt{\frac{ik}{\kappa}}a\right)+h\,I_m\left(\sqrt{\frac{ik}{\kappa}}a\right)}$$

$$\left[K_m\left(\sqrt{\frac{ik}{\kappa}}\rho\right)\left\{K\sqrt{\frac{ik}{\kappa}}\,I'_m\left(\sqrt{\frac{ik}{\kappa}}a\right)+h\,I_m\left(\sqrt{\frac{ik}{\kappa}}a\right)\right\}\right.$$

$$\left.-I_m\left(\sqrt{\frac{ik}{\kappa}}\rho\right)\left\{K\sqrt{\frac{ik}{\kappa}}\,K'_m\left(\sqrt{\frac{ik}{\kappa}}a\right)+h\,K_m\left(\sqrt{\frac{ik}{\kappa}}a\right)\right\}\right]. \quad . \quad . \quad . \quad (79)$$

By the substitution $\sqrt{\frac{ik}{\kappa}} = i\lambda$, employed in the former problem, the evaluations required can be obtained by means of the integrand

$$\lambda e^{-\kappa\lambda^2 t}\,\frac{J_m(\lambda a')[G_m(\lambda\rho)\{K\lambda J'_m(\lambda a)+h J_m(\lambda a)\} - J_m(\lambda\rho)\{K\lambda G'_m(\lambda a)+h G_m(\lambda a)\}]}{K\lambda J'_m(\lambda a)+h J_m(\lambda a)}. \quad (80)$$

When this expression is integrated round the contour employed in the preceding problem, a result similar to (72)

is obtained; namely,

$$v = \frac{q\kappa}{\pi K} \sum_{-\infty}^{+\infty} \cos m(\theta - \theta') \sum_{s=1}^{s=\infty} \lambda_s e^{-\lambda_s^2 \kappa t} \frac{J_m(\lambda_s a') J_m(\lambda_s \rho) \{K\lambda_s G'_m(\lambda_s a) + h G_m(\lambda_s a)\}}{\frac{d}{d\lambda}\{K\lambda_s J'_m(\lambda a) + h J_m(\lambda a)\}}, \quad (81)$$

where the summation with respect to s extends over the roots of

$$K\lambda J'_m(\lambda a) + h J_m(\lambda a) = 0. \quad . \quad . \quad . \quad (82)$$

Since equation (73) holds in addition to (82), it follows that at each root of (82) we have

$$K\lambda G'_m(\lambda a) + h G_m(\lambda a) = -\frac{K\lambda}{\lambda a J_m(\lambda a)}, \quad . \quad . \quad (83)$$

also

$$\begin{aligned} \frac{d}{d\lambda}\{K\lambda J'_m(\lambda a) + h J_m(\lambda a)\} &= aK\lambda J''_m(\lambda a) + K J'_m(\lambda a) + ha J'_m(\lambda a) \\ &= aK\lambda \left\{ -J_m(\lambda a) + \frac{m^2}{\lambda^2 a^2} J_m(\lambda a) \right\} + ha J'_m(\lambda a) \\ &= -J_m(\lambda a) \left\{ K\lambda \left(1 - \frac{m^2}{\lambda^2 a^2}\right) + \frac{h^2}{K\lambda} \right\} a. \quad . \quad (84) \end{aligned}$$

By means of (82) and (84), our solution given by (81) becomes

$$v = \frac{q\kappa}{\pi K a^2} \sum_{-\infty}^{+\infty} \cos m(\theta - \theta') \sum_{s=1}^{s=\infty} \lambda_s^2 e^{-\kappa \lambda_s^2 t} \frac{J_m(\lambda a') J_m(\lambda_s \rho)}{\left(\frac{h^2}{K^2} - \frac{m^2}{a^2} + \lambda_s^2\right) [J_m(\lambda_s a)]^2}, \quad (85)$$

which is also in agreement with Carslaw, 'Fourier Series and Integrals,' p. 396.

The application of the methods illustrated above to problems involving continuous heat supply, and to problems involving change of medium, would lead to further useful results.

My thanks are due to James F. Shearer, M.A., B.Sc., of this University for his friendly interest and assistance in the work.

LXXV. *The Corona Discharge in Helium and Neon.*

By L. G. H. Huxley, *B.A., New College, Oxford* *.

1. THE theory of corona discharges in gases is of particular interest, as some of the properties of positive ions and of electrons may be deduced from measurements of the potentials required to start or maintain a current between a wire and a cylinder.

It was considered desirable to investigate this type of discharge in helium and neon, especially with a view to determining the velocities of the positive ions, and their effects in ionizing the gas.

In order to determine the dimensions of an apparatus to be enclosed in a quartz cylinder, I first made a preliminary investigation with an apparatus in a brass cylinder and found that a quartz cylinder of about 6 centimetres in diameter would be sufficiently large to enable me to make accurate measurements of the velocities of positive ions, and to determine the general properties of these discharges.

It is of great advantage to have the electrodes in a transparent envelope to see whether the corona is evenly distributed along the wire, and when a quartz tube is used the whole apparatus may easily be heated to a high temperature in order to expel occluded gases from the electrodes.

2. The apparatus finally adopted is shown in fig. 1. It

Fig. 1.

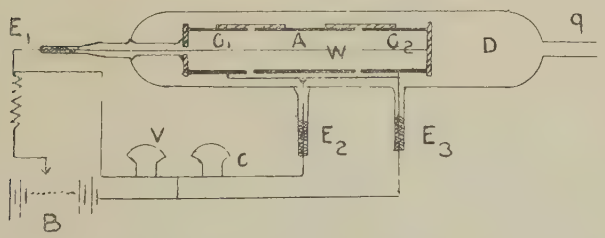

consisted of a long nickel cylinder 4·6 cm. in diameter, in three sections, the middle section A, which was 12 cm. long, being insulated by gaps of 2 mm. from the two end sections G_1 and G_2, which were each 9 cm. long.

* Communicated by Prof. J. S. Townsend, F.R.S.

The end sections acted as guard-rings, so that in the space between the wire and the central section A the electric force was along the radius.

The two sections G_1 and G_2 were fixed rigidly to the central section A by means of six quartz rods clamped by nickel cleets to the outer surface of the sections, so that the axes of the three sections coincided. Two of these rods are shown in the figure.

The two ends G_1 and G_2 were connected by a wire running through a thin quartz tube. A straight length of nickel wire 1·65 mm. in diameter was fixed along the axis of the nickel cylinder by pieces of quartz clamped to the ends of the sections G_1 and G_2. The free end of the wire at G_2 was screened from the discharge by the quartz support.

The quartz envelope was a cylinder of transparent silica 6·7 cm. diameter and 42 cm. long, thus leaving a space D about 12 cm. long near the open end of the tube in which to form an electrodeless discharge.

The nickel electrodes were placed in the quartz cylinder with the section G_1 near the closed end, and the three connectors (E_1, E_2, and E_3) to the wire W_1 the central section A_1 and the two ends G_1 and G_2 were brought through quartz tubes and made air-tight with lead seals. The apparatus was connected to the pump and the charcoal tubes used for purifying the gas through the quartz tube q, which was ground to fit a glass tube with a tap, T_1 (fig. 2). Another apparatus was also made of exactly the same dimensions with the exception of the central wire W, which was 2 mm. in diameter instead of 1·65.

The quartz work involving the sealing of the connectors E into the side tubes was carefully performed by the Mullard Radio Valve Co., and there was no trace of a leak in any of the quartz joints.

3. The current between the wire W and the central section A of the nickel tube was measured by a sensitive low resistance galvanometer C (fig. 1). The potential of the wire was adjusted by means of a battery of small accumulators, and the potential difference between the wire and the cylinder was given by the voltmeter V. The end sections G_1 and G_2 were connected through E_3 to the wire joining C and V.

4. The gas was admitted to the cylinders through the tubes G_1 and G_2 (fig 2). The ground-glass joint was made air-tight with an elastic cement, and the taps were lubricated with grease. The contamination of the gas due to the

cement and the grease was so small that in the course of twenty-four hours there was no appreciable effect due to this cause, either in the spectrum of an electrodeless discharge in D or in the conductivity of the gas between the wire and the cylinder.

When the gas had remained in the apparatus for two or three days a small effect of impurity was noticeable, which became more marked when the quartz was heated. To remove these impurities the quartz was heated to a high temperature while a discharge was passed between the electrodes, and as the gas was pumped out the impurity

Fig. 2.

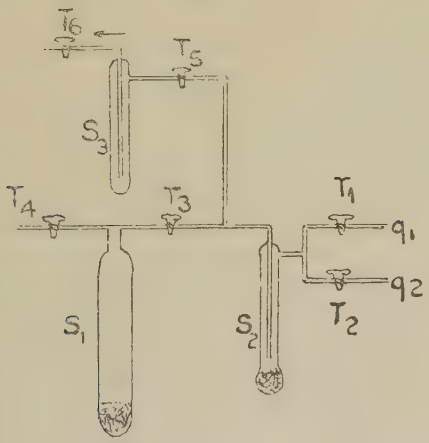

was carried with it*. This method of treating the electrodes was used by Dubois in his researches on sparking potentials, and enabled him to obtain very consistent results with diatomic gases †. When the apparatus had cooled and a fresh supply of pure gas was admitted, no impurity was observable in the spectrum of the electrodeless high frequency discharge in D, and the potentials required to maintain currents between the wire W and the cylinder A were at the same definite values, always obtained when the

* It is assumed by some experimenters that impurities may be completely removed from a gas in a vessel with electrodes, by diffusion into a side tube containing charcoal cooled with liquid air. This method is very slow, and it has been found that impurities are not removed for many hours, and in some cases for days.

† E. Dubois, *Ann. de Phys.* (9) vol. xx. Sept. & Oct. (1923).

gas was perfectly pure. Several precautions were taken to avoid impurities from other sources.

Before sealing the electrodes into the quartz tubes, the nickel apparatus was washed with carbon tetrachloride in order to remove grease due to handling. Also after the apparatus was connected to the pumps it was heated in an atmosphere of hydrogen to remove any oxide which may have formed on the nickel while the quartz was heated, during the sealing of the connectors E into the side tubes.

Two mercury vapour traps S_3 and S_2 cooled with liquid air were used between the taps T_1 and T_2 and the mercury pump, as in the preliminary experiments with the brass cylinder it was found very difficult to remove all traces of mercury. From time to time during the course of the experiments the mercury trap S_2 was heated while S_3 was cooled, in order to get rid of mercury and other impurities from the tubing near the apparatus.

In the quartz apparatus there was never any trace of mercury in the spectrum of the electrodeless discharge.

This method of avoiding any effects of impurities was found in this and other researches to be very effective, and constant results were obtained which could be easily repeated.

The gas from the apparatus was restored to the containing flask through the tube S_3 and it was also admitted to the pressure gauge through S_3. In all cases the pressure in the gauge and the pump was reduced below the pressure in the apparatus and in the tube S_2, before the taps T_5 and T_6 were opened. Thus the gas always flowed in the direction of the arrow through the tube S_3 (which was cooled with liquid air), so that no mercury vapour was carried from the pump or the gauge into the apparatus.

The gas was kept in the large tube S_1 containing charcoal which was cooled by liquid air, for about sixteen hours, before being admitted into the apparatus. All impurities except hydrogen were thus completely removed. In order to get rid of any hydrogen the gas was brought from the containing flask into the charcoal tube S_1 through a quartz tube containing copper oxide, which was heated by a coil of wire to the temperature required to convert hydrogen into water vapour. The gas was kept in the copper oxide tube for about ten minutes, and then admitted to the charcoal tube S_1 through the tap T_4. As the copper oxide tube was of comparatively small volume the operation was repeated several times in order to collect a sufficient quantity of gas in the charcoal tube.

The tube S_2, through which the pure gas was passed from S_1 to the apparatus, also contained charcoal cooled with liquid air. By these means perfectly constant results were obtained. The experiments on the currents between wires and cylinders were frequently repeated, using a fresh supply of gas each time, and the different observations at each pressure agreed within one or two per cent.

5. Experiments on corona discharges give results that determine two of the properties of positive ions in gases. They give a means of deciding as to whether electrons set free by positive ions arriving at the negative electrode are of importance compared with electrons derived from other processes. They also give a means of finding the velocities of the positive ions in the direction of the electric force for those cases in which the ratio of the electric force, X, to the pressure, p, is large.

The conclusions which may be drawn from the determinations of the potentials required to start the discharges may be considered first.

The generally accepted (S. Whitehead, 'Dielectric Phenomena, Electrical Discharge in Gases,' and W. O. Shumann 'Electrische Durchbruckfeldstarke von Gasen') theory is that given by Townsend. In this theory it is assumed that both electrons and positive ions generate others by collision with molecules of the gas, and that these two processes are predominant when the pressure of the gas is greater than that corresponding to the minimum sparking potential.

This theory gives a satisfactory explanation of the discharges between parallel plate electrodes and the corona discharges and shows that they are produced by the same processes of ionization. The results of experiments on discharges between concentric cylinders in diatomic gases were used to show that the effect of positive ions in setting free electrons from the negative electrode is negligible at the larger pressures. This conclusion may be extended to the properties of monatomic gases by considering the curves for the positive and negative discharges obtained tor helium and neon.

The potentials required to start the discharges in pure helium for the wire of 1·65 mm. diameter are given by the curves of fig. 3 *, where the ordinates represent the

* It was necessary at one stage in the experiments to open the cylinder with the wire 1·65 mm. diameter and to replace the wire by another of the same diameter. Points given by both wires are shown in the curves of fig. 3, those marked with arrows corresponding to the first wire. It is evident that both wires give points in good agreement.

Fig. 3.

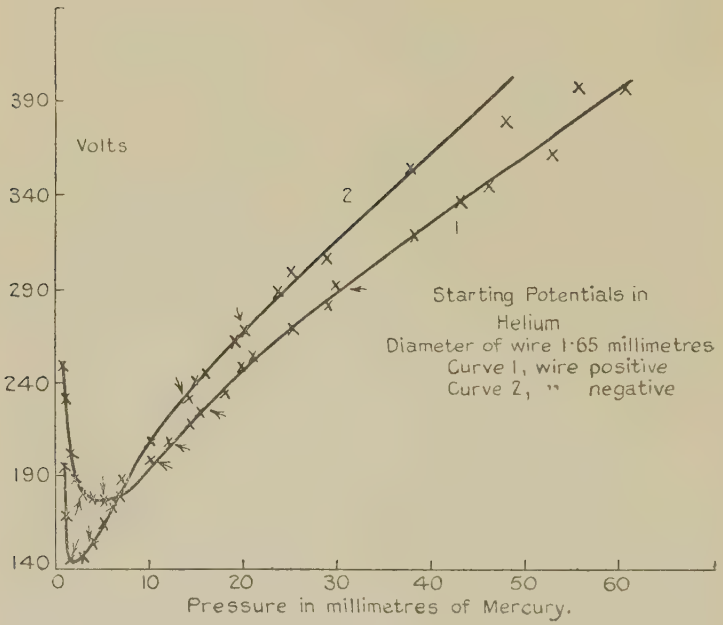
390
340
290
240
190
140
Volts
2
1
Starting Potentials in
Helium
Diameter of wire 1·65 millimetres
Curve 1, wire positive
Curve 2, " negative
0
10
20
30
40
50
60
Pressure in millimetres of Mercury.

Fig. 4.

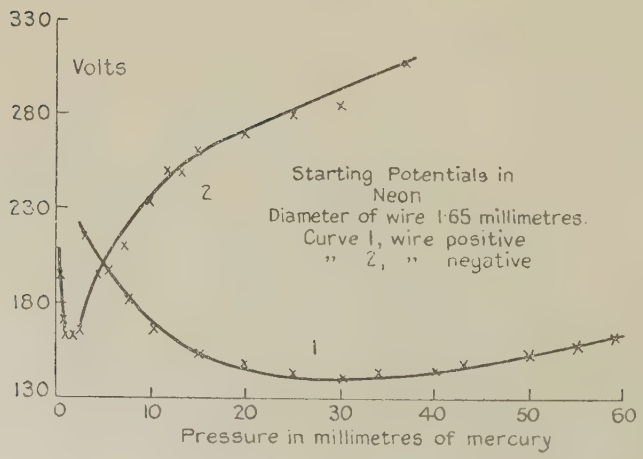
330
280
230
180
130
Volts
2
1
Starting Potentials in
Neon
Diameter of wire 1·65 millimetres.
Curve 1, wire positive
" 2, " negative
0
10
20
30
40
50
60
Pressure in millimetres of mercury

potential difference between the wire and cylinder in volts, and the abscissæ the pressure in millimetres of mercury.

Curve 1 gives the potentials with the wire positive and curve 2 with the wire negative. In fig. 4 the corresponding curves are given for pure neon. It can be seen that the curves for the discharges with the wire positive and those for the wire negative cross; at the higher pressures the positive discharge is obtained with a smaller potential than the negative.

This is of theoretical importance in determining the method by which positive ions produce new ions. By an extension of Townsend's continuity theorem (Townsend, 'Electricity in Gases,' p. 428), it may be shown that if the discharge were maintained by the action of electrons in ionizing the molecules of the gas by collision, and of the positive ions in liberating electrons from the negative electrode, the following condition must be satisfied :—

$$e^{\int_0^S \alpha\, dx} - \frac{1}{\gamma} = 1, \quad . \quad . \quad . \quad . \quad . \quad . \quad (1)$$

where α is the average number of molecules ionized by an electron in moving 1 cm. in the direction of the electric force γn the number of electrons set free from the cathode by a number n of positive ions impinging on it (γ may be supposed to depend on the velocity of impact), S the distance in centimetres between the electrodes, and x the distance along the path of the discharge measured in centimetres from the negative electrode.

This expression may be applied to the case in which the electrodes are concentric cylinders of the type under consideration. The value of the integral $\int_0^S \alpha\, dx$ is approximately the same when the integration is taken from the wire to the cylinder as when taken from the cylinder to the wire, but may be slightly greater in the former case. Thus when the field is reversed this term is practically unchanged.

If γ were independent of the velocity of impact of the positive ions on the negative electrode, the positive and negative discharges should start with the same electromotive force between the wire and cylinder. If γ depended on the velocity of impact of the positive ions, it would be greater in the negative discharge than in the positive owing to the large value of the force near the wire compared with that

near the cylinder. The negative discharge would then be started with a smaller force than the positive.

These conclusions are contrary to the results obtained experimentally. The curves in figs. 3 and 4 show that at the larger pressures the positive discharge is obtained with smaller potentials than the negative. This occurs both in helium and in neon, but is more pronounced in the latter. In helium at a pressure of 30 mm. the positive discharge starts with a potential of 290 volts between the wire and the cylinder, and the negative with 320 volts. In neon at the same pressure the positive discharge is obtained with a potential of 140 volts, and the negative with 290 volts. In view of these results it is clear that the discharges cannot be explained on the hypothesis that the current is maintained by the ionization of the molecules of the gas by electrons combined with the liberation of electrons from the negative electrode by the action of positive ions.

6. It was found by leaving gas in the apparatus that the presence of an impurity produced considerable variations in its conductivity. The effect of impurity in helium is shown in fig. 5, where curves for the potentials required to start positive discharges with the wire 2 mm. in diameter for pure and impure helium are compared. Curve 1 is for pure and curve 2 is for impure helium.

At the higher pressures the potentials required to start the discharge are greater in the pure than in the impure gas, while at the lower pressures an impurity has the opposite effect. A similar effect was obtained for the negative discharges.

For positive discharges in neon the starting potentials were greater for the impure than the pure gas at all pressures, but in negative discharges the potentials were affected in a manner similar to those in helium.

When the potentials were the same as those given in curve 1 (fig. 5) the spectrum as shown by the electrodeless discharge was that of the pure gas, but when those corresponding to curve 2 (fig. 5) the spectrum indicated the presence of impurities.

The spectrum of the impurities formed a continuous background to the characteristic lines of the pure gas, both in helium and in neon.

7. It is a well-known property of the discharges between coaxial cylinders, that the force X_1 at the surface of the inner cylinder necessary to start the discharge is independent

of the diameter of the outer cylinder, provided the latter exceeds a certain value, depending on the pressure of the gas.

This indicates that the space in which the ions are generated does not extend beyond a certain distance c from the wire, and that ions are not generated by collision when the force is less than $\frac{V}{c \log A/a}$, where V is the potential difference between the electrodes and A and a the diameters of

Fig. 5.

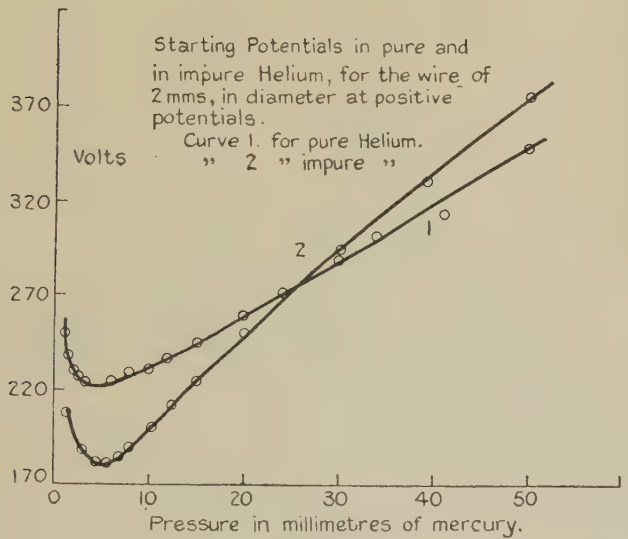

the outer and inner cylinders. In these circumstances it may be shown theoretically (Townsend, *loc. cit.* p. 367) that the quantity aX_1 depends only on the product $a \times p$, where a and X_1 have the meanings given them above and p is the pressure of the gas. This is confirmed experimentally by comparing the values of $a \times X_1$ for a given value of $a \times p$ for discharges obtained with wires of different diameters.

When aX_1 is expressed graphically as a function of ap, the points obtained from the experiments with the two wires lie on the same curve.

The curves 1 and 2 in fig. 6 are for helium, curve 1 for the positive and curve 2 for the negative discharge, the ordinates being the values of aX_1 and the abscissæ those of ap. The points given by the wire of 1 mm. diameter are

indicated by crosses, and those by the wire of 2 mm. diameter by circles.

The corresponding curves for neon are shown in fig. 7.

For the larger pressures, the value of aX_1 obtained with wire of 1·65 mm. diameter are the same as those obtained with the 2 mm. wire, and the points lie on the same curve. As the pressure is reduced the ionization extends further into the space between the electrodes and eventually touches the

Fig. 6.

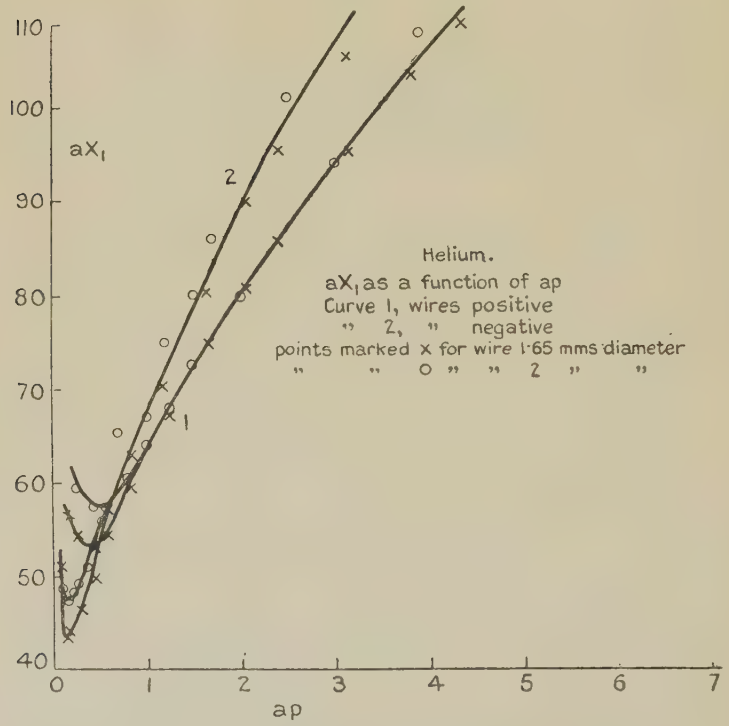

outer cylinder. For a given value of X/p the quantity c is proportional to a, and it follows that the ionization will have extended to the outer cylinder in the apparatus with the 2 mm. wire, at a higher pressure than in the apparatus with the wire 1·65 mm. diameter.

This is shown by the curves where the values of aX_1 are greater at the lower pressures for the larger wire than for the smaller, with the exception of curve 1 for the positive discharge in neon.

8. The velocities of the positive ions in the direction of the electric force were found from measurements of the currents which are maintained between a wire and a cylinder by potentials greater than those required to start the discharge.

The following equations given by Townsend (Phil. Mag., July 1914, p. 83) connect the currents with the potentials required to maintain them :—

$$\frac{(v-\mathrm{V})}{\mathrm{V}}\log \mathrm{A}/a=(1+\theta)^{\frac{1}{2}}-1+\log\frac{2}{(1+\theta)^{\frac{1}{2}}+1} \quad . \quad (2)$$

and

$$\theta=\frac{2\mathrm{I}\mathrm{A}^2}{wa^2\mathrm{Z}_1{}^2}, \quad . \quad . \quad . \quad . \quad . \quad . \quad . \quad . \quad (3)$$

Fig. 7.

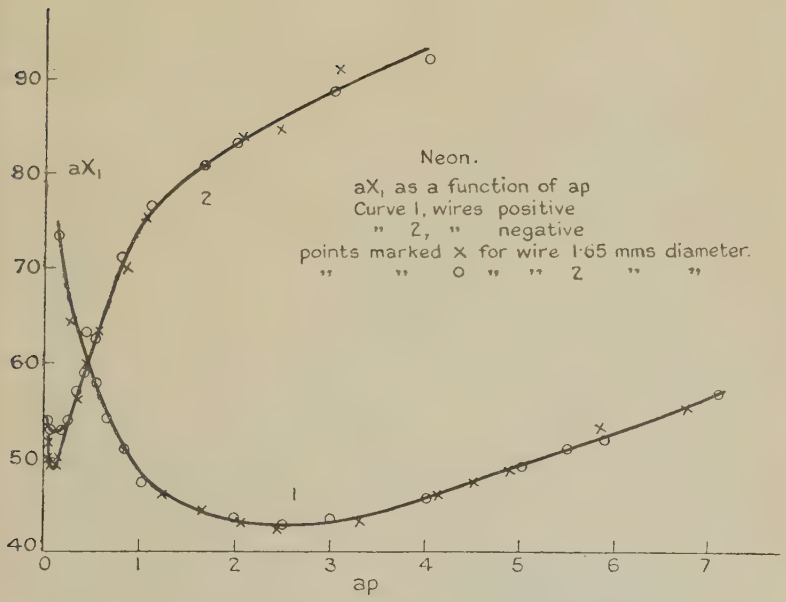

where I is the current per unit length of the wire, v the potential required to maintain the current, V the potential required to start the discharge, A and a the radii of the cylinder and the wire, wZ the velocity in centimetres per second of the ions in the direction of the electric force Z, Z_1 the force at the surface of the wire, the currents, potentials, and forces being expressed in electrostatic units.

The equations (2) and (3) serve to determine w from measurements v, V, and I.

Equation (2) is represented by the curve in fig. 8, where the ordinates are the values of θ and the abscissæ the values $(v-V)\log A/a$. Having determined the quantities v, V, and I, θ is obtained from the curve, and w from equation (2).

Fig. 8.

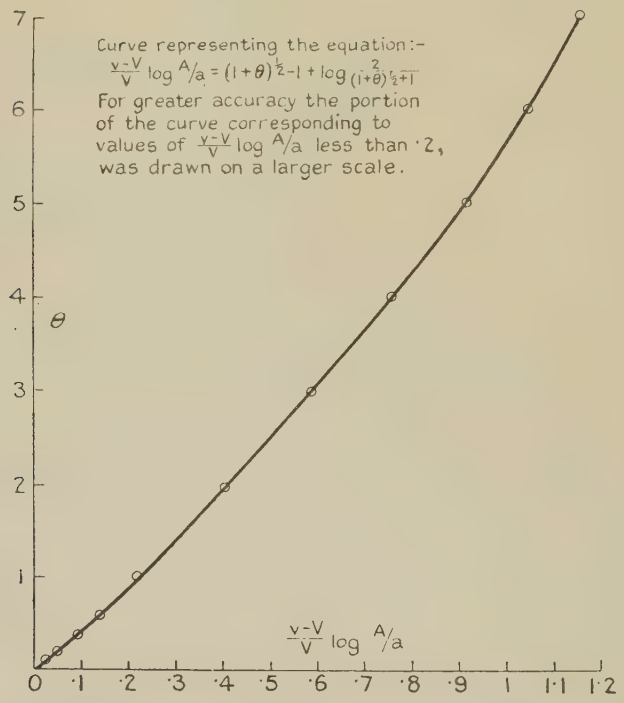
Curve representing the equation:-
$\frac{v-V}{V}\log\frac{A}{a}=(1+\theta)^{\frac{1}{2}}-1+\log\frac{2}{(1+\theta)^{\frac{1}{2}}+1}$
For greater accuracy the portion of the curve corresponding to values of $\frac{v-V}{V}\log\frac{A}{a}$ less than ·2, was drawn on a larger scale.
θ
$\frac{v-V}{V}\log\frac{A}{a}$
0 ·1 ·2 ·3 ·4 ·5 ·6 ·7 ·8 ·9 1 1·1 1·2
1 2 3 4 5 6 7

It was found impossible to measure the velocities of the negative ions in helium and neon by this method, owing to the formation of a cathode fall of potential at the wire, making the discharge disruptive.

In Table I. a series of potentials and currents with the corresponding values of w is given for helium at 57 mm. pressure, the diameter of the wire being 2 mm.

There is good agreement between the numbers found for w for different currents.

The mean values of w for pressures above 30 mm., obtained from experiments made with the two wires, are

given in Table II. The values of the product wp are also given.

Table I.

v.	$I \times 10^{-4}$.	$w \times 10^{-5}$.
1·33	0	—
1·37	5·3	1·04
1·39	10·1	1·09
1·41	13·9	1·06
1·43	19·3	1·14
1·47	25·4	1·03
1·49	29·2	1·04

Table II.

Wire 1·65 mm. diameter.			Wire 2 mm. diameter.		
Pressure p in mm. of mercury.	$w \times 10^{-5}$.	$wp \times 10^{-6}$.	Pressure p.	$w \times 10^{-5}$.	$wp \times 10^{-6}$.
93	1·74	6·9	67	·95	6·4
80	·85	6·8	57	1·1	6·3
77	·87	6·7	50	1·2	6·0
53	1·3	6·9	39	1·9	7·4
43	1·6	6·9	30	2·5	7·5
29	2·6	7·5			

Since wp is constant, for the larger pressures the velocity W of a positive ion in the direction of the electric force is given by the formula $W = bX/p$, where b is a constant equal to $2{\cdot}27 \times 10^{-4}$ when X is in volts per centimetre, and p in millimetres of mercury. This formula is applicable when X/p is less than 2·5. According to this formula the velocity of the positive ions in helium at 760 mm. pressure under a force of one volt per centimetre would be 30 centimetres per second, if the mass of the ion were the same at 760 mm. pressure as at 50 mm. pressure.

The velocities for larger values of X/p are obtained from the experiments with pressures less than about 30 mm.

At these pressures the values of w for a given pressure increase with the current and therefore also with the force.

The results obtained at pressures of 20 and 15 mm. are given in Table III. The diameter of the wire was 2 mm.

Table III.

Pressure 20 mm.				Pressure 15 mm.			
v.	$I\times10^{-2}$.	$w\times10^{-5}$.	$wp\times10^{-6}$.	v.	$I\times10^{-2}$.	$w\times10^{-5}$.	$wp\times10^{-6}$.
·833	0	...	...	·757	0	...	...
·853	8·35	3·3	6·6	·777	9·75	6·2	9·3
·880	28·6	3·9	7·8	·790	41·2	11·3	16·7
·897	36	5·1	10·2				

In these cases w increases with the electric force.

At pressures less than 12 mm. the current increases so rapidly with increase of voltage that the discharge becomes disruptive and w cannot be found.

Thus with the large values of X/p, W may be represented by the formula

$$W = bX/p, \text{ where } b \text{ increases with } X/p.$$

In neon there was no range of values of X/p for which b was constant, as in helium. Over the whole range of pressures b increased with X/p. This is illustrated in Table IV., where v, I, w are given for neon at 82 mm. pressure, with the wire of 1·65 mm. diameter.

Table IV.

v.	$I\times10^{-2}$.	$w\times10^{-6}$.
·615	0	...
·617	2·6	·45
·743	6·4	·56
·773	10·5	1·03
·807	10	1·4
·827	31·6	

The experimental results are most conveniently expressed by a curve giving the velocity W as a function of X/p.

In order to evaluate X/p it is necessary to consider the distribution of the field between the electrodes while a current is passing. It may be shown that the radial force Z at the distance r centimetres from the axis is given by the equation

$$Z^2 = \frac{a^2 Z_1^2}{r^2} + \frac{2I}{w}.$$

With the larger currents the value of Z is nearly constant for the larger values of r, and since the most effective part

Fig. 9.

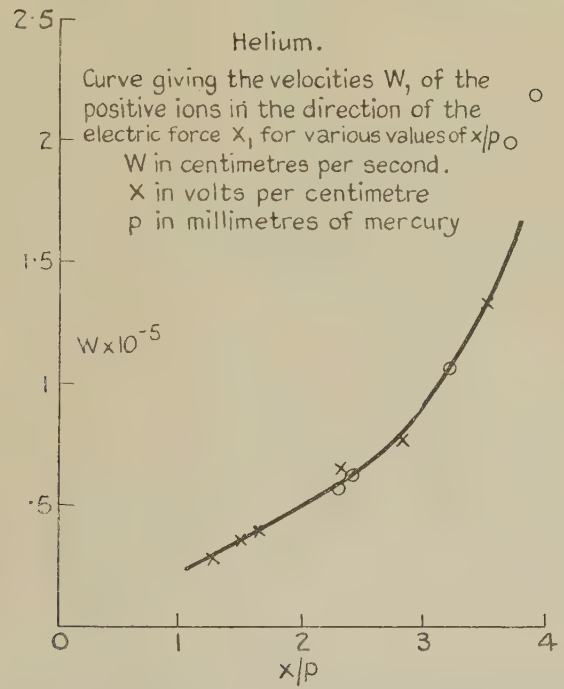

of the space charge is that near the surface of the outer cylinder, the mean value of Z over this space may be taken as the force at $r = 1{\cdot}5$ cm.

The curve in fig. 9 gives W as a function of X/p for helium, while that in fig. 10 is the corresponding curve for neon.

The ordinates have the values $W \times 10^{-5}$, and the abscissæ the values of X/p, X being in volts per centimetre, p in

millimetres of mercury, and W the velocity of the positive ions in centimetres per second. The points marked with a cross were given by the wire of 1·65 mm. diameter and those marked with a circle by the 2 mm. wire.

In both gases Wp/X increases with X/p.

The simplest theoretical formula for the velocity W of an ion in the direction of electric force is of the form

$$W = g\frac{e}{m}\frac{X}{p}\frac{l}{u},$$

where g is a constant, e and m the charge and mass of the ion, l its mean free path, and u its velocity of agitation.

Fig. 10.

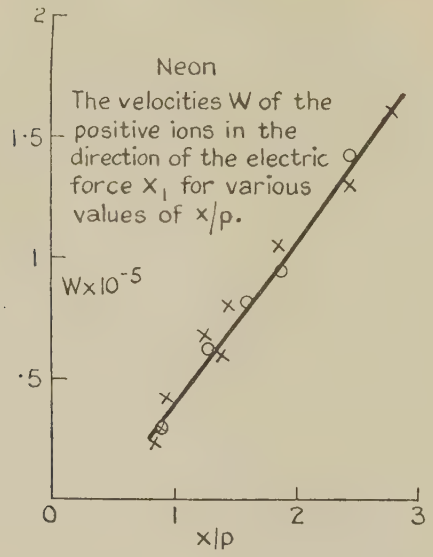

Since u does not decrease, the large increase of W with X/p must be due to an increase in the mean free path l.

The molecules of helium and neon show, then, towards positive ions of certain velocities large reductions in the effective diameter, analogous to those obtained in the study of the velocities of electrons. For the value $X/p = 2$, the velocity of the positive ions is $1{\cdot}05 \times 10^5$ in neon, and $\cdot 5 \times 10^5$ in helium. Thus the mean free paths in neon are about five times the mean free paths in helium. The corresponding result for electrons is shown by the tables for

the values of the mean free paths obtained with small velocities by Townsend and Bailey ('Motion of Electrons in Gases,' University Press, Oxford). The mean free path of electrons moving with a velocity 6×10^8 cm. per second in neon at 1 mm. pressure is ·21 cm. and in helium ·048 cm.

9. It cannot be assumed as an objection to the hypothesis of the ionization of molecules of a gas by collision with positive ions, that positive ions cannot acquire sufficient energy to ionize molecules. In view of the fact that both in helium and neon the positive ions can have long free paths and can acquire comparatively large energies, it is necessary when proposing a theory of electrical discharges in gases to consider ionization of molecules by impact with positive ions, as a possible process by which new ions may be generated.

I wish to conclude by expressing my gratitude to Professor Townsend for his constant assistance and inspiration throughout the course of the investigation.

Note.—A variation in the mean free paths of positive ions in Helium has been found by Dempster *. The ions were liberated from a hot electrode and possessed greater energies than those occurring in the above experiments.

LXXVI. *Chemical Dynamics in a Rigidly Coherent Phase.*

By D. H. Bangham, *M.A.*, *D.Sc.* †

THIS paper is an attempt to interpret the observation of Bangham and Burt ‡ that the rate at which sorption of gases takes place at a surface of glass is given in the early stages of process by an equation of the form

$$s = \text{constant} \times t^{1/m},$$

$$\frac{ds}{dt} \propto t^{-(1-1/m)} \propto s^{-m+1}. \quad . \quad . \quad . \quad . \quad . \quad (1)$$

Here s is the amount of gas accepted by the solid at time t, and m a constant greater than unity.

In the sequel it was found that this behaviour is not peculiar to glass (as an absorbent), or even to vitreous bodies in general, but that it is also met with in cases of sorption

* A. J. Dempster, Ph.D., "The Passage of Positively-charged Particles through Helium," Phil. Mag., Jan. 1927, p. 115.

† Communicated by the Author

‡ Proc. Roy. Soc. A, cv. p. 481 (1924).

by a whole variety of crystalline and semi-crystalline solids. A similar form of equation applies equally well to the taking up of iodine by charcoal *, of ammonia gas by carborundum powder and sapphire †, and of oxygen by "activated" graphite ‡.

The failure to approach anything like an equilibrium is not in all cases surprising, since it is well known that the superficial coating of a solid with a layer of adsorbed molecules—a process requiring only a short time for its completion—is often accompanied by the slow diffusion of the molecules into the interior. There is ample evidence that molecules of water can be gained or lost by the layers of glass that are beneath the surface, and there is little difficulty in crediting ammonia with the same power of penetrating a glass surface and participating in the chemical equilibrium in the interior. The other cases—those in which the sorbent is crystalline—are less readily explained. Yet the rejection of the diffusion hypothesis for the latter class rests less on the qualitative behaviour of the individual members than on the impossibility of reconciling equation (1)—established by measurements of some accuracy—with the ordinary theory of diffusion §.

After several attempts to formulate a theory that would lead to a dynamical equation in harmony with the experimental results, the author was led to examine the literature for data bearing on the rate of progress of other, and completely different, physical and chemical changes taking place in solid substances. Here he was more successful, for it soon became apparent that the "power" time-law is the rule rather than the exception where changes taking place in the solid phase are concerned—a fact not generally recognized ‖. In coming to this conclusion the author has been aided, not only by the data of those workers who have definitely set out to measure the time-changes, but also of many others who, having noticed a steady drift in the properties of the substances they were using, have observed and recorded its rate. It has frequently been assumed that this drift was following an exponential course, so that equilibrium or steady values could be calculated on the basis

* McBain and Davis, Trans. Faraday Soc. xiv. p. 202 (1919).
† Private communication from Mr. J. B. M. Herbert.
‡ Bangham and Stafford, J. C. S. cxxvii. p. 1085 (1925).
§ Bangham and Sever, Phil. Mag. xlix. p. 935 (1925).
‖ The term "solid" where used in this paper is intended to include non-crystalline bodies in which the thermal motions of the atoms are vibratory, not translatioual.

that the rate of progress was proportional to the distance from completion; but a wide survey of the subject leaves a strong impression that the number of exponential terms required to fit the experimental observations is often limited only by the range and accuracy of the latter. While the discussion below is confined to simple types of change which have been examined in sufficient detail to establish definitely the "power" type of time-law in their case, there are in fact countless others which, though less unequivocal, are quite consistent with a time-law of this type *. This generality is important since, together with the fact that typical liquids do not show a parallel behaviour (except perhaps in one or two cases of surface effects), it indicates the direction in which we are to seek an explanation of the law in question. As the surface layers of liquids are known to contain molecules in a definite condition of orientation, we may suppose the same causes to be operative here as in the case of solids.

The Non-validity of the Law of Viscous Flow in the Case of Solids.

The rate of deformation under steady loads of a large number of solid substances have been examined by Trouton and Rankine †, Larard ‡, Phillips §, and others. The general results of the authors named may be summed up in the statement that the strain (x) and the time (t) (reckoned from the moment of application of the steady stress) were found to be related by an equation of the form

$$x = a + b \log t,$$

$$\frac{dx}{dt} = bt^{-1} = be^{-\frac{x}{b}}, \quad . \quad . \quad . \quad . \quad . \quad (2)$$

where a and b are constants. This law which, as Trouton points out, is at complete variance with all established theories, holds with considerable accuracy for such widely different substances as copper, silver, lead, steel, glass, and indiarubber.

* For example: The phenomenon of photo-electric fatigue investigated by Hallwachs, H. S. Allen (Proc. Roy. Soc. A, lxxviii. p. 483, 1907; A, cxxxii. p. 161, 1909), Pochettino (*Atti dei Lincei*, xv. p. 171, 1906), and many others; the variation of capacities of lead accumulators during charging (see, for example, Hazelett, Trans. Amer. Electrochem. Soc. xxxiii. p. 95, 1909); the time-variation of the resistance of selenium on exposure to light (Brown, Phys. Rev. xxxiii. p. 410, 1911, and later papers).

† Trouton and Rankine, Phil. Mag. viii. p. 538 (1904).

‡ Larard, Proc. Phys. Soc. London, xxv. p. 83 (1912).

§ Philips. Proc. Phys. Soc. London, xix. p. 491 (1903).

Nutting *, on the other hand, suggests as the form of empirical equation most widely applicable

$$x = \text{constant} \times t^{1/n},$$

$$\frac{dx}{dt} \propto t^{-(t-1/n)} \propto x^{-n+1}, \quad . \quad . \quad . \quad . \quad . \quad (3)$$

where n is a constant greater than unity.

For reasons which will appear, it is the differential forms of these equations which are all-important. It is seen at once that differential equation (2) is but a special case of Nutting's differential equation (3), in which n is infinite. It follows that while any series of observations which shows agreement with equation (2) must also be consistent with Nutting's differential equation (3), the converse holds only when n is very great. For example, equation (3) in its integrated form represents with great accuracy the data of Trouton and Andrews † for the twist suffered by rods of pitch (at room temperature) at different times after the application of a constant torque. It is worthy of note that Trouton's own equation gives very poor agreement in this instance, even if a constant term is added to the expression for the rate, to take into account the possibility of ordinary viscous flow (that is, flow taking place without elastic storage of energy).

The Behaviour of Dielectrics.

When a potential difference is set up and maintained constant between a pair of electrodes in contact with the two sides of a plate of dielectric or poorly-conducting material, the observed current (initially relatively great) gradually decays until, at least in certain cases, it ultimately approaches zero. If the external E.M.F. is removed and the electrodes short-circuited, a current in the opposite sense makes its appearance and falls off to zero as time goes on. These effects are more noticeable in more obviously heterogeneous bodies; and in order to reconcile with them the accepted theory of dielectrics (according to which an *immediate* electric displacement depending on the material should be followed by a steady current proportional to its conductivity), Maxwell supposed the presence in the dielectric of the phases characterized by different specific inductive

* P. G. Nutting, Journ. Franklin Inst. cxcii. p. 679 (1921).

† Trouton and Andrews, Proc. Phys. Soc. London, xix. p. 47 (1904); Phil. Mag. vii. p. 347 (1904).

capacities. He considered that the energy used in forcing the current through the dielectric was not wholly degraded into heat, but was used in doing work against the elastic forces of the solid by causing a relative motion of the two phases. The anomalous discharge current he attributed to gradual return to the original state brought about by the agency of these elastic forces.

Maxwell's theory led him to an exponential expression for the decay with time of the discharge current. If i_0 be the discharge current immediately the electrodes are short-circuited, and i_t its value t minutes afterwards, then according to Maxwell,

$$i_t = i_0 e^{-ht}, \quad . \quad . \quad . \quad . \quad . \quad . \quad . \quad (4)$$

where h is a constant.

It has been abundantly proved that neither the discharge nor the charging current decays in accordance with this equation. Trouton and Russ * and also H. A. Wilson † have found that the discharge-current was practically proportional to t^{-1} (*cf.* equation (2)), while, according to Schweidler ‡, the decay of the charging current can in general be represented by the equation (*cf.* (3)) above for plastic deformation.

$$i_t = \text{constant} \times t^{-r}, \quad . \quad . \quad . \quad . \quad . \quad (5)$$

where r is a positive constant often closely approaching unity.

The Chemical Character of the Changes Considered.

An explanation of the power time-law must clearly be sought in the chemical forces which are the primary cause of rigid cohesion. The response of any rigid body to external mechanical forces—for instance, the stretching or bending of a wire or piece of indiarubber—must, in so far as it involves changed mutual relationships between the constituent atoms, be termed a chemical reaction. The same applies when a plate of insulating material is placed between charged electrodes, and when a photo-active substance such as selenium is exposed to light. In all these cases there is a well-marked drift in the properties of the solid, the extent of which depends on the time for which the disturbing influence is maintained.

To sum up, there is abundant evidence that solids, even of

* Trouton and Russ, Proc. Phys. Soc. London, xx. p. 551 (1905).
† H. A. Wilson, Proc. Roy. Soc. A, lxxxii. p. 409 (1909).
‡ Schweidler, *Ann. Physik*, xxiv. p. 711 (1907).

the simplest chemical types, have an inner complexity of structure, rendering the attainment of a reproducible minimum potential energy a matter of extreme practical difficulty in their case*. For solids and liquids alike, the well-known theory of Smits † accounts for this complexity in terms of the different energy states in which the simplest chemical unit can exist, such states being often only slowly mutually convertible. In Smits's nomenclature an ideal solid—in the sense of the ordinary theory of elasticity—should be classed as an "unary" system, since it attains a new equilibrium immediately on application of a steady load. A body showing "creep," on the other hand, must be at least "pseudo-binary," the drift of properties measuring the rate of a slow change of the fundamental chemical unit from one energy state to another, while the "elastic after-working" effect which often manifests itself on removal of the load finds a ready explanation in the setting-in of the reverse reaction.

Whatever may be the nature and size of the chemical units in terms of which the macroscopic change is ultimately expressible, the certainty that in coherent solids the rate of reaction does not depend on their chance encounters is sufficient to justify its formulation as a unimolecular reaction $A_1 \rightarrow A_2$. The only assumption made here is that similar changes of configuration are undergone by a large number of leptonic units ‡, each of which is sufficiently small (as compared with the parent body) to permit application of the usual statistical principles.

The empirical expressions (2) and (3) above are alike in taking no cognisance of any limit to the extent of the change as t approaches infinity ; and it follows that the rate can be governed neither by the nearness of approach to equilibrium

* *Cf.*, for instance, Lewis and Randall, 'Thermodynamics' (McGraw-Hill Book Co., 1923).

† Smits, 'Theory of Allotropy' (English translation, Longmans, 1924).

‡ This assumption is at least justified in the special case of india-rubber, a substance which, as already mentioned, undergoes slow deformation in accordance with a time-law of the "power" type. Katz (*Kolloid-Z.* xxxvi. p. 300, 1925) has shown by the X-ray method that, when rubber is stretched, a strongly-marked crystalline structure is developed which disappears gradually on releasing the tension. An investigation of this phenomenon by Hauser and Mark has revealed that the amount of crystalline material is increased, not by the growth of old crystallites, but by the continuous formation of new ones (Hauser and Mark, *Koll. Chem. Beih.* xxiii. p. 64, 1926; *Ambronn Festschrift.* lxiii. 1926 (*cf.* W. L Bragg, Chemical Society Annual Reports, xxiii. p. 277, 1926.)

(setting-in of the reverse reaction), nor by the falling-off in the concentration of the reactant species. The explanation of its decay may well lie, however, in the circumstance that the chemical units are not independent molecules, but are structurally bound to their neighbours. Since each unit is subject to forces which balance its own external field, it follows that the occurrence of catastrophic change of configuration on the part of any one group of atoms must have the effect of placing the others in its vicinity under a mechanical stress, which is only balanced when the elastic properties of the body as a whole are called into play. The forces knitting the groups of atoms together must therefore vary as the reaction proceeds; and since this force determines the chance that any given group will undergo change of configuration, the decay in the reaction rate becomes explicable on these lines *.

Making use of the fact that the forces binding the atomic groups, though chemical in origin, are expressible (in so far as their generalized effects are concerned) in terms of mechanical stresses, the above theory is capable of quantitative expression in cases where the solid body is originally isotropic, and the disturbing influence is such as to permit it to remain so.

It is assumed that the initial and final stages A_1, A_2 of the chemical unit A are characterized by volumes V_1, V_2, which are independent of the stress within the solid, and of the external pressure. To take into account the fact that transition from state A_1 to A_2 is possible only to groups which possess sufficient thermal energy of vibration to render them partially detached from their neighbours, we shall postulate also the transitory existence of an "activated" state A_A, the characteristic volume V_A of which far exceeds the average volume of the reactant species A_1. From this activated condition the group may relapse into either of the configurations A_1, A_2, the relative probabilities of these events depending only on the inner structure of the group. During the progress of the undirectional change the relations between the three states A_1, A_A, A_2 may then be summarized thus:

$$A_1 \rightleftharpoons A_A \rightarrow A_2.$$

* It is possible that the increased hardness characteristic of strained solids is connected with this increase in the force restraining the thermal movements of constituent units. Since it appears in vitreous as well as in crystalline solids, it cannot be due entirely to distortion of glide-planes.

If Π be the pressure with which the rigid framework as a whole opposes the expansion of any individual group of atoms, the work which must be done in the process of activation is $\Pi(V_A - V_1)$, and the rate of change, being determined by the probability of activation, should be proportional to $e^{-\frac{\Pi}{RT}(V_A - V_1)}$ if the number of A_1 groups remains sensibly constant. A comparison of this result with the two alternative empirical expressions for the rate (2 and 3 above) now tells us how the internal stress Π varies with the "strain" or extent of the reaction.

It is seen at once that Trouton's equation (2) is satisfied if

$$\frac{d\Pi}{dx} = \text{constant}, \quad . \quad . \quad . \quad . \quad . \quad (6)$$

implying a sort of extension of Hooke's law to the conditions within the solid.

Nutting's equation (3), on the other hand, requires that the relation between Π and x should take the form

$$\frac{d\Pi}{d \log x} = \text{constant}. \quad . \quad . \quad . \quad . \quad . \quad (7)$$

From the theoretical standpoint the form of this last equation is not altogether surprising, as the following discussion may serve to demonstrate. Suppose a solid body composed of the fundamental unit A to be undergoing compression under a constant hydrostatic pressure, which is causing reaction $A_1 \rightarrow A_2$ to take place. Let the change be still in progress when the fraction y of the groups of atoms are in the more compact configuration A_2. The further increase of y to $(y + dy)$ is accompanied by an increase dP in the external pressure which the body as a whole can withstand without further change; and the same applies to a block of atom-groups chosen in the interior of the solid, in regard to the pressure exerted by the rigid envelope surrounding it. The relation of dP to dy is given by the thermodynamic equation expressing the effect of pressure on the reaction constant K, which is here equal to $\frac{y}{1-y}$:

$$dP = \frac{RT}{V_1 - V_2} d \log \frac{y}{1-y}. \quad . \quad . \quad . \quad . \quad (8)$$

During the slower stages of the reaction the solid may be conceived as passing through a continuous series of false equilibria, in each of which the external pressure is opposed

partly by an active restoring force, and partly by a passive resistance due to internal stress, which opposes change in either direction. The permanence of each equilibrium state is destroyed, however, by the fortuitous internal property of the atom-groups which enables them, under certain conditions, to change their configuration. As the reaction proceeds, the active restoring force gradually decays, and the body loses to an increasing extent its power of immediate recovery, though its power of ultimate recovery remains unimpaired.

On this basis, as y increases to $(y+dy)$, some estimate of the change in the stress due to rigid cohesion should be gained by considering it equal to the accompanying change in an imaginary force-system capable of holding the existing chemical systems, before and after the change dy, in equilibrium with the constant external pressure. But this has been shown above to be equivalent simply to a negative decrease, that is, a positive increase, of pressure $d\mathrm{P}$.

In the range where y is small compared with unity, the variation of $(1-y)$ is negligibly small compared with that of y, and substituting $d\Pi$ for $d\mathrm{P}$, we have, as an approximation valid within this range,

$$d\Pi = \frac{\mathrm{RT}}{\mathrm{V}_1 - \mathrm{V}_2} d\log y. \quad . \quad . \quad . \quad . \quad . \quad (9)$$

The strain x is proportional, not to y itself, but to the increment $(y-y_0)$, reckoned from an original value y_0, which characterizes the unstressed solid. The relation (9) therefore reproduces the form of (7) above, provided y is always great compared with y_0; that is, provided the amount of the resultant species A_2 produced by the disturbing influence far exceeds that present in the original solid.

While not providing a derivation of the "power" time-law in any instance in which it has been found actually to hold, the above offers at least a partial explanation of the law, if it be supposed that Π is independent of the nature of the disturbing influence, and dependent only on the degree of the disturbance.

The rate of change being proportional to $e^{-\frac{\Pi}{\mathrm{RT}}(\mathrm{V_A}-\mathrm{V_1})}$ and dy to dx, the suggested significance of the index constant n is arrived at by using equations (3) and (9). We get

$$n = \frac{\mathrm{V_A} - \mathrm{V_2}}{\mathrm{V_1} - \mathrm{V_2}}. \quad . \quad . \quad . \quad . \quad . \quad . \quad . \quad (10)$$

It should therefore be nearly independent of the temperature.

Such experimental evidence as is available appears to support this conclusion *.

A New Aspect of the Sorption Problem.

The difficulty commonly experienced in realizing complete equilibrium in sorption experiments is not necessarily due to the occurrence of diffusion ; if the sorption follows the "power" time-law, it is to be inferred that the atomic groups forming the rigid framework of the sorbent are unable in their "average" condition to combine with gas molecules, but they require first to be activated at the expense of work done against the forces binding them. Those atomic groups which have entered into combination with gas molecules are in a configuration different from the remainder, and the change they have undergone imposes a stress on the rigid framework which surrounds them. That a porous sorbent like charcoal is actually distended in the process has recently been confirmed by the interesting experiments carried out by Meehan † at the Building Research Station, Garston. A very similar effect, the change of volume accompanying ionic exchange and variation of water-content of the zeolites, has been somewhat more fully investigated ‡.

The extension of Langmuir's well-known "chemical" theory of sorption to such generally active sorbents as charcoal requires that the ultimate chemical units of these substances should be characterized by extreme reactivity. This activity may be almost completely masked, however, when the units are rigidly bound together ; a parallel behaviour is shown by those metallic oxides which, by high-temperature ignition, are made to lose their power of rehydration. These oxides are strong *sorbents* of water, but

* It will perhaps bear emphasis that the above considerations apply only to the slow "creep" following the disturbance of a solid, and not to the initial disturbance itself. The wide application of the "power" time-equation in its integrated form is partly connected with the fact that as long as n is fairly great, the linearity of the graph on which the logarithms of the variables are plotted is but little affected by adding constants (within limits) to the variable representing the extent of the change. Since the instantaneous effects earlier referred to would give rise to such constants, which may alter considerably the slope of the logarithmic graph, it follows that conclusions based on this method of determining the index may be widely in error.

† Proc. Roy. Soc. A, cxv. p. 199 (1927).

‡ G. Schultze, *Zeitschr. f. Phys. Chem.* lxxxix. p. 168 (1915) and subsequent papers.

the reaction is retarded to such an extent by the forces of rigid cohesion as to be practically arrested.

A sorbent is normally prepared by driving out the volatile matter from a substance originally mechanically rigid. This being carried out well below the sintering-point of the residue, the latter, though somewhat shrunken, may be freely permeable to gas molecules. A rough calculation from X-ray data indicates that even the lattices of certain crystalline solids, without having part of their structure removed by heat, contain lacunæ large enough to permit small molecules to enter. Imperfections in the crystal would render its interior even more accessible, and, to go to the extreme, it is clearly illogical to attempt to estimate the internal surface of substances like charcoal.

Calling the gas molecule G and the initial, active, and final states of the sorbent atom-group A_1, A_A, A_2 respectively, our conception of the reaction may be formulated :

$$A_1 \rightleftharpoons A_A \; ; \; A_A + G \rightarrow A_2G.$$

Its rate decays with the building-up of a stress which makes it more and more difficult for the A_1 groups to attain the activated state as the reaction proceeds. It is not, of course, contended that the influence of this stress, rather than the accessibility of the gas molecules to a free surface, will invariably set a limit to the rate ; with certain types of solids, however, the conditions for accessibility and activation would be tantamount, since both require the partial detachment of the atom-group from its neighbours *.

The mechanism described goes far to explain the hysteretic effects so common in sorption and occlusion phenomena. The behaviour of a particular sorbent will depend largely on whether or not its atom-groups are capable of losing their gas without reverting to the unreactive configuration. If this is the case, the sorption-value at a particular pressure will depend largely on the past history of the sorbent. Owing to the larger number of reactive groups present, the sorption will be greater if the " equilibrium " is approached from a higher than if from a lower pressure. Moreover, if the gas is removed by exhausting at a sufficiently low temperature, the sorbent, for the same reason, will appear more active on a second exposure to the gas. Removal of gas at high temperature, on the other hand, especially if followed

* A very similar postulate forms the basis of a theory of contact catalysis recently advanced by H. S. Taylor. Taylor (Proc. Roy. Soc. A, cviii. p. 105, 1925) does not, however, require that the necessary degree of detachment should be attainable by thermal oscillation.

by slow cooling, would permit the groups to revert to the unreactive form, with consequent loss of activity. All these effects are common phenomena in sorption work.

Summary and Conclusions.

The equations of the form

$$s = \text{constant} \times t^{1/m}$$

found empirically to govern in many cases the rate of the sorption process are not peculiar to this phenomena alone, but are somewhat widely applicable to the time-course of processes involving the disturbance of the "inner equilibrium" of solid substances (either by mechanical deformation or by other physical or chemical means), provided the solid after disturbance remains rigidly coherent. It is shown that the rate of such a change may be limited by conditions which do not apply in a liquid reaction medium, and which are not concerned in any way with the distance of the reaction from completion. Owing to the incongruity of the initial and final stages of the groups of atoms undergoing transition, the partial occurence of the reaction disturbs the balance of elastic forces, and therefore influences the internal work that must be done before further groups of atoms can rearrange themselves.

On the hypothesis that the condition for rearrangement is the momentary occupation by the groups of a volume considerably greater than the average, calculations are made of the mode of variation during the progress of the reaction of the force restraining their thermal movements. A tentative explanation of the form of this variation is offered as an alternative to the linear variation required by an extension of Hooke's law to the conditions in the interior of the solid. According to this the intensity of the internal stress set up by the partial occurrence of the reaction is given by the difference between the hydrostatic pressures with which the initial and actual states of the solid would be in complete equilibrium. On this basis it is shown that the index-constant of the "power" time-equation is given by the ratio

$$\frac{V_A - V_2}{V_1 - V_2},$$

where $(V_A - V_2)$ is the difference of volume between the activated and final states of the atomic groups, and $(V_1 - V_2)$ the difference between their initial and final volumes.

Application of these ideas to the sorption problem provides

an immediate explanation of the dependence of the activity of the sorbent on its past history, and leads to a revised conception of the mutual relations of sorbent and sorbate in cases where the "power" time-equation holds. The sorbed molecules are regarded as distending the rigidly coherent structure of the sorbent, which consequently becomes stressed. This distension may occur even if the structure is a sufficiently open one to permit easy penetration by the gas molecules in their free state.

University of Manchester and
the Egyptian University.

LXXVII. *Sign Conventions applied to Flexing Problems.* By W. H. Brooks, *B.Sc.(Eng.).**

THE widespread lack of agreement respecting the sign conventions to be applied to flexing problems in general, results in unfortunate confusion and recurring discussion, especially amongst students.

Any convention may, of course, be arbitrarily chosen for any particular problem, and, if consistently applied throughout, will lead to correct results. When, however, certain fundamental equations are established by the adoption of different sign conventions for bending-moments, experience shows that confusion results from comparisons being made, and erroneous solutions may at first accrue.

For example, the Clapéyron equation for a girder continuous over spans l_1 and l_2 under distributed loading w_1 and w_2 per unit run respectively, and supported level at A, B, and C, may be written

$$M_A l_1 + 2M_B(l_1 + l_2) + M_C l_2 \pm \tfrac{1}{4}(w_1 l_1^3 + w_2 l_2^3) = 0,$$

according to the signs assumed for the moments at A, B, and C.

The writer of the present article ventures to suggest that, when applying rectangular coordinates to the solution of practical engineering problems, the well-established mathematical sign conventions shown in fig. 1 should be consistently used throughout, so that when considering any of the successive integrals: load, shearing-force, bending-moment, slope, and deflexion, an agreed criterion shall be available, to determine what sign to affix to the function considered.

* Communicated by the Author.

Consider the case of a simply-supported horizontal beam under a distributed load as shown in fig. 2 (*a*), in which at any point X the ordinate represents a load $= w$ per unit length.

Fig. 1.

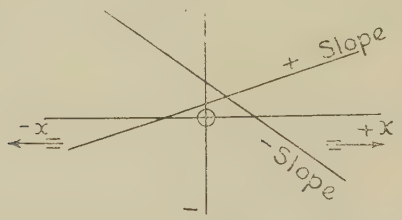

Clearly this loading will produce negative deflexion (y), as shown in fig. 2 (*e*), the form of which may be sketched, and from it the forms of the graphs (*d*), (*c*), and (*b*) may be successively derived by applying the well-known relations:

$$\text{Load } (w) \qquad = \mathrm{E_I}\frac{d^4y}{dx^4}.$$

$$\text{Shearing-force (F)} \quad = \int w\,dx = \mathrm{E_I}\frac{d^3y}{dx^3}.$$

$$\text{Bending-moment (M)} = \int \mathrm{F}\,.\,dx = \mathrm{E_I}\frac{d^2y}{dx^2};$$

$$i.\,e., \qquad \frac{d^2y}{dx^2} = \frac{\mathrm{M}}{\mathrm{E_I}}.$$

$$\text{Slope } (\theta) \qquad = \int \frac{\mathrm{M}}{\mathrm{E_I}}\,dx.$$

$$\text{Deflexion } (y) \qquad = \int \theta\,.\,dx = \int\int \frac{\mathrm{M}}{\mathrm{E_I}}\,dx\,.\,dx.$$

As a mnemonic, these relations may be written in the form:

$$\int f(x)\,dx \;\Big\updownarrow\; \begin{matrix} w \\ \mathrm{F} \\ \mathrm{M} \\ \mathrm{E_I}\,.\,\theta \\ \mathrm{E_I}y \end{matrix} \;\Big\updownarrow\; \frac{d}{dx}f(x).$$

Having inferred the form of the deflexion graph—which

represents the form taken by the neutral axis for the given loading—any ordinate in fig. 2 (*d*) may be readily derived from this curve. Thus the ordinate BC in fig. 2 (*d*) represents the positive slope $\frac{dy}{dx}$ of the deflexion curve at A in fig. 2 (*e*).

In like manner, any ordinate in fig. 2 (*c*) may be derived from consideration of the slope of the curve (*d*). Thus the ordinate DE represents $\frac{d\theta}{dx}$ at C in fig. 2 (*d*).

Fig. 2.

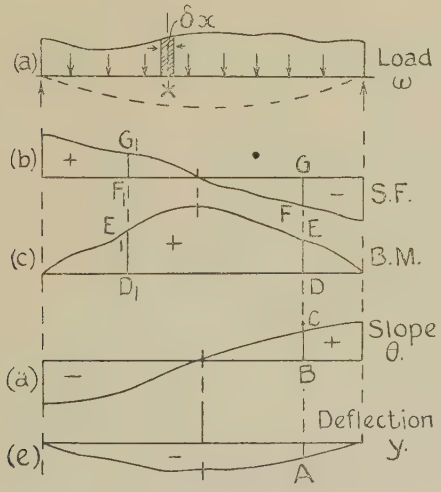

The slope of this latter curve, being positive at all points (except at the extremities, where it is zero for this case), shows that, when sagging occurs as shown in fig. 2 (*e*), the bending-moment has a positive sign. In other words, when the centre of curvature is *above* the neutral axis of the beam, the bending-moment is *positive*. Conversely, when the centre of curvature is *below* the neutral axis, the bending moment is *negative*, as may readily be deduced by inverting the curves of fig. 2.

Again, the slope at E $\left(\frac{dM}{dx}\right)$ in fig. 2 (*c*) is negative; hence the shearing-force represented by the ordinate FG in

fig. 2 (*b*) is negative. At E, in fig. 2 (*c*) $\frac{dM}{dx}$ is positive; hence the ordinate F_1G_1 in fig. 2 (*b*) is positive.

Further, since the slope at all points of the S.F. diagram is negative, and $\frac{dF}{dx} = w$, downward loading as shown should be considered negative, which sign is also consistent with that of the deflexion it produces.

If it be agreed, therefore, that the mathematical convention of signs should be consistently applied, the signs to be given to any of the functions shown in fig. 2 should not be

Fig. 3.

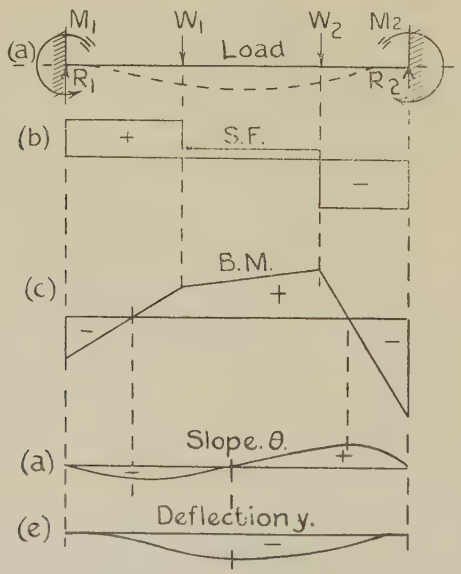

arbitrarily chosen. It will be seen that the criterion, "sagging is produced by positive BM," does not depend upon a fixed origin; the slope of any of the curves (*e*), (*d*), (*c*) of fig. 2 is not determined by the position of the origin from which x is taken, provided x is considered *positive* when taken to the *right* of a chosen origin, and *negative* when taken to the *left*, in accordance with the rule of signs, as shown in fig. 1.

In fig 3 the convention is again applied to the case of an encastré beam, loaded as shown in fig. 3 (*a*). Proceeding

as in the foregoing example, figs. 3 (*d*), (*c*), and (*b*) are successively derived from fig. 3 (*e*), which is first inferred from the load diagram. In this case the fixing couples M_1 and M_2 send the centre of curvature below the beam, and consequently are considered as negative. The test should also be applied—when working from fig. 3 (*e*) to fig. 3 (*b*)—

Fig. 4.

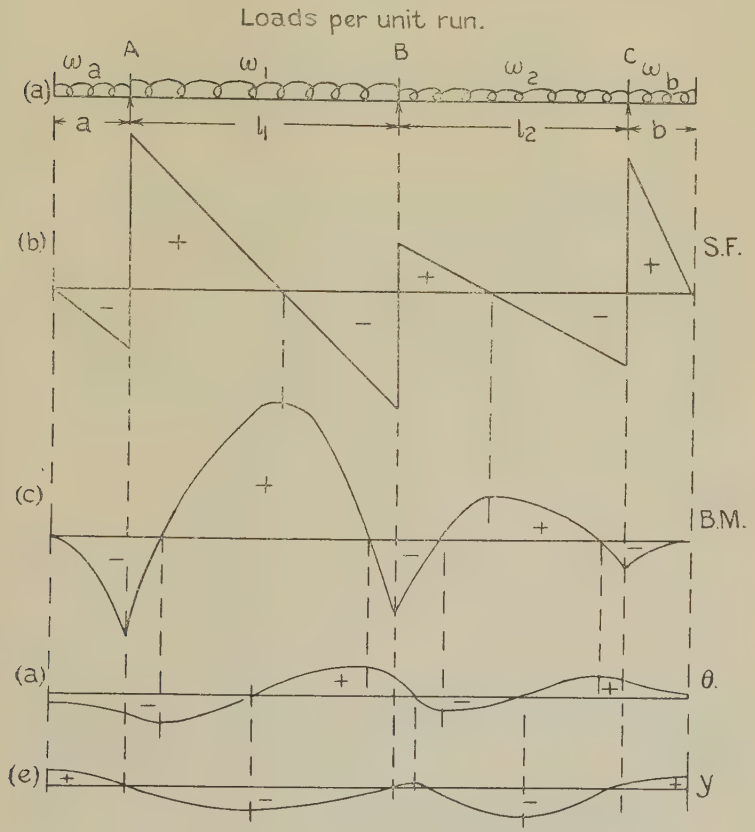

that the slope of any curve is represented in sign and magnitude by the ordinate of the curve immediately above.

Again, consider the case of a beam continuous over three supports A, B, and C at the same level, and loaded as shown in fig. 4 (*a*). Applying the mathematical sign convention

the equation giving M_B is

$$M_A l_1 + 2M_B(l_1 + l_2) + M_C l_2 + \tfrac{1}{4}(w_1 l_1^3 + w_2 l_2^3) = 0,$$

assuming M_B is *positive*.

The overhanging load to the left of A, results in a negative position for the centre of curvature of the beam at A. Similarly at C. Hence the bending-moment at A should be written

$$M_A = -\tfrac{1}{2} w_a a^2 \quad \text{and} \quad M_C = -\tfrac{1}{2} w_b b^2.$$

Thus

$$-\tfrac{1}{2} w_a a^2 l_1 + 2M_B(l_1 + l_2) - \tfrac{1}{2} w_b b^2 l_2 + \tfrac{1}{4}(w_1 l_1^3 + w_2 l_2^3) = 0,$$

giving

$$M_B = \frac{1}{4(l_1 + l_2)} \{ w_a a^2 l_1 + w_b b^2 l_2 - \tfrac{1}{2}(w_1 l_1^3 + w_2 l_2^3) \}.$$

When $w_a a^2 l_1 + w_b b^2 l_2 = \tfrac{1}{2}(w_1 l_1^3 + w_2 l_2^3)$, $M_B = 0$; *i. e.*, the centre of curvature for the point B is at infinity.

When $w_a a^2 l_1 + w_b b^2 l_2 < \tfrac{1}{2}(w_1 l_1^3 + w_2 l_2^3)$, M_B is *negative*, showing that the centre of curvature is *below* the beam.

When $w_a a^2 l_1 + w_b b^2 l_2 > \tfrac{1}{2}(w_1 l_1^3 + w_2 l_2^3)$, M_B is *positive*, showing that the centre of curvature is *above* the beam.

In the special case $a = b = c$ say, $l_1 = l_2 = l$ say, and $w_a = w_1 = w_2 = w_b = w$ say,

$M_B = 0$, negative or positive, according as

$$2c^2 = l^2, < l^2 \text{ or } > l^2 \text{ respectively.}$$

In sketching the graphs of fig. 4, it has been assumed that

$$w_a a^2 l_1 + w^b b^2 l_2 < \tfrac{1}{2}(w_1 l_1^3 + w_2 l_2^3).$$

In cases such as this, where the bending-moment over a support may be either positive or negative, it is important that an agreed criterion should be applied so as to determine whether the beam is sagging or hogging over the supports, otherwise erroneous values are likely to be obtained for the reactions of the piers at these points.

Thus, applying the sign conventions used in the foregoing, when $M_B = 0$, taking moments about B, clearly

$$R_A l_1 = w_a a\left(l_1 + \frac{a}{2}\right) + w_1 \frac{l_1^2}{2};$$

$$\therefore \quad R_A = w_a a\left(1 + \frac{a}{2l_1}\right) + w_1 \frac{l_1}{2}.$$

Similarly

$$R_C = w_b b\left(1 + \frac{b}{2l_2}\right) + w_2 \frac{l_2}{2}.$$

When M_B is negative, it is causing hogging at B, and therefore operating, as shown in fig. 5, on the left-hand portion of the beam.

Fig. 5.

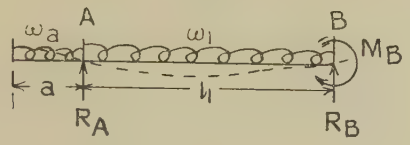

For equilibrium, therefore,

$$M_B + R_A l_1 = w_a a\left(l_1 + \frac{a}{2}\right) + w_1 \frac{l_1^2}{2};$$

$$\therefore \quad R_A = w_a a\left(1 + \frac{a}{2l_1}\right) + w_1 \frac{l_1}{2} - \frac{M_B}{l_1}.$$

Similarly

$$R_C = w_b b\left(1 + \frac{b}{2l_2}\right) + w_2 \frac{l_2}{2} - \frac{M_B}{l_2}.$$

When M_B is positive, it is causing sagging at B, and

Fig. 6.

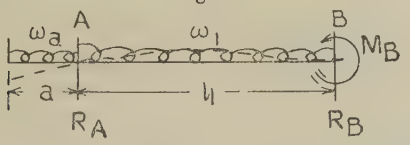

therefore operating as shown in fig. 6. Here, for equilibrium,

$$R_A l_1 = w_a a\left(l + \frac{a}{2}\right) + w_1 \frac{l_1^2}{2} + M_B;$$

$$\therefore \quad R_A = w_a a\left(1 + \frac{a}{2l_1}\right) + w_1 \frac{l_1}{2} + \frac{M_B}{l_1}$$

Similarly

$$R_C = w_b b\left(1 + \frac{b}{2l_2}\right) + w_2 \frac{l_2}{2} + \frac{M_B}{l_2}.$$

In all three cases, of course,

$$R_B = (w_a a + w_b b + w_1 l_1 + w_2 l_2) - (R_A + R_C),$$

and may be alternately found and checked by taking moments about either A or C.

When a graphical construction is used for the purpose of drawing the S.F. and B.M. diagrams for a given loading, a little consideration will show that, when the load-line is drawn to the *left* of the origin chosen for the polar diagram, the resulting funicular polygon giving the B.M. diagram becomes inverted, because drawn from a negative base. This accounts for the reversal in sign often apparent between S.F. and B.M. diagrams.

To avoid this inversion, clearly a *positive* base must be used in the polar diagram, so making

$$F = \frac{dM}{dx} \text{ at all points in the S.F. diagram.}$$

LXXVIII. *A Simple Method for Determining the Orientation and Structure of Crystals with X-Rays.* *By* W. E. Dawson, *M.Sc., Assistant for Physics, Technische Hoogeschool, Delft (Holland)* *.

1. Preliminary Discussion.

THE principal object of the present experiments has been the devising of a simple method for determining the orientation and structure of crystals showing no well-developed faces, such, for example, as crystal fragments and metal crystallites.

For the purpose of defining the orientation, it is sufficient to define the directions of three non-parallel lines in the crystal, preferably the crystal axes, and to this end one may imagine the latter as radius vectors of a sphere, whose directions may then be given by the polar coordinates of their points of intersection with the surface.

A photograph taken with a single crystal rotating in a Debye-Scherrer camera will have two axes of symmetry, perpendicular and parallel respectively to the axis of rotation. The photographic spots produced by the reflected pencils fall thus into groups of four, each group arising from a single set of reflecting planes in the crystal, and yielding sufficient

* Communicated by Prof. A. D. Fokker, Ph.D.

data to determine the inclination of the normal to these planes to the axis of rotation. If, in addition, the structure of the crystal be known, so also are the angles between the various normals, but in no case can the azimuth of a normal, measured from an arbitrary plane containing the axis of rotation, be determined.

In the case, then, of a rod containing several crystals of known structure, a Debye-Scherrer photograph is sufficient to determine the orientation of each with respect to an axis, but not the amount of its rotation about the latter. Their mutual orientations cannot thus be found unless separate exposures be made with the crystal rotating about three non-parallel axes, which in view of the time demanded and the restrictions imposed on the specimen, is not very convenient.

The present method has been devised to overcome this drawback, and is based upon the observation first made by Weissenberg * that, if the rotation of the crystal be accompanied by a proportional movement of the recording film, the angle turned through by the crystal between successive reflexions may be obtained, and sufficient data are thus provided for determining uniquely the direction of the normal belonging to each set of atomic reflecting planes, and hence also the orientation and space-lattice of the crystal.

The arrangement used, which may also be called an X-ray goniometer, is depicted diagrammatically, though not to scale, in fig. 1. OA is the axis of rotation of a small crystal at C and of a wheel WHL. The latter bears against a photographic plate holder PP, which is constrained to move along a straight line perpendicular to OA. Thus as the crystal and wheel rotate together, the recording plate suffers a proportionate tangential displacement. IC, the incident pencil of X-rays, is perpendicular both to the axis OA and plane of the plate.

Let us suppose that CR is a reflected pencil of X-rays meeting the plate in R, and that CN is the normal to the set of atomic reflecting planes responsible for the reflexion. Let η be the co-latitude of the normal measured from OA, and α its azimuth measured in the clockwise direction from the plane ACI (fig. 1) defined by the axis and the incident pencil. The direction of the normal is then defined by α and η.

The incident beam produced meets the plate in C′, and the lines C′X and C′Y through C′, parallel and perpendicular

* K. Weissenberg, *ZS. f. Phys.* xxiii. p. 229 (1924).

respectively to the axis of rotation, may be taken as axes of reference for the photographic spots. If, then, x and y are

Fig. 1.

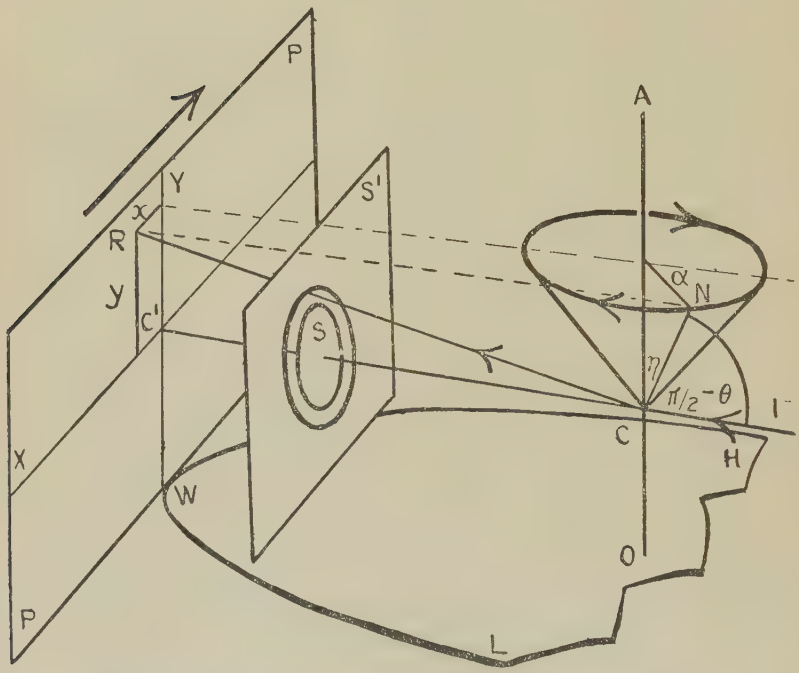

the coordinates of the spot produced at R by the reflected pencil CR, the following relations are deduced :—

$$\cos\eta = \frac{y}{l}\cdot\frac{\cos\theta}{\tan 2\theta}, \quad \ldots\ldots (1)$$

$$\tan\alpha' = \frac{x}{l}\cdot\frac{\cot\theta}{\tan 2\theta}, \quad \ldots\ldots (2)$$

$$x^2+y^2 = l^2\,.\tan^2 2\theta, \quad \ldots\ldots (3)$$

where l is the distance from crystal to plate, α' is the value of α when reflexion occurs, and θ is the angle (measured from the reflecting plane) satisfying the Bragg reflexion

condition: viz.,

$$\lambda = 2d \cdot \sin\theta,$$

in which λ is the wave-length of the reflected X-rays, and d the spacing of the reflecting planes.

(1) and (2) are not independent, and, eliminating x, y, and l with the aid of (3), we obtain

$$\tan^2\alpha' = \left(\frac{\sin\eta}{\sin\theta}\right)^2 - 1 \quad . \quad . \quad . \quad . \quad . \quad (4)$$

For given values of η and θ, (4) gives four real values of α' or none, according as η is greater or less than θ. Reflexion is obviously impossible in this latter case. If η is greater than θ, and α' is the smallest positive value of α satisfying (4), then as the crystal rotates in the clockwise direction, successive reflexions will occur when the normal occupies positions determined respectively by the azimuths,

$$\alpha', \quad \pi - \alpha', \quad \pi + \alpha', \quad 2\pi - \alpha'.$$

Suppose, now, that the crystal makes one complete revolution. Two types of photograph are possible according to the initial position of the normal CN. These are shown in figs. 2 *a* and 2 *b*, which correspond, respectively, to the patterns to be expected when the normal begins with an azimuth given by

$$\alpha' > \alpha > -\alpha' \quad . \quad . \quad . \quad . \quad . \quad . \quad . \quad (5)$$

or $$\pi - \alpha' > \alpha > \alpha' \quad . \quad . \quad . \quad . \quad . \quad . \quad . \quad (6)$$

Inverted the same figures would correspond to the normal starting from the diametrically opposite positions, given respectively by

$$\pi + \alpha' > \alpha > \pi - \alpha' \quad . \quad . \quad . \quad . \quad . \quad . \quad (7)$$

and $$2\pi - \alpha' > \alpha > \pi + \alpha' \quad . \quad . \quad . \quad . \quad . \quad . \quad (8)$$

The numbers indicate the order in which the reflexions occur when the plate moves in direction of the arrow. The upper and lower pairs correspond respectively to the azimuths $\pm\alpha'$ and $\pm(\pi - \alpha')$.

The distance S separating the upper or lower pair of spots is expressed either by

$$S = 2\pi r - 2(r\alpha' + x) \quad . \quad . \quad . \quad . \quad . \quad (9)$$

or $$S = 2(r\alpha' + x), \quad . \quad . \quad . \quad . \quad . \quad . \quad . \quad (10$$

depending upon the initial conditions, r, representing the linear displacement of the plate per unit angular displacement of the crystal, or otherwise the effective radius of the wheel WHL. The distance separating the upper pair is in either figure given either by (9) or (10), according as the initial azimuth of the normal to the reflecting planes lies within or without the region of α defined by the limits $\pm\alpha'$. The same is also true of the lower pair when we substitute for the limits $\pm(\pi-\alpha')$. In this latter case also, the value S given by (9) becomes negative when $x>r\ (\pi-\alpha')$ and the numbers by the corresponding pair of spots need interchanging.

The difference of the abscissæ of spots 1 and 3 or 2 and 4 is in either figure equal to πr; the linear displacement of the film accompanying half a revolution of the crystal. A means is thus afforded of determining the constant r. It may also be noted that the sum of the distances separating the upper and lower pairs in fig. 2 *a* amounts to $2\pi r$.

The lines joining the upper and lower pairs respectively stand at a distance $2y$ apart. These joins have in fig. 2 *a* a common perpendicular bisector whose position on the photograph corresponds to that of the crystal in which the normal has the azimuths 0 or π, according as the distance separating the upper pair is identical with (9) or (10). This latter is easily ascertained since the two values of S are calculable, α' being found from (4), and x from (2) or (3), in which r and y are obtained from the photograph, and θ is calculated from the Bragg reflexion condition, or, in case the lattice dimension d is unknown, determined from an exposure with stationary plate.

A similar significance attaches to the perpendicular bisectors in fig. 2 *b*, the upper and lower ones corresponding respectively to the azimuths 0 and π.

The azimuthal angle of the normal measured from a plane containing the axis of rotation may therefore be found, and this in conjunction with the co-latitude η, given by (1), determines its direction completely.

Sufficient data are also obtained when the crystal performs only half a revolution, but in this case the interpretation of the photographs becomes somewhat more involved and the results less accurate, as only two spots are then recorded, the upper or lower pair or one member of each, according to the initial conditions.

When only the orientation of a crystal is desired, it is of course unnecessary to record all the reflexions rendered possible by the monochromatic radiation employed. In the

present experiments with aluminium crystals, for example, it was sufficient to record the reflexions arising from the cube faces ((100) planes). These determine the orientations of the cubic axes and so also that of the crystal. As in this case the other reflexions only serve to complicate the photograph, they were screened off by interposing between the crystal and plate two lead screens, S and S′ (fig. 1)*, the

Figs. 2 *a* & 2 *b*.

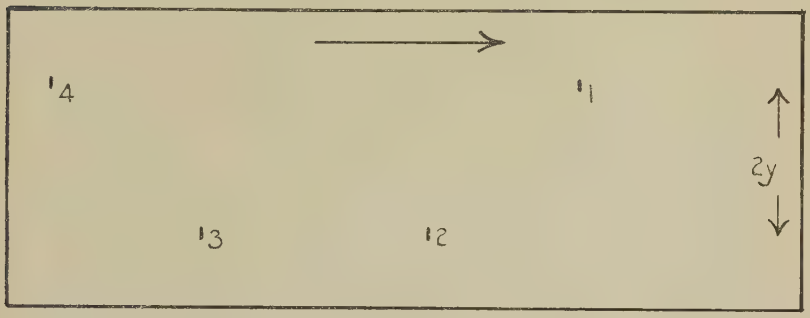

Fig 2a

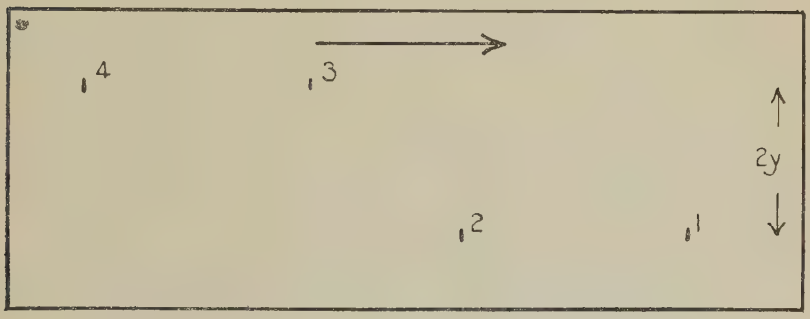

Fig 2b.

* In the arrangement described by Weissenberg (*loc. cit.*), the reflected pencils are allowed to emerge only through an annular apertnre concentric with the axis of rotation, and are recorded on a cylindrical film moving parallel to the latter. The reflexions photographed make thus a constant angle with the axis, determined by the dimensions of the aperture. Reflexions from planes having different indices may be simultaneously recorded, but then only one of the two possible pairs given by each set of reflecting planes. The elucidation of the photographs would, it seems, under these circumstances be somewhat more difficult than with the present arrangement, where the reflected pencils make a constant angle with the incident pencil, and proceed thus from atomic planes having the same indices.

one S, a circular plate, and the other S′, a rectangular plate, having a concentric circular aperture of somewhat greater diameter. The disk S was further pierced centrally with a pin-hole which could be opened or closed at will by a small lead cover, and served both for making reference marks by allowing the incident pencil to fall directly on to the film and for setting the screens correctly in position, viz., so as to be traversed centrally and normally by the incident pencil *. In this way the photographic plate was exposed only over a narrow annular region equidistant from the trace of the incident pencil and subtending at the crystal a circular cone of semi-vertical angle designed to admit only the second-order reflexions from the cube-faces. As is well known, the corresponding first-order reflexions are destroyed by interference owing to the face-centred structure of aluminium.

Under the above circumstances, a complete photograph should show twelve spots produced by the four reflexions arising from each of the three sets of (100) planes. If, however, θ be greater than 54° 44′, no reflexions need occur, as the possibility exists of the normals to the reflecting faces simultaneously having co-latitudes η less than θ (*cf.* (4)). Similarly, if θ be less than 54° 44′ but greater than 45°, only one set of (100) planes need reflect. In these cases, which indeed are improbable, either a new axis of rotation would have to be chosen, or reflexions from planes of different spacing would have to be recorded. When, finally, θ is less than 45°, two sets of cube-faces are certain to reflect, and at least eight spots will appear in the resulting photograph. Just sufficient data are then provided for determining the orientation of the crystal. In the present investigation copper Kα radiation was employed ($\lambda = 1{\cdot}537$ Å.). θ was therefore fixed at 22° 11′, and this being less then 45°, the sufficiency of the photographic material was ensured from the beginning. As a precautionary measure, however, a stationary plate,

* Such screens may easily be prepared by cutting two pieces of cardboard to the same size and shape as the lead and pasting each to a sheet of good thin paper. For the sake of rigidity, the sheet bearing the disk may be furnished with a narrow cardboard frame. The lead screens are then superimposed on and fastened to the cardboard. When the two are mounted concentrically and parallel, a narrow ring of paper remains, transparent to X-rays. The angular aperture subtended by the ring at the crystal may be varied by displacing the screens with respect to the latter or each other, as the case may be. Reflexions from planes of given spacing may thus be recorded or eliminated according to choice.

which may be placed in front of the annular aperture and exposed simultaneously with the moving plate, serves to indicate all the available reflexions. Such a preliminary exposure is of course indispensable when dealing with crystals of unknown structure.

When, on the other hand, it is desired to determine the structure of a crystal, it would be more expedient to expose the plate over a considerable range, or even over the the whole range (θ to $\pi/2$) of θ, at once.

2. Experimental.

In the arrangement employed, which was made throughout of brass, the photographic plate moved 20·33 cm. to a single revolution of the crystal, the coupling being effected by means of a toothed wheel engaging a toothed bar fixed to the plate-holder. The distance l from the axis of rotation to the plate was $3{\cdot}28_5$ cm., and, as appeared from the subsequent photographs, the effective radius r of the coupling-wheel was $3{\cdot}23_5$ cm. The plates themselves were 30 cm. long by 9 cm. wide. Obviously, if $W = 2 \,.\, l \,.\, \tan 2\theta$ be the least permissible dimension of the plate parallel to the axis of rotation, the other dimension should be not less than $W + 2 \,.\, \pi \,.\, r$, or $W + \pi \,.\, r$ if only half a revolution be utilized, in order to ensure of no reflexions being missed.

The crystals were of aluminium in the form of cylindrical rods 1·5 mm. in diameter, prepared after the method due to Carpenter *. They were rotated with a uniform angular velocity of one revolution in half an hour, and as a complete exposure occupied four hours, four revolutions were made in either direction, the reversing being performed automatically. Connexion between the goniometer and driving arrangement was made with a cardan coupling, enabling the former to be adjusted with respect to the X-ray beam. Provision was also made whereby the rod under examination could be given a pure displacement along its axis, either for the purpose of bringing a different crystal into the X-ray beam, or for allowing the latter to impinge directly on the photographic plate and produce reference marks.

X-rays were supplied by a Philips tube, having a water-cooled anticathode of metallic copper working under an

* H. C. H. Carpenter, 'Nature,' cxviii. p. 266 (1926).

Figs. 3 *a*, 3 *b* & 4 *a*, 4 *b*.

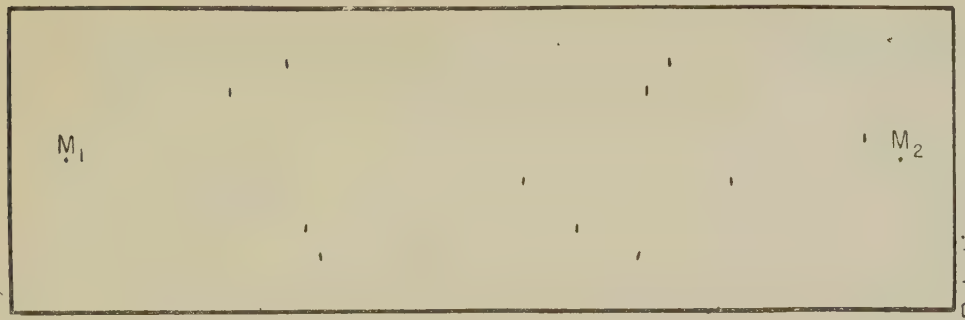

Fig 3a

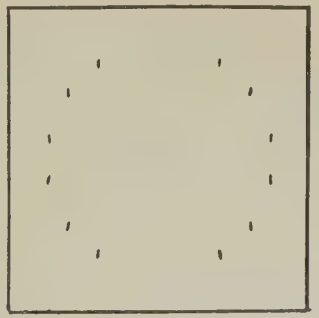

Fig 3b

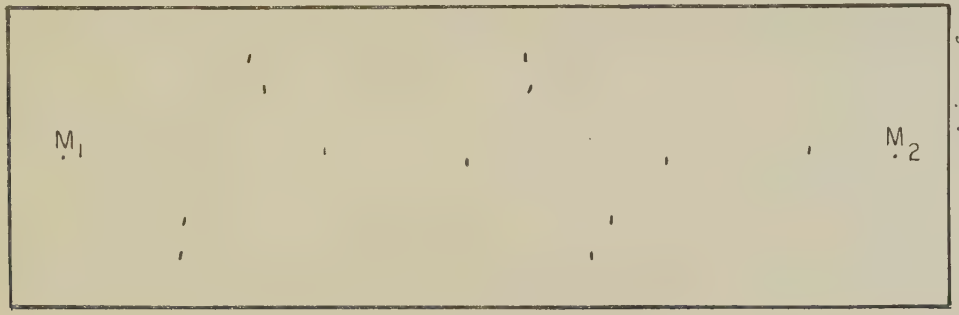

Fig 4a

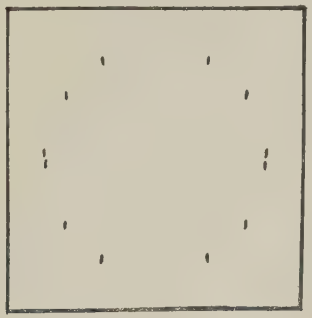

Fig 4b

alternating potential difference of 33 KV at 50 cycles, and taking a current of 8 *m*A. They were filtered through the aluminium window of the tube, 3 100 mm. thick, and a sheet of nickel 1/50 mm. thick, and were limited to suitable dimensions by passing through a cylindrical hole of circular cross-section, 4·5 cm. long and 1·5 mm. diameter, bored through a plug of lead. The intensity of the copper Kβ radiation was in this way so far reduced by selective absorption that only the reflexions arising from the copper Kα-radiation appeared in the photographs.

The specimen actually examined was a rod of aluminium 14 cm. long, comprising two single crystals which met at a point 6 cm. from one end of the rod.

Figs. 3 *a* and 4 *a* are scale drawings reduced to about one-half the original size of the photographs obtained. Each plate showed all twelve possible spots. Exposures made with the same crystals and stationary plates are similarly depicted in figs. 3 *b* and 4 *b* respectively. The upper photographs belong to the upper and shorter crystal as the specimen stood in the goniometer. M_1 and M_2 are reference marks, so chosen that, if the two figures be superposed, the M_1's and M_2's on each being made to coincide respectively, the resulting figure will represent the photograph to be expected when the two crystals are exposed simultaneously, as might be done by passing the X-rays through their junction. As follows from the foregoing discussion, and is to be seen from the figures, M_1 M_2 is a screw axis of symmetry, characterized by a linear displacement of πr and a rotation of π. The spots are also seen to fall into groups of four, the members of the same group being equidistant from M_1 M_2. Each figure resolves thus into a superposition of three of the type of fig. 2 *a*.

The only measurements which have to be made are the coordinates of the spots referred to a pair of axes parallel and perpendicular respectively to M_1 M_2 and the distance of the axis of rotation from the plate. In evaluating the measurements, the procedure followed consisted in first taking the difference $2y$ of the ordinates of the upper and lower pairs in each group. η was then calculated from (1) and α' from (4). Next, x was obtained from either (2) or (3), and hence the values of $2(r\alpha' + x)$ in (10). Then, by inspection of the photograph, it was ascertained whether the latter values were identical with the distances separating the upper or lower pairs of the various groups, and so, too, whether the mid-point of a pair corresponded with a normal in

the position $\alpha=0$ or $\alpha=\pi$. The azimuths of the normals reckoned from some plane common to the two crystals and containing the axis of rotation, *e.g.* that corresponding to M_1 or M_2, were then determined. The results for the two crystals are exhibited in the following table, in which the azimuths are all reckoned from that of the first normal taken as zero.

Upper Crystal.

	α.	η.	χ.
	° ′	° ′	°
1	0 0	54 51	(23) 89 58
2	96 44	79 45	(31) 89 52
3	200 40	36 50	(12) 89 32

Lower Crystal.

	α.	η.	χ.
	° ′	° ′	° ′
1	68 48	87 9	(23) 89 1
2	160 43	56 33½	(31) 89 34
3	335 9	32 25	(12) 90 18

The interaxial angles χ were also calculated with the aid of the well-known formula :

$$\cos\chi=\cos\eta_1\,.\,\cos\eta_2\,.\,+\sin\eta_1\,.\,\sin\eta_2\,.\,\cos(\alpha_1-\alpha_2),$$

where the symbols have an obvious significance and their values are given in the last column. Their deviations from the theoretical value of 90° afford an estimate of their accuracy.

Denoting the axes 1, 2, 3, of the upper crystal by the symbols X_1, Y_1, Z_1, and those of the lower crystal by X_2, Y_2, Z_2, the angles included between the axes of the two crystals are shown below.

	X_1.	Y_1.	Z_1.
	°	°	°
X_2	71·1	28·7	111·1
Y_2	109 1	62·7	34·5
Z_2	27·8	97·3	63·3

On inspection of these figures, we observe that, among the nine angles, there seem to be three pairs of nearly equal angles: viz., $Y_1\ X_2 = 28°{\cdot}7$ and $X_1\ Z_2 = 27°{\cdot}8$; $Z_1\ X_2 = 111°{\cdot}1$ and $X_1\ Y_2 = 109°{\cdot}1$; and $Y_1\ Y_2 = 62°{\cdot}7$ and $Z_1\ Z_2 = 63°{\cdot}3$, where $Y_1\ X_2$ denotes the angle between Y_1 and X_2 etc. If these angles are in reality equal, it is seen that one crystal is the image of the other; and taking 28°, 110°, and 63° as the mean values of the three pairs respectively, the symmetry plane is found to have the indices $(4\bar{5}2)$ *. The crystals form thus a kind of twin, though this may be accidental, since the most common twinning plane with cubic crystals is the (111).

From the mode of preparation of these crystals, there is no obvious reason to suspect that they lie otherwise than at random. The data obtained from the two crystals here examined are scarcely sufficient to test this conclusion, but we may avail ourselves of the results found by F. Yoshida and K. Tanaka †. They prepared aluminium crystals after the same method, and determined their orientations by a modification of the Laue method, using a divergent pencil of heterogeneous X-rays. The results for the co-latitudes of the cubic axes measured from the axis along which stretching had occurred (identical in our case with the axis of rotation) are given in the first six columns of the following table, and our results in the last two columns. Their values for the azimuths are not available.

Crystal		1	2	3	4	5	6	7	8
		°	°	°	°	°	°	°	°
η		87	87	85	88	89	89	80	87
		62	57	65	63	61	61	55	56·5
		29	34	26	27	28	30	37	32·5

The observation made by Yoshida and Tanaka, that these angles are for each crystal nearly the same and that each crystal has one axis nearly perpendicular to the direction of stretching, is more or less borne out. It may be pointed out, however, that, when the crystals are distributed at random, the latter circumstance is only to be

* The actual values found for the indices are 4·00, −5·15, 2·00.

† N. Yoshida and K. Tanaka, 'Nature,' p. 913, Dec. 1926.

expected, since the average values of the greatest, intermediate, and least angles included between the cubic axes and an arbitrary line are respectively

$$81°,\quad 58°{\cdot}5,\text{ and }36°,$$

approximately. These values are found by actually taking averages for the directions of the arbitrary line given by all the indices between [600], [660], and [666]; *i. e.*, the directions obtained by substituting all possible combinations of the integers 0, 1, 2, 3 ... 6 for the two noughts in the first.

From the results of Yoshida and Tanaka, it is seen that the individual values, and hence also the averages, viz.

$$87°{\cdot}5,\quad 61°{\cdot}5,\text{ and }29°\text{ respectively,}$$

show consistent deviations from the theoretical values (except for the angle 57° of crystal 2 in the table) ; and so it seems that the crystals are not orientated at random about the direction of stretching, which lends favour to the view that the crystals grow more readily when stretched in a certain direction.

This, again, is contradicted by the present results, where the deviations from the theoretical values seem more haphazard.

In conclusion, I should like to express my thanks to Professors A. D. Fokker and H. B. Dorgelo, the former for suggesting this research, and both for the interest they have shown during its progress. I am particularly indebted to Mr. P. van den Akker, chief of the workshop, for his skill and resourcefulness in constructing the apparatus.

The Physical Laboratories,
College of Technology,
Delft, Holland.

LXXIX. *A Theory of the Birefringence induced by Flow in Liquids.* *By* Prof. C. V. Raman, *F.R.S.*, *and* K. S. Krishnan *.

1. *Introduction.*

THAT a viscous liquid such as Canada balsam exhibits optical anisotropy when mechanically agitated appears to have been first observed by Clerk Maxwell. The subject was later pursued by other investigators, notably by Kundt and his pupils, whose work will be found well summarized in an article by G. de Metz †. An extensive series of observations on the subject has been made recently by Vorländer and Walter ‡ with the arrangement, originally suggested by Maxwell, of placing the liquid in the gap between two coaxial cylinders and rapidly rotating the inner cylinder. A beam of plane-polarized light traversed the column of liquid in a direction parallel to the axis of the cylinders, and with the help of a suitable analyser and an auxiliary spectroscope, measurements were made of the birefringence exhibited by it. Vorländer and Walter examined in this way no fewer than 172 liquids, and have greatly extended our knowledge of the subject. An important outcome of their work is to show that mechanical birefringence is observable in numerous common liquids having a definite chemical composition, including several which do not possess an exceptionally high viscosity ; they found also that careful purification and removal of suspended "colloidal" matter from the liquids studied, by vacuum distillation, leaves the birefringence unaffected. Their work obliges us to conclude that the power to exhibit birefringence under mechanical flow is just as much a characteristic of pure liquids as, for instance, the power of exhibiting birefringence when placed in an electrostatic field.

It is proposed in this paper to develop a molecular theory of mechanical birefringence in liquids based on ideas somewhat similar to those successfully employed by Langevin and Born to explain electric double-refraction in liquids. The birefringence is regarded as arising from the optical anisotropy of the molecules, taken together with a tendency for them to orientate under the mechanical stresses within

* Communicated by the Authors.

† G. de Metz, *Scientia*, Gauthier-Villars, no. 26, Jan. 1906; see also Winkelmann's 'Handbuch der Physik,' Optik, pp. 1230–1236 (1906).

‡ D. Vorländer and R. Walter, *Zeits. Phys. Chem.* vol. cxviii. p. 1 (1925).

the fluid. The effective cause of such orientation is taken to be the non-spherical shape of the molecules.

It will be seen in the sequel that the theory succeeds not only in explaining the general features of the observed phenomena, but also in giving a value for the "Maxwell constant" in good agreement with observation.

2. *Molecular Orientation in Flowing Liquid.*

Stokes, in his memoir * on the internal friction of fluids, discussed the character of the stresses arising from viscous flow, and showed that in the case of a simple sliding motion

Fig. 1.

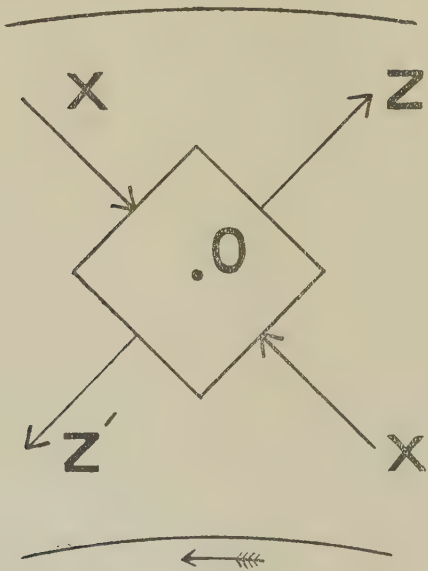

parallel to a plane the tangential stresses acting along the plane may be replaced by two sets of stresses, one set consisting of tensions and the other set of pressures acting along two directions which are mutually perpendicular and inclined at 45° to the line of flow. The direction of the tensions is parallel to the axis of extension and of the pressures to the axis of compression (see fig. 1, which represents a section of the fluid between the two cylinders, perpendicular to their common axis). The inner cylinder is assumed to rotate in the direction of the arrow, the outer one remaining fixed. The tensions and pressures shown in the figure are

* Sir George Stokes, Math. and Phys. Papers, Camb. Univ. Press, vol. i. p. 91.

each equal to $\eta \frac{v}{c}$ per unit area, where η is the coefficient of viscosity and $\frac{v}{c}$ is the radial velocity-gradient at O.

It is clear that if the molecules are highly asymmetrical in shape, the set of tensions and pressures pictured in fig. 1 would tend to cause them to orient in the fluid, in such manner that the longest dimension of a molecule lies along the axis of tensions and the shortest one along the axis of pressures. For such orientation would evidently result in the fluid (regarded as a densely-packed assemblage of molecules) expanding along the axis of z and contracting along the axis of x, the total volume remaining constant, thus allowing the system of stresses acting in the medium to do work. This orientative tendency of the molecules is, however, opposed by their thermal agitation, which tends to throw them into disarray. The resulting state of statistical equilibrium can be found by an application of the Boltzmann Principle.

In order to define the orientations of the molecules, we choose (see fig. 1) the direction of tension as the z-axis, the direction of pressure as the x-axis, and a direction perpendicular to these two (*i. e.* parallel to the common axis of the cylinders) as the y-axis, of a coordinate system $x\ y\ z$ fixed in space. We also consider the principal geometrical axes of each molecule as the axes of another coordinate system $\xi\ \eta\ \zeta$ fixed in it. Let the orientations of these axes with reference to the axes of the former system be given by the Eulerian angles θ, ϕ, ψ. Then the cosines of the various angles between the two sets of axes are as below :—

TABLE I.

	x.	y.	z.
ξ	$\alpha_{11} = \cos\theta\cos\phi\cos\psi - \sin\phi\sin\psi$.	$\alpha_{12} = \cos\theta\sin\phi\cos\psi + \cos\phi\sin\psi$.	$\alpha_{13} = -\sin\theta\cos\psi$.
η	$\alpha_{21} = -\cos\theta\cos\phi\sin\psi - \sin\phi\cos\psi$.	$\alpha_{22} = -\cos\theta\sin\phi\sin\psi + \cos\phi\cos\psi$.	$\alpha_{23} = \sin\theta\sin\psi$.
ζ	$\alpha_{31} = \sin\theta\cos\phi$.	$\alpha_{32} = \sin\theta\sin\phi$.	$\alpha_{33} = \cos\theta$.

For allowing the Principle of Boltzmann to be applied to our present problem, we require an expression for the

potential energy of each molecule in the fluid in terms of its orientation with respect to the fixed coordinate axes $x\,y\,z$. A suitable form of expression is suggested by the following considerations. The stress acting in the medium is, as we have seen, $\eta\frac{v}{c}$, and if we divide this by the number of molecules ν per unit volume in the fluid, we obtain a quantity $\eta\frac{v}{c}\cdot\frac{1}{\nu}$, which has the physical dimensions of energy. It is therefore permissible to assume that the energy of each molecule, as determined by its orientation with respect to the axes of these stresses, is proportional to $\eta\frac{v}{c}\cdot\frac{1}{\nu}$, the coefficient of proportionality being a function of the angle-variables, which is physically dimensionless. Since by hypothesis the orientation of the molecules arises from their non-spherical shape, and since the positive and negative directions are necessarily equivalent, the potential energy of a molecule will remain unaffected if we rotate it through 180° round any of the ξ-, η-, ζ-axes.

In view of what has been said above, and considering for the present only the effect of the *tensions* along the z-axis, we may assume the potential energy of each molecule to be given by the expression

$$u=-(\omega_1\alpha_{13}^2+\omega_2\alpha_{23}^2+\omega_3\alpha_{33}^2)\cdot\eta\frac{v}{c}\cdot\frac{1}{\nu}, \qquad (1)$$

where ω_1, ω_2, ω_3 are constants determined by the geometric form of the molecule, which will later be evaluated. Then, from Boltzmann's theorem, the number of molecules per unit volume whose orientations, when under thermal equilibrium, are given by the range $\sin\theta\,d\theta\,d\phi\,d\psi$, is equal to

$$Ce^{-\frac{u}{kT}}\sin\theta\,d\theta\,d\phi\,d\psi, \qquad (2)$$

where C is the constant given by the relation

$$\nu=C\int_{\theta=0}^{\theta=\pi}\int_{\phi=0}^{\phi=2\pi}\int_{\psi=0}^{\psi=2\pi}e^{-\frac{u}{kT}}\sin\theta\,d\theta\,d\phi\,d\psi. \qquad (3)$$

In the orientated state the average potential energy per molecule in the medium is given by

$$u=\frac{\iiint e^{-\frac{u}{kT}}u\sin\theta\,d\theta\,d\phi\,d\psi}{\iiint e^{-\frac{u}{kT}}\sin\theta\,d\theta\,d\phi\,d\psi}$$

the limits of integration being the same as in (3),

$$= -\frac{\omega_1+\omega_2+\omega_3}{3} \cdot \eta \frac{v}{c} \cdot \frac{1}{\nu} - \frac{2}{45kT}\left[(\omega_1-\omega_2)^2+(\omega_2-\omega_3)^2 + (\omega_3-\omega_1)^2\right] \cdot \left(\eta \frac{v}{c} \cdot \frac{1}{\nu}\right)^2 . \quad . \quad (4)$$

If, on the other hand, the molecules are orientated entirely at random, then the average energy per molecule will be given by

$$\bar{u}_0 = \frac{\iiint u \sin\theta \, d\theta \, d\phi \, d\psi}{\iiint \sin\theta \, d\theta \, d\phi \, d\psi} = -\frac{\omega_1+\omega_2+\omega_3}{3} \cdot \eta \frac{v}{c} \cdot \frac{1}{\nu} . \quad . \quad . \quad . \quad . \quad (5)$$

The difference $u_0 - \bar{u}$ multiplied by ν gives the diminution of potential energy per unit volume in orientating the molecules contained in it, and is equal to

$$(\bar{u}_0 - \bar{u})\nu = \frac{2}{45kT}\left[(\omega_1-\omega_2)^2+(\omega_2-\omega_3)^2 + (\omega_3-\omega_1)^2\right] \cdot \left(\eta \frac{v}{c}\right)^2 \cdot \frac{1}{\nu} . \quad (6)$$

3. *The Optical Effect of Molecular Orientation.*

We now proceed to find the double refraction which arises from this orientation of the molecules, here again confining our attention at first to the result of the tensions acting along the z-axis. Since the optic axes of the molecule will not, in general, coincide with its geometric axes $\xi\,\eta\,\zeta$, when a field (due to a light-wave) is incident along any one of these axes, say along the ξ-axis, the moment induced in the molecule will not be wholly along the ξ-axis, but will have components also along the η- and ζ-axes. Thus for unit field actually acting on the molecule along the ξ-axis, let b_{11}, b_{12}, b_{13} be the moments induced in it along its ξ-, η-, and ζ-axes respectively; and let b_{21}, b_{22}, b_{23}, and b_{31}, b_{32}, b_{33} be similar induced moments for unit field acting along the η- and ζ-axes respectively: $b_{ij}=b_{ji}$. We have two special cases to consider.

Case I.—The electric vector of the incident light-wave lies along the z-axis—*i. e.*, along the direction of the tension.

Let the optical field actually acting on each molecule in the same direction be denoted by E. Then the moments induced in the molecule under consideration along its axes,

when resolved along the direction of E, are together equal to

$$(b_{11}\alpha_{13}^2+b_{22}\alpha_{23}^2+b_{33}\alpha_{33}^2+2b_{12}\alpha_{13}\alpha_{23}+2b_{23}\alpha_{23}\alpha_{33}+2b_{31}\alpha_{33}\alpha_{13})\mathrm{E} \quad . \quad . \quad . \quad (7)$$

$$=m_z\mathrm{E}, \text{ say.} \quad . \quad . \quad . \quad . \quad . \quad . \quad . \quad (8)$$

Then the average value of m_z taken over all the molecules in the medium will be given by

$$\bar{m}_z=\frac{\iiint e^{-\frac{u}{kT}} m_z \sin\theta\, d\theta\, d\phi\, d\psi}{\iiint e^{-\frac{u}{kT}} \sin\theta\, d\theta\, d\phi\, d\psi}$$

$$=\frac{b_{11}+b_{22}+b_{33}}{3}+2\Theta\eta\frac{v}{c}\cdot\frac{1}{\nu}, \quad . \quad . \quad . \quad (9)$$

where

$$\Theta=\frac{1}{45kT}[(\omega_1-\omega_2)(b_{11}-b_{22})+(\omega_2-\omega_3)(b_{22}-b_{33}) +(\omega_3-\omega_1)(b_{33}-b_{11})]. \quad . \quad (10)$$

Case II.—The light-vector lies along the x-axis.

Let us denote the actual field acting on each molecule along the x-axis by E. The moments induced in any molecule along its axes, when resolved along the x-axis, are together equal to

$$(b_{11}\alpha_{11}^2+b_{22}\alpha_{21}^2+b_{33}\alpha_{31}^2+2b_{12}\alpha_{11}\alpha_{21}+2b_{23}\alpha_{21}\alpha_{31}+2b_{31}\alpha_{31}\alpha_{11})\mathrm{E} \quad . \quad . \quad . \quad (11)$$

$$=m_x\mathrm{E}, \text{ say.} \quad . \quad . \quad . \quad . \quad . \quad . \quad . \quad (12)$$

The average value of m_x taken over all the molecules can be calculated as in the previous case, and comes out equal to

$$\bar{m}_x=\frac{b_{11}+b_{22}+b_{33}}{3}-\Theta\eta\frac{v}{c}\cdot\frac{1}{\nu}. \quad . \quad . \quad . \quad (13)$$

From (9) and (13)

$$\bar{m}_z-\bar{m}_x=3\Theta\eta\frac{v}{c}\cdot\frac{1}{\nu}. \quad . \quad . \quad . \quad (14)$$

Hitherto we have considered only the effect of the tensions $\eta\frac{v}{c}$ acting along the z-axis. The effect of the pressures of the same magnitude acting along the x-axis can be calculated in exactly the same way by considering them as tensions $=-\eta\frac{v}{c}$ along the x-axis, and thus we get

$$\bar{m}_x-\bar{m}_z=3\Theta\times-\eta\frac{v}{c}\cdot\frac{1}{\nu}.$$

Thus, when the two effects are superposed, as in the actual liquid, we get for the difference in the values of the mean induced moments, for directions of vibration of the incident light along the z- and x-axes, the expression

$$\bar{m}_z - \bar{m}_x = 6\,\Theta\,\eta\,\frac{v}{c}\cdot\frac{1}{\nu}. \quad . \quad . \quad . \quad . \quad (15)$$

If we denote by n_z and n_x the refractive indices of the medium for light-vibrations along the z- and the x-axes respectively, by differentiating the well-known expression for refractivity

$$\frac{n^2-1}{n^2+2} = \frac{4\pi}{3}\nu\,.\,m, \quad . \quad . \quad . \quad . \quad . \quad (16)$$

we have

$$n_z - n_x = \frac{(n^2-1)(n^2+2)}{6n}\cdot\frac{\bar{m}_z-\bar{m}_x}{m}$$

$$= \frac{(n^2-1)(n^2+2)}{n}\cdot\frac{\Theta}{m}\cdot\eta\frac{v}{c}\cdot\frac{1}{\nu}, \quad . \quad . \quad (17)$$

where n is the refractive index and m is the mean moment induced in a molecule per unit field actually acting on it, in the randomly orientated state of the molecules. Obviously

$$m = \frac{b_{11}+b_{22}+b_{33}}{3}. \quad . \quad . \quad . \quad . \quad . \quad (18)$$

All the quantities in expression (17) for the birefringence of the medium are experimentally determinable, except Θ, which involves, as is evident from (10), the optical constants of the molecule and the constants ω_1, ω_2, ω_3 appearing in expression (1) for the potential energy. We shall now proceed to consider how the quantities ω_1, ω_2, ω_3 may be connected with the geometric form of the molecules.

4. *Molecular Shape and Molecular Orientation.*

Since, by hypothesis, the orientation of the molecules is the result of their non-spherical form, we may proceed to connect them in the following way. We idealize the molecules and consider them to have the form of ellipsoids with three unequal diameters, a_1, a_3, a_3. If we imagine the molecules to be arranged in contact with each other, their axes parallel, in the form of a rectangular parallelopiped having s molecules in each of its edges, the length of the latter would be sa_1, sa_2, sa_3 respectively. This is an extreme case, which illustrates the general principle that the effect of any general tendency of the molecules to orientate in

specific directions is to cause the density of molecules per unit length in different directions to become different. It is difficult to express this principle with complete precision in a mathematical form, particularly in the case of liquids, where the molecules are not always necessarily in contact with each other. Considering, however, the fact that the density of the type of liquid with which we are concerned here is usually not very different from that in the solidified state, the error in considering the molecules to be in contact with each other all the time would not be serious in any event ; and since we are only concerned with ratios, the inaccuracy involved can practically be eliminated by considering the "effective" dimensions of a molecule in the liquid to be slightly different from what they are in the solidified state. Subject to these remarks, we may assume that a molecule arbitrarily orientated contributes to the linear dimension of the aggregate measured along the z-axis a length equal to

$$a_1\alpha_{13}^2 + a_2\alpha_{23}^2 + a_3\alpha_{33}^2. \quad . \quad . \quad . \quad . \quad (19)$$

If the molecules are arbitrarily orientated, the average effective length of the molecule along the z-axis is simply

$$\frac{\iiint (a_1\alpha_{13}^2 + a_2\alpha_{23}^2 + a_3\alpha_{33}^2) \sin\theta \, d\theta \, d\phi \, d\psi}{\iiint \sin\theta \, d\theta \, d\phi \, d\psi} = \frac{a_1+a_2+a_3}{3}; \quad . \quad . \quad . \quad . \quad . \quad (20)$$

that is to say, the mean of the three diameters of the ellipsoid. Considering, however, the tendency of the molecules to orientate, due to the tensions along the z-axis in the fluid, we find the average length to be

$$\frac{\iiint e^{-\frac{u}{kT}} (a_1\alpha_{13}^2 + a_2\alpha_{23}^2 + a_3\alpha_{33}^2) \sin\theta \, d\theta \, d\phi \, d\psi}{\iiint e^{-\frac{u}{kT}} \sin\theta \, d\theta \, d\phi \, d\psi},$$

where u is given by expression (1),

$$= \frac{a_1+a_2+a_3}{3} + \frac{2}{45kT}\left[(\omega_1-\omega_2)(a_1-a_2) + (\omega_2-\omega_3)(a_2-a_3) + (\omega_3-\omega_1)(a_3-a_1)\right]\eta\frac{v}{c}\cdot\frac{1}{\nu}. \quad (21)$$

The difference between (21) and (20) divided by (20) gives the effective expansion per unit length, along the z-axis, owing to the orientation of the molecules, as

$$\frac{2}{15kT}\cdot\frac{(\omega_1-\omega_2)(a_1-a_2)+(\omega_2-\omega_3)(a_2-a_3)+(\omega_3-\omega_1)(a_3-a_1)}{a_1+a_2+a_3}\times\eta\frac{v}{c}\cdot\frac{1}{\nu}. \quad . \quad . \quad . \quad . \quad (22)$$

Multiplying this by the tension $\eta\frac{v}{c}$ along the z-axis, we obtain the work done per unit volume resulting from the orientation of the molecules contained in it, an expression for which was obtained in an entirely different way in (6) above. Equating the two expressions, we have

$$(\omega_1-\omega_2)^2+(\omega_2-\omega_3)^2+(\omega_3-\omega_1)^2 = 3\frac{(\omega_1-\omega_2)(a_1-a_2)+(\omega_2-\omega_3)(a_2-a_3)+(\omega_3-\omega_1)(a_3-a_1)}{a_1+a_2+a_3} \quad . \quad . \quad . \quad (23)$$

The form of the equation immediately suggests as a solution

$$\frac{\omega_1-\omega_2}{a_1-a_2}=\frac{\omega_2-\omega_3}{a_2-a_3}=\frac{\omega_3-\omega_1}{a_3-a_1}=\frac{3}{a_1+a_2+a_3}, \quad . \quad (24)$$

which is readily seen to satisfy (23). For the special cases in which the molecule has the form of a prolate or oblate spheroid of revolution, the validity of (24) is rigorously demonstrable, and it seems justifiable to assume that it is generally true.

5. *Expression for the Maxwell Constant.*

Substituting (24) in (17) and (10) we obtain as the final expression for the birefringence

$$n_z-n_x=\frac{(n^2-1)(n^2+2)}{5n\nu kT}\times\frac{(a_1-a_2)(b_{11}-b_{22})+(a_2-a_3)(b_{22}-b_{33})+(a_3-a_1)(b_{33}-b_{11})}{(a_1+a_2+a_3)(b_{11}+b_{22}+b_{33})}\times\eta\frac{v}{c}. \quad . \quad . \quad . \quad . \quad . \quad . \quad . \quad . \quad (25)$$

$$=\nabla\cdot\eta\frac{v}{c}, \quad . \quad . \quad . \quad . \quad . \quad . \quad . \quad . \quad (26)$$

where ∇ is the constant of mechanical birefringence in the fluid, which may appropriately be called the Maxwel

constant, in honour of the discoverer of the effect. It will be seen from the equation that the value of the constant depends jointly upon the optical anisotropy of the molecule and upon the anisotropy of its geometric form.

We shall now proceed to consider how the theory set out above compares with the phenomena as observed in their general features.

Axes of Birefringence.—The theory indicates in agreement with observation that the two principal directions of vibration are mutually perpendicular, and inclined at 45° to the plane of sliding within the liquid.

Positive or Negative Birefringence?—The theory indicates that the sign of the birefringence depends on whether the expression

$$[(a_1-a_2)(b_{11}-b_{22})+(a_2-a_3)(b_{22}-b_{33})+(a_3-a_1)(b_{33}-b_{11})] \quad . \quad . \quad . \quad (27)$$

is positive or negative. It is easily seen that if $a_1>a_2>a_3$ and $b_{11}>b_{22}>b_{33}$, the expression in question is positive and the birefringence is therefore positive, while if $a_1>a_2>a_3$ and $b_{11}<b_{22}<b_{33}$, the birefringence will be negative. In other words, the sign of the double refraction depends on whether the optical constants of the molecule along its three axes follow the same sequence as the linear dimensions or follow the reverse order. If we can regard the chemical molecule as roughly equivalent to an ellipsoid of isotropic dielectric material, the former condition would be satisfied. It is thus readily understood why the great majority of the liquids examined by Vorländer and Walter exhibit positive birefringence. In fact, the only cases of negative birefringence contained in their table of results are the sodium and potassium salts of some of the higher fatty acids; the corresponding fatty acids themselves show positive birefringence.

Influence of Speed, Viscosity, and Temperature.—The theory indicates that the observed birefringence should be proportional to the speed of rotation. The experimental evidence appears to indicate that this is actually the case with most pure liquids. Where divergences appear, it seems not unlikely that they are due to disturbing causes, *e. g.*, departure from the assumed stream-line flow of the liquid, or a rise of the temperature of the liquid as a result of the rotation. The theory indicates a rapid fall of the birefringence with rising temperature, primarily because of the fall of the viscosity, the variation of the Maxwell constant itself with temperature being much less important. The experimental evidence fully supports this inference from theory.

Influence of Molecular Form.—The theory shows that, apart from the viscosity of the liquid, the birefringence should be specifically influenced by the form of the molecule, being greatest when the molecule is highly elongated and least when its form approaches spherical symmetry. The observations of Vorländer and Walter furnish ample evidence in support of this. They found that increasing the length of the chain in the fatty acid series increased the specific birefringence (or Maxwell constant as we call it), and introducing side-chains in the molecule diminishes it notably.

Influence of Optical Anisotropy.—The theory indicates that for molecules of given form the Maxwell constant should increase with increasing optical anisotropy and with increasing refractive index. Now it is known that organic liquids of the aromatic series exhibit in light-scattering a much higher degree of optical anisotropy than the aliphatic series, besides having usually a higher refractive index. On the other hand, the geometry of the benzene ring ensures a greater symmetry of form for simple benzene derivatives than for the aliphatic compounds. The two effects would thus set each other off to a considerable extent in the case of the simpler benzene derivatives. If, however, we consider long-chain compounds in which the benzene ring also appears, we may reasonably expect the increased optical anisotropy to manifest itself in an increased value for the Maxwell constant. Similarly it is known from observations on light-scattering that unsaturated carbon compounds show a high degree of optical anisotropy, and it follows that they should have a large Maxwell constant. Ample support for these inferences from theory is furnished by the observations of Vorländer and Walter.

Dispersion of Double-Refraction.—From our formula it will be seen that the wave-length does not appear explicitly in our formula. Since, however, the Maxwell constant is proportional to $(n^2-1)(n^2+2)/n$, where n is the refractive index, a not negligible degree of dispersion may be expected, as has indeed been observed in experiment.

6. *Absolute Value of Birefringence.*

To calculate the Maxwell constant for any liquid, we require to know the refractive index of the liquid, its molecular weight and density, the optical anisotropy of the molecules and their geometric form. The optical anisotropy of the molecules can be completely determined from measurements of the light-scattering in the liquid if the molecule has an axis of symmetry, and can at least be estimated in other cases from such measurements. The geometrical form

of the molecules is known, at least approximately, from chemical considerations and from X-ray studies. It is thus possible to calculate the value of the Maxwell constant absolutely for any liquid for which the data referred to above are available. Unfortunately, few of the liquids for which the mechanical birefringence is known have been investigated for light-scattering. We may, however, test the theory in the following way. The range of variation of the quantities appearing in the expression for the Maxwell constant is well known. The refractive index of most organic liquids ranges between 1·4 and 1·7. The ratio of molecular weight to density for the type of compounds under consideration ranges between 80 and 240. The ratio of the longest to the shortest dimension of the molecule may of course range theoretically from 1 to large values, but practically it may be taken as lying between 2 and 5 for most compounds which are liquids and show an appreciable birefringence under flow. The ratio of the maximum and minimum polarizabilities of the molecule along its different axes is known from the extensive investigations on light-scattering carried on at Calcutta for different types of organic compounds. It is usually about 1·1 for aliphatic hydrocarbons and saturated cyclo-compounds, 1·5 for aliphatic compounds containing strongly refractive groups, 1·9 for simple benzene derivatives, and about 2·3 for very highly anisotropic compounds such as chloronaphthalene, quinolene *, etc. We may group the data in such order as to have four representative classes, in which we have respectively very low, moderate, high, and very high values of the Maxwell constant as theoretically calculated. This has been done in Table II., in which, for simplicity of calculation, the molecule is assumed to have an axis of symmetry. The temperature assumed is 293° absolute.

For comparison with the values shown in Table II. we have analysed the data given by Vorländer and Walter in their paper. Of the 172 liquids studied, 37 were of very low viscosity and naturally did not yield any results. 15 other liquids having moderate or high viscosities also showed no indication of birefringence. This is not surprising in view of the fact that their optical arrangements did not permit a difference of path of less than 2 millimicrons to be detected. A liquid of moderately high viscosity, say 50 times that of water and having a Maxwell constant less than $0{\cdot}01 \times 10^{-9}$, would have shown no detectable birefringence in their experiments. The limit of detectability would

* These values give the *effective* anisotropies determined from observations of light-scattering in *the liquid state*.

be correspondingly larger for liquids of lower viscosity. It appears certain that an adequate explanation (viz., a low viscosity, or an insufficient optical or geometric anisotropy

TABLE II.—Calculated values of the Maxwell constant.

Class.	Refractive index.	Ratio of molecular weight to density.	Ratio of geometric axes $\frac{a_1}{a_2}=\frac{a_1}{a_3}$.	Ratio of optic axes $\frac{b_{11}}{b_{22}}=\frac{b_{11}}{b_{33}}$.	Maxwell constant $\times 10^9$.
I.....	1·4	80	2	1·1	0·03
II.....	1·5	120	3	1·5	0·4
III.....	1·6	180	4	1·9	1·5
IV.....	1·7	240	5	2·3	3·7

of the molecules) would be forthcoming in most cases in which they failed to detect any effect. It must also be remembered that in the expression

$$(a_1-a_2)(b_{11}-b_{22})+(a_2-a_3)(b_{22}-b_{33})+(a_3-a_1)(b_{33}-b_{11})$$

appearing in the Maxwell constant, b_{11}, b_{22}, b_{33} are the optical polarizabilities of the molecule, *not along its optic axes, but along its geometric axes.* Consequently, special cases may arise, if the optic and geometric axes are suitably inclined to each other, when the above expression will have very small values, even if the molecule possesses a large geometric and optical anisotropy.

Excluding the 52 liquids in which no effect was found, and the 12 compounds of potassium and sodium with the fatty acids which showed a negative birefringence, we have 108 liquids in which a normal effect was observed. From the dimensions of their apparatus (length of liquid column 4·68 cm., radii of the cylinders 1·15 cm. and 1·05 cm., and width of gap therefore =0·10 cm.), and the known viscosity of water at 20° C., relative to which the values for the different liquids are expressed, and the specific birefringence as tabulated by them, the values of the Maxwell constant in C.G.S. units can be ascertained. In Table III. the observed values of the Maxwell constant have been grouped into five classes and are shown for comparison with the figures in Table II.

It appears highly significant that the observed values for the great majority of the liquids cluster round that calculated on the reasonable assumptions that the refractive index is about 1·5, the molecular weight about 120, the density about 1, the ratio of length of the molecule to its thickness

TABLE III.—Observed values of the Maxwell constant ($\times 10^9$) for 108 liquids.

Observed values of $\nabla \times 10^9$.	Below 0·03.	Between 0·03 and 0·4.	Between 0·4 and 1·5.	Between 1·5 and 3·7.	Above 3·7.
Number of aliphatic and hydro-aromatic liquids.	12	44	12	—	—
Number of aromatic liquids.	—	22	15	2	1

about 3, and the ratio of its maximum and minimum optical polarizabilities about 1·5. It is equally significant that all the low values of the Maxwell constant belong to the aliphatic or hydro-aromatic compounds, and all the high values to the aromatic compounds, and that the average values for the two sets of compounds differ just in the way we should expect in view of the greater refractive index and optical anisotropy of benzene and its derivatives.

Finally, as an example of the degree of quantitative agreement to be expected, we shall take the case of *n*-octyl alcohol. We may approximately consider this as a prolate spheroid whose major axis is 12·6 Å.U. and whose minor axis is 4·9 A.U. Its refractive index is 1·430 and the molecular weight is 130·1.

The scattering of light in octyl alcohol has not been studied. We have, however, data for heptane and octane and also for ethyl, propyl, butyl, and amylic alcohols, and for all these compounds, assuming the optical ellipsoids of the molecules to be also prolate spheroids of revolution whose axes coincide with their respective geometric axes, the ratio $b_{11} : b_{22}$ is equal to 1·15. We may therefore with confidence assume the same value for *n*-octyl alcohol. From these data we find the Maxwell constant for *n*-octyl alcohol to be

$$\textit{Calculated value of } \nabla = 0{\cdot}125 \times 10^{-9}.$$

From the measurements of Vörlander and Walter, taking the viscosity of octyl alcohol at 20° C. = 0·0895 (Landolt Tables),

$$\textit{Observed value of } \nabla = 0{\cdot}13 \times 10^{-9}.$$

7. *Summary.*

In this paper a theory is developed for the effect discovered by Maxwell—viz., that a liquid in a state of viscous flow exhibits birefringence. The state of stress in the fluid consists of tensions and pressures in directions perpendicular to each other and inclined at 45° to the plane of sliding.

When the molecules have an elongated form, these stresses tend to orientate them so that their direction of greatest length lies along the axis of tension, and that of shortest length along the axis of pressure. The tendency to orientation is, however, resisted by their thermal agitation, and the resulting state of statistical equilibrium may be found by the application of Boltzmann's Principle. The optical anisotropy of the molecules, taken together with the orientations referred to, causes the medium to become birefringent. The magnitude of the effect is proportional to the product of the viscosity and the velocity-gradient. The constant of proportionality, which is referred to as the Maxwell constant for the liquid, is evaluated in terms of the optical and geometrical anisotropies of the molecule, the refractive index, density, and molecular weight of the liquid, and Boltzmann's constant.

The data for 172 liquids recently obtained by Vorländer and Walter are critically discussed, and it is shown that the theory succeeds not only in giving an explanation of the general features of the phenomena observed, but also in giving quantitatively the observed values of the Maxwell constant.

210 Bowbazar Street,
Calcutta, India.
September 15, 1927.

LXXX. *Frequency Variations of the Triode Oscillator. A Note on Mr. D. F. Martin's Paper.* *By* Lieut.-Col. K. E. Edgeworth, *D.S.O., M.C., A.M.I.E.E.**

I HAVE just obtained a copy of the Phil. Mag. for November 1927 containing a paper by Mr. D. F. Martin on the Frequency Variations of the Triode Oscillator.

It is evident that the author has overlooked the paper which I read in December 1925 on the same subject before the Institute of Electrical Engineers (Wireless Section).

So far as they cover the same ground, the experimental results appear to be in agreement, and the explanations offered are substantially the same. The main cause of frequency variations is associated with damping of one sort or another in the grid circuit, and, other things being equal, the magnitude of the frequency variation is proportional to the amount of the damping. This type of frequency variation is referred to in my paper as a frequency variation of the first type.

My paper takes matters a good deal further, however. It is shown that the frequency variations of the first type are reversible ; that is to say, the sign depends upon the direction of the coupling. With normal reactive coupling an increase

* Communicated by the Author.

of filament current produces a decrease of frequency, but with reversed reactive coupling the opposite effect is produced. By employing resistance coupling the frequency variation of the first type can be eliminated altogether.

It is mentioned incidentally that, when the grid and anode circuits are tuned to different frequencies, the frequency of the oscillations approximates to the lower resonant frequency with normal coupling and to the higher frequency with reversed coupling.

The paper then proceeds to show that there are other sources of frequency variation which are irreversible ; that is to say, they are independent of the direction of the coupling. They are usually much smaller than the frequency variations of the first type, but assume importance when the grid damping is made small enough.

When an oscillator is employed with an untuned grid circuit and heavy grid bias, the two types of oscillation may cancel out so that a circuit of constant frequency is obtained. It is suggested in the paper that these subsidiary variations are associated with the fact that the ordinary valve oscillator is single-acting, giving its impulses only during one-half of each cycle ; but further research is undoubtedly required to place the matter on a proper footing.

The paper therefore discloses two types of constant frequency circuit ; namely, the resistance coupled circuit and the untuned grid circuit with small grid current. Yet another type of constant frequency circuit is described by Fromy*.

As regards the practical value of these constant frequency circuits, the untuned grid circuit with small grid current is undoubtedly the most convenient for wave-meters, and variations of frequency due to changes in the supply voltage can be reduced to less than one part in 10,000 without any particular difficulty. The necessary grid bias is most conveniently produced by means of a grid leak, as the oscillations are then self-starting. If a battery is used, some special expedient may be necessary for starting the oscillations.

The circuit is also suitable for master oscillators, but has received less attention than it deserves on account of the rapid development of oscillators employing crystal control.

The resistance coupled oscillator is a convenient circuit for small transmitters, and a number of transmitters working on this principle are now under construction for the Sudan Government.

Khartoum, 30th December, 1927.

* ' L'Onde Electrique,' 1925 : 4e année, p. 433.

LXXXI. *Coefficient of Absorption in Lead of the γ-Rays from Thorium C″ and Radium C.* *By* L. Bastings, *M.Sc., B.A., The University, Durham* *.

Introduction.

THE intensity of a beam of homogeneous radiation has in the past been regarded as reduced exponentially by its passage through an absorbing medium, the quality of the transmitted beam meanwhile remaining unaltered. Recently, however, Compton † has shown both theoretically and experimentally, that when the absorption of a beam of X-rays is accompanied by scattering, there is a definite change in the average quality of the beam, corresponding to an increase in the wave-length of the portion scattered. The magnitude of this increase is independent of the wave-length, and is determined only by the angle of scattering. Now, if the same phenomenon also occurs with γ-rays, the effect should be of relatively greater importance, since the increase in wave-length predicted by Compton's theory is comparable, in the γ-ray region, with the wave-length of the incident radiation.

Moreover, it is now generally accepted that in the X-ray region the absorption coefficient is a direct function of the cube of the wave-length; and Ahmad ‡ has furnished evidence to show that the same law is applicable to the γ-ray region.

If, then, a homogeneous beam of γ-rays is in part scattered in passing through a filter, the average wave-length of the emergent beam should be greater, and the absorption coefficient of the beam should also show an increase, which would be greater the larger the amount of scattered radiation included in the emergent beam considered. The absorption would not then be strictly exponential.

Now this quantum theory of Compton further involves a distribution of scattered radiation differing markedly from the classical prediction. The applicability of the theory to γ-rays has recently been tested by Ahmad §, who has found reasonable agreement with the formulæ obtained by Compton for the scattering; but the alteration in absorption coefficient

* Communicated by Prof. Sir E. Rutherford, O.M., P.R.S.

† Compton, Phys. Rev. xxi. p. 483 (1923), xxii. p. 409 (1923); Phil. Mag. xlvi. p. 897 (1923).

‡ Ahmad, Roy. Soc. Proc. A, cv. p. 507 (1924).

§ Ahmad, Roy. Soc. Proc. A, cix. p. 206 (1925).

in the scattered beam was not sufficiently pronounced to substantiate the theory.

Experiments with strictly homogeneous beams of γ-rays are unfortunately impracticable. It is now well established that the radiation emitted by radium in equilibrium, or by its emanation in equilibrium, consists of a number of homogeneous rays, stretching over a range of several octaves. The presence of a continuous background of γ-radiation has been suggested, but not definitely proved.

The case of thorium was believed to be similar: but recently Black * has deduced evidence from β-ray spectra of an isolated γ-ray from Th C'' of very much higher frequency than that of any other monochromatic ray. As we shall see below, this γ-ray must carry a very considerable proportion of the total energy of the radiation, and the effect of filtering through large thicknesses of lead should be to increase very considerably the importance of this ingredient; so that eventually we might expect to produce a beam more nearly homogeneous than any other available. For this purpose it is obvious that a large source of Th C'' must be available.

Previous Experiments.

Although the literature on the absorption coefficient of radium is abundant, very little has been done with thorium. The first measurements were made by Russell and Soddy †, who determined μ in lead, iron, and aluminium in two different experimental dispositions. In the first the absorber was placed next to the source and some distance from the ionization chamber. The values obtained were: in lead 0·462; and in aluminium 0·0916. In the second disposition the absorber formed the base of the ionization chamber, and the sources were placed some distance away. In this case μ in lead was 0·408, and in aluminium 0·0971. In both cases the source was covered with from 6·4 to 10 mm. of lead to absorb the very soft radiation.

Next, Rutherford and Richardson ‡, adopting the first disposition above, measured the coefficient in aluminium, and found that all the softer rays from a Th C source were absorbed in 2 mm. of the metal, and that the residual beam had a coefficient of 0·096 in aluminium of up to 9 cm. in thickness. This result is in approximate agreement with the earlier measurements.

* Black, Roy. Soc. Proc. A, cix. p. 166 (1925).
† Russell & Soddy, Phil Mag. xxi. p. 130 (1911).
‡ Rutherford & Richardson, Phil. Mag. xxvi. p. 937 (1913).

No further experiments seem to have been made with Th C″.

The great amount of work done with radium shows clearly that the experimental disposition very considerably affects the results obtained. Most of the recent work in this field has been directed to distinguishing between the true absorption (photo-electric) and the apparent absorption due to scattering. Obviously, if the absorber is close to the ionization chamber, much of the radiation scattered in the forward direction will enter the chamber, and the observed coefficient will for this reason be smaller than when the absorber is removed to a distance, and so subtends a smaller solid angle at the chamber. This is confirmed in the case of thorium by the results of Russell and Soddy above, and in the case of radium by Ahmad *.

In previous determinations of the coefficient over any considerable thickness of absorber, the method adopted has been to measure the ionization obtained through successively increasing thicknesses of absorber, plotting points representing logarithm of activity against thickness, and, if these are reasonably on a straight line, drawing the best such line through the points. From the slope of this line μ is determined. This method entirely fails to detect any small change in μ as the thickness of absorber is increased.

Experimental Details.

The method adopted in the present experiments consisted in measuring the absorption in a selected piece of material, of accurately known thickness, sufficiently great to reduce the ionization to about one-half. Other absorbers (or "filters") of less accurately measured thickness served, when required, to cut down the intensity of the beam. Thus the actual coefficient in the selected absorber is deducible with great precision for various thicknesses of filter. Since this absorber could be accurately replaced in a specified position, the results should clearly reveal any small change in μ as the thickness of filter is increased.

Since the chief aim was to investigate a possible change in μ due to the influence on the absorption of the rays scattered in the forward direction, the absorber was placed in immediate contact with the outside of the ionization chamber. The source was kept in a fixed position, and as close to the chamber as to allow just sufficient room for the insertion of the maximum thickness of filter employed. The

* Ahmad, Roy. Soc. Proc. A, cvi. p. 507 (1924).

electroscope was completely covered externally with 3 mm. of lead. The absorber consisted of ten layers of sheet-lead (99½ per cent. purity), aggregating $1{\cdot}62_5$ cm. in thickness and 13 cm. square. The source was enclosed in a sealed glass tube inserted in a cavity in a lead block so that the rays had to penetrate walls of minimum thickness 2·4 cm. The face of the block was placed 8·5 cm. from the outer surface of the electroscope, and two lead filters $13 \times 13 \times 3{\cdot}4$ cm. could be inserted between this and the standard absorber. Thus attention was concentrated on measuring the coefficient in this standard absorber when the rays were filtered in turn through 2·4, 5·8, and 9·2 cm. of lead.

The Sources.

Two Th C″ sources have been used. Both were radiothorium preparations obtained from mesothorium by precipitation with ammonium hydroxide with the aid of a trace of added thorium. The precipitates were dried and sealed up in glass tubes about 6 mm. in diameter and 5 cm. long. The actual material occupied less than ¼ c.c. and so they may be regarded as point sources. The precipitates, a week after being sealed up, had grown sufficient Th C″ to allow measurements to be made. The maximum γ-ray activity occurs about four weeks after preparation, and then falls off by about 0·07 per cent. per day. The first source (*a*) had a maximum activity about equal to that due to 5 mg. of radium in equilibrium (as measured through 3 mm. of lead), and had been precipitated as described a large number of times. It seemed unlikely, therefore, that it should contain any appreciable trace of mesothorium, and its behaviour indicated that it was reasonably pure. The second source (*b*) had a maximum activity of about 15 mg., and was prepared in the same way, but was precipitated only twice. In consequence there was a greater likelihood of its containing an appreciable amount of mesothorium. Its subsequent behaviour lent colour to this possibility; and some attempt was made to determine the amount of this contamination by following its curve of rise and decay, and also by the absorption-coefficient method of Bothe *. This method is not at present very reliable for determining the mesothorium content of a radiothorium preparation, owing to our lack of accurate information on the absorption coefficient of pure mesothorium. The rise and decay method is of doubtful utility. Consequently a number of rather

* Bothe, *Zeit. f. Phys.* xxiv. p. 10 (1924).

widely differing values for the proportion of mesothorium were obtained, ranging from 5 to 15 per cent. In consequence of this consideration, it was to be expected that the sources should give slightly different results for the absorption coefficient under similar conditions.

The Results.

The absorption coefficient was invariably determined by making ten observations of the movement of the gold leaf, with and without the absorber, correcting for natural leak, and also, where necessary, for change in temperature and pressure of the air in the ionization chamber between sets of readings.

The values obtained with the two sources were not quite consistent, but the discrepancy is satisfactorily accounted for if we make the assumption, already shown to be highly probable, that source (*b*) owed some 5 per cent. of its maximum activity to mesothorium. With this adjustment, the average values of μ were :—

0·417 through 2·4 cm. of lead,
0·419 „ 5·8 „ „ ,
0·425 „ 9·2 „ „ ,

with probable error of about 1 in 300.

Such an increase in μ has not previously been recorded, either for Th C″ or for any other γ-ray product. A further discussion of this important result will be reserved till later.

The Case of Radium C.

At this stage it was thought advisable to re-examine the problem in regard to Ra C by the present method. Two large emanation sources were therefore prepared, the first initially of about 100 millicuries, the second about 300. They were contained in tubes as nearly as possible the same size and shape as in the thorium experiments.

As thicker filters were to be used in these experiments than in the previous ones, it was necessary to move the source further from the electroscope when these filters were employed ; in consequence, the solid angle was different, as also the proportion of scattered radiation entering the absorber. Results at this stage will not therefore be strictly comparable with those for Th C″.

All the values obtained for Ra C are represented in fig. 1. Results indicated by circles were obtained with some small radium sources ; those indicated by crosses, with the emanation sources. The value obtained with a 15-mgm. radium source acting through 9·2 cm. of lead gives the only suggestion of an increase in μ with distance : it is however based on very doubtful evidence, owing to the very small value of the ionization involved. All the remaining results show a consistent fall in μ as the filter thickness is increased.

Fig. 1.

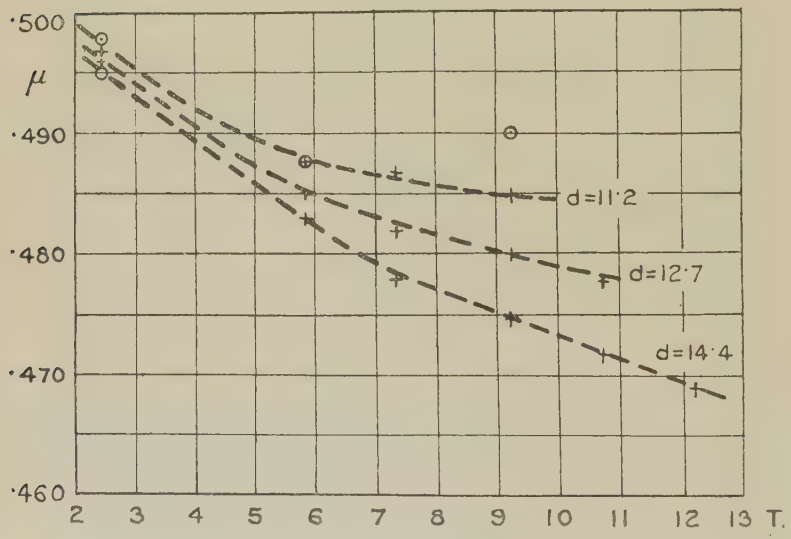

Variations of μ with thickness of filter (T) for various distances (d).

But an examination of the figure shows that the decrease in μ becomes more marked as the source distance is increased. This seems to suggest that if we could sufficiently reduce the source distance, and still obtain an extensive μ-T curve (as, *e.g.*, if an absorber and filter of much higher density were available), the curve might be found to bend upwards, at some stage, in somewhat the same way as the Th C″ curve has been shown to do above. The use of platinum, or even tungsten, might possibly elucidate this matter, but the quantity required would be almost prohibitive.

These data point, then, to the conclusion that in the case of Ra C, under the conditions actually investigated, the absorbability of the γ-rays in lead does not increase with increasing thickness of absorber, as occurs in the case of Th C″.

Discussion of Comparative Results.

The difficulty in arriving at a just estimate of the value of these results in providing support for Compton's ideas depends partly on the complex nature of the beams of γ-rays employed, and partly on the even more complex sequence of events which probably occur during the scattering and the subsequent absorption. We may attempt to simplify the picture somewhat in the former respect by assuming the original beam to be composed of only a few monochromatic rays, and endeavouring to assign an effective wave-length and intensity to these. This may be attempted with sufficient accuracy for the present purpose if we divide the whole range of wave-lengths into three groups, and, having assigned relative intensities to the lines, we average the wave-lengths in each group with due regard to the intensities of the component lines. Now, Ellis & Wooster * have recently outlined a valuable methed for estimating these relative intensities, and their results for Ra C have been employed. Their method has also been extended to the case of Th C″ by operating on the data published by Black †. The conclusions are set out in Table I.

Table I.

Effective Wave-lengths and Energy of γ-Ray Groups.

Group.	No. of lines.	Range of λ. (X.U.)	Average λ. (X.U.)	Per cent. energy.	Approx. μ.
Ra C I.	4	21–9	12·5	21	·50
II.	2	9–6	8·1	68	
III.	1	5·6	5·6	11	
Th C″ I.	6	59–42	45·1	2 3	·42
II.	2	24–17	22·5	9·3	
III.	1	4·7	4·7	88·4	

Some of the low-frequency lines have been omitted in either case; their energy-content is negligible for the purpose in hand.

* Ellis & Wooster, Proc. Camb. Phil. Soc. xxiii. p. 717 (1927).

† Black, Roy. Soc. Proc. A, cix. p. 166 (1925).

These conclusions, although based on data of only moderate accuracy, and deduced by a process of averaging of the roughest kind, are sufficiently valid to substantiate most unequivocally the difference between the two γ-ray products.

In the case of Ra C the rays are distributed over a moderate range of wave-lengths, with no outstanding gaps, or preponderating concentration of energy. But with Th C'' nearly 90 per cent. of the energy is resident in the high-frequency monochromatic wave, which is removed over two octaves from the centre of gravity of the next group. We are thus justified in our assumption that a Th C'' source approximates very closely to a monochromatic irradiator.

No account has here been taken of the continuous background of γ-radiation which may be present. The data available are inadequate to enable us to deal with it even as cursorily as we have done with the line spectrum. But it is unlikely to affect our conclusions materially, for Ellis and Wooster * have shown that the continuous γ-ray spectrum is probably of weak intensity.

As has already been indicated, the total absorption has been shown by Ahmad † to be a function of λ of the form

$$AZ + B\lambda^3 Z^4,$$

where A and B are independent of λ, and Z is the atomic number of the absorber. The relative importance of the two terms is not sufficiently established to justify accurate deductions. But Ahmad estimates that for $\lambda = 20$ X.U. the two terms are comparable in magnitude. It is probable, then, that for waves two octaves below this, μ is considerably smaller. The data in Table I. broadly support this conclusion.

It follows from these considerations that, in the absence of any further complexity, the passage of these hypothetical radiations through the same filter should result in a much greater proportionate concentration of the energy in the high-frequency group with Th C'' than with Ra C. The resulting coefficient for the Th C'' should thus fall more rapidly with increasing filter thickness than for Ra C.

But the further complexity—the change in quality on scattering, postulated by Compton—will act counter to this. The scattered portion of the beam suffers an increase in λ, and in consequence an increase in the average μ which is measured. This effect will be at least twice as important for Th C'' III. as for Ra C III. under similar conditions.

* Ellis & Wooster, Proc. Camb. Phil. Soc. xxiii. p. 717 (1927).
† Ahmad, Roy. Soc. Proc. A, cvi. p. 8 (1924).

The net effect which is observed will be determined by the relative importance of these two factors in each case.

This picture of the process involves very considerable simplifying assumptions ; but still it seems sufficiently valid to indicate the reason for the difference in the behaviour of the two radioactive bodies. With Ra C the hardening effect under the experimental conditions outlined seems everywhere to be of greater importance than the Compton effect, and μ to decrease continually in consequence ; but with Th C″ the latter effect appears to be of greater importance, and the coefficient increases. The magnitude of the increase evidently depends on the experimental conditions, especially in so far as these control the proportion of scattered radiation which is included in the absorption measurements. But as the distribution of scattered radiation is again an uncertain and complex function of the wave-length, it is apparent that much more detailed information on all these matters and a much more elaborate analysis must be evolved before we can hope to obtain satisfactory quantitative agreement between this phase of Compton's theory and γ-ray absorption measurements.

Summary.

Careful measurements on the absorption of γ-rays in lead have shown that the coefficient increases with the thickness of lead penetrated in the case of Th C″, but decreases in the case of Ra C. The difference is shown to be in general agreement with the consequences of Compton's theory of scattering.

The important fact evolves that Th C″ acts almost as a monochromatic source of γ-radiation.

Acknowledgments.

I have much pleasure in recording my indebtedness to Sir Ernest Rutherford for his helpful interest during the prosecution of these measurements ; also to Dr. J. Chadwick for advice, and especially for preparing and placing at my disposal the large Th C″ sources used.

The work was rendered possible through a grant from the Department of Scientific and Industrial Research, for which I am deeply grateful.

The University, Durham.
July 28, 1927.

LXXXII. *Bubbles, Drops, and Stokes' Law.* (Paper 2.) *By* W. N. Bond, *M.A., D.Sc., F.Inst.P., Lecturer in Physics, University of Reading, and* Dorothy A. Newton, *B.Sc., a Senior Scholar, University of Reading* *.

Summary.

In a previous paper by one of the authors it was shown that spherical drops or bubbles surrounded by a more viscous fluid might have a terminal velocity as great as one and a half times that of a solid sphere of equal size and mass. The present paper shows experimentally and theoretically that the surface-tension of the surface of the drop or bubble decreases the terminal velocity. For any radii appreciably less than a certain critical value the drop or bubble behaves almost like a rigid sphere. After a fairly rapid transition, for all radii appreciably larger than the critical the effect of surface-tension is small. Experiments on the terminal velocity for air in water-glass, air in syrup, mercury in syrup, and water in castor-oil, all give critical radii of the order predicted ; but the different media show appreciably mutual disagreement, the cause of which is not yet certain.

Introduction.

In a previous paper by one of us †, Stokes' calculations for the slow rectilinear motion of a solid sphere through viscous fluid were extended, in the way he outlined, to the case where the sphere is composed of fluid. For a drop of radius a, and density ρ', falling through an infinite extent of fluid of density ρ and viscosity μ, the terminal velocity may be written

$$V_\infty = \frac{1}{k}\left\{\frac{2}{9}\frac{(\rho'-\rho)ga^2}{\mu}\right\}. \quad . \quad . \quad . \quad . \quad (1)$$

It was shown that, *if the surface of the drop did not itself exert any tangential force,*

$$k = \frac{2/3+\mu'/\mu}{1+\mu'/\mu}, \quad . \quad . \quad . \quad . \quad . \quad . \quad (2)$$

where μ' is the viscosity of the fluid forming the drop.

* Communicated by the Authors.

† Bond, Phil. Mag. (7) vol. iv. No. 24, pp. 889–898 (Nov. 1927).

According to this theory, if the fluid composing the drop has a very large viscosity compared with that of the surrounding fluid, the drop will behave as a solid sphere ($1/k=1$); conversely, if the fluid of the drop be relatively very inviscous, the drop should move one and a half times as fast as a solid sphere of equal size and density ($1/k=\frac{3}{2}$), there being now no tangential force at the surface of the sphere.

It was also recorded in the former paper * that air-bubbles were found to rise in viscous liquid at a speed corresponding to $1/k=1{\cdot}43$—almost that predicted. Fluctuations in the measurements, and the relatively small velocities obtained in the few experiments with water drops in castor-oil, were attributed to tangential forces exerted by the spherical surface that were then considered probably due to surface contamination. The present paper records an attempt to investigate this surface-effect further.

Theory.

At first it might be thought that surface-tension, without contamination, would not influence the phenomenon, as the area and shape of the common surface are constant. But further consideration (as well as the experimental results) shows that surface-tension will itself have an effect.

The fluid just inside and outside the surface has, in general, a common tangential velocity. Because this velocity varies from zero at the two points on the axis of motion of the sphere to a maximum at points in (or near) the equatorial plane, the area of an element of the common surface must at first grow from zero, then attain a maximum, and finally decrease again to zero. This change in area will require a local supply or removal of energy, and will call into play tangential forces not considered in deriving equation (2). It appears likely that, as this effect becomes important, k will change from the value given by equation (2) towards unity (a rigid sphere).

Without making a detailed calculation, it may be assumed that one extra variable, the surface-tension, T, of the common surface, is all that need be considered (the conditions being sensibly isothermal). We then obtain dimensionally the most general form of relationship between the variables

$$f\left(\frac{a\mu \mathrm{V}_\infty}{\mathrm{W}},\quad \frac{\mu'}{\mu},\quad \frac{a\mathrm{T}}{\mathrm{W}}\right)=0, \quad . \quad . \quad . \quad . \quad (3)$$

* Bond, *loc. cit.*

where W is the apparent weight of the drop or bubble after allowing for buoyancy. This equation may be written

$$V_\infty = \left\{ \phi\left(\frac{\mu'}{\mu}, \quad \frac{aT}{W}\right) \right\} \left\{ \frac{2}{9} \frac{(\rho'-\rho)ga^2}{\mu} \right\} . \quad . \quad . \quad (4)$$

Thus $1/k$ of equation (1) will be a function not only of μ'/μ as given by equation (2), but also of $\frac{aT}{W}$. For large drops or bubbles, $\frac{aT}{W}$ is small, and $1/k$ should approach the value given by equation (2), being a maximum ($1/k = \frac{3}{2}$) when μ'/μ is also small. And for small drops or bubbles $\left(\frac{aT}{W} \text{ large}\right)$ it was suggested above that $1/k$ should in all cases tend to unity (rigid sphere).

The surface-tension would probably become of moderate importance if $\frac{aT}{W}$ were of the order unity *. Or, changing to more convenient variables, we may define a critical radius, $\bar{a}$, near which the transition would be expected to occur, by

$$\bar{a} = \sqrt{\frac{T}{|(\rho'-\rho)| \cdot g}} . \quad . \quad . \quad . \quad . \quad . \quad (5)$$

It might be thought that when surface-tension became of small importance $\left(\frac{aT}{W} \text{ small}\right)$ the large drops or bubbles would depart from the spherical form. It appears, however, from equation (4) of the previous paper † that, when there is no tangential force at the surface of the sphere (and when the kinetic energy of the fluid is negligible), the departure from sphericity is only due to the hydrostatic pressure being slightly different at the top and bottom of the drop, and is therefore very small.

Experiments.

In order to investigate the effect of surface-tension on the terminal velocity, the viscosity of the fluid inside the sphere was kept very small compared with that outside.

* For rapidly moving air-bubbles in water a change in effect has been found at a critical radius of about 0·165 cm. (O. Miyagi, Tôhoku Univ. Technol. Reports, (5) No. 3, pp. 1–33, 1925). This effect, also, seems to be due to surface-tension, and the order of the critical radius is given by equation (5) above.

† Bond, *loc. cit.*

The ratio of the terminal velocity to that of a solid sphere of equal size and density (*i.e.*, $1/k$ defined by equation (1)) was then measured for various sizes of drop or bubble $\left(i.e.,\text{ for various values of } \frac{a\mathrm{T}}{\mathrm{W}}\right)$. For no tangential force due to the surface of the sphere this ratio should be $1/k=\frac{2}{3}$, as given by equation (2) when μ'/μ is very small; but in general it might be less, being a function of $\frac{a\mathrm{T}}{\mathrm{W}}$, ϕ of equation (4).

Experiments were carried out with air in golden syrup, mercury in golden syrup, and water in castor-oil. Also the previous results on air in water-glass and air in golden syrup were analysed on the present basis. The velocities were in all cases such that the forces accelerating the liquid outside were negligible in comparison with those overcoming viscous resistance to relative motion (*i.e.*, $\mathrm{V}_\infty a\rho/\mu$ was small compared with unity). The temperature varied during the experiments between about 13° C. and 20° C.

The terminal velocities were found using a vertical brass box of internal cross-section 4·75 cm. square, containing about 13 cm. length of liquid column (as in the previous work). A pair of adjacent sides had plate-glass windows, and the drops or bubbles were viewed with a microscope, in front of a white background crossed by a number of horizontal dark lines. In some experiments on large water drops in castor-oil a glass cylinder was used (internal diameter 7·5 cm.; height 13½ cm.). To allow for the effect of the walls and ends, a curve was constructed for both vessels from observations of solid spheres of various sizes falling in golden syrup. As the size of sphere was increased, the correction began to exceed that given by Ladenburg's formula, being considerably in excess for the largest spheres.

The diameters of the slower drops and bubbles were found by measuring the time they took to move a distance equal to their diameter; the size of the larger mercury drops was found by previous weighing, and of the larger water drops by forming them from calibrated pipettes.

The viscosity of the surrounding liquid was found by measuring the terminal velocity of steel spheres before and after each experiment.

Since it was shown in the previous paper* that the wall-correction for drops and bubbles is in general less than for a

* Bond, *loc. cit.*

solid sphere (being closely proportional to k), the unmodified wall-correction was first applied, yielding a first estimate of k. This was used to modify the wall-correction and obtain a second approximation to k. This again changes slightly the estimated wall-correction ; and for large drops the approximation was carried out to three or four stages, the estimates being successively above and below the required value. The accuracy of this allowance for the wall-correction is confirmed by the agreement of the results, using two different containing-vessels (see Water in Castor-oil, fig. 1).

The surface-tension of the surface common to the two fluids was chiefly found by use of a large flat drop (Quincke's method), so as to have conditions nearly like those occurring during the main experiment.

Discussion of Results.

The values of $1/k$ (defined by equation (1)) are plotted against values of the radius of the drop or bubble (fig. 1).

It is seen that in three cases $1/k$ reaches the value $\frac{2}{3}$ (given by equation (2) for $\mu'/\mu=0$) for large drops or bubbles. In the case of the mercury, drops of radii larger than 0·13 cm. were not used, as they were non-spherical. This was evidently due to the large kinetic energy of the mercury in the drop, combined with the large difference in density between the mercury and the surrounding syrup. For the large water drops also, $V_\infty a\rho'/\mu'$ was not small compared with unity. But in this case ρ and ρ' differed little, and the drops remained sensibly spherical for the largest diameters recorded. No obvious evidence of turbulence inside the drops was noticed, and for the largest drops the tangential forces required to circulate the inner fluid were evidently small, as $1/k$ became very close to $\frac{3}{2}$ in value.

For small diameters of drop or bubble the value of $1/k$ approaches unity very closely (*i. e.*, Stokes' Law is obeyed). This is in general agreement with the predictions, assuming surface-tension to affect the problem. If there is very small velocity at the spherical surface, no appreciable work will be done in stretching the surface, and the problem reduces to that of a solid sphere. But the action of surface-tension has not been elucidated in detail.

Finally, let us consider the transition case (say $1/k=1{\cdot}25$). It is found that this occurs for a radius of the order predicted by equation (5) for the considerable range of values of T and $(\rho'-\rho)$ covered by the experiments. The agreement

Fig. 1.

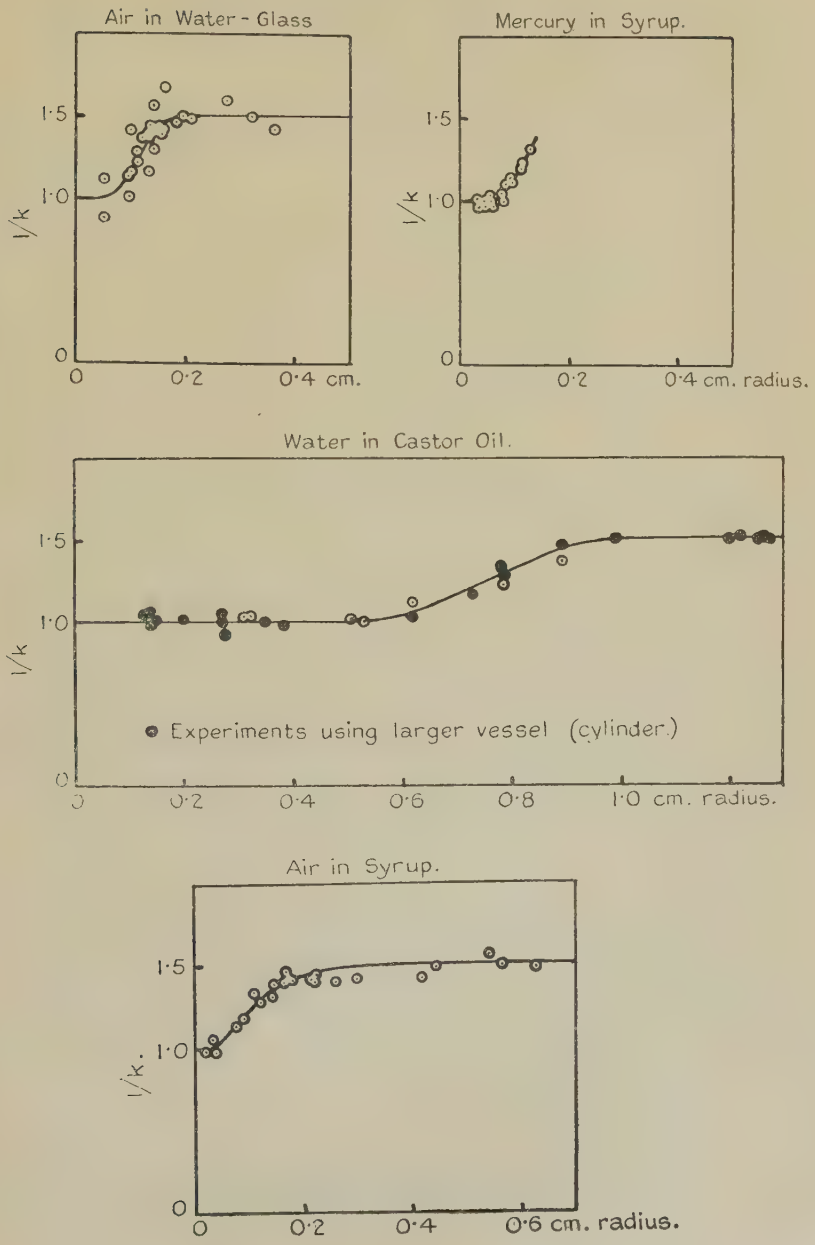
Air in Water-Glass
1·5
1·0
1/k
0
0
0·2
0·4 cm.
Mercury in Syrup.
1·5
1/k 1·0
0
0
0·2
0·4 cm. radius.
Water in Castor Oil.
1·5
1·0
1/k
Experiments using larger vessel (cylinder.)
0
0·2
0·4
0·6
0·8
1·0 cm. radius.
Air in Syrup.
1·5
1/k . 1·0
0
0
0·2
0·4
0·6 cm. radius.

between the results for different fluids is not at all perfect, but there is enough evidence to show that surface-tension is the main cause of the departure from the value of $1/k$ given by equation (2).

The values may be put in tabular form :—

	μ'/μ.	T.	$\rho'-\rho$.	$\bar{a}=\sqrt{\frac{T}{\lvert(\rho'-\rho)\rvert \cdot g}}$	Observed radius for $1/k=1{\cdot}25$.
Air in water-glass...	10^{-7}	10·4	−1·69	0·25 cm.	$0{\cdot}10_5$ cm.
Air in golden syrup	10^{-6}	91	−1·48	0·25	0·11
Mercury in golden syrup.	10^{-4}	285	12·1	$0{\cdot}15_5$	0·12
Water in castor-oil.	10^{-3}	18·0	0·037	0·70	0·77

The variation in the ratio of (observed radius for $1/k=1{\cdot}25$) to ("critical radius," a) may be due to surface contamination. It seems impossible that it can be due to the conditions not being isothermal. The variation may also be due to the surface-tension changing with time. The surface-tension of water to castor-oil was found to decrease with time. Finally, the variation might possibly be due to the effect of the kinetic energy of the liquid inside the drops ; or even, conceivably, to the ratio of μ' to μ being changed.

It is now clear that the variation in the values of $1/k$ found in the previous work, and the low values found in some experiments at the start of the present work, were due to the action of surface-tension. Also surface-tension will cause Stokes' Law to be applicable in experiments such as those of J. J. Thomson and of Millikan, referred to in the former paper.

The authors would like to thank Professor Crowther, in whose laboratories the work was carried out, for his kind encouragement and interest in the work; thanks are also due to Mr. J. S. Burgess, the laboratory steward, for continued help in regard to apparatus.

Department of Physics,
University of Reading,
December 31st, 1927.

[*The Editors do not hold themselves responsible for the views expressed by their correspondents.*]

THE

LONDON, EDINBURGH, AND DUBLIN

PHILOSOPHICAL MAGAZINE

AND

JOURNAL OF SCIENCE.

[SEVENTH SERIES.]

SUPPLEMENT, MAY 1928.

LXXXIII. *The Sæcular Changes in Electronic Orbits in a Magnetic Field.* *By* W. M. Hicks, *F.R.S.**

THE use which has been made of Larmor's theorem to explain the Zeeman effect on the quantum basis is well known. On the supposition that the effect of H^2 on the motion may be neglected, the motion of a single electron round a nucleus is compounded of an elliptic orbit in some plane inclined to H which at the same time regredes with angular velocity $\omega = HE/2mc$. Now, such an electron in orbits of atomic dimensions makes about a billion circuits in 1/1000 sec. Thus during the life even of an excited orbit there is time for sæcular effects to produce very large changes in the orbital constants. It is the purpose of the present investigation to determine these changes, and at the same time to find the conditions that H^3 and higher powers may be neglected. Shortly, the principal results may be summarized as follows :—

(1) If the initial orbits are parallel or perpendicular to H their planes remain fixed, but the line of apses regredes.

* Communicated by the Author.

(2) If the initial orbit be a circle, it will remain a circle, with the inclination of its plane unaltered, but the nodal line progredes at a constant rate of the second order of magnitude.

(3) In other cases the nodes, apses, eccentricity, and inclination of plane all change. There are two categories of cases:

(3 *a*) The apses continually regrede. An orbit initially with its axis in the nodal line has its maximum inclination at that instant. As the axis moves back to a line perpendicular to the node, the inclination diminishes to a minimum at that stage. The nodal line progredes continuously and the eccentricity changes so that

$$(1-e^2)\cos^2\alpha = \text{const.}$$

(3 *b*) The apses oscillate on either side of the line perpendicular to the node. The plane of the orbit swings up and down with its maximum and minimum inclinations now both when the apsidal line is perpendicular to the node. In the maximum position the axis is swinging in the same direction as the electron is moving (*i. e.* progredes), whilst in the minimum it is moving oppositely (regredes). No orbit can belong to this category whose inclination is less than

$$\sin^{-1}\sqrt{\cdot 8} = 63^\circ\ 26'\ 6''.$$

For numerical examples, see § 8.

The conclusion is drawn that, for orbits of 10^{-8} cm. and H of the order of 30,000 gauss, we are justified in regarding H^2 as a small disturbing effect, but not for those of 10^{-6} or larger. The energy of the whole motion remains constant, also that of the standard portion if we regard $-\omega^2\rho$ as a force with potential $-\frac{1}{2}\omega^2\rho^2$. The angular momentum round H of the standard portion remains constant, but that of the whole motion or of the regressive portion is not. If the field has been imposed on a previously existing orbit, the standard cannot possibly be the same as the original *, and, in any case, its actual form would depend on the instant at which, and on the way in which, the field was imposed. The problem is considered only in its dynamical aspects, and no discussion is taken as to its application to various physical theories.

1. Taking fixed axes, with the axis of z along the field H, using cylindrical coordinates ρ, ϕ, z, and denoting the

* Larmor, 'Æther and Matter,' p. 343. Also see Nat. cxv. p. 978 (1925).

distance from the nucleus at the origin by r, the equations of motion are

$$\left.\begin{aligned} \frac{d^2\rho}{dt^2} - \rho\left(\frac{d\phi}{dt}\right)^2 &= -\frac{E^2\rho}{mr^3} + \frac{HE}{mc}\rho\frac{d\phi}{dt}, \\ \frac{d}{dt}\left(\rho^2\frac{d\phi}{dt}\right) &= -\rho\frac{HE}{mc}\frac{d\rho}{dt}, \\ \frac{d^2z}{dt^2} &= -\frac{E^2z}{mr^3}. \end{aligned}\right\} \quad . \quad . \quad (1)$$

Write $HE/(2mc)=\omega$ and $E^2/m=p$. Integrating the second gives

$$\rho^2\frac{d\phi}{dt} + \omega\rho^2 = h.$$

Replacing $\frac{d\phi}{dt}+\omega$ by $\frac{d\theta}{dt}$, the equations become

$$\left.\begin{aligned} \frac{d^2\rho}{dt^2} - \rho\left(\frac{d\theta}{dt}\right)^2 &= -\frac{p\rho}{r^3} - \omega^2\rho, \\ \rho^2\frac{d\theta}{dt} &= h, \\ \frac{d^2z}{dt^2} &= -\frac{pz}{r^3}. \end{aligned}\right\} \quad . \quad . \quad (2)$$

The *form* of these equations is that of orbits referred to fixed axes, under the central attraction combined with one *towards* the axis of z proportional to ρ. Hence the actual motion is that of an orbit determined by equations (2) referred to fixed axes, which is at the same time subject to a uniform regression ω. In determining the motion, therefore, we may pay no attention to the regressive part, whatever the magnitude of ω may be. The orbit as determined by equations (2) we shall call the standard orbit. If ω^2 is negligible, the standard will be a plane elliptic orbit, and this regredes with angular velocity ω. This is Larmor's theorem.

The energy of the whole motion is given by

$$\left.\begin{aligned} \frac{2p}{r} - \frac{2W}{m} &= \left(\frac{d\rho}{dt}\right)^2 + \left(\frac{dz}{dt}\right)^2 + \rho^2\left(\frac{d\phi}{dt}\right)^2 \\ &= \left(\frac{d\rho}{dt}\right)^2 + \left(\frac{dz}{dt}\right)^2 + \rho^2\left(\frac{d\theta}{dt}\right)^2 - 2\omega h + \omega^2\rho^2, \end{aligned}\right\} \quad (3)$$

where W is the energy-defect of the whole motion, and $W - m\omega h$ that of the standard.

Eliminating the time variable in the usual way and writing $1/\rho = u$, $z/\rho = zu = \mathrm{X}$, it is easily shown that

$$\left.\begin{aligned} \frac{d^2u}{d\theta^2} + u &= \frac{p}{h^2(1+\mathrm{X}^2)^{3/2}} + \frac{\omega^2}{h^2u^3}, \\ \frac{d^2\mathrm{X}}{d\theta^2} + \mathrm{X} &= \frac{\omega^2\mathrm{X}}{h^2u^4}, \end{aligned}\right\} \quad . \quad . \quad . \quad (4)$$

and the energy equation becomes

$$\left(\frac{du}{d\theta}\right)^2 + \left(u\frac{d\mathrm{X}}{d\theta} - \mathrm{X}\frac{du}{d\theta}\right)^2 + u^2 = \frac{2p}{h^2}\frac{u}{\sqrt{(1+\mathrm{X}^2)}} - \frac{\omega^2}{h^2u^2} + \frac{2\omega}{h} - \frac{2\mathrm{W}}{mh^2}. \quad (5)$$

2. If the effect of ω^2 is negligible, these give a fixed plane elliptic orbit. If the effect is not negligible but small, the standard motion may be regarded as taking place in an instantaneous ellipse whose constants are subject to continuous variation. The condition of negligibility, however, does not depend on ω alone, but on the size of the actual orbit. This is evident from the fact that, if the orbit is very large, its form will depend almost wholly on H, whilst when it is sufficiently small, it depends chiefly on the electric forces. We shall assume here that ω^3 may be neglected, and determine later the conditions under which the assumption is permissible.

If l denote the semi-latus rectum of an orbit, lu is of order unity Replacing lu for u, the disturbing terms in (4, 5) appear with the numerical coefficient

$$k = \frac{l^4\omega^2}{h^2} = l^3\frac{\omega^2}{p} = \frac{\mathrm{H}^2}{4mc^2}l^3.$$

With a field of $30{,}000\,x$ gauss and an orbit of the order of 10^{-8} cm. this becomes $k = 2{\cdot}7\,x^2 \times 10^{-10}$.

3. In fig. 1 let the plane of the orbit cut a spherical surface round O in the great circle PNA, the plane of xy in $x\mathrm{N}y$, the radius vector to the particle in P and that to perihelion in A. Also let

a = inclination of orbital plane = PNm,
b = nodal angle xON,
c = angle from node to perihelion = NOA,
ϕ = angle PN *,
θ = angle xOm.

* Not, of course, the ϕ of § 1, which we shall no longer require.

The equation of the instantaneous ellipse in its own plane will be of the form

$$\frac{l'}{r} = 1 + e\cos(\phi + c).$$

Here $l' = h_1^2/p$, where $\frac{1}{2}h_1$ is the rate of description of area in the plane of motion. The areal rate in the projection of the path on xy is the absolute constant $\frac{1}{2}h$ of equation (2).

Fig. 1.

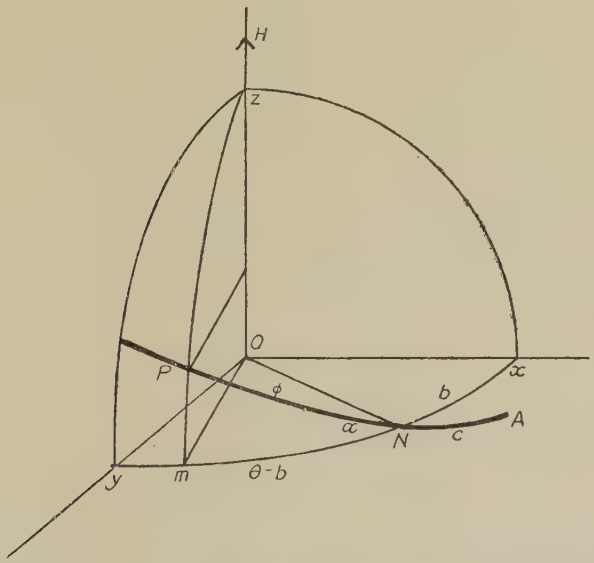

Hence $h = h_1 \cos a$. Write $h^2/p = l$, also an absolute constant however a may alter. Then

$$\frac{lu\cos \mathrm{P}m}{\cos^2 a} = 1 + e\cos\phi\cos c - e\sin\phi\sin c,$$

also

$$\mathrm{X} = z/\rho = \tan \mathrm{P}m.$$

Now

$$\tan \mathrm{P}m = \tan a \sin(\theta - b)\ ; \quad \tan(\theta - b) = \cos a \tan\phi.$$

Hence it is easy to show that

$$\left.\begin{aligned} \frac{lu}{\cos^2 a} &= \sqrt{(1+\mathrm{X}^2)} + e\left\{\cos c\cos(\theta - b) - \frac{\sin c}{\cos a}\sin(\theta - b)\right\}, \\ \mathrm{X} &= \tan a \sin(\theta - b). \end{aligned}\right\} \quad \ldots \quad (6)$$

If, however, ω^2 be neglected—ON fixed—it is more convenient to express the relations in ϕ, and then

$$lu\sqrt{Y} = 1+e\cos(\phi+c) \quad . \quad . \quad . \quad . \quad (7)$$

with

$$Y = 1-\sin^2 a \sin^2\phi.$$

$$\cos(\theta-b) = \cos\phi/\sqrt{Y}\ ; \quad \sin(\theta-b) = \cos a \sin\phi/\sqrt{Y}.$$

When ω^2 is small, a, b, c, e may be regarded as slowly changing. In settling these changes, equations (6) must be used, and not (7), which assumes a, b always constant. *After*, however, the variations of the orbital constants have been introduced into our equations, ϕ may be regarded as a mere transformation of coordinates from θ, and the corresponding expressions be used while integrating round a single orbit.

4. *Variation of* X, i. e. of a, b.—We shall denote throughout variations of the constants by the corresponding Greek letters. The equation in X is

$$\frac{d^2X}{d\theta^2}+X = \frac{kX}{l^4u^4}.$$

Multiply by $\frac{dX}{d\theta}$ and integrate

$$\left(\frac{dX}{d\theta}\right)^2+X^2 = 2k\int\frac{X\,dX}{l^4u^4}.$$

In the small term on the right we may use values for the undisturbed motion, viz.:

$$X = \tan a \sin(\theta-b) = \sin a \sin\phi/\sqrt{Y},$$

$$\frac{dX}{d\phi} = \frac{\sin a\cos\phi}{Y^{3/2}}.$$

Hence, writing $1+e\cos(\phi+c) = D$,

$$\left(\frac{dX}{d\theta}\right)^2+X^2 = 2k\frac{\sin^2 a}{\cos^8 a}\int\frac{\sin\phi\cos\phi}{D^4}d\phi.$$

In the disturbed motion let X become $X+\xi$; then

$$\frac{dX}{d\theta}\frac{d\xi}{d\theta}+X\xi = k\frac{\sin^2 a}{\cos^8 a}\int\frac{\sin\phi\cos\phi}{D^4}d\phi.$$

Now $\frac{d\theta}{d\phi} = \frac{\cos a}{Y}$, whence

$$\cos\phi \sqrt{Y}\frac{d\xi}{d\phi} + \xi\cos^2 a\frac{\sin\phi}{\sqrt{Y}} = k\frac{\sin a}{\cos^6 a}\Big\} \ldots$$

$$\cos\phi\frac{d}{d\phi}(\xi\sqrt{Y}) + \sin\phi\xi\sqrt{Y} = \ldots.$$

It will be convenient to write $\xi\sqrt{Y} = \lambda\zeta\sin a$, $k = \lambda\cos^6 a$

$$P = \int\frac{\sin\phi\cos\phi}{D^4}d\phi, \qquad Q = \int\frac{\sin^2\phi}{D^4}d\phi.$$

Then

$$\cos\phi\frac{d\zeta}{d\phi} + \zeta\sin\phi = P, \quad \ldots \quad (8)$$

$$\frac{d}{d\phi}\left(\frac{\zeta}{\cos\phi}\right) = P\sec^2\phi = P\frac{d}{d\phi}(\tan\phi),$$

$$\zeta = P\sin\phi - Q\cos\phi. \quad \ldots \quad (9)$$

Since

$$X = \tan a\sin(\theta - b),$$

$$\xi = \sec^2 a\sin(\theta - b)\alpha - \tan a\cos(\theta - b)\beta,$$

$$\xi\sqrt{Y} = \frac{\sin\phi}{\cos a}\alpha - \frac{\sin a}{\cos a}\cos\phi\,.\,\beta.$$

Hence, comparing with equation (9),

$$\left.\begin{aligned}\alpha &= \lambda\sin a\cos a\,P,\\ \beta &= \lambda\cos a\,Q.\end{aligned}\right\} \quad \ldots \quad (10)$$

In the integrals,

$$D = 1 + e\cos(\phi + c) = 1 + e\cos\chi \text{ (say)}.$$

If I_n denote $\int\frac{d\chi}{D^n}$,

$$\int\frac{\cos\chi}{D^n}d\chi = -\frac{1}{n-1}\frac{d}{de}I_{n-1},$$

also

$$\int\frac{\sin\chi}{D^n}d\chi = \frac{1}{n-1}\frac{1}{e}\frac{1}{D^{n-1}}.$$

Let Δ stand for the operator d/de. Then

$$P = \int \frac{\sin\chi\cos\chi\cos 2c - \sin c\cos c(2\cos^2\chi - 1)}{D^4}\,d\chi$$

$$= -\tfrac{1}{6}\cos 2c\,\Delta\left(\frac{1}{eD^2}\right) - \tfrac{1}{6}\sin 2c\,\Delta^2 I_2 + \sin c\cos c I_4,$$

so

$$Q = \tfrac{1}{6}\sin 2c\,\Delta\left(\frac{1}{eD^2}\right) - \tfrac{1}{6}\cos 2c\,\Delta^2 I_2 + \cos^2 c I_4.$$

As we require to find the changes in a, b after one revolution of the particle, the integration limits are χ_0, $\chi_0 + 2\pi$. The first terms in the above for P, Q then disappear, and the I stand for the complete integrals. To find these we note that

$$e\Delta I_n = -\int n\,\frac{e\cos\chi}{D^{n+1}} = -n\int\left(\frac{1}{D^n} - \frac{1}{D^{n+1}}\right) = -n(I_n - I_{n+1}).$$

Thus

$$I_n = \left(\frac{1}{n-1}e\Delta + 1\right)I_{n-1}.$$

The I_n depend then on I_1, viz.:

$$I_1 = \int \frac{d\chi}{1+e\cos\chi} = \frac{2}{\sqrt{(1-e^2)}}\tan^{-1}\left(\sqrt{\frac{1-e}{1+e}}\,.\tan\tfrac{1}{2}\chi\right).$$

It is easily seen that the indefinite I_n is of the form

$$A_n\tan^{-1}(\ldots) + \left(\frac{B_1}{D} + \ldots + \frac{B_{n-1}}{D^{n-1}}\right)\sin\chi.$$

These will give the complete values of α, β at any point of the orbit. For our purpose, however,

$$I_1 = \frac{2\pi}{\sqrt{(1-e^2)}} = 2\pi Z \text{ (say)}.$$

Here

$$e\Delta Z^n = n(Z^{n+2} - Z^n),$$

whence

$$\left.\begin{aligned} I_2 &= (e\Delta + 1)I_1 = 2\pi Z^3, \\ I_3 &= (\tfrac{1}{2}e\Delta + 1)I_2 = \pi(3Z^5 - Z^3), \\ I_4 &= (\tfrac{1}{3}e\Delta + 1)I_3 = \pi(5Z^7 - 3Z^5), \\ \Delta^2 I_2 &= 6\pi(5Z^7 - 4Z^5), \\ \Delta^3 I_1 &= 6\pi e(5Z^7 - 2Z^5). \end{aligned}\right\} \quad . \quad . \quad (11)$$

Substituting, it will be found that

$$\alpha = -\tfrac{5}{2}\pi\lambda \frac{\sin a \cos a}{(1-e^2)^{5/2}}\left(\frac{1}{1-e^2}-1\right)\sin 2c,$$

$$\beta = \pi\lambda \frac{\cos a}{(1-e^2)^{5/2}}\{1+5(Z^2-1)\sin^2 c\}.$$

We shall find in the next section that $Z = C\cos a$, where C is a constant. Hence, replacing λ by $k/\cos^6 a$,

$$\left.\begin{aligned}\alpha &= -\tfrac{5}{2}\pi k C^5 \sin a(C^2\cos^2 a-1)\sin 2c,\\ \beta &= \pi k C^5\{1+5(C^2\cos^2 a-1)\sin^2 c\}.\end{aligned}\right\} \quad . \quad (12)$$

5. *The eccentricity.*—In any elliptic orbit (major axis = 2a) the energy defect is given by $W' = mp/2a$ and $l' = a(1-e^2)$, whence $1-e^2 = 2W'l'/mp$. In the present case the effective elliptic energy is not constant:

$$W' = W - m\omega h + \tfrac{1}{2}m\omega^2\rho^2\ ; \quad l' = l/\cos^2 a\ ; \quad l = h^2/p.$$

Hence

$$\begin{aligned}(1-e^2)\cos^2 a &= 2(W-m\omega h)\frac{l^2}{mh^2}+\frac{l^2\omega^2}{h^2u^2}\\ &= \text{const.}+\frac{k}{l^2u^2}.\end{aligned}$$

$$\therefore \quad e\eta\cos^2 a = -(1-e^2)\sin a\cos a\,.\,\alpha - \frac{k}{2l^2u^2}. \quad . \quad (13)$$

Since $l^2\omega^2/(hu)^2$ is periodic, it follows that $(1-e^2)\cos^2 a$ is unaltered after a complete revolution; or throughout the sæcular motion

$$(1-e^2)\cos^2 a = \text{const.} = (1-e_0^2)\cos^2 a_0,$$

where e_0, a_0 are initial values. It is convenient to put the constant $= \dfrac{1}{C^2}$. Some interesting conclusions follow at once. *E. g.*:

(1) Since $1-e^2$ is always < 1, $\cos^2 a > (1-e_0^2)\cos^2 a$. Hence, even if α increases, a can never be greater than $\cos^{-1}\{\surd(1-e_0^2)\cos a_0\}$.

(2) If initially the plane of the orbit is parallel to H, it must always remain so, for then the constant is zero and $(1-e^2)\cos^2 a = 0$ always, *i. e.* either $\cos a = 0$ or $e = 1$, the latter denoting a line orbit. The same result also follows from the fact that, in this case, the areal rate projected on

the plane of xy is zero, and by equation (2) is constant and therefore zero always. This can only happen when the orbital plane remains perpendicular to xy.

(3) Any finite change in the inclination must involve simultaneous changes in the shape of the orbit, so that, if ϵ denote the ratio of the axes, $\epsilon \cos a$ is constant.

6. *The orientation of axis or* c.—Equation (5), the analogue of the energy equation, is

$$\left(\frac{du}{d\theta}\right)^2 + \left(u\frac{d\mathrm{X}}{d\theta} - \mathrm{X}\frac{du}{d\theta}\right)^2 + u^2 + \frac{2\omega}{h} + \frac{k}{l^4u^2} = \frac{2u}{l\sqrt{(1+\mathrm{X}^2)}} - \frac{2\mathrm{W}}{mh^2}.$$

If the disturbed value of u is $u+v$,

$$\frac{du}{d\theta}\frac{dv}{d\theta} + \left(u\frac{d\mathrm{X}}{d\theta} - \mathrm{X}\frac{du}{d\theta}\right)\left\{u\frac{d\xi}{d\theta} - \xi\frac{du}{d\theta} + v\frac{d\mathrm{X}}{d\theta} - \mathrm{X}\frac{dv}{d\theta}\right\} + uv - \frac{v}{l\sqrt{(1+\mathrm{X}^2)}} + \frac{u\mathrm{X}\xi}{l(1+\mathrm{X}^2)^{3/2}} = -\frac{k}{2l^4u^2}.$$

In this we may now transform to ϕ with $\frac{d\theta}{d\phi} = \frac{\cos a}{\mathrm{Y}}$. Now, in general,

$$\mathrm{W}\left(\mathrm{U}\frac{d\mathrm{V}}{d\phi} - \mathrm{V}\frac{d\mathrm{U}}{d\phi}\right) = \mathrm{U}\sqrt{\mathrm{W}}\frac{d}{d\phi}(\mathrm{V}\sqrt{\mathrm{W}}) - \mathrm{V}\sqrt{\mathrm{W}}\frac{a}{d\phi}(\mathrm{U}\sqrt{\mathrm{W}}),$$

whence, dashed letters denoting the corresponding letters $\times \sqrt{\mathrm{Y}}$,

$$\frac{du}{d\phi}\frac{dv}{d\phi}\frac{\mathrm{Y}^2}{\cos^2 a} + \frac{1}{\cos^2 a}\left(u'\frac{d\mathrm{X}'}{d\phi} - \mathrm{X}'\frac{du'}{d\phi}\right)\left(u'\frac{d\xi'}{d\phi} - \xi'\frac{du'}{d\phi} + v'\frac{d\mathrm{X}'}{d\phi} - \mathrm{X}'\frac{dv'}{d\phi}\right) + uv - \frac{v'}{l} = -\frac{u'\mathrm{X}'\xi'}{l} - \frac{k}{2l^4u^2}.$$

Now,

$$\mathrm{X}' = \mathrm{X}\sqrt{\mathrm{Y}} = \sin a \sin\phi; \qquad \frac{1}{1+\mathrm{X}^2} = \mathrm{Y};$$

$$lu\sqrt{\mathrm{Y}} = (1+e\cos\chi)\cos^2 a;$$

$\therefore$ multiplying by l^2,

$$l^2\frac{du}{d\phi}\frac{dv}{d\phi}\frac{Y^2}{\cos^2 a}+\sin^2 a(D\cos\phi+e\sin\phi\sin\chi)\left(v'\cos\phi-\sin\phi\frac{dv'}{d\phi}\right)+l^2uv-lv'$$

$$=-\sin a\cos^2 a(D\cos\phi+e\sin\phi\sin\chi)\left(D\frac{d\xi'}{d\phi}+e\sin\chi\xi'\right)-\sin a\cos^2 a\,D\sin\phi\xi'-\frac{k}{2l^2u^2}.$$

Now,

$$\sqrt{Y}\frac{dv}{d\phi}=\frac{dv'}{d\phi}+\frac{\sin^2 a\sin\phi\cos\phi}{Y}v'.$$

The coefficient of $l\dfrac{dv'}{d\phi}$

$$=-eY\sin\chi+D\sin^2 a\sin\phi\cos\phi-\sin^2 a\,D\sin\phi\cos\phi-e^2\sin^2 a\sin^2\phi\sin\chi$$

$$=-e\sin\chi(1-\sin^2 a\sin^2\phi)-e\sin^2 a\sin^2\phi\sin\chi$$

$$=-e\sin\chi;$$

coefficient of lv'

$$=\frac{\sin^2 a\sin\phi\cos\phi}{Y}(-eY\sin\chi+D\sin^2 a\sin\phi\cos\phi)+D\sin^2 a\cos^2\phi+e\sin^2 a\sin\phi\cos\phi\sin\chi+\frac{D\cos^2 a}{Y}-1$$

$$=D\sin^2 a\left(\frac{\sin^2 a\sin^2\phi\cos^2\phi}{Y}+\cos^2\phi\right)+\frac{D\cos^2 a}{Y}-1$$

$$=D\frac{\sin^2 a\cos^2\phi}{Y}+\frac{D\cos^2 a}{Y}-1=D-1=e\cos\chi.$$

Hence the left-hand side of the equation is

$$-e\sin\chi\frac{d}{d\chi}(lv\sqrt{Y})+e\cos\chi(lv\sqrt{Y})=-e\sin^2\chi\frac{d}{d\chi}\frac{lv\sqrt{Y}}{\sin\chi}.$$

The right-hand side :

$$=-\lambda\cos^2 a\frac{Y}{2D^2}-\lambda\sin^2 a\cos^2 a\times\left\{(\cos\phi+e\cos c)\left(D\frac{d\zeta}{d\chi}+e\zeta\sin\chi\right)+D\sin\phi.\zeta\right\}.$$

Hence

$$\frac{e\sin^2\chi}{\lambda\sin^2 a\cos^2 a}\frac{d}{d\chi}(lv\sqrt{\mathrm{Y}})$$

$$= \frac{\mathrm{Y}}{2\mathrm{D}^2\sin^2 a} + (\cos\phi + e\cos c + e\cos\phi\cos\chi + e^2\cos c\cos\chi)\frac{d\zeta}{d\chi}$$
$$+ \{e\sin\chi(\cos\phi + e\cos c) + \sin\phi(1+e\cos\chi)\}\zeta$$

$$= \frac{\mathrm{Y}}{2\mathrm{D}^2\sin^2 a} + \cos\phi\frac{d\zeta}{d\phi} + \zeta\sin\phi$$
$$+ e(2\cos\phi\cos\chi + \sin\phi\sin\chi + e\cos c\cos\chi)\frac{d\zeta}{d\chi}$$
$$+ e(2\sin\phi\cos\chi + \sin c + e\cos c\sin\chi)\zeta$$

$$= \frac{\mathrm{Y}}{2\mathrm{D}^2\sin^2 a} + (1+2e\cos\chi)\left(\cos\phi\frac{d\zeta}{d\chi} + \zeta\sin\phi\right)$$
$$+ e^2\cos c\left(\cos\chi\frac{d\zeta}{d\chi} + \zeta\sin\chi\right)$$
$$+ e\left(\sin\chi\frac{d}{d\chi} - \cos\chi\right)(\zeta\sin\phi).$$

Since

$\sin\chi\dfrac{d}{d\chi} - \cos\chi$ on $\sin\phi$; $\cos\phi$ produce $\sin c$; $-\cos c$

$\cos\chi\dfrac{d}{d\chi} + \sin\chi$ on „ „ „ $\cos c$; $\sin c$

and (8, 9)

$$\cos\phi\frac{d\zeta}{d\chi} + \zeta\sin\phi = \mathrm{P}, \qquad \zeta = \mathrm{P}\sin\phi - \mathrm{Q}\cos\phi,$$

$$\cos\chi\frac{d\zeta}{d\chi} + \zeta\sin\chi$$
$$= \cos\chi\left(\sin\phi\frac{\sin\phi\cos\phi}{\mathrm{D}^4} - \cos\phi\frac{\sin^2\phi}{\mathrm{D}^4}\right) + \mathrm{P}\cos c - \mathrm{Q}\sin c$$
$$= \int\frac{\sin\phi\cos\chi}{\mathrm{D}^4}d\chi = \mathrm{P}_1 \quad \text{(say)};$$

$$\therefore \frac{e\sin^2\chi}{\lambda\sin^2 a\cos^2 a}\frac{d}{d\chi}\left(\frac{lv\sqrt{\mathrm{Y}}}{\sin\chi}\right)$$
$$= e\sin^2\chi\frac{d}{d\chi}\left(\frac{\zeta\sin\phi}{\sin\chi}\right) + \frac{\mathrm{Y}}{2\mathrm{D}^2\sin^2 a}$$
$$+ (1+2e\cos\chi)\mathrm{P} + e^2\cos c\,\mathrm{P}_1.$$

Divide by $\sin^2\chi$ and integrate

$$\frac{e}{\lambda\sin^2 a\cos^2 a}\frac{lv\sqrt{Y}}{\sin\chi}$$
$$= \frac{e\zeta\sin\phi}{\sin\chi} - \left(\frac{Y}{2D^2\sin^2 a} + P + e^2\cos c\, P_1\right)\cot\chi - 2eP\operatorname{cosec}\chi$$
$$+ \frac{1}{2\sin^2 a}\int \cot\chi\frac{d}{d\chi}\left(\frac{Y}{D^2}\right)d\chi$$
$$+ \int\{(\sin\phi\cos\phi + e^2\cos c\sin\phi\cos\chi)\cos\chi + 2e\sin\phi\cos\phi\}\frac{d\chi}{D^4\sin\chi}.$$

Now

$$\int \cot\chi\frac{d}{d\chi}\left(\frac{Y}{D^2}\right)d\chi = \int\cot\chi\left(2e\sin\chi\frac{Y}{D^3} - \frac{2\sin^2 a\sin\phi\cos\phi}{D^2}\right)d\chi;$$

$$\therefore \frac{elv\sqrt{Y}}{\lambda\sin^2 a\cos^2 a}$$
$$= e\zeta\sin\phi - 2eP - \left(\frac{Y}{2D^2\sin^2 a} + P + e^2\cos c P_1\right)\cos\chi$$
$$+ \frac{e\sin\chi}{\sin^2 a}\int\frac{Y\cos\chi}{D^3}d\chi + \sin\chi\int\frac{d\chi}{D^4\sin\chi}\times$$
$$[-D^2\cos\chi\sin\phi\cos\phi + \sin\phi\cos\phi\cos\chi + e^2\cos c\sin\phi\cos^2\chi + 2e\sin\phi\cos\phi].$$

Substituting $D = 1 + e\cos\chi$ in the expression in [ ], gives

$$2e\sin\phi\cos\phi(1-\cos^2\chi) + e^2\sin\phi\cos^2\chi(\cos c - \cos\phi\cos\chi)$$
$$= e\sin\chi(2\sin\phi\cos\phi\sin\chi + e\sin^2\phi\cos^2\chi);$$

$$\therefore \frac{elv\sqrt{Y}}{\lambda\sin^2 a\cos^2 a}$$
$$= e\zeta\sin\phi - 2eP - \left(\frac{Y}{2D^2\sin^2 a} + P + e^2\cos c P_1\right)\cos\chi$$
$$+ \frac{e\sin\chi}{\sin^2 a}\int\frac{\cos\chi}{D^3}d\chi$$
$$+ e\sin\chi\int\{-(1+e\cos\chi)\sin^2\phi\cos\chi + 2\sin\phi\cos\phi\sin\chi + e\sin^2\phi\cos^2\chi\}\frac{d\chi}{D^4}$$
$$= \ldots + e\sin\chi\int(\sin\phi\sin c + \sin\phi\cos\phi\sin\chi)\frac{d\chi}{D^4}. \quad (14)$$

It is now necessary to express v in terms of the variations of the orbital constants. To do this we must use equation (6), which gives u in terms of θ, viz.:

$$lu=\cos^2 a\left\{\surd(1+\mathrm{X}^2)+e\left(\cos c\cos(\theta-b)-\frac{\sin c}{\cos a}\sin(\theta-b)\right)\right\};$$

$$\therefore\ lv=\cos^2 a\left\{-\frac{2\mathrm{D}}{\surd\mathrm{Y}}\tan a-e\frac{\sin a}{\cos^2 a}\sin c\sin(\theta-b)\right\}\alpha$$

$$+\cos^2 a\left\{\frac{\mathrm{X}\xi}{\surd(1+\mathrm{X}^2)}+\frac{\eta\cos\chi}{\surd\mathrm{Y}}\right\}$$

$$+\cos^2 a\left[-e\left\{\sin c\cos(\theta-b)+\frac{\cos c}{\cos a}\sin(\theta-b)\right\}\gamma\right.$$

$$\left.+e\left\{\cos c\sin(\theta-b)+\frac{\sin c}{\cos a}\cos(\theta-b)\right\}\beta\right].$$

Transforming to ϕ, χ

$$\frac{lv\surd\mathrm{Y}}{\cos^2 a}=\lambda\sin^2 a\sin\phi\,.\,\zeta-e\sin\chi\,.\,\gamma$$

$$+\eta\cos\chi+(-2\mathrm{D}-e\sin c\sin\phi)\tan a\,.\,\alpha$$

$$+e\left(\cos c\cos a\sin\phi+\frac{\sin c}{\cos a}\cos\phi\right)\beta.$$

Now

$$\alpha=\lambda\sin a\cos a\,.\,\mathrm{P},\qquad\beta=\lambda\cos a\,.\,\mathrm{Q},$$

$$e\eta=-\frac{\lambda\mathrm{Y}}{2\mathrm{D}^2}-\lambda(1-e^2)\sin^2 a\,.\,\mathrm{P}\quad\text{(from 13)}.$$

Hence

$$\frac{elv\surd\mathrm{Y}}{\lambda\sin^2 a\cos^2 a}$$

$$=-\frac{e^2\sin\chi}{\lambda\sin^2 a}\gamma+e\zeta\sin\phi-\frac{\mathrm{Y}\cos\chi}{2\mathrm{D}^2\sin^2 a}-(1-e^2)\mathrm{P}\cos\chi$$

$$+e(-2\mathrm{D}-e\sin c\sin\phi)\mathrm{P}+e^2\left(\frac{\sin\chi}{\sin^2 a}-\cos c\sin\phi\right)\mathrm{Q}$$

$$=-\frac{e^2\sin\chi}{\lambda\sin^2 a}\gamma+e\zeta\sin\phi-\frac{\mathrm{Y}\cos\chi}{2\mathrm{D}^2\sin^2 a}-2e\mathrm{P}$$

$$+\{-\mathrm{P}+(-\mathrm{P}\cos^2 c+\mathrm{Q}\sin c\cos c)e^2\}\cos\chi$$

$$+e^2\sin\chi\left\{\frac{\mathrm{Q}}{\sin^2 a}-\mathrm{P}\sin c\cos c-\mathrm{Q}\cos^2 c\right\}.$$

Combining this with the former value for $lv\sqrt{Y}$, all the terms, except those in $\sin\chi$, cut out, since

$$-P\cos^2 c + Q\sin c\cos c = -P_1\cos c,$$

and there results

$$\frac{e^2\gamma}{\lambda\sin^2 a} = e^2\frac{Q}{\sin^2 a} - e^2\cos c\int\frac{\sin\phi\sin\chi}{D^4}d\chi - \frac{e}{\sin^2 a}\int\frac{\cos\chi}{D^3}d\chi$$
$$-e\int(\sin\phi\sin c + \sin\phi\cos\phi\sin\chi)\frac{d\chi}{D^4}.$$

As we require only the definite integral χ_0 to $\chi_0+2\pi$, odd powers of $\sin\chi$ disappear and

$$\frac{e}{\lambda\sin^2 a}\gamma = -\frac{1}{\sin^2 a}\int\frac{\cos\chi}{D^3}d\chi$$
$$+\frac{e}{\sin^2 a}\int\frac{\cos^2 c - \cos 2c\cos^2\chi}{D^4}d\chi$$
$$-e\cos^2 c\int\frac{1-\cos^2\chi}{D^4}d\chi$$
$$+\sin^2 c\int\frac{\cos\chi}{D^4}d\chi - \cos 2c\int\frac{\cos\chi-\cos^3\chi}{D^4}d\chi,$$

whence

$$\frac{e}{\lambda\sin^2 a}\gamma = \frac{1}{\sin^2 a}\{\tfrac{1}{2}\Delta I_2 + e\cos^2 c I_4 - \tfrac{1}{6}e\cos 2c\Delta^2 I_2\}$$
$$-e\cos^2 c\{I_4 - \tfrac{1}{6}\Delta^2 I_2\} - \tfrac{1}{3}\sin^2 c\Delta I_3 + \cos 2c\{\tfrac{1}{3}\Delta I_3 - \tfrac{1}{6}\Delta^3 I_1\}.$$

Substituting the values of I from (11), it will be found that

$$\frac{e}{\lambda\sin^2 a}\gamma = \frac{\pi e}{\sin^2 a}\{4Z^5 + 5(Z^7 - Z^5)\sin^2 c\} - 5\pi e Z^7\sin^2 c,$$
$$\gamma = \pi\lambda Z^5\{4 + 5(Z^2-1)\sin^2 c - 5\sin^2 a\sin^2 c Z^2\}$$
$$= \frac{\pi k}{\cos a}C^5\{4 + 5(C^2\cos^4 a - 1)\sin^2 c\}. \quad . \quad . \quad (15)$$

Here γ gives the change of perihelion from the nodal line. It is therefore composite and measures the combined effect of the change of perihelion in space and the effect of the motion of the nodal line. In fig. 2 let the two successive orbital planes cut the sphere of reference in PN_1A_1, PN_2A_2, P denoting the projection of the particle at any instant.

Then γ is increased N_1n by the motion of the node, and $dc = mA_2$ by the motion of the line of apses.

$$N_1n = N_1N_2 \cos a = \beta \cos a;$$

$$\therefore \quad \gamma = dc + \beta \cos a,$$

whence, combining equations (15, 12),

$$dc = \gamma - \beta \cos a = \frac{\pi k C^5}{\cos a} \{3 + \sin^2 a - 5 \sin^2 a \sin^2 c\}. \quad (16)$$

Fig. 2.

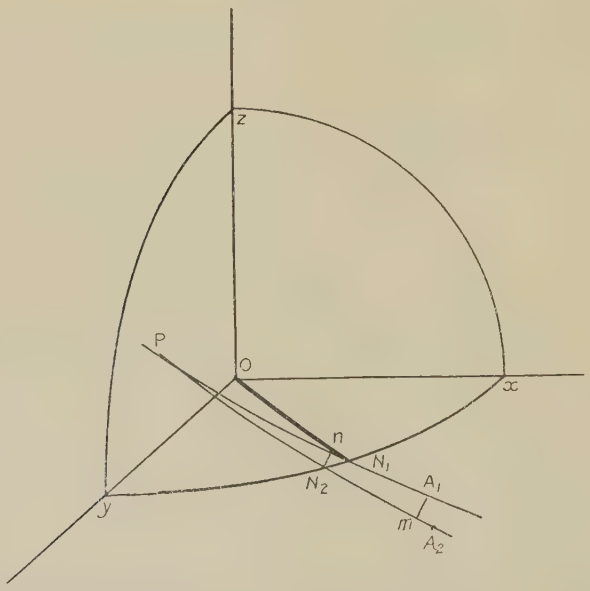

For the general cases of motion the line of apses will be referred to the nodal line and be given by (15).

7. *Discussion of the motions.*—Collecting the equations of change,

$$\delta a = -\tfrac{5}{2}\pi k C^5 \sin a (C^2 \cos^2 a - 1) \sin 2c,$$

$$\delta b = \quad \pi k C^5 \{1 + 5(C^2 \cos^2 a - 1) \sin^2 c\},$$

and $dc = \gamma$ (eq. 15). It is seen that the nature of the sæcular changes is quite independent of the magnitude of H (provided, of course, powers higher than H^2 are negligible). The individual orbits depend on C^{-1}, which is the value of $\sqrt{(1-e^2)} \cos a$ in any, say, initial configuration. The value of H merely affects the rate at which the changes take place.

The above equations give the change in a, b, c, whilst the particle makes one complete revolution in its orbit, say their annual variation. If 2 a denote the major axis of an ellipse, the period is

$$\frac{2\pi}{\sqrt{p}}a^{3/2}=\frac{2\pi}{\sqrt{p}}\left(\frac{l'}{1-e^2}\right)^{3/2}=\frac{2\pi l^{3/2}}{\sqrt{p}}\{(1-e^2)\cos^2 a\}^{-\frac{3}{2}}=\frac{2\pi l^2}{h}C^3.$$

It is thus constant throughout the sæcular changes. The da, ... are produced in this time. The final effect is the same as if these values are produced by continuous change during a period.

Now

$$\pi kC^5\Big/\left(\frac{2\pi l^2}{h}C^3\right)=\frac{khC^2}{2l^2}=\tfrac{1}{2}\omega^2\frac{l^2}{h}C^2=\tfrac{1}{2}\omega\sqrt{k}C^2.$$

Hence we may write:

$$\left.\begin{aligned}\frac{da}{dt}&=-\tfrac{5}{4}\omega\sqrt{k}C^2\sin a(C^2\cos^2 a-1)\sin 2c,\\ \frac{db}{dt}&=\tfrac{1}{2}\omega\sqrt{k}C^2\{1+5(C^2\cos^2 a-1)\sin^2 c\},\\ \frac{dc}{dt}&=\tfrac{1}{2}\omega\sqrt{k}\frac{C^2}{\cos a}\{4+5(C^2\cos^4 a-1)\sin^2 c\}\end{aligned}\right\}\quad(17)$$

with $$\frac{da}{dc}=-\tfrac{5}{2}\frac{\sin a\cos a(C^2\cos^2 a-1)\sin 2c}{4+5(C^2\cos^4 a-1)\sin^2 c}.$$

If $\cos a=y$, $\sin^2 c=x$, the last may be written:

$$\frac{dy}{dx}=\frac{y(1-y^2)(C^2y^2-1)}{4+5(C^2y^4-1)x}.$$

These formulæ are valid for all the motions possible, except that they become nugatory when the orbital plane tends to become perpendicular to the plane of xy, for in this case the k tend to zero. The reason is that the constant areal rate h becomes zero and the actual orbits indeterminate. In fact, $k=l^4\omega^2/h$, where $l=l'\cos^2 a$, $h=h'\cos a$, l', h' being the values of l, h in the actual orbit. Hence k becomes $l'^4\omega^2\cos^6 a/h'^2$, which tends to zero as $a\to\frac{\pi}{2}$. But at the same time $C^5\cos^5 a=(1-e^2)^{-\frac{5}{2}}$. Hence, in the expressions for da, db, dc, kC^5 must be replaced by $k'\cos a$, where $k'=l'^4\omega^2/h'^2$, so that as the plane approaches parallelism to H, a, b tend to become constant, *i. e.* the plane fixed,

as it clearly should be, since the disturbing force $-\omega^2\rho$ lies in the plane, whilst the apse regression is given by

$$dc = \frac{\pi k'}{(1-e^2)^{5/2}}(4-5\sin^2 c). \quad . \quad . \quad . \quad (18)$$

This has also been verified by direct calculation.

The first conclusion we draw from the equations (16) is that, if ever $\sin a=0$, $\cos a=0$, or $C^2\cos^2 a-1=0$, they maintain these values. For, writing $da/dt=f(a)\,.\,F$, where $f=0$ has roots $a_1, a_2 \ldots$ and F and its differentials are finite,

$$\frac{da}{dt} = 0 \text{ for } a=a_1, \text{ or } a_2 \ldots,$$

$$\frac{d^2a}{dt^2} = f(a)\frac{dF}{dt} + \frac{df}{dt}\cdot\frac{da}{dt} = 0 \text{ for } a=a_1 \text{ or } a_2 \ldots,$$

and so on.

Thus $(d/dt)^n a=0$ for any root value. Consequently, if $a=a_1$ or $a_2 \ldots$ at any instant, it will always retain that value. Here we have the three cases: A, $\cos a=0$: B, $\sin a=0$; C, $C^2\cos^2 a-1=0$.

A. This corresponds to a plane parallel to H. The motion of the apses is given by equation (18). If c_0 is the least value of $\sin^{-1}\sqrt{\cdot 8}$, $dc=0$ when $c=c_0, \pi-c_0, \pi+c_0, 2\pi-c_0$. If initially $c<c_0$, dc is positive and c grows asymptotically to c_0. If initially $c>c_0$, dc is negative and c decreases back to c_0. Thus c_0 is a stable position for the apsidal line. On the other hand, $\pi-c_0$ is an unstable position, for if c is less, dc is negative, etc.; but $\pi+c_0$ is again a stable position, giving the same apsidal position as c_0, but perihelion and aphelion reversed. The stable position is that in which the ellipse is tilted in the direction of the orbital motion. During a revolution the apsidal line makes small oscillations about this stable position.

B. Plane perpendicular to H. Here

$$\frac{da}{dt} = 0, \qquad \frac{db}{dt} = \tfrac{1}{2}\omega\sqrt{k}C^2\left(1+\frac{5e^2}{1-e^2}\sin^2 c\right),$$

$$\frac{dc}{dt} = \tfrac{1}{2}\omega\sqrt{k}C^2\left(4+\frac{5e^2}{1-e^2}\sin^2 c\right).$$

These hold quite close up to the limit $a=0$, but when $a=0$ they give the changes expressed in terms of a moving axis,

viz. an imaginary nodal line, without anything to show its relation to the motions in the plane. To express in terms of a fixed axis, recourse must be had to equation (16), which gives

$$\frac{db}{dt} = 0, \quad dc = 3\pi k C^5 \quad \text{or} \quad \frac{dc}{dt} = \tfrac{3}{2}\omega\sqrt{k}\frac{1}{1-e^2}.$$

This has been verified by direct calculation for this case.

C. $C^2\cos^2 a - 1 = 0$ corresponds to $1/(1-e^2) = 1$ or $e = 0$, *i. e.* to a circular orbit. This gives the important result that, for every circular orbit, the inclination remains unchanged by sæcular variations. But the nodal line progredes at a constant rate $= \frac{1}{2}\omega\sqrt{k}/\cos^2 a$, or an annual rate $\pi k/\cos^5 a$. In other words, the Larmor regression ω is decreased by this small amount. Also

$$\frac{dc}{dt} = \tfrac{1}{2}\omega\sqrt{k}\frac{4 - 5\sin^2 a \sin^2 c}{\cos^3 a},$$

with the apparent paradox of a circle possessing a definite apse. To understand this, it must be remembered that we have been dealing with the complete changes produced after a single revolution in the orbit. If we take account of what goes on during a period, we never get the same instantaneous orbit persisting. It is only at certain instants that the true circle appears, and between these the orbit has been elliptic with its apse moving. The angle through which this has gone in a complete revolution is that given by the above equation. As the particle in a circle is always at an apse, it is to be supposed that the "apse" is at the point where the particle is at the moment of change, and is again in a circle after it has moved through $2\pi - dc$. This could be definitely settled by working out the details, but there is no interest in doing so.

Returning now to the consideration of the general case, we shall take a given initial orbit (i. e. e_0, a_0, c_0) and trace the subsequent changes. In all cases these changes are symmetric on both sides of the nodal line as also of a line perpendicular to this. We may then confine the discussion to initial configurations between $c = 0$ and $\frac{1}{2}\pi$. Since $C^2\cos^2 a - 1$ is necessarily positive, $-da$, db are positive everywhere, so that within this region ($\sin 2c$ positive) a continually decreases, and $\cos a$, b continually increase as c increases from 0 to $\frac{1}{2}\pi$.

Consider, first, that category of orbits in which during their sæcular changes their line of apses coincides at some

instant with the node. The rates of increase of a vanish at $c=0$ and $c=\frac{1}{2}\pi$, increase up to a maximum at some point which depends on a_0 and C, and then decrease up to $c=\frac{1}{2}\pi$. Starting from an initial value a_0 at the node, a increases to some final value a_1 at $c=\frac{1}{2}\pi$, which, again, is dependent on the C of the orbit as well as on a_0. This a_1 will be less than $\cos^{-1}(1/C^2)$. This follows because if it ever attained this value it would continue in this state and the orbit remain a circle. Failing the integration of equations (17), the actual value of a_1 cannot be given explicitly, but in any special case it can be determined to any desired degree of accuracy by numerical calculation (see § 8).

The course of the changes in c is not so simple, since for certain categories of orbits dc may become negative in certain regions. dc is necessarily positive at the start, since then $\sin c$ is too small to make dc negative. If at the start $C^2\cos^4 a>1$, it will continue so, dc must always be positive, and c continually increase up to $\frac{1}{2}\pi$. If, however, $C^2\cos^4 a<1$, dc depends on $4-5(1-C^2\cos^4 a)\sin^2 c$, and whether it ever becomes zero or negative depends on the relative changes in a and c. In any case, if $\sin c$ reaches a value given by

$$5(1-C^2\cos^4 a)\sin^2 c = 4,$$

$dc=0$, $\sin c$ is stationary, whilst $1-C^2\cos^4 a$ goes on decreasing, and dc now again becomes positive. In such cases c rises to a stationary state at a certain value and then goes on again increasing to $\frac{1}{2}\pi$. Thus, for orbits in this category, dc can never become negative, or the line of apses always regredes.

Nevertheless, we can choose an orbit so that dc is negative. For this to happen we must have

$$C^2\cos^4 a-1<0, \qquad \cos^2 a<1-e^2, \qquad \sin a>e,$$

$$5(1-C^2\cos^4 a)>4, \qquad \sin^2 a>\cdot 8+\cdot 2e^2,$$

$$\sin^2 c>\tfrac{4}{5}(1-C^2\cos^4 a)^{-1}.$$

Since $\cdot 8+\cdot 2e^2>e^2$, the second condition is sufficient as well as necessary. Orbits in this category, therefore, must have large inclinations $>\sin^{-1}\sqrt{\cdot 8}$ or $63°\,26'\,6''$. Also, $\sin c$ cannot be $<\sqrt{\cdot 8}$, or c must be $>63°\,26'\,6''$. When these conditions for a, c are fulfilled, $\sin c$ decreases, but this cannot continue up to $\sin c=0$, for, apart from the constantly increasing $\cos a$, $\sin^2 c$ at last reaches a point which contravenes the third of the above conditions. After

reaching this, dc again becomes positive, $\sin^2 c$ now increases and is enabled to increase to 1 on account of the simultaneous increase of $\cos a$, which keeps dc positive. This is clear, since the longer $\sin c$ exists, the larger becomes $\cos a$ until $C^2 \cos^4 a - 1 > 0$, after which dc is necessarily positive. The point where $\sin^2 c$ reaches its smallest value is given by $dc = 0$, or

$$\sin^2 c_0 = \frac{4}{5} \frac{1-e^2}{\sin^2 a - e^2}.$$

In other words, if we choose as our initial configuration an orbit of eccentricity e, with inclination $a > a_0$, where $\sin^2 a_0 = \cdot 8 + \cdot 2e^2$, and with its axis at an angle given by the above value for $\sin^2 c_0$, the apses will move from c_0 to $\pi - c_0$, and will never coincide with a nodal line.

The question arises : How did the orbit arrive at the configuration in question? To see this we trace back. Here $\cos a$ decreases, dc is to be treated as positive, until at last $\sin c$ becomes unity. In other words, we must start with the line of apses perpendicular to the nodal line, and the configuration of such a nature that dc is negative. This will be a position of maximum inclination with the apses progreding at their maximum rate. They reach a position c_0 and then regrede, the inclination still decreasing and reaching its minimum when the apses are again perpendicular to the nodal line.

There are thus two categories of sæcular variations, distinguished as follows :—

I. The line of apses continually regredes, at a maximum rate, when they are perpendicular to the nodal line ; the orbital planes swing up and down with the maximum inclination when the apses coincide with the nodal line and the minimum when perpendicular. The nodal line constantly progredes.

II. The line of apses oscillates about the line perpendicular to the nodal line; the orbital planes swing up and down with their maximum and minimum inclinations, both at instants when the apses are perpendicular to the nodal. The greatest inclination occurs when the apses are swinging from left to right in the diagram, *i. e.* when they are swinging in the same direction as that of the particle in its orbit. Again the nodal line constantly progredes.

The transition state between these two categories occurs

for $e=0$. The orbit is then circular and inclined at the angle 63° 26′ 6″.

8. The period of these sæcular variations will clearly be of the order of magnitude of the $(\frac{5}{2}\omega\sqrt{k}\mathrm{C}^2)^{-1}$ of equation (16), say $1/q$ of this. Thus the number of cycles per sec.$=\frac{5}{2}q\omega\sqrt{k}\mathrm{C}^2$. Here

$$\sqrt{k}=\frac{\omega l^2}{h}=\frac{\mathrm{HE}}{2mc}\times\frac{\sqrt{m}}{\mathrm{E}}\,l^{3/2}=\frac{\mathrm{H}}{2c\sqrt{m}}\,l^{3/2}.$$

$$\text{The electron year}=\frac{2\pi}{\sqrt{p}}\mathrm{a}^{3/2}=2\pi\frac{\sqrt{m}}{\mathrm{E}}\mathrm{a}^{3/2}.$$

These results may be expressed thus, with $\mathrm{H}=30000\,x$ gauss :—

Electron years per sec. ..... $=2{\cdot}52\times10^{3}\,\mathrm{a}^{-3/2}$

Larmor cycles per year ..... $=1{\cdot}66\,x\times10^{7}\,\mathrm{a}^{3/2}$

Sæcular cycles per Larmor ..... $=2{\cdot}62\,q\mathrm{C}^2x\times10^{8}\,l^{3/2}$

„ „ „ electron year $=4{\cdot}35\,q\mathrm{C}^2x^2\times10^{15}\,\mathrm{a}^{3/2}\,l^{3/2}$

As $l=\mathrm{a}(1-e^2)$, l, a are of the same order.

We are now in a position to make some estimate of the orders of magnitude of H and of "a" below which we may treat their effects as small, *i. e.* for which we may neglect the effect of H^3 and higher orders. Taking, as examples, the two cases of orbits of order 10^{-8} and 10^{-6}, we get the following table :—

	10^{-8}.	10^{-6}.
Electron years per sec.	$2{\cdot}52\times10^{15}$	$2{\cdot}52\times10^{12}$
Larmor cycles per year	$1{\cdot}66\,x\times10^{-5}$	$1{\cdot}66\,x\times10^{-2}$
Sæcular cycles per Larmor ...	$2{\cdot}62\,\mathrm{A}x\times10^{-4}$	$2{\cdot}62\,\mathrm{A}x\times10^{-1}$
„ „ per year	$4{\cdot}35\,\mathrm{A}x^2\times10^{-9}$	$4{\cdot}35\,\mathrm{A}x^2\times10^{-3}$

Here A denotes $q\mathrm{C}^2$, and $\mathrm{H}=30000\,x$ gauss. The sæcular change for the 10^{-6} cm. orbit, or 360° per 1000 years, can certainly not be regarded as small. That for 10^{-8} is well within this limit.

To illustrate the foregoing analysis, a numerical computation has been carried out for one example from each category. The inclinations and apsidal regressions have been calculated from equations (17) by steps of $\frac{5}{2}\omega\sqrt{k}\mathrm{C}^2t$ at successive

intervals $=\cdot1$. The cases chosen are:

Cat. I. $a = 45°$; $e = \sin 45°$ when apse and node coincide.

„ II. $a = 70°$; $e = \sin 32° 26' = \cdot5363$; $c = 78° 8'$ for stationary position.

These require $C^2=4$ for I. and $C^2=12$ for II. The results are:

I. The orbital plane swings from 45° to 25° 55′ in $1\cdot08/(\frac{5}{2}\omega\sqrt{k}C^2)=\cdot108/(\omega\sqrt{k})$ seconds, whilst the apsidal line moves through 90°. Hence a complete cycle of one revolution of apse and two of the inclination takes place in $\cdot43/(\omega\sqrt{k})$ secs.

II. The plane swings from 72° 15′ through 70° to 64° 4′ and the apsidal line has oscillated from 90° to 78° 8′ and back to 90° in $2\cdot17/(\frac{5}{2}\omega\sqrt{k}C^2)=11\cdot9/(\omega\sqrt{k})$ sec. A complete cycle is twice this. The times from 90° to 78° 8′ and back to 90° are in the ratio ·98 : 1·19, say 5 : 6.

The numerical values for 10^{-8} and 10^{-6} are:

	I.		II.	
	10^{-8}.	10^{-6}.	10^{-8}.	10^{-6}.
Sæcular per Larmor	$2\cdot4x\times10^{-4}$	$2\cdot4x\times10^{-1}$	$7\cdot22x\times10^{-4}$	$7\cdot22x\times10^{-1}$
„ „ year ...	$4x^2\times10^{-9}$	$4x^2\times10^{-3}$	$1\cdot19x^2\times10^{-8}$	$1\cdot19x^2\times10^{-2}$

LXXXIV. *On the characteristic Infra-Red Vibrations of certain Crystals of the Rock-Salt Type.* *By* L. G. Carpenter, *B.A., B.Sc., Lecturer in Physics, and* L. G. Stoodley, *B.Sc., Research Student in Physics, University College, Southampton* *.

Introduction.

In a recent series of papers † in the Proceedings of the Royal Society, J. E. Lennard-Jones has shown how the

* Communicated by the Authors.

† Proc. Roy. Soc. A, cvi. pp. 441, 463, 709 (1924); A, cvii. pp. 157, 636 (1925); A, cix. pp. 476, 584 (1925); A, cxii. pp. 214, 230 (1926). These papers will be referred to below as Papers I. to IX.

force fields of certain atoms and ions may be deduced from one or more of the following data :—

1. The variation of viscosity of gases with temperature.
2. The equation of state of gases.
3. X-Ray measurements of interatomic distances in crystals.
4. Certain measurements of ionic refractivities by Wasastjerna.
5. The compressibility of certain crystals.

Lennard-Jones has classified the forces which occur between ions whose electronic structure is similar to that of the inert gases under four heads*:—(1) electrostatic forces; (2) van der Waals' attractive forces ; (3) intrinsic repulsive forces ; and (4) forces due to polarization. In crystals of a high degree of symmetry, such as rock-salt, the polarization forces need not be considered ; the van der Waals' attractive forces can also be neglected in comparison with the electrostatic forces. There remain, therefore, the electrostatic forces and the intrinsic repulsive forces. The electrostatic forces are of the inverse square type and depend on the valency of the ions concerned ; while the intrinsic repulsive forces are known from the work of Lennard-Jones.

Lennard-Jones proceeds on the assumption that the intrinsic repulsive fields of the atoms and ions with which he deals may be regarded as spherically symmetrical, the field being represented by a formula of the type $\lambda_n r^{-n}$. This treatment of atomic and ionic fields on the basis of inverse power laws must be considered as approximate merely, to be replaced by more accurate methods when our knowledge of the disposition and motion of electrons in atoms is more complete †.

Born and Brody ‡ have shown that, for regular diatomic crystals of the rock-salt type, electrostatic cohesive forces, together with other forces, proportional to r^{-n} suffice for the explanation of expansion phenomena, elastic properties and infra-red frequencies. It is with these last that we are concerned here. Using density and compressibility data Born and Brody obtained values of n for the crystals dealt with, and calculated the frequencies of the characteristic infra-red vibrations. The values so obtained, when corrected by a method due to Försterling § for the difference

* Paper IX.
† Paper I. p. 441.
‡ *Zeits. f. Phys.* (11) vi. p. 327 (1922).
§ *Ann. d. Phys.* (4) lxi. p. 577 (1920).

between characteristic frequencies and residual ray frequencies, are in good agreement with the experimental values obtained by Rubens.

It is the object of the present paper to point out that, using the data of Lennard-Jones, characteristic infra-red frequencies of the salts NaCl, KCl, KBr, and KI may be calculated which are in fair agreement with those obtained by Born and Brody from the compressibility and density of crystals. The method of treatment here given is a rough approximation; it will be seen that the agreement with the results of Born and Brody is, except in the case of NaCl, within about 10 per cent. Lennard-Jones has calculated the force constants for argon-like and neon-like * ions without making use of data derived from the compressibility in the *solid* state. The values obtained in the present paper for the infra-red frequencies of NaCl and KCl are therefore also independent of compressibility measurements on solid crystals, and hence it is of especial interest to compare them with those obtained by Born and Brody.

In the case of xenon-like and krypton-like † ions Lennard-Jones has deduced values λ_n and n from the interatomic distances and compressibilities of solid crystals, together with the refractivity data of Wasastjerna. The infra-red frequencies of KBr and KI calculated in this paper are, therefore, dependent on these data also.

Method of Treatment.

We here calculate the frequency of the characteristic infra-red vibrations of NaCl, KCl, KBr, and KI on the following assumptions :—

1. In a crystal the two oppositely charged ionic lattices may be represented as vibrating as wholes relatively to one another.
2. The frequency of this vibration is identical with that of characteristic infra-red vibration of the crystal.
3. The oscillations are of sufficiently small amplitude to be taken as simple harmonic ; *i. e.*, the restoring force is proportional to the first power of the displacement.

* In Paper VI. page 485, he chose the model of Ne by comparison with the observed interatomic distance in NaF. In Paper VIII., however, he showed that the choice of this model was independently confirmed by the fact that it was the one which gave the best concordance between isotherm measurements and measurements of viscosity and thermal conductivity

† Paper VII.

4. The restoring force on an ion in a displaced lattice of one sign depends only on the presence of the 14 nearest ions in the lattice of the opposite sign, the effect of the remaining ions being neglected.

The frequency with which the positive lattice of mass M_1 and the negative lattice of mass M_2 oscillate relatively to each other is easily shown by simple dynamical reasoning to be

$$\nu = \frac{1}{2\pi}\sqrt{\frac{F_1(M_1+M_2)}{M_1M_2}}, \quad . \quad . \quad . \quad . \quad (1)$$

where F_1 is the restoring force on one lattice per unit displacement relative to the other.

If there are N ions of each sign in the lattice, then

$$F_1 = Nf_1, \quad . \quad . \quad . \quad . \quad . \quad . \quad . \quad (2)$$

where f_1 is the restoring force per unit displacement on one ion. This is evidently the case, since, by symmetry, all the ions are acted upon by similar forces, so that the total restoring force on the lattice is the arithmetic sum of the forces on individual ions. Similarly,

$$M_1 = Nm_1, \quad . \quad . \quad . \quad . \quad . \quad . \quad (3)$$

$$M_2 = Nm_2, \quad . \quad . \quad . \quad . \quad . \quad . \quad (4)$$

where m_1 and m_2 are the masses of the positive and negative ions respectively.

Hence the frequency of relative vibration of the lattices is

$$\nu = \frac{1}{2\pi}\sqrt{\frac{f_1(m_1+m_2)}{m_1m_2}} \quad . \quad . \quad . \quad . \quad . \quad (5)$$

We therefore calculate f_1 taking only the 14 neighbouring ions of opposite sign into account, and substituting in (5) deduce the corresponding frequency. It is convenient first to obtain a general expression for the restoring force per unit displacement on a displaced ion, due to another ion, for an inverse pth power law, the direction of displacement making any angle θ with the line joining the centres of the two ions.

Calculation of Restoring Force for Small Displacements.

Let P be an ion at a distance ϵ from another ion. Let the force between P and Q be represented by

$$F = \lambda_p \epsilon^{-p}.$$

Then the resolved part of this force in direction X′ X is

$$\frac{\lambda_p}{\epsilon^p}\cos\theta.$$

Let P be displaced by an amount Δx (small compared with ϵ) in the direction X′ X. Then, the restoring force

$$= -\Delta F,$$

where $\Delta F = \frac{d}{dx}\left(\frac{\lambda_p}{\epsilon^p}\cos\theta\right)\Delta x,$

$$= \lambda\left[\frac{-p\,d\epsilon}{\epsilon^{p+1}dx}\cos\theta - \frac{1}{\epsilon^p}\sin\theta\frac{d\theta}{dx}\right]\Delta x,$$

$$= \lambda_p\left[\frac{p}{\epsilon^{p+1}}\cos^2\theta - \frac{1}{\epsilon^p}\frac{\sin^2\theta}{\epsilon}\right]\Delta x,$$

Fig. 1.

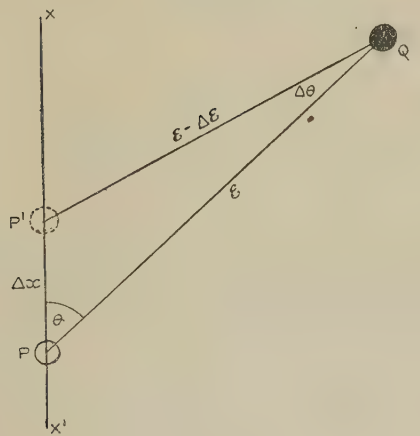

since $\frac{\Delta\epsilon}{\Delta x} = -\cos\theta$ and $\epsilon\Delta\theta = \Delta x\sin\theta,$

$$\therefore \quad \frac{\Delta F}{\Delta x} = \frac{\lambda}{\epsilon^{p+1}}\left[p\cos^2\theta - \sin^2\theta\right] \quad . \quad . \quad . \quad . \quad (6)$$

Let fig. 2 represent the structure of crystals of the rock-salt type, the black and white points representing positive and negative ions respectively. Let ϵ be the shortest distance between a positive and a negative ion. Calculate the restoring force per unit displacement of the ion P along the line AB parallel to the X X′ axis.

(*a*) In the case of ions 2 and 4, $\theta = 0°$;

$$\therefore \quad \frac{\Delta F}{\Delta x} = \frac{2\lambda_p}{\epsilon^{p+1}} \cdot p. \quad . \quad . \quad . \quad . \quad . \quad . \quad (7)$$

(*b*) In the case of ions 1, 5, 3, 6, $\theta = 90°$;

$$\therefore \quad \frac{\Delta F}{\Delta x} = -\frac{4\lambda_p}{\epsilon^{p+1}}. \quad . \quad . \quad . \quad . \quad . \quad (8)$$

Fig. 2.

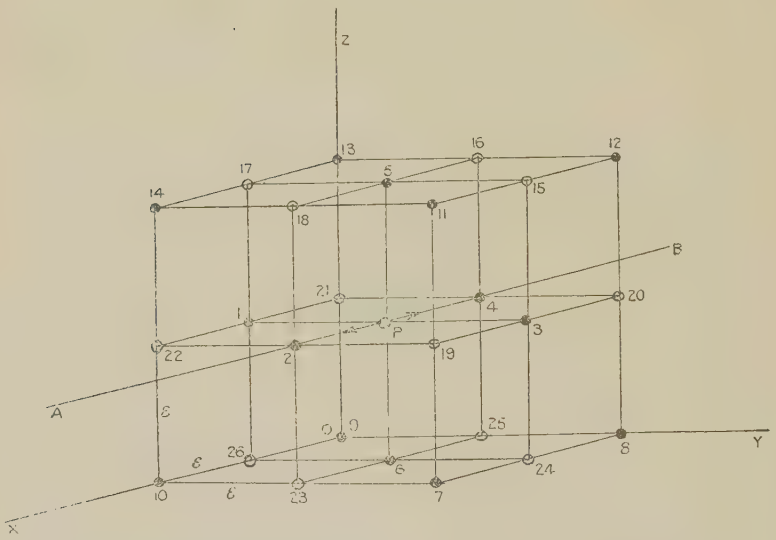

(*c*) In the case of ions 7–14 consider the effect of ions 7, 8, 13, 14 on P ; (fig. 3),

$$\cos\theta = \frac{1}{\sqrt{3}},$$

$$\sin\theta = \sqrt{\frac{2}{3}},$$

$$\therefore \quad \frac{\Delta F}{\Delta x} = \frac{4\lambda_p}{(\sqrt{3}\epsilon)^{p+1}}\left[\frac{p}{3} - \frac{2}{3}\right],$$

$$= \frac{4\lambda_n}{3^{\frac{p+3}{2}}\epsilon^{p+1}}[p-2].$$

The effect of the ions 9, 10, 11, 12 is precisely similar. Hence, for the ions 7–14, the total effect is given by

$$\frac{\Delta F}{\Delta x} = \frac{8\lambda}{3^{\frac{p+3}{2}}\epsilon^{p+1}}[p-2]. \quad . \quad . \quad . \quad . \quad . \quad . \quad (9)$$

Fig. 3.

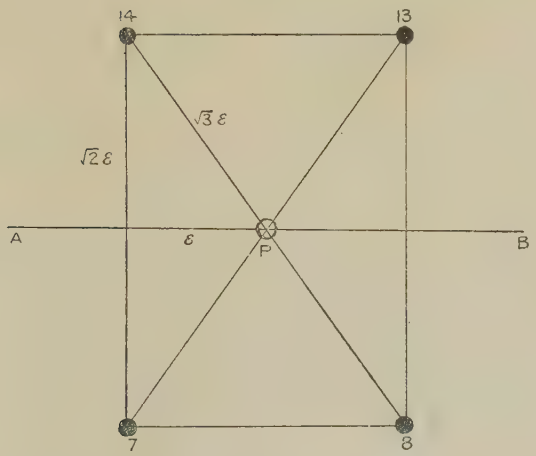

Hence, the total effect of the 14 nearest ions of one sign on an ion of the opposite sign is given by adding equations (7), (8) and (9), and f_1, the restoring force per unit displacement is given by

$$f_1 = \frac{2\lambda_p}{\epsilon^{p+1}}[p-2]\left[1+\frac{4}{3^{\frac{p+3}{2}}}\right]. \quad . \quad . \quad . \quad (10)$$

This equation is, of course, strictly true only for vibrations of infinitely small amplitude.

Numerical Results.

The repulsive force constants (λ_n), and the indices of the repulsive power law (n) * for the four crystals considered,

* Paper IX.

are given below in Table I., together with values of ϵ the shortest distance between a positive and a negative ion as determined by X-ray measurements.

Table I.

	λn.	n.	ϵ.
NCl	$2{\cdot}12\times10^{-80}$	10	$2{\cdot}814\times10^{-8}$
KCl	$1{\cdot}59\times10^{-72}$	9	$3{\cdot}13\times10^{-8}$
KBr	$1{\cdot}95\times10^{-72}$	9	$3{\cdot}285\times10^{-8}$
KI	$1{\cdot}15\times10^{-79}$	10	$3{\cdot}525\times10^{-8}$

From these are calculated, by means of equation (10), the corresponding values of f_1. It will be noticed that in equation (10), f_1 vanishes when $p=2$. Hence, the contribution of the inverse square electrostatic attraction to the restoring force per unit displacement is zero within the body of the crystal. The charge on the ions affects the frequency through the effect on ϵ.

The value of $\frac{m_1m_2}{m_1+m_2}$ is calculated, taking the mass of the hydrogen atom as $1{\cdot}66\times10^{-24}$ gram. Substituting in equation (5), we obtain the frequency of the characteristic infrared vibrations: the results are given in Table II.

Table II.

	f_1.	$\frac{m_1m_2}{m_1+m_2}$.	ν.
NaCl	$3{\cdot}88\times10^{4}$	$2{\cdot}30\times10^{-23}$	$6{\cdot}54\times10^{12}$
KCl	$2{\cdot}47\times10^{4}$	$3{\cdot}06\times10^{-23}$	$4{\cdot}52\times10^{12}$
KBr	$1{\cdot}87\times10^{4}$	$4{\cdot}32\times10^{-23}$	$3{\cdot}32\times10^{12}$
KI	$1{\cdot}77\times10^{4}$	$4{\cdot}92\times10^{-23}$	$3{\cdot}02\times10^{12}$

Finally, the results, converted to wave-lengths, are compared in Table III. with those of Born and Brody*; the observations of the residual rays by Rubens are included in the third column.

TABLE III.

	Wave-lengths.		
	Calculated.	Born and Brody.	Residual rays.
NaCl	45·9 μ	61·6 μ	52·0 μ
KCl.....	66·4	74·5	63·4
KBr	90·5	88·0	82·6
KI	99·5	108·3	94·1

The agreement with the calculations of Born and Brody is least satisfactory in the case of NaCl, for which the wave-length 45·9 μ is evidently too low; it is less than the wave-length of the residual rays.

The repulsive force constants determined by Lennard-Jones and used in the calculations of this paper are believed† to be accurate within about 10 per cent. The uncertainty from this cause in the values of the characteristic infra-red wave-lengths here deduced should therefore be about 5 per cent., since these wave-lengths are inversely proportional to the square roots of the force constants.

The wave-lengths of the characteristic infra-red vibrations are seen to differ from those of the residual rays, as indeed they should. The magnitude of the difference theoretically to be expected between the wave-lengths obtained by Born and Brody and those observed by Rubens has been calculated by Försterling‡, who finds satisfactory agreement with experiment.

In conclusion, our thanks are due to Professor F. A. Lindemann and to Mr. F. G. Maunsell, with whom we have discussed the subject matter of this paper.

Note added in proof.—Since the above paper was written,

* *Loc. cit.*
† Paper IX. p. 234.
‡ *Loc. cit.*

a paper * by O. Reinkober has come to our notice, in which an experimental value of 74μ is given for the wave-length of the residual rays of rubidium chloride. Lennard-Jones has given the numerical data representing the repulsive force between a rubidium and a chlorine ion, and the crystal structure of rubidium chloride has been determined and is of the rock-salt type †. It is, therefore, of interest to calculate the wave-length of the fundamental vibration in the manner already described. The result is given in the table below :—

TABLE IV.

λn.	n.	ϵ.	γ.	$\frac{m_1 m_2}{m_1+m_2}$	Wave-length.	
					Calculated.	Residual Rays.
$2{\cdot}1\times10^{-72}$	9	$3{\cdot}267\times10^{-8}$	$2{\cdot}13\times10^{4}$	$4{\cdot}13\times10^{-23}$	$82{\cdot}9\ \mu$	74μ

It is seen that the wave-length of the fundamental vibration is greater than that of the residual rays, as it is in the case of the other crystals considered (except NaCl), and that if the residual ray wave-length be placed in numerical order between KCl and KBr in Table III., then the calculated fundamental wave-length lies between those of the same two salts.

LXXXV. *An Extension of Dulong and Petit's Law to Gaseous Compounds and Mixtures.* By Prof. A. PRESS ‡.

IN deriving the laws pertaining to adiabatic processes (see Phil. Mag., Dec. 1927), the writer deduced the following formulæ which held simultaneously

$$\left.\begin{aligned} pv_\gamma &= \text{constant} \\ pv &= (\gamma-1) \end{aligned}\right\} \quad . \quad . \quad . \quad . \quad . \quad . \quad (15)$$

* *Zeits. f. Phys.* xxxix. 5-6, p. 437 (1926).
† Bragg, 'X-Rays and Crystal Structure,' 5th ed. p. 306.
‡ Communicated by the Author.

The latter were derived from the relation

$$\gamma = -\frac{v}{p} \cdot \frac{dp}{dv} = 1 + \frac{d(pv)^*}{dU} \quad . \quad . \quad . \quad . \quad (12)$$

It is easily checked that the latter amounts to *proving* that

$$p \cdot dv + dU = 0.$$

The anomalies of Thomson and Joule (see Birtwistle, 'Thermodynamics,' p. 76) have therefore to be accounted for on the basis that the γ components of specific heat varied during the process of the experiment.

Turning, then, to the second of (15), there is clearly a relation indicated with the usual equation of state,

$$pv = R\theta, \quad . \quad . \quad . \quad . \quad . \quad . \quad . \quad . \quad (8)$$

which, as known, applies rather well to all so-called fixed gases. We should therefore expect to find that, by equating the respective right-hand terms to each other, the following formula should hold, viz.:

$$(\gamma - 1)U = \alpha R\theta.$$

This would indicate at once by differentiating with respect to θ that

$$\frac{\partial U}{\partial \theta} = \alpha \frac{R}{\gamma - 1}.$$

On the basis of Avogadro's law it is known that we have

$$R = 2 \text{ calories per gram-molecule.}$$

If, then, we substitute with M = molecular weight, as follows:

$$R = \frac{2}{M},$$

$$\left(\frac{\partial U}{\partial \theta}\right)_p = \text{specific heat} = s,$$

then it results that

$$2\alpha = (\gamma - 1) \cdot s \cdot M.$$

This formula is, of course, very much different from that of Leray, mentioned in Preston's 'Theory of Heat,' p. 295.

* The error of sign, *l. c.*, should be corrected.

The constancy of the factor α is indicated by the following tabulation :—

Substance *.	γ.	$\gamma-1$.	s.	M.	2α calc.
Air	1·4	·4	·238	28·8	2·74
Alcohol	1·136	·136	·453	46·06	2·84
Ammonia	1·31	·31	·523	17	2·78
Bromine	1·293	·293	·0553	159·9	2·59
CO_2	1·3	·3	·201	44	2·65
CO	1·4	·4	·243	28	2·73
CS_2	1·2	·2	·16	76·1	2·43
Chlorine	1·32	·323	·1125	71	2·58
Chloroform	1·106	·106	·149	119·4	1·89
Ether	1·029	·029	·456	74·1	·98
HCl	1·395	·395	·194	36·5	2·8
H_2	1·41	·41	·3406	2	2·79
H_2S	1·276	·276	·245	34·1	2·3
Methane	1·316	·316	·593	16·03	3·0
Nitrogen	1·41	·41	·244	28	2·8
Nitrous Oxide	1·291	·291	·221	44	2·82
SO_2	1·26	·26	·7544	64·1	2·57
Steam	1·3	·3	·43	18	2·32
Argon	1·6	·6	·123	39·9	2·95
Oxygen	1·4	·4	·2175	32	2·78
Benzol	1·4	·4	·299	78	·936

* Similarly, it can be shown that, taking provisionally that the specific heat of mercury vapour is ·03 and $\gamma=1·6$, we have $2\alpha=·6\times200\times·03=3·6$.

Thus, the improved form of Dulong and Petit's formula is the following :

$$2\alpha=s\mathrm{M}(\gamma-1),$$

in which, of course, the expression $2\alpha/(\gamma-1)$ becomes, for solids,

$$\frac{2\alpha}{\gamma-1}\equiv6·4.$$

1314–18th St., N.W.,
Washington, D.C., U.S.A.
Dec. 24, 1927.

LXXXVI. *On Relativistic Cosmology.* *By* H. P. Robertson, *Ph.D., National Research Fellow in Mathematics**.

THE general theory of relativity considers physical space-time as a four-dimensional manifold whose line element coefficients $g_{\mu\nu}$ satisfy the differential equations

$$G_{\mu\nu} = \lambda g_{\mu\nu} \quad . \quad . \quad . \quad . \quad . \quad . \quad (1)$$

in all regions free from matter and electromagnetic field, where $G_{\mu\nu}$ is the contracted Riemann-Christoffel tensor associated with the fundamental tensor $g_{\mu\nu}$, and λ is the cosmological constant †. An "empty world," *i. e.* a homogeneous manifold at all points of which equations (1) are satisfied, has, according to the theory, a constant Riemann curvature, and any deviation from this fundamental solution is to be directly attributed to the influence of matter or energy. In considerations involving the nature of the world as a whole the irregularities caused by the aggregation of matter into stars and stellar systems may be ignored ; and if we further assume that the total matter in the world has but little effect on its macroscopic properties, we may consider them as being determined by the solution for an empty world ‡.

The solution of (1), which represents a homogeneous manifold, may be written in the form :

$$ds^2 = -\frac{d\rho^2}{1-\kappa^2\rho^2} - \rho^2(d\theta^2 + \sin^2\theta d\phi^2) + (1-\kappa^2\rho^2)c^2d\tau^2, \quad (2)$$

where $\kappa = \sqrt{\lambda/3}$. If we consider ρ as determining distance from the origin (the measured distance being then $\sin^{-1}\kappa\rho/\kappa$) and τ as measuring the proper-time of a clock at the origin, we are led to the de Sitter spherical world ; the astronomical

* Communicated by Prof. A. S. Eddington, F.R.S.

† A. Einstein, "Die Grundlage der allgemeinen Relativitätstheorie," *Ann. d. Physik*, xlix. p. 769 (1916); 'Kosmologische Betrachtungen zur allgemeinen Relativitätstheorie,' Berlin, Sitzungsberichte, 1917, p. 142; W. de Sitter, "On Einstein's Theory of Gravitation and its Astronomical Consequences." Monthly Notices, R. A. S. lxxvi. p. 699, lxxvii. p. 155, lxxviii. p. 3 (1916-17). The notation here used is that of A. S. Eddington, 'The Mathematical Theory of Relativity,' Cambridge, 1923.

‡ This view, due to de Sitter, is an alternative to one proposed by Einstein in which the existing matter is considered uniformly spread throughout the world. The equations (1) are not applicable in this latter case, as terms involving the density must then be added to the right-hand side.

consequences of this interpretation have been discussed by de Sitter, Eddington and Weyl *. Important among these is the prediction that the spectral lines in light from distant sources should be displaced toward the red; this would be interpreted as Doppler effect due to a larger motion of recession of the source, and seems to be in accord with the known facts concerning the radial velocities of spiral nebulæ. The singularity $\rho = \frac{1}{\kappa}$ of the line element creates the illusion of a "mass-horizon" which recedes as we approach it and concerning which we can obtain no direct information, as light emitted from it never reaches us.

It is the purpose of this paper to replace (2) by a mathematically equivalent solution which is susceptible of a perhaps simpler interpretation and in which many of the apparent paradoxes inherent in (2) are eliminated; aside from this, it offers a convenient method of investigating the properties of the de Sitter form. The last paragraph will be devoted to a discussion of the analogous solution for a spherically symmetric mass.

1. *Kinematics.*—If we subject the de Sitter solution (2) to the transformation

$$\rho = re^{\kappa ct}, \qquad \tau = t - \frac{1}{2\kappa c}\log(1-\kappa^2 r^2 e^{2\kappa ct}),$$

we obtain

$$ds^2 = -e^{2\kappa ct}(dx^2 + r^2 d\theta^2 + r^2 \sin^2\theta d\phi^2) + c^2 dt^2,$$

or, on changing to rectangular coordinates,

$$x = r\sin\theta\cos\phi, \qquad y = r\sin\theta\sin\phi, \qquad z = r\cos\theta,$$

$$ds^2 = -e^{2\kappa ct}(dx^2 + dy^2 + dz^2) + c^2 dt^2. \quad . \quad . \quad . \quad (3)$$

The space-time manifold, which is described in the de Sitter interpretation with the aid of the variable ρ with finite range $0 < \rho \leqq 1/\kappa$, is here described with the aid of r with infinite range, and the singularity $\rho = 1/\kappa$ is removed from the finite region.

Interpreting t as the proper-time of a clock at the origin, the distance, measured at time t with a rigid scale, from the origin to a point whose spacial coordinates are (r, θ, ϕ) is $l = re^{\kappa ct}$. The proper-times of all observers at points $(r, \theta, \phi) = \text{constant}$ coincide with that of an observer at the origin,

* De Sitter, *l. c.* (third paper); Eddington, *l. c.* chap. v.; H. Weyl, "Zur allgemeinen Relativitätstheorie," *Phys. Zeits.* xxiv. p. 230 (1923).

and such observers will be called *equivalent*. The line element (3) is "dynamical" in that its coefficients depend on the time t, whereas (2) is not. That the properties of the manifold are, however, independent of t may be seen by introducing a change of scale and time origin by means of the transformation

$$\bar{r} = re^{\kappa c t_0}, \qquad \bar{t} = t - t_0.$$

A perhaps more serious objection is that the world is on this interpretation of infinite extent, but, as will be seen later, its closed character is maintained in the sense that the only events of which we can be aware must occur within a sphere of finite radius. In common with the special relativity world, and in contradistinction to the de Sitter world, the geometry of space is euclidean and the velocity of light is independent of its direction. The properties which distinguish the space-time defined by (3) from that of special relativity are thus to be sought in its kinematics.

The velocity of a point moving along the x-axis, measured by an observer at the origin, is

$$V_x = (x' + \kappa c x)e^{\kappa c t} = x' e^{\kappa c t} + \kappa c l_x \qquad \left(x' = \frac{dx}{dt}\right),$$

the time rate of change of its measured distance $l_x = xe^{\kappa c t}$. An equivalent observer at x, whose coordinate velocity x' must by definition be zero, will thus have a measured velocity $\kappa c l_x$ relative to 0, and light travelling along the x-axis, whose coordinate velocity is by (3) $\gamma = ce^{-\kappa c t}$, will have as measured velocity $c(1 + \kappa l_x)$. The measured velocity along the y- and z-axes may be similarly defined, and, by means of its three components, the motion of an arbitrarily moving point described. We shall usually refer to these quantities simply as distance and velocity, and it is to be remembered that they are measured with respect to some definite observer; the quantities x and x' will always be called the coordinate distance (or interval) and coordinate velocity.

2. *Geodesics.*—The geodesics of the manifold defined by (3), in terms of the time t as parameter, are obtained by minimizing the integral

$$\int_{t_0}^{t} \mathrm{F}(tx'y'z')\,dt, \qquad x' = \frac{dx(t)}{dt}, \text{ etc.},$$

where

$$\mathrm{F}(tx'y'z') = \frac{ds(t)}{dt} = \sqrt{-e^{2\kappa c t}(x'^2 + y'^2 + z'^2) + c^2}.$$

Since F does not depend on x, the Euler equation

$$\frac{\partial}{\partial t}\frac{\partial F}{\partial x'} - \frac{\partial F}{\partial x} = 0$$

yields immediately

$$\frac{x' e^{2\kappa c t}}{F(t x' y' z')} = \text{const.},$$

and the corresponding integrals for y and z are obtained in the same way. Solving for x', y', z', and choosing the constants of integration in such a way that these quantities assume the values δ_x, δ_y, δ_z at time $t = t_0$, we find

$$x' = \delta \frac{e^{-2\kappa c(t-t_0)}}{\sqrt{1-\left(\frac{\delta}{\gamma_0}\right)^2(1-e^{-2\kappa c(t-t_0)})}} = \delta_x \frac{\beta_0 e^{-2\kappa c(t-t_0)}}{\sqrt{1+\left(\frac{\delta\beta_0}{\gamma_0}\right)^2 e^{-2\kappa c(t-t_0)}}}, \text{ etc.,} \quad (4)$$

where $\gamma_0 = c e^{-\kappa c t_0}$, the initial coordinate velocity of light,

$$\delta^2 = \delta_x^2 + \delta_y^2 + \delta_z^2,$$

and $\beta_0 = \left(1-\left(\frac{\delta}{\gamma_0}\right)^2\right)^{-\frac{1}{2}}$.

The coordinates themselves are, on integrating (4),

$$x - x_0 = \delta_x \frac{\gamma_0}{\kappa\delta^2} e^{\kappa - c t_0}\left(1 - \frac{1}{\beta_0}\sqrt{1+\left(\frac{\delta\beta_0}{\gamma_0}\right)^2 e^{-2\kappa c(t-t_0)}}\right), \text{ etc.} \quad . \quad . \quad (5)$$

These are, according to the postulates of the general theory of relativity, the equations of motion of a free particle.

The minimal geodesics, giving the equations of motion of light, are

$$\left.\begin{aligned} x' &= \delta_x e^{-\kappa c(t-t_0)}, \qquad \delta = \gamma_0, \\ x - x_0 &= \frac{\delta_x}{\kappa\gamma_0} e^{-\kappa c t_0}(1 - e^{-\kappa c(t-t_0)}), \text{ etc.} \end{aligned}\right\} \quad . \quad . \quad (6)$$

Since

$$\frac{x-x_0}{\delta_x} = \frac{y-y_0}{\delta_y} = \frac{z-z_0}{\delta_z},$$

the motion of a free particle or light is rectilinear in the x, y, z coordinate space.

A particle, starting from $(x_0, 0, 0)$ at time $t=t_0$ with coordinate velocity $(-\delta, 0, 0)$, approaches the limiting position defined by

$$x_0 - \frac{\gamma_0}{\delta\kappa} e^{-\kappa c t_0}\left(1-\frac{1}{\beta_0}\right);$$

so, unless the initial measured distance

$$l_0 = x_0 e^{\kappa c t_0} < \mathrm{L}\left(\frac{\delta}{\gamma_0}\right) = \frac{1}{\kappa}\frac{\gamma_0}{\delta}\left(1-\sqrt{1-\left(\frac{\delta}{\gamma_0}\right)^2}\right),$$

it can never reach an observer at the origin. For a beam of light this becomes

$$l_0 < \mathrm{L}(1) = \frac{1}{\kappa},$$

and since $\mathrm{L}(\zeta)$ is a monotonic increasing function of ζ, it follows that all particles or light which reach an observer at the origin are initially within a sphere of measured radius $\mathrm{R}=1/\kappa$. Hence the only events concerning which we can obtain any knowledge must occur within this sphere; it constitutes, therefore, our observable universe. According to recent evidence, celestial objects as distant as 10^{26} cm. have been observed, so R must be greater than this—the interpretation given below of data concerning spiral nebulæ indicates that it is of order between 10^{27} and 10^{28} cm. Considerations involving the whence and whither of celestial objects lead to results of a rather paradoxical nature—all matter and light within our observable universe must have started from the boundary and will be eventually lost to it;—but such long-time predictions cannot be taken too literally, as we have neglected their influence on the line element, an influence which undoubtedly plays an important role in such questions.

3. *Representation in Euclidean 5-Space. Transformations of Space-Time.*—Since the manifold defined by (3) has constant Riemann curvature, it must be possible to imbed it in euclidean space of five dimensions. This representation will be of value in finding the transformations relating the measurements of observers in relative motion—the analogue of the Lorentz transformations in special relativity.

We can, in fact, write (3) in the form:

$$ds^2 = -(d\alpha^2+d\beta^2+d\gamma^2)+d\zeta^2-d\eta^2, \quad . \quad . \quad (7)$$

where

$$\left.\begin{aligned} \alpha &= x\,e^{\kappa ct}, \qquad \zeta = \frac{1}{\kappa}\sinh \kappa ct + \tfrac{1}{2}\kappa r^2 e^{\kappa ct}, \\ \beta &= y\,e^{\kappa ct}, \qquad \eta = \frac{1}{\kappa}\cosh \kappa ct - \tfrac{1}{2}\kappa r^2 e^{\kappa ct}, \\ \gamma &= z\,e^{\kappa ct}. \end{aligned}\right\} \quad . \quad . \quad (8)$$

The equation of space-time is then

$$\alpha^2+\beta^2+\gamma^2-\zeta^2+\eta^2 = \frac{1}{\kappa^2}, \quad . \quad . \quad . \quad . \quad (9)$$

and it may therefore be considered as a hyper-sphere in the euclidean 5-space (7). A geodesic is the intersection of a (two-dimensional) plane through 0 with this hyper-surface.

Now, any rotation of this 5-space, *i. e.* any transformation under which (7) and (9) are invariant, will generate a transformation of the space-time variables which leaves (3) invariant. To obtain the explicit form of these latter it is only necessary to solve the equations:

$$\left.\begin{aligned} \bar{\alpha} &= a_{11}\alpha + a_{12}\beta + \ldots a_{15}\eta, \\ \bar{\beta} &= a_{21}\alpha + \ldots \\ &\vdots \\ \bar{\eta} &= a_{51}\alpha + \ldots \qquad a_{55}\eta, \end{aligned}\right\} \quad . \quad . \quad . \quad . \quad (10)$$

defining the rotation of the 5-space, where α, β, etc. are the functions of x, y, z, t given by (8), and $\bar{\alpha}$, $\bar{\beta}$, etc. are the same functions of the transformed space-time variables $\bar{x}$, $\bar{y}$, $\bar{z}$, $\bar{t}$. But four of these five equations are independent, as the constants a_{ij} must be so chosen that

$$\bar{\alpha}^2+\bar{\beta}^2+\bar{\gamma}^2-\bar{\zeta}^2+\bar{\eta}^2 = \alpha^2+\beta^2+\gamma^2-\zeta^2+\eta^2,$$

and on substituting (8) this leads to an identity, so we have just enough equations to solve for $\bar{x}, \bar{y}, \bar{z}, \bar{t}$ as functions of x, y, z, t.

In order to effect the complete solution of this problem, we may consider the general transformation (10) as composed of ten elemental rotations, in each of which only the coordinates of one (two-dimensional) plane are involved. Because of the symmetry existing between α, β, γ, this number can be reduced to four, say those in the (β, γ), (ζ, η), (α, η), (α, ζ) planes; in place of the third, however, it is found simpler to consider a rotation in a certain plane of the (α, ζ, η) 3-space.

The first of these elemental transformations obviously leads to a rotation of the y and z axes. The second, which may be written

$$\bar{\zeta} = \cosh\epsilon\zeta - \sinh\epsilon\eta, \quad \bar{\alpha} = \alpha, \quad \bar{\beta} = \beta,$$
$$\bar{\eta} = -\sinh\epsilon\zeta + \cosh\epsilon\eta, \quad \bar{\gamma} = \gamma,$$

to

$$\bar{x} = xe^{\epsilon}, \quad \bar{y} = ye^{\epsilon}, \quad \bar{z} = ze^{\epsilon}, \quad t = \bar{t} - \frac{\epsilon}{\kappa c};$$

i. e., a change of time origin, with corresponding change of scale. The third rotation, defined by

$$\bar{\alpha} = \alpha - \epsilon\zeta - \epsilon\eta, \qquad \bar{\beta} = \beta, \quad \bar{\gamma} = \gamma,$$
$$\bar{\zeta} = -\epsilon\alpha + \left(1 + \frac{\epsilon^2}{2}\right)\zeta + \frac{\epsilon^2}{2}\eta,$$
$$\bar{\eta} = \epsilon\alpha - \frac{\epsilon^2}{2}\zeta + \left(1 - \frac{\epsilon^2}{2}\right)\eta,$$

gives rise to a change of x origin. These three types are rather trivial, representing the transformations of euclidean 3-space with change of time origin. The most general rotation which can be built from them gives the relations between the coordinates of equivalent observers.

The only type remaining to be considered is a rotation in the $(\alpha\zeta)$ plane:

$$\bar{\alpha} = \cosh\epsilon\alpha - \sinh\epsilon\zeta, \qquad \bar{\beta} = \beta, \qquad \bar{\gamma} = \gamma.$$
$$\bar{\zeta} = -\sinh\epsilon\alpha + \cosh\epsilon\zeta, \quad \bar{\eta} = \eta,$$

On solving for x, y, z, t, we find

$$\left.\begin{aligned}
\bar{x} &= -\frac{1}{\kappa}\coth\frac{\epsilon}{2}\,\frac{1 - 2\coth\epsilon\kappa x + \kappa^2 r^2 - e^{-2\kappa c\bar{t}}}{\coth^2\frac{\epsilon}{2} - 2\coth\frac{\epsilon}{2}\kappa x + \kappa^2 r^2 - e^{-2\kappa c\bar{t}}},\\
\bar{t} &= t + \frac{1}{\kappa c}\log\left\{\sinh^2\frac{\epsilon}{2}\left(\coth^2\frac{\epsilon}{2} - 2\coth\frac{\epsilon}{2}\kappa x + \kappa^2 r^2 - e^{-2\kappa c\bar{t}}\right)\right\},\\
\bar{y} &= ye^{\kappa c(t-\bar{t})}, \qquad z = ze^{\kappa c(t-\bar{t})}.
\end{aligned}\right\} \quad . \quad . \quad . \quad . \quad (11)$$

To interpret this transformation, we solve the first three of equations (11) for x, y, z, in terms of t when $\bar{x}, \bar{y}, \bar{z}$ vanish, and find

$$x = \frac{1}{\kappa}\coth\epsilon\left\{1 - \sqrt{1 - \tanh^2\epsilon(1 - e^{-2\kappa ct})}\right\}, \quad y = 0, \quad z = 0.$$

Comparing this with (5), it is seen that the point $\bar{x}, \bar{y}, \bar{z} = 0$

describes a geodesic passing through the origin at time $t=0$, with initial coordinate velocity $\delta = c\tanh\epsilon$. Hence we may interpret $\bar{x}$, $\bar{y}$, $\bar{z}$, and $\bar{t}$ as the spacial coordinates and proper-time of an observer in motion along the x-axis relative to the observer with coordinates x, y, z, t. We have thus found the analogue of the Lorentz transformations for the space-time here considered; here as there, the transverse measured distances are the same for both observers, since

$$\bar{y}e^{\kappa c\bar{t}} = ye^{\kappa ct}, \quad \bar{z}e^{\kappa c\bar{t}} = ze^{\kappa ct}.$$

We have arrived at an interpretation of the relations existing between the data of freely moving observers similar to that given by Minkowski for special relativity—that in our case they may be represented by the rotation of a hyper-sphere in flat 5-space *. The transformations could, of course, be obtained directly by requiring that the transformation leave (3) invariant; but in this way we avoid the integration of rather cumbersome differential equations and obtain a more comprehensible view of the process.

4. *Parallax. Doppler Effect.*—The measured distances considered above, which are obtained by comparing the intervals involved with a rigid scale, are themselves ideal constructions when applied to celestial, or even large terrestrial, distances. Since, however, the path of light is rectilinear in the x, y, z coordinate space, the usual triangulation methods are valid; we can deduce the coordinate and, on multiplying by $e^{\kappa ct}$, the measured distances of objects not susceptible of direct measurement, provided we know the length of the base. The usual method of determining the parallax of celestial objects is then applicable if we know the mean distance of the earth from the sun; this is again reducible to a triangulation whose base is a measurable distance on the earth, provided we know the solution of the one-body problem. The latter is considered in the following section, and it suffices here to state that the required solution

* This interpretation is valid not only for the particular space-time here considered, but also for de Sitter's or any other space-time of constant Riemann curvature. The relation between this interpretation and Minkowski's, which is applicable for the case $\kappa=0$, is seen from the fact that the equation (9) of the hyper-sphere, referred to origin at $(0, 0, 0, 0, 1/\kappa)$, becomes on letting $\kappa \to 0$

$$x^2+y^2+z^2-c^2t^2=0.$$

This is the equation of the light "cone" in special relativity, and the rotations considered by Minkowski are the transformations of x, y, z, t space under which it is invariant.

and the data necessary for the measurement of the solar distances can be obtained.

The measurement of velocities can, in principle at least, be reduced to the measurement of distances. Transverse velocities of celestial objects are in practice determined in this way, but the measurement of the radial component offers more difficulty; in practice it is accomplished by means of the Doppler effect, so we must develop the theory of this effect for the space-time here considered.

The simplest case is that in which the light from a distant equivalent point-source is examined by an observer at the origin. Light emitted from the source in the time interval t_0, t_0+dt_0 arrives at 0 in the interval t, $t+dt$, and it can be shown with the aid of (6) above that

$$dt=\frac{dt_0}{1-\kappa l_0}, \quad . \quad . \quad . \quad . \quad . \quad . \quad (12)$$

where l_0 is the measured distance of the source from 0 at time $t=t_0$. Since the proper-times of vibration of atoms situated at 0 and the equivalent point-source are the same (neglecting the Einstein effect due to mass), this leads to a shift $\Delta\lambda$, of a spectral line of wave-length

$$\frac{\Delta\lambda}{\lambda}=\frac{dt}{dt_0}-1=\frac{\kappa l_0}{1-\kappa l_0}. \quad . \quad . \quad . \quad . \quad (13)$$

This shift toward the red would be attributed in practice to the Doppler effect due to a velocity of recession v according to the formula

$$\frac{\Delta\lambda}{\lambda}=\sqrt{\frac{1+\frac{v}{c}}{1-\frac{v}{c}}}-1. \quad . \quad . \quad . \quad . \quad (13')$$

On comparing this with (13), it is seen that a velocity

$$v=c\kappa l_0(1+O[\kappa]) \quad . \quad . \quad . \quad . \quad . \quad (14)$$

would be assigned as the cause of the shift; this velocity coincides to terms of first order in κ with the "measured" velocity $c\kappa l_0$ of the source.

In the more general case, where the source has a non-vanishing coordinate velocity, account must be taken of the fact that the proper-time of vibration of the moving atom is not the same as the time interval measured by a stationary observer. For this the transformation (11) must be used,

and it can then be shown that the shift is given by

$$\frac{\Delta\lambda}{\lambda}=\frac{1+\frac{\delta_r}{\delta_0}}{\sqrt{1-\left(\frac{\delta}{\delta_0}\right)^2}}\cdot\frac{1}{1-\kappa l_0}-1, \quad . \quad . \quad (15)$$

where δ_r is the radial component of the coordinate velocity δ, and γ_0 is the coordinate velocity of light at time t_0. This shift would be attributed to a velocity v_r, where

$$\frac{\Delta\lambda}{\lambda}=\frac{1+\frac{v_r}{c}}{\sqrt{1-\left(\frac{v}{c}\right)^2}}-1, \quad . \quad . \quad . \quad . \quad (15')$$

and on identifying the transverse component of v with the corresponding "measured" quantity, we find that the radial component v_r is

$$v_r=e^{\kappa ct_0}\delta_r+c\kappa l_0\left(1+O\left[\left(\frac{\delta}{\delta_0}\right)^2\right]\right)+O(\kappa^2). \quad . \quad (16)$$

Hence the ordinary interpretation of Doppler effect leads to a radial velocity which is to terms of order $\kappa\left(\frac{\delta}{\delta_0}\right)^2$, *the same as the corresponding "measured" component*, and may therefore for practical purposes be taken as measuring it.

If we assume that there is no systematic correlation of coordinate velocity with distance from the origin, we should expect that the Doppler effect would indicate a residual positive radial velocity of distant objects because of the term $c\kappa l_0$ in (16). Although we cannot, from Doppler effect alone, distinguish between proper motion and this distance effect, we should nevertheless expect a correlation

$$v\simeq c\frac{l}{\mathrm{R}} \quad . \quad . \quad . \quad . \quad . \quad . \quad . \quad (17)$$

between assigned velocity v, distance l, and radius of the observable world R*.

* Weyl, *l. c.*, has deduced a similar relation on the de Sitter hypothesis, which is also given by (17) to first order, assuming that the geodesics concerned form a diverging pencil. L. Silberstein ('Nature,' March 8, April 26, June 7, 1924; Monthly Notices, R. A. S. lxxxiv. p. 363, lxxxv. p. 285, 1923 24, Phil. Mag. xlvii. p. 907, xlviii. p. 619, 1924–25) has supplemented this with a converging pencil, which allows him to write (17) for either positive or negative velocities, and he and K. Lundmark (Monthly Notices, R. A. S. lxxxiv. p. 747, 1924) have discussed the motion of various cla ses of celestial objects and arrived at a value of R of the order 10^{26} cm. There is no possibility of introducing the negative sign in our case, unless we change the sign of κ, and then the positive sign could not appear!

Comparing the data given by Hubble * concerning the value of l for the spiral nebulæ with that of Slipher † concerning the corresponding radial velocities, we arrive at a rough verification of (17) and a value $R=2\times10^{27}$ cm. This is somewhat lower than Hubble's value $8{\cdot}5\times10^{28}$ cm., which was obtained on Einstein's cosmology from the computed value of the mean density of matter ; the fact that the two values do not differ more is rather remarkable, considering the radical difference in the methods by which they were determined.

5. *Central-symmetric Solution.*—The de Sitter line element (2) for an empty world can be obtained from the Schwarzschild solution

$$ds^2=-\gamma^{-1}d\rho^2-\rho^2(d\theta^2+\sin^2\theta\,d\phi^2)+\gamma c^2dt^2, \quad . \quad (18)$$

where

$$\gamma=1-\frac{2m}{c^2\rho}-\kappa^2\rho^2,$$

which represents the field of a spherically symmetric mass, on setting $m=0$. If the interpretation we have given for (3) is to have physical significance, it should be possible to derive it from a solution of the one-body problem by the same process. That such a solution exists can be shown by subjecting (18) to the transformation

$$\left.\begin{aligned}\rho&=re^{\kappa ct}\left(1+\frac{m}{2c^2re^{\kappa ct}}\right)^2\\ \tau&=t+8\frac{m^2\kappa}{c^5}\mathrm{F}\left(\frac{1-\frac{m}{2c^2re^{\kappa ct}}}{1+\frac{m}{2c^2re^{\kappa ct}}}\right)\end{aligned}\right\}, \quad . \quad . \quad . \quad (19)$$

where

$$\mathrm{F}(\zeta)=\int\frac{d\zeta}{(1-\zeta^2)\left[\zeta^2(1-\zeta^2)^2-4\frac{m^2\kappa^2}{c^4}\right]};$$

* E. Hubble, "Extra-galactic Nebulæ," Astrophys. Journ. lxiv. p. 321 (1926).

† See Eddington, *l. c.* p. 162, for Slipher's Table of Radial Velocities.

whence

$$\left.\begin{aligned} ds^2 = &-\left(1+\frac{m}{2c^2 re^{\kappa ct}}\right)^4 e^{2\kappa ct}(dr^2+r^2d\theta^2-r^2\sin^2\theta\, d\phi^2) \\ &+c^2\left(\frac{1-\dfrac{m}{2c^2re^{\kappa ct}}}{1+\dfrac{m}{2c^2re^{\kappa ct}}}\right)^2 dt^2\ *. \end{aligned}\right\}. \quad (20)$$

On setting $\kappa=0$ the usual isotropic form of the static Schwarzschild solution for the case $\kappa=0$ is obtained †.

The observational tests of the general theory of relativity within the solar system (the advance of perihelion of Mercury, deflexion of light grazing the limb of the sun, and shift of spectral lines in the solar spectrum (mass effect)) are, in so far as the observational data are concerned, the same in the field defined by (20) as in Schwarzschild's. This can be most readily shown from the fact that the equations of the geodesics of (20) differ from those of (18) by terms of order κct, and for the tests under consideration this can at worst only lead to an insignificant correction. For this reason we do not attempt to give a full discussion of the rather complicated solar field. The rigorous discussion must be in terms of measured distances and proper-times ; as an example of the method, we here derive the radial component of the measured distance and apply it to the advance of perihelion of a particle.

The radial component at coordinate time t of the distance between two points whose coordinates are r_0, r is

$$l(re^{\kappa ct})-l(r_0e^{\kappa ct}),$$

where

$$l(\zeta)=\int\left(1+\frac{m}{2c^2\zeta}\right)^2 d\zeta=\zeta+\frac{m}{c^2}\log\zeta-\frac{m^2}{4c^4\zeta}.$$

This can obviously not be measured from the origin ; but this difficulty can be avoided by measuring it from a surface

* This solution was originally found by solving (1) for all dynamical manifolds expressible in orthogonal coordinates in which the velocity of light is isotropic (Trans. Amer. Math. Soc. xxix. April 1927). It was there shown that of the three solutions of the problem, (20) is the only one of physical significance. Furthermore, it is the simplest orthogonal isotropic form of (18).

† Eddington, *l. c.* p. 93.

$re^{\kappa ct} = \text{const.}\ \alpha$, say that for which $l(\alpha) = 0$*. An orbit, *i. e.* geodesic, of (18) will be an orbit of (20) on transforming its equations by (19), and its measured distance will be $l(re^{\kappa ct})$. As $re^{\kappa ct}$ is a function of ρ alone, the directions θ, ϕ of perihelion and aphelion, *i. e.* points at which the *measured* distance has an extremum, will be the same in both cases; in particular, leaving the numerical values of the constants of integration involved unchanged, the advance of perihelion will be the same here as in the Schwarzschild solution.

6. In conclusion, a system of cosmology based on (3), which is mathematically equivalent to that of de Sitter but differs from it in its physical interpretation, has been developed in which the "mass-horizon" and "arrest of time at the horizon" paradoxes do not occur, and in which space and the velocity of light are isotropic. In addition, it has the advantage of simplicity, since the geometry of space is euclidean, the motion of particles and light is rectilinear in coordinate space, and the proper-times of observers at relative rest in this coordinate space are the same. On the other hand, t appears explicitly in the line element, and consequently natural processes are not reversible, but space-time is isotropic in time in the sense that at any time the line element has the same form as at any other, provided the spacial scale is appropriately chosen. Although space is unlimited the observable world is not, and objects at an appreciable fraction of its radius should show a residual motion of recession; assuming that the known excess of recessional velocity of spiral nebulæ is due to this cause, the radius of the observable universe is found to be 2×10^{27} cm.

The relations existing between observers in relative motion, the analogue of the Lorentz transformation, can be represented by the rotation of a hyper-sphere in a flat 5-space; and this is true for any cosmology in which space-time is considered as a manifold of constant Riemann curvature. Finally, the corresponding solution of the one-body problem is given, the predictions of which are indistinguishable from

* The justification of this procedure consists in the fact that the circular orbits of the Schwarzschild field give, on applying (19), orbits $re^{\kappa ct} = \text{const.}$ coplanar with 0. On choosing $\theta = \frac{\pi}{2}$, $\frac{d\phi}{dt}$ and $\frac{ds(t)}{dt}$ are constant, and these orbits may be taken as the "circular" orbits of (20); on choosing one of them as origin of measured distance (considering a ring of particles travelling in it), the other circular orbits are at constant distance from it. The equation $\phi = \sqrt{(m, l)}(t - t_0)$ for such orbits yields the analogue of Kepler's third law, and can be used for the determination of solar distances as required by (4) above.

those of Schwarzschild's (to which it is mathematically equivalent) within the solar system.

On replacing κ by $-\kappa$ the solution (3) still satisfies Einstein's equations, as this is equivalent to the transformation $\bar{t} = -t$. The consequences of this can be obtained from the foregoing by interchanging past and future; but the known facts concerning the spiral nebulæ indicate that this is not desirable.

Göttingen, Germany.

LXXXVII. *The Resistance of Sputtered Films.* *By* Russell Sturgis Bartlett, *Ph.D.* (*Yale*) *.

MANY observers † have remarked the peculiar electrical properties of thin metallic films on glass, whether deposited by chemical means, by cathode sputtering, or by evaporation and condensation. Many hypotheses have been advanced to explain these properties, though none has proved entirely satisfactory. It seems probable, however, that the true and complete explanation will include much that has already been suggested. The purpose of the present paper is to present some new experimental evidence, and to suggest a means, hitherto apparently overlooked, whereby many of the peculiarities can be explained.

It seems advisable, before proceeding further, to summarize briefly the peculiarities mentioned above. The specific resistance for the thinnest films is almost infinite, and decreases rapidly with increasing thickness up to a certain point. Beyond this point a further increase in thickness produces only a small change in the specific resistance. This critical thickness has been variously estimated by different experimenters, and appears to depend upon the rate of deposit and on the metal, but is in general in the neighbourhood of 5×10^{-7} cm., assuming normal

* Communicated by Sir J. J. Thomson, O.M., F.R.S.

† Longden, Phys. Rev. xi. pp. 40, 84 (1900); Patterson, Phil. Mag. iv. p. 652 (1902); Kolschütter & Noll, *Zeits. Electrochem.* xviii. p. 419 (1912); Swann, Phil. Mag. xxviii. p. 467 (1914); King, Phys. Rev. x. p. 291 (1917); Kahler, Phys. Rev. xviii. p. 210 (1921); Koller, Phys. Rev. xviii. p. 221 (1921); Holmes, Phys. Rev. xxi. p. 386 (1923); Mackeown, Phys. Rev. xxiii. p. 85 (1924); and Reynolds, Phys. Rev. xxiii. p. 302 (1924) have worked with sputtered films. Stone, Phys. Rev. vi. p. 1 (1898); Vincent, *Ann. de Chimie et Phys.* (7) xix. p. 421 (1900); Grimm, *Ann. d. Physik*, (5) ii. p. 448 (1901); Weber & Oosterhuis, *K. Akad. Amst. Proc.* xix. p. 567 (1917); and Steinberg, Phys. Rev. xxi. p 22 (1923) have dealt with evaporated or chemically deposited films.

density. The thinnest films have a negative temperature coefficient of resistance, changing through zero to a small positive coefficient for thicker films. Again, all show a permanent irreversible change in resistance with time, with heating, with passage of a heavy current, etc. This phenomenon, which is generally known as ageing, is usually an increase in resistance for very thin or high resistance films, and a decrease for thick and low resistance films. Bismuth always shows an increase of resistance with ageing, and always has a negative temperature coefficient. The presence of various gases or of vacuum affects the ageing in a rather irregular manner. Finally, the thermoelectric force, the change of resistance of bismuth in a magnetic field, and the photoelectric emission all show peculiarities.

Experimental Procedure and Results.

The author has in general verified the results of previous experimenters, and has gone further to push the ageing process in certain cases to its ultimate limits. Gold films were used for the greater part of the observations ; the subsequent considerations have shown that platinum would, perhaps, have been a more fortunate choice. However, some observations were made on sputtered films of platinum, palladium, copper, silver, bismuth, and tellurium.

The films were sputtered in a bell-jar in the usual manner. The electrode of the metal to be sputtered, in the form of a flat plate, was suspended horizontally near the top of the bell-jar. Beneath that, at a distance of from 2 to 4 cm., depending upon the metal used and other circumstances, was supported the glass plate for receiving the deposit. To ensure uniform thickness, the region of the plate to be used was always considerably smaller than the sputtering electrode. An unrectified current from a step-up transformer was used, with a variable resistance in the primary circuit to control the current. An aluminium electrode in the base of the bell-jar was sufficiently removed so that no sputtering from this could affect the metallic deposit at the top. The wax joints were carefully protected from the discharge, as previous experience had shown that muddy and dirty deposits were produced with grease or wax vapour in the bell-jar.

The thickness of the films was determined by weighing, a method which does not admit of great accuracy. But all methods are open to question in some way, and this one

seemed adequate. The absorption of light in the films was used also as a means of comparing thickness, and proved reasonably satisfactory.

But where it was desirable that two or more films should be identical, or nearly so, special precautions were taken. In some cases they were sputtered side by side, even on the same piece of glass. If this was impracticable, care was taken to maintain all conditions the same ; and a good check on this was possible. The pressure, measured on a McLeod gauge, and the resistance in the primary of the transformer were maintained the same for two cases. If, then, the current in the primary and the size of the cathode dark space were also the same for both cases, it may be taken as a fair indication of identical conditions. Finally, the glass plates were similarly located, the sputtering continued for the same length of time, and the absorption of light in the two was found to be the same.

The ends were heavily sputtered to ensure good contact with brass clamps. In some cases the film was carefully ruled in a sort of gridiron pattern to increase the resistance, thus reducing the resistance of contacts and leads to a negligible factor. Both Wheatstone bridge and potentiometer methods were used to measure the resistance.

The films were placed in an electric oven and heated slowly, resistance measurements being made from time to time. At intervals during the ageing process the films were cooled again to room-temperature and sometimes to liquid-air temperature, and the temperature coefficient of resistance was measured.

It was found that, when a film was heated to a temperature above that which it had previously reached, the resistance changed rapidly at first, but more slowly as time went on, and appeared to approach a limiting value asymptotically. At any time a slight increase in temperature would increase the rate of change of resistance. It was also found that the temperature coefficient of resistance increased with ageing. There was no evidence of any sudden change in resistance at any temperature. Fig. 1 is a typical example of change of resistance with temperature, the temperature being maintained in so far as possible at a steady value till the resistance ceased to change.

From measurements of the temperature coefficient of resistance at different stages of ageing, the readings were all reduced to resistances at room-temperature, 15° C. A typical example of variation of resistance with time, showing the corresponding temperatures, is given in fig. 2. From a

Fig. 1.

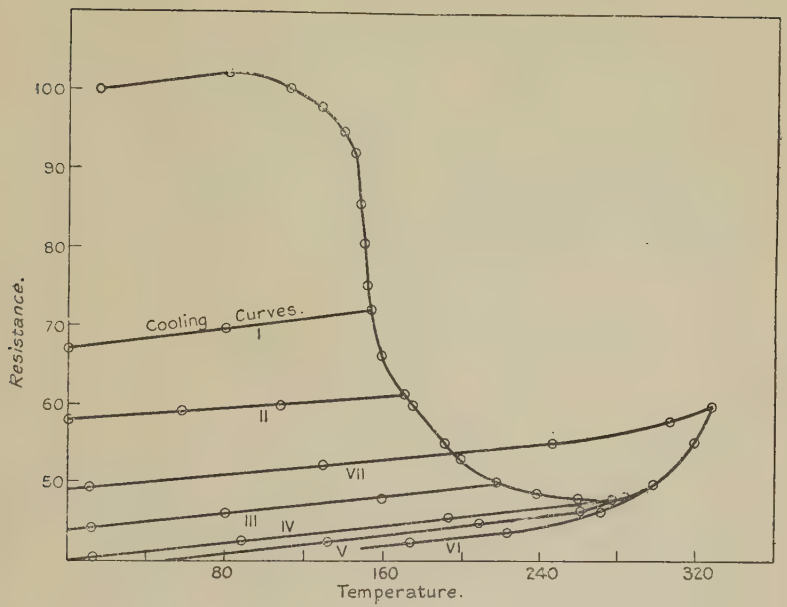

Changes of resistance with temperature of ageing.

Fig. 2.

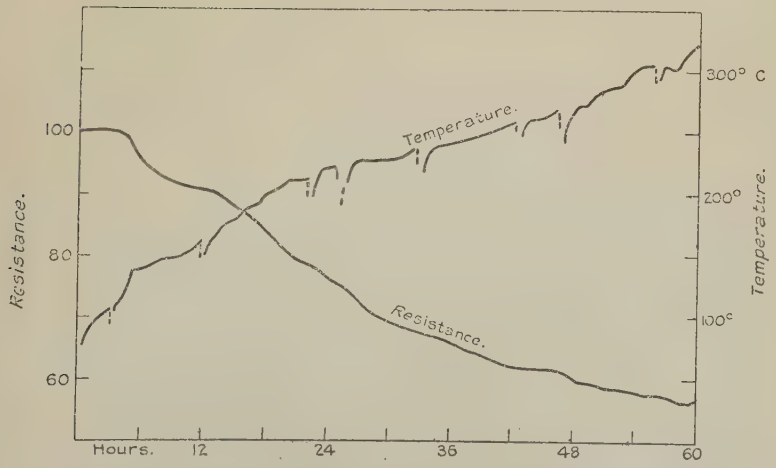

Changes of resistance with time, showing corresponding temperatures.

number of such curves it was possible to deduce the nature of the change of resistance with time at a given temperature, and thus to fix the limiting resistance reached after long ageing at any temperature. It was found that all films decreased in resistance with increasing temperature up to a certain point, where the resistance went through a minimum and began to increase with further increase in temperature. The temperature for this minimum resistance varied slightly with different films, but was in the neighbourhood of 300° C. for the films examined, varying in thickness from 3×10^{-6} up to 7×10^{-6} cm.

Fig. 3.

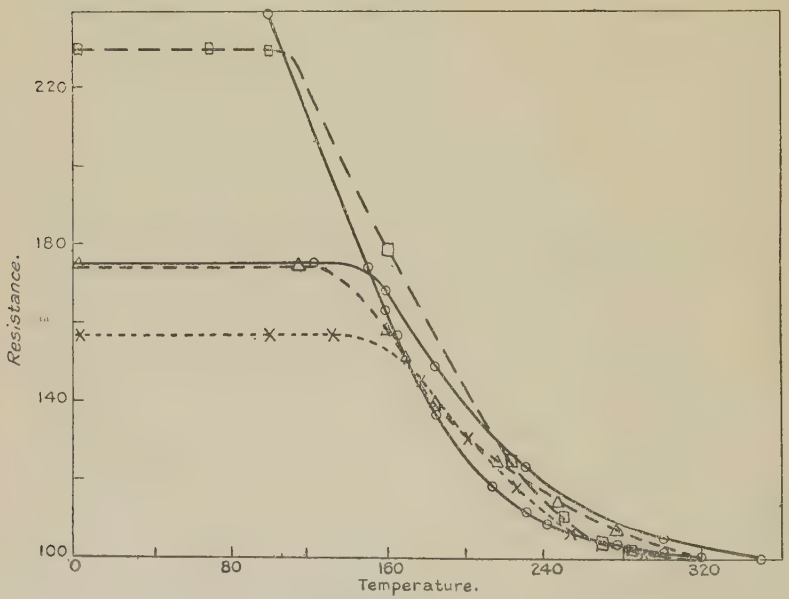

Resistances plotted as percentages of final value.

The specific resistance of these films cannot be fixed accurately because of the uncertainty as to the thickness, but it is worthy of note that for gold all reached nearly the same limiting value of 8×10^{-6} ohm per cm. cube, though starting with as widely differing values as 18×10^{-6} and 12×10^{-6} ohm per cm. cube. This suggested a means of comparison for a number of films. The resistances were plotted against temperature as before, but as percentages of the final value reached, which was assumed to be the same for all cases. These results are shown in fig. 3. It will be

observed that the curves for all films follow the same general course at higher temperatures, breaking away at various lower temperatures. These differences appear to depend upon the previous history of the film, temperature reached during sputtering, etc.

To determine, if possible, whether this ageing is caused by the escape of occluded gas, two films sputtered side by side were placed in the oven together, one in an evacuated tube and the other in air. The presence of air was found merely to retard the ageing process without having any effect on the final value reached. For temperatures above 240° C., the films behaved in exactly the same manner.

Fig. 4.

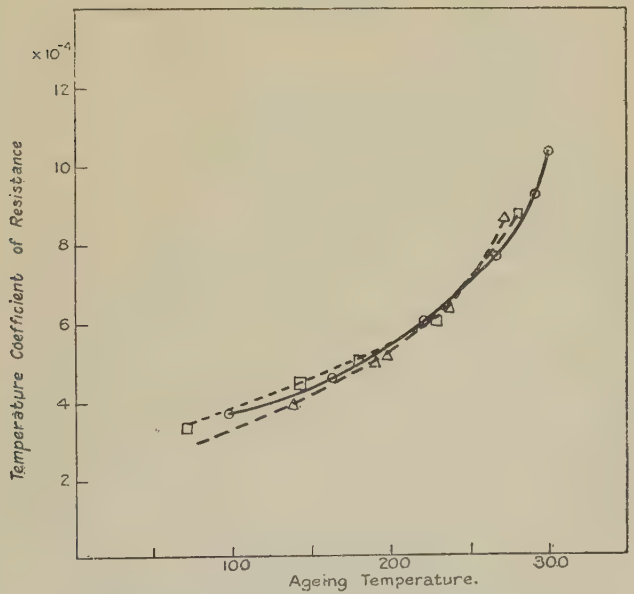

Changes of temperature coefficient of resistance with temperature of ageing.

Fig. 4 shows the temperature coefficient of resistance for a number of films as a function of the ageing temperature. The agreement is fairly good for a short range. At higher temperatures very marked increases occur which are of particular interest, and will be discussed later. One curious point is that in general the absolute change of resistance per degree centigrade remained nearly the same during ageing, the change in the temperature coefficient being caused

almost entirely by the permanent decrease in resistance. As others have noted, once a film has been thoroughly aged at a given temperature, its behaviour below that temperature is reversible and reproducible.

The results of a few other attempts at ageing will be noted here. The instantaneous passage of a heavy current, of a current density of the order of 3×10^5 amperes per square centimetre, reduced the resistance to 35·7 per cent. and 36·6 per cent. of its original value in two cases. A further increase of the current to double this value produced no appreciable change. In the case of heating externally, the greatest reduction observed was to 37·5 per cent. of the original value. And any increase in temperature beyond the optimum value caused a rapid increase in resistance. The question then arises whether the passage of a heavy current does not contribute to the ageing in some way besides the heating effect.

A film subjected to strong mechanical vibration during heating showed no more change than one similarly heated without the vibration. Another, heated in a discharge-tube by positive ion bombardment, showed no unusual change. And when the bombardment was increased sufficiently to produce appreciable sputtering, from a sputtered film, the change in resistance so produced did not indicate the ejection of appreciable chunks of metal from the film, but rather an evaporation, molecule by molecule or atom by atom.

An Explanation of the Properties of Sputtered Films.

Swann and King have suggested different theories of granular structure and incomplete covering to account for the high specific resistance of these films. Koller has shown that occluded gas is certainly a factor in ageing. He goes so far as to suppose that in sputtering small crystals are ejected from the cathode and deposited on the film. These are then kept from intimate contact by gas molecules which are gradually released. Kahler, from X-ray analysis, concludes that sputtered films are crystalline, identical with bulk metal, while evaporated films are amorphous. Steinberg does not agree with this, finding evaporated films identical in structure with bulk metal. Weber and Oosterhuis have shown that the granular structure of sputtered films may be quite as fine as that of evaporated films. There seems to be some difference of opinion as to the size of the granular structure, but this could be readily explained by differences in conditions of evaporation or sputtering.

One can point, then, confidently to occluded gas as the first cause of the peculiar properties of these thin films, particularly the ageing process. We can invoke Koller's granular structure held apart by gas-molecules. Or we can assume that the large amounts of gas in the metal increase its resistance in the same manner as the smaller quantities of gas in metal wires and foils, but to a much greater extent *. In any case, it is the escape of this gas, with, perhaps, a settling together of the metal atoms, which causes the reduction in resistance known as ageing.

The granular or irregular structure, the second factor, is important, particularly in the variation of specific resistance with thickness; but it can also explain the negative ageing (increase of resistance) of high-resistance films. We do not need to suppose that crystals are deposited on the glass, though Longden's suggestion of crystallization at the edge of the cathode dark space would favour such an idea if the glass were far removed from the cathode (as it was for the films used in Kahler's X-ray analysis). For it is known that crystals of varying sizes may be produced in electrolysis by varying the rate of deposition. Electrolysis is not an exact parallel to condensation or sputtering deposition. But a similar arrangement of condensing atoms in groups is quite a probable occurrence, since the forces of attraction between two metal atoms are greater than between metal and glass. This is supported by the fact that, under suitable conditions, a sputtered film may be stripped from the glass and remain continuous. We may suppose, then, that metal atoms condense about those already on the glass, forming groups; and not until these groups have grown to a considerable size does the conductivity approach a reasonably steady value, at which point the glass is presumably completely covered. Further deposition adds to the thickness of the film irregularly, so that it will never be of a uniform thickness, and will always have a high specific resistance. Variation of the rate of deposition would vary the size and spacing of the aggregates, and thus cause the variations in the thickness at which the film shows a fairly constant specific resistance, as noted by different observers. One can go through mathematical calculations to justify these assumptions and obtain suitable values of specific resistance, but they would not carry much weight, and so will be omitted.

* Fisher, *Ann d. Physik*, xxi. p. 503 (1906); Kleine, *Zeits. f. Physik*, xxxiii. p. 391 (1925); Herrmann, *Ann. d. Physik*, lxxvii. p. 503 (1925); and Janitzky, *Zeits. f. Physik*, xxxi. p. 277 (1925), have all studied this phenomenon.

If a very thin film is heated, while still far from the melting-point, a rearrangement of the molecules begins, particularly towards the aggregates and massive centres of condensation, and away from the thinly-populated regions between. This may be aided by a variation with temperature of the cohesive forces of metal to metal and metal to glass, but increased thermal agitation could also be the cause of the rearrangement; and the result, of course, is a permanent increase in resistance. The same thing takes place for thicker films, but at a higher temperature. At first the outgassing of the metal decreases the resistance, but at higher temperatures the other becomes effective, and the resistance finally increases. This probably combines with the tension effect noted below, though that is still effective when the film is of so great a thickness as to be sensibly uniform. Weber and Oosterhuis have noted that silver does not attain a constant specific resistance until much thicker than platinum or tungsten, which means that the silver aggregates are larger than those for the other metals. It is also notable that silver shows negative ageing at greater thicknesses, attributable to the same larger aggregates.

There is another factor, hitherto apparently overlooked, which should in most cases contribute towards several of the properties noted above. This factor is the difference in the coefficients of thermal expansion of the sputtered film and the material used to receive the deposit. A brief statement of the case will suffice to show what changes would be expected from this.

In most cases the coefficient of expansion of the metal is greater than that of the backing. When the film is cooled, its greater contraction produces a state of tension. Bridgeman * has shown that most metals show an increase of resistance under tension, but the effect is so small as to be quite immaterial in the present instance. However, if we take the common case of gold films on glass, the tension on the gold is of the order of 5 kg./cm.^{2} per degree centigrade of cooling; so that cooling of 100° would produce a tension as great as that applied by Bridgeman experimentally, and for a slightly greater range of temperature the elastic limit, or even the breaking-stress, of the gold would be exceeded. Taking into account the generally accepted hypothesis of a granular structure, we may justifiably suppose a process of opening or closing gaps in the film as the temperature falls or rises. This should produce an increase of resistance with

* Bridgeman, Proceedings of the American Academy of Arts & Sciences, lx. p. 423 (Oct. 1925).

cooling, opposing the normal decrease, and resulting in the observed low or negative-temperature coefficient.

To test this hypothesis experimentally, gold was sputtered on three plates placed side by side in the discharge-tube, one of quartz crystal cut perpendicular to the axis, one of glass, and one of fused quartz. These have coefficients of expansion of about 13·7, 7·5, and $0{\cdot}42\times10^{-6}$ per degree centigrade respectively, whereas gold has a coefficient of about 13·9, almost identical with that of quartz crystal. A similar procedure was carried out for platinum, which corresponds roughly to glass in coefficient of expansion. The specific resistances of these films were then determined, and their temperature coefficients of resistance over the range from 15° C. to −185° C. The results are given below :—

Metal.	Backing.	$\Delta R/R_0(T_2-T_1)$.	Specific resistance.
Gold	Quartz crystal.	$7{\cdot}06\times10^{-4}$	$19{\cdot}8\times10^{-6}$
Gold	Glass.	6·38	21·6
Gold	Fused quartz.	5·27	28·6
Platinum	Glass.	4·41	75
Platinum	Fused quartz.	3·71	82

The figures in the first column, showing the lowest temperature coefficient of resistance where the difference in coefficients of expansion is greatest, are in accord with the above hypothesis. The data on specific resistance are necessarily inaccurate, but are useful for comparison, since the samples of gold were sputtered at the same time and in the same discharge-tube. If the film and backing are heated during sputtering, as is often the case, on cooling to room-temperature the tension should give rise to a high specific resistance, greatest where the greatest tension occurs. The figures in the last column show the expected differences, though somewhat larger than the observed differences in temperature coefficient would indicate. Reynolds has shown that films deposited on cold and on warm glass have markedly different properties, a fact which supports this view.

We may then point to the unequal coefficients of expansion of film and backing, with the attendant tension on the film, as a third factor contributing to the low-temperature coefficient of resistance, and probably, in some cases, to a part of the high specific resistance.

As noted above, consistent results are obtainable with

these films only at temperatures appreciably below those reached previously during sputtering or ageing, so that in most cases we are dealing with a stretched film. When a film is heated to a temperature in the neighbourhood of the highest previously reached, it will reach a state in which the gaps are all closed and the texture is fairly uniform. For a short range above this point the temperature coefficient of resistance should be more normal. Further increase in temperature should cause the film to buckle and heap up, giving rise, on cooling, to larger gaps than ever and an increased resistance. Fig. 1, typical of all the films examined, shows all these features. Over a short range the temperature coefficient of resistance was about 90 per cent. of that for bulk metal, whereas for the rest of the temperature range it was as low as 20 to 25 per cent.

Sputtered films of bismuth have in all cases a negative-temperature coefficient of resistance, a fact which can be attributed to its larger coefficient of expansion.

At 350° C., for gold in bulk, the specific resistance is about 6×10^{-6} ohm per centimetre cube, while for these films, when thoroughly aged, it was only 50 per cent. greater. If the abnormal temperature coefficient persisted, the specific resistance of the sputtered film would, at somewhat higher temperatures, be less than that of the bulk metal. But if we accept the effect of tension outlined above, this difficulty vanishes : for the abnormal temperature coefficient persists only to the previous temperature reached in sputtering or ageing, which was in the neighbourhood of 350° C. for most cases dealt with.

Much work has been done with films of platinum sputtered on glass, in which case the coefficients of expansion are nearly the same, and this reasoning would not apply ; but the properties of platinum films on glass are closer to those of the metal in bulk than is the case for any other metal.

It appears that most of the discrepancies and disagreements between previous workers are caused by differences in the manner of obtaining deposits, both as to the rate of deposition, determining the size of the aggregates, and as to conditions, nature of gas and pressure, etc., affecting the gas-content of the metal. Experimental evidence on these points would be interesting, and would do much to prove or disprove the theories advanced. Deposits of platinum on glass, where the deposition is slow and the glass is heated from below, should be free from the tension troubles suggested above.

Summary.

The ageing of sputtered films is shown to depend on the temperature to which the film is raised. The resistance decreases to a minimum value and then increases as the temperature is further increased. The dependance of the temperature coefficient of resistance on degree of ageing and on temperature is shown. Other experimental evidence is brought forward in support of the theoretical considerations suggested below.

It is shown that the peculiar electrical properties of thin metallic films on glass may be attributed to three principal causes. Occluded gas contributes towards the high specific resistance, and particularly the decrease in resistance with ageing, brought about by the outgassing of the metal. A granular or irregular structure explains the dependance of specific resistance on thickness and the negative ageing of very thin films. A state of tension in the film, produced by unequal coefficients of expansion of film and backing, opens or closes gaps in the film as the temperature changes, giving rise to the low or negative-temperature coefficient of resistance and other peculiarities. Experimental evidence of the author and others is advanced to justify these proposals. The importance of the conditions of deposition in determining the properties of the film is pointed out.

Finally, the author wishes to acknowledge his indebtedness to Sir Ernest Rutherford and others at the Cavendish Laboratory for their kindness, and in particular to Sir J. J. Thomson for his interest and assistance in this work.

LXXXVIII. *Space-Charge Effects.* *By* E. W. B. Gill, *M.A., B.Sc., Fellow of Merton College, Oxford* *.

1. SOME time ago † I described experiments with a three-electrode gas-free valve in which the current from the filament to the plate was investigated, the plate being kept at a few volts and the grid at from 20 to 30 volts positive to the filament. It was found that the space-charge between the grid and the plate had a considerable effect on the electric field in that region, and when the current was sufficiently increased discontinuous changes took place in the field. The theory which was given has recently been

* Communicated by Professor Townsend, F.R.S.

† Phil. Mag., May 1925, p. 993.

extended by Tonks *. The present investigation comprises a further extension of the experiments to the case in which the plate is a little negative to the filament. Normally no electrons can reach the plate if it is negative to the filament, and another method is required to investigate the field.

2. The valve used was a modified Marconi MT 5 type, the same one as before. The spiral grid was 5 mm. and the plate 25 mm. in diameter. The plate lead was brought out at the top of the glass, and the insulation of this electrode is therefore much better than in an ordinary valve. No trace whatever of residual gas could be detected in the valve. In what follows the plate potential was measured by connecting it to a quadrant electrometer, the potential on insulating being the same as that of the negative end of the filament. This point will be taken as being at zero potential.

Fig. 1.

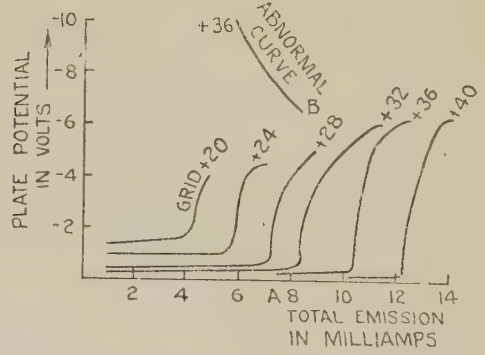

An experiment consisted in passing different currents through the grid kept at a fixed positive potential and observing the potential assumed by the plate, the plate being always earthed while the current was being varied. This variation of current was effected by adjustment of the filament heating. The plate current being zero, all the electrons set free from the filament must finally arrive at the grid, and the grid current, which was measured, represents the total electron emission from the filament.

The curves in fig. 1 represent the plate potentials thus obtained when the grid was kept at +20, +24, +28, &c.

* Lewi Tonks, Phys. Rev., Oct. 1927, p. 501.

volts plotted against the emission current. It will be observed that in all cases the plate acquires a small negative potential for the smaller currents, but a point is reached at which there is an abrupt increase in the value of this negative potential. The emissions at which this abrupt change occurs increase as the grid potential isincreased. The curve for the grid at +36 volts labelled "abnormal curve" was obtained under conditions to be described later.

In order to explain the large abrupt increase of the plate potential the following questions may be considered :—

1. What is the distribution of the electric field between the grid and the plate ?

2. How is this field initially set up ?

3. As a preliminary it may be noted that no ionization or photo-electric effects can account for the curves. The amount of gas in the valve was, as stated, quite appreciable, but in any case the grid being positive to the plate no ionization or photo-electric effect can cause the plate to attain a negative potential.

The general current distribution inside the valve is indicated diagrammatically in fig. 2. The filament grid and plate are

Fig. 2.

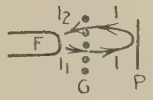

represented respectively by F, G, and P; F and P are at the same potential and G positive to both of them. At any instant in the space between F and G a current i_1 flows towards G ; part of this current is collected by the grid, and the remainder i flows towards P. Since P and F are at the same potential, the electrons in the space between P and G return towards the grid, that is a current i also flows towards G, of which a part is collected on G and the remainder i_2 flows towards F. As with the stream i, i_2 is reversed and forms part of i_1. The total current collected by the grid is $i_1 - i_2$, and this is the same as the emission current from the filament.

It is not possible to measure i, i_1, and i_2 separately with any accuracy, but only $i_1 - i_2$. The current i_1, and in many cases the currents i and i_2 are larger than the total emission current $i_1 - i_2$, so that there is always the possibility with

this arrangement that there may be large space-charges in the valve even if the emission is comparatively small.

In the first part of the curves, where the ordinary small plate potential of about one volt is obtained, this potential is due to the velocity of emission of the electrons from the hot filament in addition to contact differences of potential between the plate and the filament. The plate potential is, however, measured from the negative end of the filament, while the fastest electrons come from about the middle of the filament whose potential alters as the filament current is varied. The reason for the curves not coinciding over this range is that in passing the grid the electrons are deviated and lose velocity in the direction normal to the plate, and this deviation increases with the voltage of the grid.

4. The abrupt increases in the negative potential of the plate are due to space-charge effects between the grid and

Fig. 3.

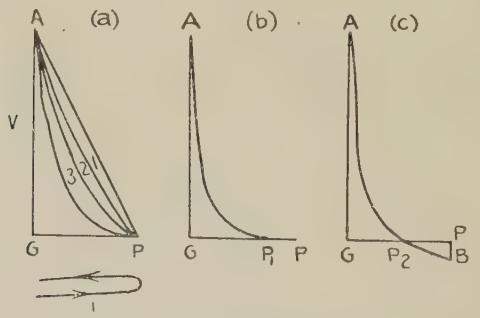

the plate. To simplify the explanation the grid and plate may be regarded as parallel planes, all electrons may be supposed to move at right angles to them, and the distribution to be uniform over any plane parallel to the electrodes. The velocities of emission and contact differences of potential will be neglected. The space-charges between the grid and plate are exactly the same as those due to a current $2i$ carried by electrons leaving the plate with zero velocity and moving towards the grid, and the well-known results of Child and Langmuir can therefore be easily applied to this case.

Fig. 3 represents the distribution of potential between the plate P and grid G, the ordinates representing potentials at the different planes and the abscissæ the distances of the planes from the grid. The grid potential $+V$ is represented by GA, the plate potential being zero.

When no current flows the straight line AP represents the potential distribution. A small current flowing in the space gives the potential distribution represented by curve 1, a larger current gives curve 2, and, finally, a current is reached which gives curve 3, in which GP is a tangent to the curve at P. This is the maximum current which can flow in this space provided that the electrons penetrate just to the plate before their direction of motion is reversed. Langmuir's equation for this saturation current gives $2i = k\frac{V^{3/2}}{GP^2}$ k being a constant.

If the current forced through the grid from the filament side exceeds this value, two different types of distribution are possible.

One of these is represented by the curve of fig. 3 (*b*), where the electrons penetrate as far as P_1, the space between the planes G and P_1 carrying the maximum current, involving GP_1 being the tangent to the curve at P_1. In this distribution the space between P and P_1 has no charge, and all points in it are at zero potentiel.

As GP_1^2 replaces GP^2 in the denominator of Langmuir's equation, this distribution carries a larger current than that represented by curve 3 in fig. 3 (*a*).

The other possible distribution of potential is shown in fig. 3 (*c*). In this case the electrons only penetrate as far as P_2, where GP_2 is less than GP_I and the space GP_2 is not carrying its maximum current. The part of the curve from P_2 to B is a straight line touching the curve at P_2 since the electric force is continuous, and there is no charge in the space between the planes P_2 and P. This distribution requires the plate *to have a negative potential* PB. It is evident that for a given current there are an infinite number of distributions of this type each with a different plate potential. The one actually set up depends on the amount of negative electricity which the plate can receive, which will be discussed in paragraph 5.

The curves of fig. 1 are explained by the distributions indicated by the curves of fig. 3. The early parts of the curves correspond to distribution (*a*) in which the plate potential remains constant; and the currents at which the discontinuities occur give distribution (*a*) 3, for which i is proportional to $V^{1.5}$. As explained, the current i is not the same as the total emission, but is probably roughly proportionate to it, and the emission currents at the points where the curves suddenly rise are within errors of experiment proportional to $V^{1.5}$.

The remainder of the curves in which the plate is negative corresponds to distributions of the type (*c*).

Distribution (*c*) is also an alternative to (*a*), which explains the abnormal curve in fig. 1 for the grid at 36 volts. Similar curves can be obtained for the other voltages by a method to be described later.

5. It remains to explain by what process the distribution represented by the curve fig. 3 (*c*) is set up, as it involves negative electricity from the filament reaching the plate to charge it to a negative potential. Under static conditions this is impossible, as no electron from the filament can reach an electrode at a potential negative to the filament.

If, however, there is any disturbance of the field, it is possible for the plate to receive negative charge. This will be seen from the following considerations:—If a small increase in the filament emission occurs when the current is

Fig. 4.

adjusted to the critical value giving the saturation distribution 3 (fig. 3 (*a*)) there is a sudden increase in the number of electrons entering the space between G and P. This space becomes momentarily super-saturated, and the field readjusts itself to something like fig. 3 (*b*). If this change is very sudden the electrons originally between P and P_1 are still in that space when the zero of potential moves to P_1, and thus for an instant these electrons produce the potential distribution shown by the dotted part of the curve in fig. 4.

This distribution is unstable, and some of the electrons in it move on to the plate and charge it negatively. If the plate only goes slightly negative for this first disturbance so that in the distribution set up the space carrying the current is nearly saturated, further slight disturbances will cause more electrons to move to the plate, and the final potential of the plate depends on the total charge it has received.

The fact that distribution 3 (*c*) is always obtained instead of 3 (*b*) shows that the emission from a filament, though very steady, is not steady enough to prevent the above process occurring.

Even the stable distribution of the type *a*(1) can be changed to type *c*; the abnormal curve was obtained by establishing the normal field indicated by a point such as A (fig. 1) for a low emission, and then momentarily brightening the filament by shortening a few turns of the filament rheostat, the plate in this case being insulated. The electrometer at once showed a large negative deflexion to a point B which remained permanent when the emission returned to its original value.

The ease with which a static field can be upset by the minutest variation in the source of electrons constitutes a real danger in the interpretation of certain experiments. In the above experiments, if it had been assumed that the fields were always static, it would not have been possible to interpret the results in any other way than by saying that the electrons in their passage across the valve had picked up from other sources energies of several volts.

Although V is the greatest fixed potential difference in the system, some of the electrons attain an energy greater than *e*V.

Professor Townsend has given me much advice and criticism.

LXXXIX. *A Contribution to the Theory of Torsional Oscillations in Plastic Solids.* *By* James P. Andrews, *M.Sc.*, *East London College* *.

FROM time to time, explanations of the phenomenon of flow in solids have been attempted, various reasonable hypotheses being advanced to explain particular aspects. However different in other respects, these suggestions have one factor in common, namely, that during flow the solid possesses a certain fluidity which prevents parts of it from withstanding stress. The primary aim of this work is to embody that fact in an approximate equation of motion which will be of such a form as to allow specific hypotheses to be considered in some detail. A secondary aim is to demonstrate that the application of this theory leads to a

* Communicated by the Author.

general explanation of the variation of logarithmic decrement with amplitude in torsional oscillations, even in cases where the amplitude is so small that the elastic limit is not surpassed.

This is not the first occasion upon which such an explanation has been put forward, for I have since found that Wiechert * expressed similar fundamental ideas in a theory of the elastic after-effect, in which he has, however, restricted his attention to a particular hypothesis from the start; and Prof. Peddie † has developed a hypothesis as to the molecular alterations in a strained plastic substance, which has certain points nearly in common with the present theory. In this paper, however, a development not restricted to particular hypotheses is attempted.

Experimental results with which to compare this theory are almost entirely confined to the investigations of the logarithmic decrement, and a brief review of the chief conclusions is appropriate. Among the first investigators H. Streintz ‡ concluded that logarithmic decrement was independent of the amplitude of vibration, of the dimensions of the wire under observation—apart from the effect considered to be due to change of period,—and of the moment of inertia of the vibrating body suspended from the wire. For oscillations of longer period, the logarithmic decrement was smaller. This invariability of log. dec., although scarcely borne out by the contemporaneous work of Pisati §, agrees well with Boltzmann's theory of the after-effect ||. On the other hand, Prof. Peddie and his collaborators have given a definite law of variation of decrement with amplitude according to which, if y is the decrement and x the number of oscillations from the start, $y^n(x+a)=b$. Moreover, in some at least of their experiments, the motion was not simple periodic, motion outward being more rapid than motion inward. Similarly, we have the results of K. E. Guthe and L. P. Sieg ¶, which show that Platinum-Iridium and Bismuth wires—both brittle materials,—when oscillating with rather large amplitudes, exhibit a rapid decrease of both log. dec. and period as the oscillation dies down. Then

* Wiechert, *Wied. Ann.* l. pp. 348 and 546 (1893).

† W. Peddie, Proc. Roy. Soc. Edin. p. 225 (1912–3).

‡ H. Streintz, *Wien. Ber.* lxix. Abt. 2, p. 337 (1874), & lxxx. Abt. 2, p. 397 (1879).

§ G. Pisati, *Gaz. Chim. Ital.* t. vi. (1876), t. vii. (1877).

|| L. Boltzmann, *Abh.* i. p. 616.

¶ K. E. Guthe and L. P. Sieg, Phys. Rev. xxx. p. 132 (1910). L. P. Sieg, Phys. Rev. xxxi. p. 421 (1910).

Bouasse and Carrière * have shown that an iron wire exhibits a clearly defined maximum decrement for a particular value of the amplitude. Kei Iokibe and S. Sakai † find again that the log. dec. decreases as the oscillation decays, but this time not for large amplitudes only ; and, finally, G. Subrahmaniam and D. Gunnaiya ‡ show a variety of curves for different substances, where, even for small amplitudes, the log. dec. sometimes is constant, sometimes increases, but generally decreases at a decreasing rate, as the motion dies away. It appears fairly well established that the log. dec. varies in some cases in a rather complicated way, even for small amplitudes. We may perhaps conclude with G. Masing that the matter is not yet sufficiently unravelled to allow of a simple theory to include all cases. A little more generality is secured in this paper by avoiding hypotheses connected with the actual mechanism of the physical changes which occur.

Consider, then, a rod of the material of length l, and cross-section a circle of radius r_0. Let the upper end be maintained always at rest, and the lower end, to which is attached a body of moment of inertia I, let us suppose to be twisted through an angle θ about the axis of the rod. I is to be so large that the moment of inertia of the rod itself about its axis is negligible in comparison. Let the whole be placed in an evacuated chamber.

Select a cylindrical element as in fig. 1, coaxial with the wire, of radii r and $r+dr$, and length unity. Its lower end is twisted through an angle α_0 relatively to the upper end, where, if we may assume as usual that the twist is uniform, $\alpha_0=\theta/l$ (fig. 1).

If no flow occurs, the shear stress on this element may be shown to be $n\alpha_0 r$, where n is the rigidity. If, however, flow has occurred, α_0 will be greater for a given couple than ordinary elastic theory would lead us to expect. Since α_0 is the actual angle of twist, we must therefore write for the stress called forth by the deformation $n(\alpha_0 r-\psi_0)$ where ψ_0 is (or may be) a function of α_0, r, t, where t is the time. We shall take account later of forces elicited by the motion, or change of deformation. It is conceivable that if flow occurs, a straight line drawn in the material, as the radius

* Bouasse and Carrière, *Ann. de Chem. et de Phys.* 8me ser. p. 190, t. 14.

† Kei Iokibe and S. Sakai, Phil. Mag. xlii. p. 397 (1921)

‡ G. Subrahmaniam and D. Gunnaiya, Phil. Mag. xlix. p. 711 (1925). G. Subrahmaniam, Phil. Mag. l. p. 716 (1925).

of a section, will not remain straight; that is, α_0 may be a function of r. In any case, we have insufficient data to determine this function, and since we shall deal only with small oscillations, we shall take α_0 to be independent of r. The function ψ_0, related to α_0, is also unknown; but a plausible and sufficiently general assumption is that

$$\psi_0(\alpha_0, r, t) = \mathrm{R} \,.\, \psi(\alpha_0, t),$$

Fig. 1.

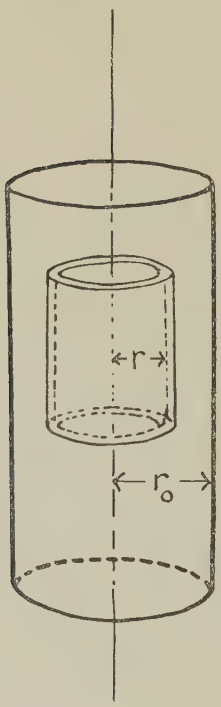

where R is some function of r alone, and ψ does not contain r. On these assumptions, the restoring couple at any instant is

$$\mathrm{C} = \int_0^{r_0} 2\pi r^2 n(\alpha_0 r - \psi_0)\, dr$$

$$= \frac{n\pi r_0^4 \alpha_0}{2} - n\psi(\alpha_0, t) \int_0^{r_0} 2\pi r^2 \mathrm{R}\, dr.$$

Now $\int_0^{r_0} 2\pi r^2 \mathrm{R}\, dr = \mu$, is a constant whose value depends only on the radius of the rod, so that we may write

$$\mathrm{C} = \frac{n\pi\alpha_0 r_0^4}{2} - n\mu\psi(\alpha_0, t). \quad . \quad . \quad . \quad . \quad . \quad (1)$$

Defining Q as μ/R_0, where R_0 is the value of R at r_0, again a constant depending only on the radius, we may write this equation

$$n\mathrm{Q}(\alpha_0 r_0 - \mathrm{R}_0\psi) + n\alpha_0 r_0\left(\frac{\pi r_0^3}{2} - \mathrm{Q}\right) = \mathrm{C},$$

or
$$n\mathrm{Q}\phi + \frac{n\theta r_0}{l}\left(\frac{\pi r_0^3}{2} - \mathrm{Q}\right) = \mathrm{C}, \quad . \quad . \quad . \quad . \quad (2)$$

where $\phi = (\alpha_0 r_0 - \mathrm{R}_0\psi)$* is a convenient measure of the elastic strain in a particular wire ; for it is the quantity to which the stress on the bounding element is proportional. We shall employ it later as a parameter with this meaning.

To obtain an idea of the possible magnitude of Q, let us imagine, as a rough test only, that R varies as the mth power of r. Then Q lies between 0 and $\frac{2\pi r_0^3}{3}$. This is sufficient to indicate that Q is of the same order as, or less than, $\frac{\pi r_0^3}{2}$.

Angular velocities are to be small, but the solution of this problem clearly depends in an important way upon the resistance due to motion, and it may not be sufficient to assume resistance proportional to velocity, even when $\dot{\theta}$ is small. Let the resistance in the first case be $\Omega\dot{\theta}$, where Ω is a function which may depend explicitly on the time. Then the equation of free motion of the suspended body may be written (see equation (1))

$$\mathrm{I}\ddot{\theta} + \Omega\dot{\theta} + b\theta = \mathrm{A}\psi \quad . \quad . \quad . \quad . \quad . \quad (3)$$

where $\mathrm{A} = n\mu$.

The solution of the equation depends on the form of the functions Ω and ψ, of which the latter is a measure of the flow. The following investigation shows, that if Ω is not a constant and both Ω and ψ are chosen to make the equation integrable, only by rather arbitrary assumptions can the solution be made to conform with experience. It was undertaken, however, at the suggestion of Prof. Lees, with

* This is closely related to the "Katastasic" strain of Wiechert.

the object of tracing more accurately, if possible, the way in which the flow must enter the equations. Thus :—(1) If $\Omega = \alpha/t$, then the equation reduces to Euler's form

$$I\ddot{\theta} + \frac{\alpha}{t}\dot{\theta} + \frac{b''\theta}{t^2} = f(t)$$

provided $A\psi = b\left(\theta - \frac{b'\theta}{t^2}\right) + f(t)$, a not altogether unwarrantable assumption, where α, b', b'', are constants. Euler's form, however, for any reasonable assumption regarding $f(t)$, leads to a kind of oscillation in which the period very rapidly increases as the amplitude decreases. Nothing of this kind is known.

(2) Let $\Omega = 1/t$, and $A\psi = \left(b - 1 + \frac{n^2}{t^2}\right)\theta$ where n^2 is a constant. Then eqn. (3) may be written

$$t^2\ddot{\theta} + t\dot{\theta} + (t^2 - n^2)\theta = 0,$$

which is Bessel's equation of the nth order. We note first, that when t is fairly large, this becomes

$$\ddot{\theta} + \frac{\dot{\theta}}{t} + \theta = 0$$

which is Bessel's equation of zero order, the most general solution of which is

$$\theta = AJ_0(t) + BY_0(t),$$

where Y_0 is Weber's function of zero order.

By choosing the origin of time suitably, we make $B = 0$ and the solution, using the asymptotic expansion is then

$$\theta = A_1 \frac{1}{\sqrt{t}} \cdot \cos\left(t - \frac{\pi}{4}\right).$$

Very clearly this is the right form of variation of amplitude. Unfortunately, the limiting value of the log. dec. is zero, as otherwise appears from the original equation, which becomes when t is very large,

$$\ddot{\theta} + \theta = 0,$$

the equation of undamped periodic motion. I know of no such case. This may, however, be circumvented by modifying Ω and ψ.

(3) Let $\Omega=\left(\alpha+\frac{\mathrm{I}}{t}\right)$, and $\mathrm{A}\psi=\left(b+\frac{\alpha^2}{4\mathrm{I}}+\frac{\alpha}{2t}+1\right)\theta$.

Write $\frac{\alpha}{\mathrm{I}}=2a$ where α is constant.

Then a particular solution to this equation is

$$\theta=\mathrm{A}_0e^{-at}\mathrm{J}_0(t)=\mathrm{B}\frac{1}{\sqrt{t}}e^{-at}\cos\left(t-\frac{\pi}{4}\right)\text{ approx.},$$

and this will suffice as solution to this case, if we choose the origin of time correctly.

This represents a similar variation to that before obtained, but one which now gives us a log. dec.$=\pi a$, for infinitely small amplitudes. This is the type of variation most often found in practice, and this solution indicates that a decrease of the resistance with time (which has already been denoted "Accommodation" by early investigators), and an interdependence of the flow and the resistance of the kind indicated, can account for the variation of logarithmic decrement.

On the other hand, there is admittedly something very artificial about this method of searching for the solution, and a more simple method, if it will produce similar results, is clearly preferable. We therefore proceed with the exploration, after mentioning that many other equations have been tried without success, by putting $\Omega=$constant, as the simplest, and try likely functions for $\mathrm{A}\psi$.

Forms to be tried are limited to those which will make the equation integrable, and the simplest may be tried first.

(1) Let $\mathrm{A}\psi=g\theta+ht$ where g and h are constants. This is the simplest way of allowing the time effect to continue increasing. It is equivalent to the notion of a flow which, once started, proceeds to relax the stresses at a constant pace until they are reduced to zero.

This leads without difficulty to the solution

$$\theta+\mathrm{H}=\mathrm{G}t+\mathrm{A}e^{x_1t}+\mathrm{B}e^{x_2t},$$

where G and H are formed from the constants of the original equation, A and B are arbitrary, x_1, x_2 are

$$-\frac{\alpha}{2\mathrm{I}}+\sqrt{\frac{\alpha^2}{4\mathrm{I}^2}-\frac{b-g}{\mathrm{I}}}\quad\text{and}\quad-\frac{\alpha}{2\mathrm{I}}-\sqrt{\frac{\alpha^2}{4\mathrm{I}^2}-\frac{b-g}{\mathrm{I}}}.$$

In the periodic case this indicates an ordinary damped vibration of constant logarithmic decrement, but whose equilibrium position is drifting at a constant angular speed

in the positive or negative direction of θ, according as g is less than, or greater than, b.

(2) Let $A\psi = c\theta t$ where c is a positive constant. This will have a similar interpretation to the last. It makes equation (3)

$$\ddot{\theta} + \frac{\alpha}{I}\dot{\theta} + \theta\left(\frac{b}{I} - \frac{ct}{I}\right) = 0.$$

With the substitutions $\theta = ve^{-\frac{1}{2}\frac{\alpha}{I}t}$, and $y = h - kt$, where h and k are constants, this becomes an alternative form of Riccati's equation, viz.,

$$\frac{d^2v}{dy^2} + \frac{1}{k^2}yv = 0,$$

the solution of which in Bessel functions is *

$$v = y^{\frac{1}{2}}\left[AJ_{\frac{1}{3}}\left(\frac{2}{3k}y^{\frac{3}{2}}\right) + BJ_{-\frac{1}{3}}\left(\frac{2}{3k}y^{\frac{3}{2}}\right)\right],$$

where A and B are constants. The meaning being that, as the oscillation proceeds and the restoring force is gradually reduced to zero, the oscillation dies out: in a finite time however. After this, the solution will correspond to an unstable condition, in which θ proceeds at an increasing rate in one direction only. Only the first part can we regard as approximating to any likely case.

Clearly, simplest assumptions regarding flow do not lead to very satisfactory solutions, and we may therefore proceed to the more complicated.

(3) Let $A\psi = A_1 p\theta(1 - e^{-qt})$ where A, p, and q are constants. This represents a flow, or at least an increase in the deformation, proportional to the angle of twist, reversing its direction with the twist; and also increasing independently with the lapse of time, from zero to a steady value, in such a way that the partial derivative with respect to time continually diminishes.

Equation (3) must now be written

$$I\ddot{\theta} + \alpha\dot{\theta} + b_1\theta = -B\theta e^{-qt}$$

were $b_1 = (b - A_1 p)$, and $A_1 p = B$.

The character of the solution is well brought out by successive approximations, commencing by neglecting the right-hand member of the equation, which is permissible if B is small. The solution thus obtained is then used to

* Forsyth 'Differential Equations.'

evaluate $-B\theta e^{-qt}$, and a second approximation is made. After a few repetitions, it becomes clear that the solution may be expressed by an infinite series

$$\theta = \sum_{m=0}^{m=\infty} \left[A_m e^{\left\{-\left(\frac{a}{2I}+mq\right)+\sqrt{\frac{a^2}{4I^2}-\frac{b_1}{I}}\right\}t} + B_m e^{\left\{-\left(\frac{a}{2I}+mq\right)-\sqrt{\frac{a^2}{4I^2}-\frac{b_1}{I}}\right\}t} \right]$$

in which the constant coefficients of the first two terms are arbitrary, the remainder related to them. Further

$$A_{r-1} > A\ , \quad B_{r-1} > B_r \text{ for all values of } r,$$

so that the coefficients form a convergent series. Clearly, we need only retain the first few terms of the series, since the higher terms are smaller, and decay more rapidly. If the motion is oscillatory, as we are to consider, the series may be written

$$\theta = \sum_{m=0}^{m=\infty} C_m e^{-\left(\frac{a}{2I}+mq\right)t} \cos(nt+\delta_m),$$

where δ_m is a const. and $n = \sqrt{\frac{b_1}{I} - \frac{a^2}{4I^2}}$.

We may arrange initial conditions so that $\delta_0 = 0$, and it then follows that $\tan \delta_1 = \frac{2n}{q}$, and similarly for other δ's, so that in the event of q being large, we may write

$$\theta = \cos nt \sum_{m=0}^{m=\infty} C_m e^{-\left(\frac{a}{2I}+mq\right)t} \text{ approx.}$$

This type of solution is to be discussed in detail later (case 4), and it will be sufficient to say here that it represents an oscillation of nearly constant periodic time, whose logarithmic decrement diminishes as the amplitude decreases, in a manner very suggestive of certain experimental results. If, however, q is not large, we must replace $\cos nt$ by $\cos(nt+\delta)$ in the solution, where δ is a function of the time, which reduces to a constant after a long time ; the oscillation ending, as it dies out, as an ordinary damped vibration with a constant logarithmic decrement.

It is nevertheless very important to notice that both the periodic time and the log. dec. are related to the quantity n, which is a definite function of the dimensions of the wire.

(4) Let $A\psi = A_2 e^{p\theta}(1-e^{-qt})$ where A_2, p, and q are positive

constants. This is merely a variant on the last, being mathematically rather simpler, but representing the flow as being non-symmetrical, since $e^{p\theta}$ is not symmetrical with respect to θ. This will resemble the case of a rod which has been twisted too far in one direction before the experiment began.

Equation (3) becomes

$$I\ddot{\theta}+\alpha\dot{\theta}+b\theta=A_2e^{p\theta}(1-e^{-qt}), \quad . \quad . \quad . \quad . \quad (4)$$

or, writing

$$\theta=\omega e^{p\theta},\ k_1=p+\frac{\alpha}{2I};\ N^2=p^2+\frac{\alpha}{I}p+\frac{b}{I};\ A_3=\frac{A_2}{I};$$

$$\ddot{\omega}+2k_1\omega+N^2\omega=A_3-A_3e^{-qt},$$

the solution of which by the ordinary rules is

$$\omega=A_3\left(1-\frac{1}{B_2}e^{-qt}\right)+B_1e^{(-k_1+\sqrt{k_1^2-N^2})t}+C_1e^{(-k_1-\sqrt{k_1^2-N^2})t},$$

where $$B_2=q^2-2k_1q+N^2,$$

and where, if $N^2>k^2$, the system oscillates in the manner given by

$$\omega=A_3\left(1-\frac{1}{B_2}e^{-qt}\right)+Ee^{-k_1t}\cos\left(\sqrt{N^2-k_1^2}\,t+\beta\right), \quad (5)$$

E and β being arbitrary constants.

Whether the system oscillates or not, after a long time it returns to rest at a new position of equilibrium given by $\omega=A_3$ or $\theta=$constant. This angular distance depends on the radius of the rod, and the moment of inertia of the suspended body.

Since θ is always to be small, $p\theta$ may be taken as a small quantity also, so that

$$\omega=\theta e^{-p\theta}=\theta\left(1-p\theta+\frac{p^2\theta^2}{2}+\ldots\right)\text{ approx.}$$

The solution in the form of equation (5) may then be interpreted to mean that the oscillations are not symmetrical, in such a way that excursions in the positive direction of θ exceed the value given by

$$\theta=A_3+Ee^{-k_1t}\cos\left(\sqrt{N^2-k_1^2}\,t+\beta\right),$$

and on the negative side fall short of this value, by quantities which are roughly proportional to the squares of the amplitudes, if q is large enough.

The two roots of the approximate equation

$$p\theta^2-\theta+A+Ee^{-k_1t}=0$$

give us the equations to the two curves upon which the maximum and minimum values of θ will lie. From these we may derive information concerning the decrement. It is easy to verify that if p and k are small, the decrement (and therefore the log. dec.) increases or decreases from one steady value to another as the amplitude diminishes, according as the constant E is positive or negative. The experimental results contain both kinds of variation.

It might be further pointed out that the conditions for oscillation in both cases (3) and (4) show that we may pass from the oscillatory to the aperiodic condition by changing the dimensions of the rod and of the vibrating body. No essential change is made by retaining $\frac{A_3}{B_2}e^{-qt}$.

Second Method.

We may now try a method of expression in which the assumption as regards time is less arbitrary and the forms tried are more definite in meaning.

First, let $\frac{d\psi_0}{dt} = f(\phi)$, where ϕ has the parametric meaning already assigned to it. This expresses the idea that the rate of flow depends on the elastic or "katastasic" part of the strain.

Since $$\psi_0 = R\psi, \quad R\frac{d\psi}{dt} = f(\phi). \quad . \quad . \quad . \quad . \quad (6)$$

From (3) if $\Omega = \alpha$, a constant,

$$R_0\psi = \frac{I}{nQ}\ddot{\theta} + \frac{\alpha}{nQ}\dot{\theta} + \frac{b}{nQ}\theta.$$

Hence

$$R_0\dot{\psi} = \frac{1}{nQ}(I\dddot{\theta} + \alpha\ddot{\theta} + b\dot{\theta}) = f_0(\phi), \quad . \quad . \quad . \quad (7)$$

where $f(\phi) = f_0(\phi)$ when $R = R_0$.

Also, since

$$\phi = (\alpha_0 r_0 - R_0\psi)$$

$$\phi = -\left[\frac{I}{nQ}\ddot{\theta} + \frac{\alpha}{nQ}\dot{\theta} + \theta\left(\frac{b}{nQ} - \frac{r_0}{l}\right)\right]. \quad . \quad . \quad (8)$$

Also $$f_0(\phi) = \frac{R_0}{R}f(\phi).$$

So that the problem is now to obtain a solution of the simultaneous differential equations (7) and (8) for θ, after suitable assumptions as to $f(\phi)$ have been made. In general the equations are too complicated for exact solution, and recourse must be had to approximations, to reveal the character of the motion.

(5) Let $f_0(\phi) = k\phi$ where k is a small positive constant.

This requires $f(\phi) = \left(\frac{k \cdot R}{R_0}\right)\phi$.

Our equation of motion then reduces to

$$\frac{I}{nQ}\dddot{\theta} + \ddot{\theta}\left(\frac{\alpha}{nQ} + \frac{kI}{nQ}\right) + \dot{\theta}\left(\frac{b}{nQ} + \frac{\alpha k}{nQ}\right) + k\theta\left(\frac{b}{nQ} - \frac{r_0}{l}\right) = 0.$$

But if k is small enough, we may neglect the last term, whereupon, one integration gives

$$I\ddot{\theta} + (\alpha + kI)\dot{\theta} + (b + k\alpha)\theta = A \text{ where A is constant,}$$

or if $$\omega = \theta - \frac{A}{b + k\alpha},$$

$$I\ddot{\omega} + (\alpha + kI)\dot{\omega} + (b + k\alpha)\omega = 0,$$

the solution of which is

$$\omega = Be^{x_1 t} + Ce^{x_2 t},$$

where $$x_1, x_2 = -\frac{-\alpha + kI}{2I} \pm \sqrt{\left(\frac{\alpha + kI}{2I}\right)^2 - \frac{b + k\alpha}{I}},$$

(B and C are constants)

an ordinary damped motion, in which, if

$$b + k\alpha > \frac{\alpha^2}{4I^2} + \frac{k}{2} + \frac{k^2 I}{4},$$

the system performs damped oscillations about a position $\theta = \frac{A}{b + k\alpha}$, with constant period $T = \frac{2\pi I}{b + k\alpha}$, and constant log. dec.

$$\lambda = \frac{\pi}{2}\frac{(\alpha + kI)}{b + k\alpha}. \quad . \quad . \quad . \quad . \quad . \quad . \quad . \quad (9)$$

The interest of this result lies in the demonstration that a constant log. dec. is possible in the complete absence of

resistance or "internal friction"; for if α is put equal to zero in (9), $\lambda_0 = \frac{\pi}{2}\frac{kI}{b}$, and the constant log. dec. would then determine k. The first assumption of this case is not unreasonable, since it merely implies that the rate of flow is proportional to the elastic stresses in those portions of the material which remain capable of withstanding them; or, in short, the flow is proportional to the force producing it, if $f(\phi)$ contains R as shown above.

(6) Let $f_0(\phi) = p\phi^3$ where p is a positive constant, and not large.

This requires $f(\phi) = \frac{p\mathrm{R}}{\mathrm{R}_0}\phi^3$.

In this instance rate of flow is taken proportional to the cube of the forces producing it, to exemplify the law $f(\phi) = p\phi^m$. For symmetry, m must be odd.

A numerical example will be found helpful in this instance, and I have selected an aluminium wire and vibrating body, specified as follows :—$l = 100$ cm., $r = \cdot 05$ cm. $n = 2\cdot 6 \times 10^{11}$ dynes/cm.^{2}, $\mathrm{I} = 2 \times 10^5$ gram. cm.^{2}; so that b is about 3×10^4; the approx. time of vibration $\mathrm{T} = 15$ sec.; and if successive maximum amplitudes are reduced in the ratio 10 : 9, we may take α to be 5×10^3 (or less—see result of Case (5)). The value of Q may be roughly estimated in the way already indicated.

In (8) the first term has the largest coefficient, the third a coefficient of the order one tenth or less of the first, and the second a much smaller coefficient still. In order to obtain the essentials of the solution with moderate ease, we shall neglect the second and third terms in comparison with the first. The equation of motion may then be written

$$\mathrm{I}\ddot{u} + \alpha\dot{u} + bu = -\frac{p\mathrm{I}^3}{n^2\mathrm{Q}^2}(\dot{u})^3,$$

where $u = \dot{\theta}$.

Now $\frac{p\mathrm{I}^3}{n^2\mathrm{Q}^2}$ is, in general, small compared with the other coefficients, and the usual method of successive approximation may be used as in Case (1). The algebra, though laborious, is straightforward, and need not occupy space here. At every stage, very small terms are dropped, the numerical example helping in such selection. The results of the first

three approximations are as follows :—

1st approx. $u_1 = Be^{-\frac{\alpha}{2I}t}\cos(\rho t+\delta)$,

where $\rho = \sqrt{\frac{b}{I} - \frac{\alpha^2}{4I^2}}$.

2nd approx. $u_2 = Be^{-\frac{\alpha}{2I}t}\cos(\rho t+\delta)$

$$-3Ee^{-\frac{3\alpha}{2I}t}\cos(\rho t+\delta),$$

in which 3E is small compared with B.

3rd approx. $u_3 = u_2 +$ a term much smaller still.

Succeeding approximations merely add terms which are not only smaller in amplitude, but which die out quicker. We need only attend to the solution as given in u_2.

Let us now choose initial conditions so that $\delta = 0$, and we have, finally,

$$u = \left(Be^{-\frac{\alpha}{2I}t} - 3Ee^{-\frac{3}{2}\frac{\alpha}{\theta}t}\right)\cos\rho t,$$

and therefore

$$\theta - G = -\frac{I\rho}{b}B\sqrt{1+\frac{\alpha^2}{4I^2\rho^2}}e^{-\frac{\alpha}{2I}t}\cos(\rho t+\epsilon)$$

$$-\frac{\rho}{\frac{b}{I}+\frac{2\alpha^2}{I^2}}3E\sqrt{1+\frac{9}{4}\frac{\alpha^2}{I^2\rho^2}}e^{-\frac{3}{2}\frac{\alpha}{I}t}\cos(\rho t+\sigma),$$

where $\tan\epsilon = \frac{2I\rho}{\alpha}$ and $\tan\sigma = \frac{1}{3}\tan\epsilon$.

In general, $\tan\epsilon$ is large—near 40 in the numerical example, and is probably greater—and little error will therefore be made in the approximation if ϵ is taken equal to σ, which indeed is probably correct to two or three per cent., and each of these equal to $\frac{\pi}{2}$ so as to allow us to write, abbreviating the coefficients,

$$\theta - G = -\sin\rho t\left\{H_1e^{-\frac{\alpha}{2I}t} + H_2e^{-\frac{3}{2}\frac{\alpha}{I}t}\right\},$$

in which it appears that H_2 is considerably smaller than H_1, both of them depending, however, on the arbitrary constant B, and H_2 on the constant p; both H_1 and H_2 are positive. The motion is clearly an oscillation whose amplitude decays in a rather complicated way. As this is an important case, a numerical example has been calculated by putting $H_1 = 1$, $H = \cdot1$, other quantities being as laid down. The unbroken curve in fig. 2, to which scale A applies, gives the result of

this calculation, and the broken curves show the experimental results for aluminium and copper wires, from Subrahmanian. I have selected those curves which are in best agreement with the calculation. Scales B and C apply to these (fig. 2).

In this case the motion is clearly similar to that sometimes obtained practically, and it is suggested that the explanation of the variation of log. dec. is that given here. Case (4) clearly shows, however, that the magnitude of the log. dec. for infinitesimal amplitudes depends primarily on the resistance measured by α, the flow being responsible for the rate

Fig. 2.

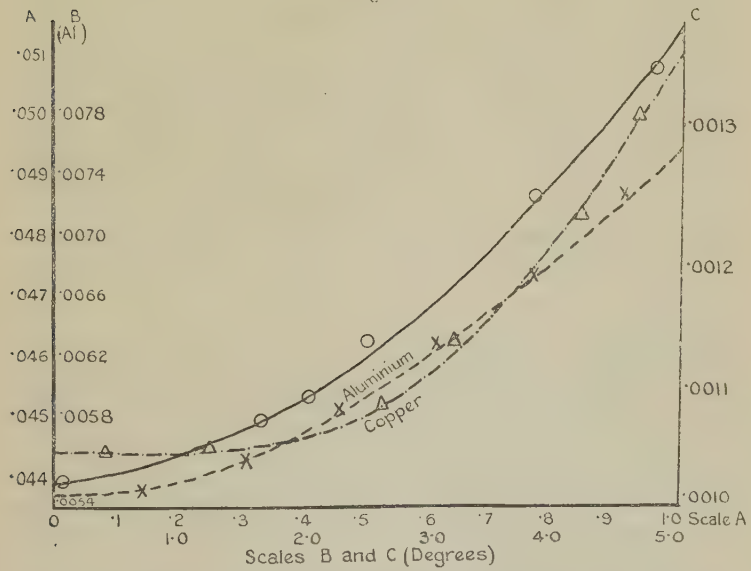

For the sake of a clear diagram, the curves in fig. 2 are drawn separated; but obviously, by a small adjustment of the scales, they could be made to lie more nearly along one another; the aluminium curve, indeed, would almost coincide with the calculated one. This last would present the same appearance whether drawn for large or small amplitudes, so that it is the shape only which is important.

of change of decrement. Now, many experiments have shown that when the dimensions of the wire are changed so that the period is increased, the log. dec. for a given amplitude is decreased. This indicates that α is a function of the dimensions, which always diminishes for any change of dimensions which increases the period. For changes in the radius this is clearly the case; when the length increases

for a given angular velocity of the vibrating body, the relative angular velocity between the two ends of the element considered at the beginning is inversely proportional to the length of the wire. With this in view the condition may be fulfilled, and the theory is not in any way contradictory to practice.

Other Cases.—It becomes clear that the law $A\psi = k(\phi)^{2m+1}$ will not lead to any fundamentally different kinds of motion, but will only introduce decaying terms in the amplitudes, whose rates of decrease will depend on other multiples of $\alpha/2I$. It is, however, possible that the phase angles such as ϵ, σ, in the above, will not be nearly equal. In such an event we must include a phase angle in the result, which phase angle will be a function of the time.

With this always allowable, we may conclude from the fact that our differential equations are linear (in the approximate method), that solutions found for various powers of ϕ are additive, in the sense that if $\theta = M$ is the solution when $A\psi = k_m\phi^m$, and $\theta = N$ when $\theta\psi = k_n\phi^n$, then $\theta = M + N$ when $A\psi = k_m\phi^m + k_n\phi^n$. Hence, except for a different rate of change of logarithmic decrement with amplitude, nothing new is introduced if we assume

$$A\psi = k_1\phi + k_3\phi^3 + k_5\phi^7 + \text{etc.},$$

all the constants being positive.

Other trials could be made, but the calculations are sufficient to justify the hypotheses employed to explain those aspects of the phenomenon of flow dealt with here. It appears, too, that the assumption that flow is proportional to an odd power of the elastic stresses does lead to the prediction of a variation of logarithmic decrement which agrees with experiment. It is suggested that this affords an explanation of this effect, at least in some metals.

For encouragement and valuable advice during the course of the work, my thanks are tendered to Prof. C. H. Lees.

Summary.

The equations of motion of a torsional pendulum whose suspension is a wire of plastic material, are worked out in two different forms which are kept as general as possible. The first form is employed to trace by trial the manner in which the flow varies with the time and the twist. With the second form, a definite hypothesis, that the rate of flow is proportional to an odd power of the elastic stresses, is developed, and is shown to lead at once to an explanation of the observed variation of logarithmic decrement with amplitude.

XC. *The Mobilities of the Positive Ions formed by Alpha Rays in Air, Hydrogen, and Helium.* *By* J. S. Rogers, *B.A., M.Sc., Senior Lecturer in Natural Philosophy, University of Melbourne* *.

Introduction.

THE mobility of positive ions has been shown to vary with the life of the ion by Erikson † and Wahlin ‡. These authors have found that the mobility of the "normal" positive ion in air was 1·4 cm./sec. per volt/cm.; but if the mobility was measured in a very short time after the ion was formed (of the order of 1/50 sec.), the value obtained was 1·89 cm./sec., which is approximately the same as that of the negative ion. In addition to these values of the mobility, Nolan § has reported evidence of many more types of positive ions—mobilities as high as 12·4 cm./sec. having been obtained. Later, Wahlin ‖ found mobilities of positive air-ions as low as ·970 cm./sec.

The dependence of the mobility of positive ions on their life has been investigated in air, hydrogen, and helium. The method employed was a modification of the original method of Rutherford ¶, in which an alternating potential was produced by means of a commutator. The ionization was produced by alpha rays which, by means of a sectored metal disk carried on the shaft of the commutator, were allowed to enter the mica window of the ionization vessel once only in every revolution. With the arrangement used the life of the ion could be measured accurately.

In addition, the apparatus was devised to examine helium for the presence of doubly-charged positive ions which had been reported by Millikan ** and Wilkins ††.

Description of the Apparatus.

The apparatus consisted of an ionization chamber and a compensating chamber, the upper insulated electrodes of each being connected to the same quadrant of a Dolezalek

* Communicated by Sir E. Rutherford, O.M., P.R.S.
† Erikson, Phys. Rev. xx. p. 117 (1922).
‡ Wahlin, Phys. Rev. xx. p. 267 (1922).
§ Nolan, Proc. Roy. Irish Acad. xxxvi. p. 74 (1923).
‖ Wahlin, Phil. Mag. xlix. p. 566 (1925).
¶ Rutherford, Phil. Mag. v. p. 95 (1903).
** Millikan, Phys. Rev. xviii. p. 456 (1921).
†† Wilkins, Phys. Rev. xix. p. 210 (1922).

electrometer. The sensitivity of the instrument was 600 mm. per volt when the needle potential was 200 volts and the lamp and scale 150 cm. from the electrometer.

The ionization vessel (see fig. 1) consisted of a hollow brass cylinder 10 cm. in diameter and 12 cm. high. The bottom of the vessel was made of ebonite 1 cm. thick. The curved side of the brass vessel fitted into a ring of brass

Fig. 1.

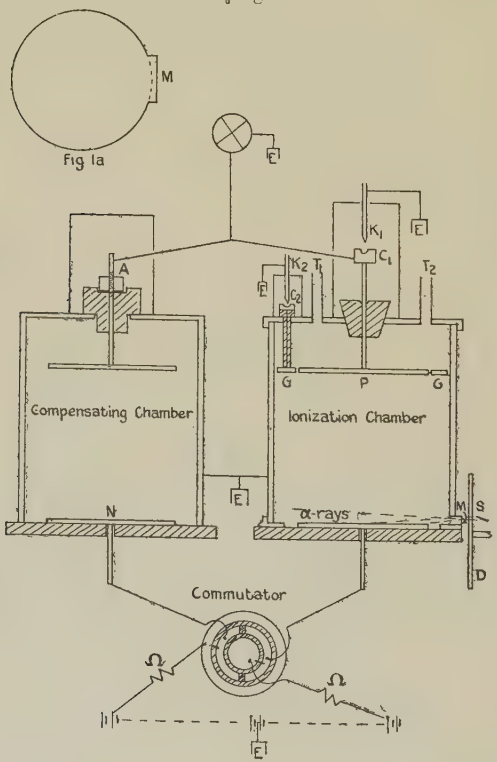

which was screwed down to the ebonite. This curved side was fastened to the ring with picein, while soft wax made the ring-ebonite joint air-tight. An insulated plate L about 8 cm. in diameter was placed on the ebonite, and connexion was made between this plate and the commutator by a lead which passed through the ebonite. The upper plate P of the ionization vessel and the guard-ring G were carried by the lid of the vessel. The lead to the plate passed through an amber stopper, and could be earthed by the key K_1.

The guard-ring could be earthed by the key K_2. The source of α-rays was polonium on a copper plate about 2 cm. long and 3 mm. wide, which was mounted with its long edges horizontal and with the other edges at an angle of 30° to the horizontal. This was so inclined to prevent the rays from the lower edge of the source, S, passing into the upper part of the chamber. The ideal ionizing beam for the work would have been a thin parallel horizontal one ; but as this was not practicable, the beam of rays entered the chamber so that the majority of them grazed the lower plate L. The rays entered the chamber through a mica window M which had a stopping power of about 1·3 cm. of air. It was not possible to construct a window of thinner mica which would remain intact when the vessel was evacuated; in fact, there was considerable difficulty in supporting a mica window of the above thickness. It was possible to do so by soldering a flange on to the lower portion of the curved side where the mica was to be placed, as is indicated in fig. 1*a*. The openings in this flange consisted of three holes 4 mm. square side by side, the thickness of the metal between holes being 2 mm. The piece of mica for the window was then fastened by picein to a brass strip in the form of a grid, the holes in which corresponded to the holes in the flange. This strip, with the mica, was then fastened on to the flange with soft wax. As the melting-point of the soft wax is considerably lower than that of picein, it was possible to do this without disturbing the seal between mica and brass strip. This vessel, with the numerous wax joints, proved difficult to make gas-tight, and the difficulty was finally overcome by painting all the joints over with shellac dissolved in methylated spirits. Two brass tubes T_1 and T_2 were soldered on to the lid of the vessel, and glass tubes were passed into these and secured by picein. Through one of these tubes, T_1, the various gases were introduced, and through the other, T_2, the vessel was evacuated. For evacuation a Cenco Hyvac pump was used. The pressure attained by this was indicated by a discharge-tube connected to the apparatus. When the vessel was evacuated the alternative spark-gap between points was at least 2 cm., and on occasion exceeded 2 inches. After the vessel had been evacuated and left for several days, the cathode dark space was still found to be 1·5 cm., and from the colour of the discharge the gases present appeared to be vapours which arose from the various sealing agents used. The amount of these vapours was thus too small to affect seriously the purity of the gases employed.

The Commutator.

Difficulty was experienced in obtaining a suitable commutator. This difficulty was occasioned by two factors—first the uneven bearing of the brushes on the commutator, and second the presence of metallic dust, which caused short circuits between the insulated segments of the commutator.

All the commutators used were constructed on ebonite cylinders carried by an axial steel shaft which rotated within ball-bearings. The conducting strips were made of brass, the difference between the various commutators being merely in the nature of the end insulation separating the central segments.

In the first commutator the insulation between these central segments was of bakerlite 1·2 cm. wide, and brass brushes cut from strip ·5 mm. thick were used. Four brushes were required; two bearing on the side brass cylinders were connected respectively to the positive and negative sides of the small storage-cells which provided the potential applied to the lower plate of the ionization vessel, and two diametrically opposite, bearing on the central segments, were connected to the lower plates of the ionization and compensating vessels. To protect the cells, megohms were inserted in the leads from the cells to the commutator.

The width of the insulation strip (1·2 cm.) introduced an uncertainty, for it was necessary to know how long the brush in contact with an insulating segment remained at the potential of the last conducting segment with which it had been in contact. This was ascertained by replacing the bakerlite strips with an air-gap 2 mm. wide; and by comparing readings obtained with these two commutators, it was concluded that the brush remained at the same potential the whole of the time it was in contact with the bakerlite insulation. The air-gap commutator was found to be useless for high speeds of rotation, for the brushes did not bear evenly on the commutator, and considerable irregularities were introduced into the readings.

In the final commutator the brass brushes were replaced by brushes of thin phosphor-bronze strip. The ends of these brushes, which touched the commutator, were cut with a fine saw, so that they resembled the tooth of a comb. This ensured a more even pressure on the commutator. These phosphor-bronze brushes produced a very much smaller quantity of brass dust than the brass brushes. The end insulation was here of mica, 1·7 mm. wide. This commutator proved to be much more satisfactory than any of

the previous types. The surface of the mica had, however, to be scraped lightly occasionally to remove traces of metallic dust.

To one end of the steel shaft of the commutator was attached the revolution counter, and to the other was a brass disk D (fig. 1) about ·7 cm. in diameter, which moved between the source S and the mica window M. A sector of 15° was cut in this disk, and thus the rays could enter the ionization chamber only when the sector was between S and M. This disk was fastened by means of a screw to the steel shaft, and the position of the sector with regard to the remainder of the commutator could thus be varied. The purpose of this sector was to allow a beam of rays to be shot into the gas while the bottom plate was positively charged, and then only for a limited time. The commutator was rotated by a shunt-wound D.C. motor driven by large storage cells, and a sliding rheostat was placed in series with the motor. The rate of rotation could be maintained constant within 1 per cent. for a series of readings lasting for two hours. During every reading of the ionization current one reading at least was taken of the rate of rotation of the commutator.

The Compensating Chamber.

If the source of α-rays was removed and L was charged positively (say to +200 volts), and the keys K_1 and K_2 raised, then the electrometer would register no charge.

If, now, the commutator were turned by hand until the potential of L were negative (−200 volts, say), the spot of light would be reflected completely off the scale, owing to the charge induced on the upper plate. The compensating chamber was used to overcome this; it was an earthed shielded vessel with the lower plate M connected to the commutator so that its potential was always opposite in sign to that of L and the upper insulated plate was connected to the electrometer. The distance between the upper and lower plates could be varied by means of the screw A, and when this vessel had the same capacity (electrostatic) as that of the ionization chamber, the reversal of the potential on L caused no deflexion of the electrometer. The actual experimental method employed was to turn the screw A until there was no deflexion on reversing the commutator. Whatever potentials were then applied to L and N, the whole apparatus remained compensated for induced charges. This adjustment was quite a sensitive one, as 1/8 of a turn of A could be readily detected. When the apparatus was compensated

and the commutator rotated by the motor, the earthing-keys could be raised and the electrometer was unaffected. The leads from the top plates of the ionization and compensation chambers passed through amber insulators within earthed tubes. All the insulation except the stopper at the top of the compensation chamber was of amber, the last being of sulphur. The electrostatic leak of the whole apparatus was very small ; about 1 mm. in 5 min. near the zero, *i. e.* in the region where the final ionization was measured.

The potentials applied to the lower plates of the two chambers were supplied by 248 small storage-cells. One point of this battery was earthed. The potentials were measured by means of a Weston multi-range D.C. voltmeter.

Preparation of Gases used.

Air.—Before the air passed into the apparatus it was dried in a side-tube containing a tightly-fitting plug of phosphorus pentoxide. This plug occupied about one-third of the volume of the drying vessel. Before the air passed into the apparatus it was stored for at least an hour, and usually for very much longer, in this side-tube.

Hydrogen.—This was prepared by the electrolysis of water (plus a little sodium carbonate), nickel electrodes being used. An inverted burette was placed over the cathode, and the hydrogen as produced displaced the solution from this burette. The top of the burette was connected by a piece of pressure-tubing to the drying-tube of phosphorus pentoxide mentioned above. The hydrogen was stored in this tube for at least an hour, usually longer, before being passed into the apparatus. Hydrogen was passed through the apparatus several times before the sample, on which readings were taken, was introduced.

Helium.—The helium used was very generously sent to Australia by Sir Ernest Rutherford. When this arrived it was contained in a glass bulb with a drawn-out side-tube and contained nitrogen as an impurity. The tube was broken under mercury, and the helium was, by means of a mercury transfer-pump, passed backwards and forwards through finely broken-up coconut charcoal contained in a narrow tube immersed in liquid air until there was no further diminution in volume. The charcoal column was about 24 cm. long, and the charcoal had been carefully prepared and activated. During the process of the purification the charcoal was several times heated in a bath of boiling sulphur for some hours while the Hyvac pump was running.

The helium was then stored over mercury. For each experiment the helium was, on its path to the ionization chamber, again passed slowly through charcoal immersed in liquid air, and after each experiment the gas passed through the same purifier before being stored over mercury.

Method of calculating the Mobility.

The method consisted in allowing a beam of rays to enter the chamber near the bottom plate when this plate was positively charged. The positive ions then proceeded towards the top insulated plate. If their velocity was sufficiently great, they would reach the latter plate before the potential of the lower plate changed in sign. On the other hand, if the velocity was insufficient, they would, on the reversal of the potential gradient, be drawn downwards to the lower plate. If x cm. is the distance between the plates, and X volts the potential applied to the lower plate when no charge is registered by the electrometer, p mm. the pressure of the gas, and K cm./sec. per volt/cm. the mobility at a pressure of 760 mm. of the fastest ion present in the gas, then $\frac{x^2}{\mathrm{K}} = \frac{760\,\mathrm{X}t}{p}$, where t sec. is the interval elapsing from the instant when the last ions were formed by the α-rays to that when the potential on the lower plate became negative. This quantity t is thus the *life of the ion.* It was determined by the product of two factors—the first was the rate of rotation of the commutator, and the second was what will subsequently be termed the reduction factor. This was obtained by dividing the circumference of the commutator into the distance that the positively-charged portion of the central part of the commutator moved under the brush connected to the ionization chamber (plus the width of the insulation strip) after the last α-rays had entered the chamber. The reduction factor could be varied by changing the position of the rotating sector on the shaft of the commutator with regard to the rest of the commutator. The commutator was rotated in such a direction that the last α-rays to enter the ionization chamber were those which grazed the lower plate.

Influence of Different Values of Negative Potential.

The first point that was investigated after the compensation chamber had been adjusted was the influence that different values of the negative potential applied to one-half

of the commutator had on the readings when the positive potential applied to the other remained constant. A typical curve is shown in fig. 2. It was found that, as the negative potential was increased, the ionization current decreased to a certain value which then remained constant. This constant value was reached when the negative potential was approximately 25 per cent. greater than the positive. As the purpose of the negative potential was merely to sweep back to the lower plate those positive ions which were unable to reach the upper plate, it was arranged, in all readings described below, that the negative potential was at least 25 per cent. greater than the highest potential used.

Fig. 2.

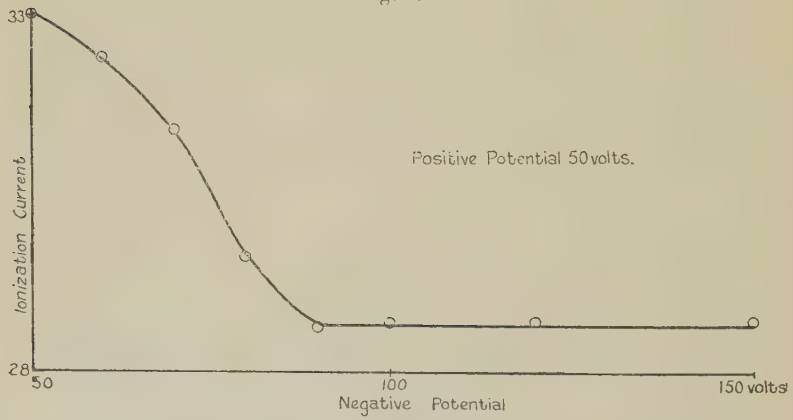

It is considered the reason that a larger ionization current was obtained when the negative and positive potentials were equal was that either certain of the positive ions did not proceed directly between the plates, or else certain ions were formed in parts of the ionization chamber where the potential gradient had not its maximum value.

Experimental Results.

(a) *Method.*

After the gas had been introduced, and sufficient time had elapsed for the commutator to be rotating uniformly, readings of the ionization current were taken for differ values of the positive potential applied to the lower plate

the ionization vessel. Two consistent readings were made for each value of the positive potential. The ionization currents were then plotted against the positive potential, and the intercept of this curve on the potential axis gave the value of X. To find the reduction factor, the commutator was turned by hand until the α-rays just failed to enter the ionization vessel. The distance that the positive portion of the central segment had still to run could then be readily measured.

(b) *The Curves.*

Fig. 3 represents typical curves for air, hydrogen, and helium respectively. It will be noticed that for the higher potentials the curve runs parallel to the potential axis, showing that for such potentials all the positive ions were reaching the top plate. As the potential was further decreased, the curve began to slope off gradually, while the final portion is a straight line, and the intercept of the straight line on the potential axis gave the value of X mentioned above. Under ideal conditions for these experiments, after the straight horizontal portion of the curve the remainder would be a vertical descent to the potential axis. This cannot, however, be realized for the following reasons :—

Firstly, such a curve would be realized only when the ionizing beam was a thin, parallel, horizontal one which grazed the bottom plate of the ionization chamber. If the beam was not parallel, then the ions would be formed in the chamber at different distances from the top plate so that those which were produced near the bottom of the chamber would have greater distances to travel than those produced higher up. In consequence, as the positive potential was decreased, the "lower" ions would fail to reach the upper plate, while the "upper" ions still continued to do so. The source was so arranged that the majority of the rays were directed on this lower plate so that the ionization was limited to that portion of the chamber near the lower plate. It was impracticable with polonium sources to produce a parallel beam. The mica window, through which the rays entered the chamber, had to be equal to 1·3 cm. of air at least to withstand atmospheric pressure, and the α-rays which entered the chamber had to have an emergent range over 1 cm. so that the source could not be placed further from the mica window than 1 cm. Even if a parallel beam of rays had been realizable, the ideal curve would not have

Fig. 3.

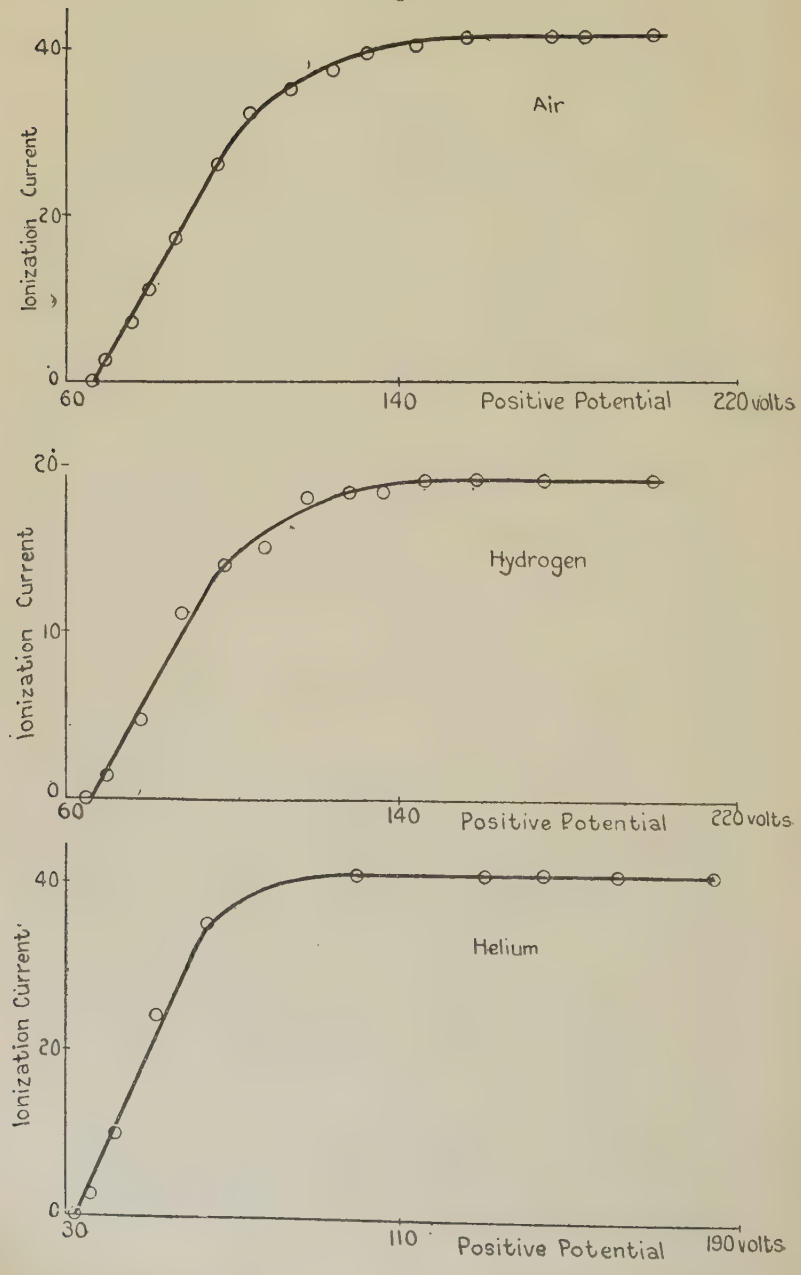
40
20
0
Ionization Current
Air
60
140
Positive Potential
220 volts
20
10
0
Ionization Current
Hydrogen
60
140
Positive Potential
220 volts
40
20
0
Ionization Current
Helium
30
110
Positive Potential
190 volts

been obtained unless this beam were very thin, for a beam of finite thickness would produce ions at different vertical distances from the lower plate. In order that this effect should be as small as possible, the distance between lower and upper plates was made approximately 8 cm., so that the width of the beam would be small in comparison with the distance that the ions travelled in the chamber.

On the other hand, the thinner the beam of rays the less was the ionization current, and consequently either very intense sources were required or very sensitive detectors of the ionization current.

Secondly, in order to obtain the ideal curve the ionizing beam must enter the chamber momentarily once in each revolution. If the time in which the beam was present in the chamber was of any duration, those ions which were first formed would be moving towards the top plate before the last ones were formed. This could only be prevented by making the rotating sector of very small angle. Very small sectors necessitated, however, very intense sources if the ionization currents were to be appreciable. A compromise had thus to be arrived at between the ideal small-angled sector and one which would allow ionization currents to be measured in reasonable times.

If such ideal conditions could be realized, the presence of ions of more than one mobility in a gas could be readily shown. The existence of slower ions under the actual experimental conditions would be more difficult to show, as they would cause a somewhat slight discontinuity in the curves obtained. However, in the actual curves there was no definite evidence of ions of more than one mobility present at the same time.

In order to determine the mobilities of the ions when the life of the ion was very short, the whole curve was not obtained, but merely the last portion, *i.e.* that just before the ionization current disappeared. Sufficient points were obtained to allow the straight line to be drawn which determined the intercept.

Fig. 4 represents two end portions of the curves for helium and air respectively, and is typical of the type of curve obtained. The curves are quite straight, and thus show that there is only one type of ion present. The mobility obtained from (*a*) was 5·53 cm./sec. per volt/cm., and from (*b*) 1·65 cm./sec. Practically the whole of the curves were of this type, and thus represent the presence of one type of ion alone.

Fig. 4.

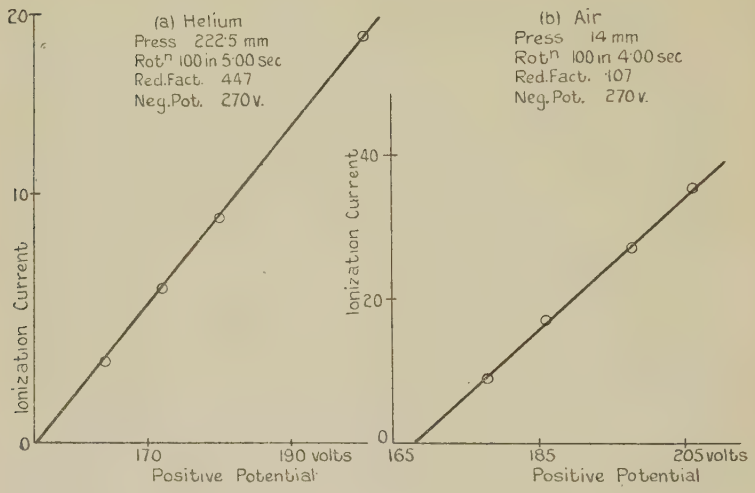

(c) *Values of the Mobilities.*

(i.) *Air.*—Table I. represents the results obtained with air. The table is arranged so that the life of the ion decreases as one reads down the table. It will be seen that, for lives between ·138 and ·0139 sec., the value of x^2/K remains constant within the limits of experimental error although the pressure varies between 98 and 22 mm., the rate of rotation of the commutator between 3·8 and 22 seconds for 100 revolutions, and the intercept on the potential axis between 15 and 164 volts. Further, these values were obtained with the three different commutators mentioned above.

For lives of ions between ·00947 to ·00675 sec. the value of x^2/K appears to be constant, so that these values have been bracketed, and the same applies to the values between ·00428 and ·00229 sec. The mobilities corresponding to the different values x^2/K are given in the last column. It was assumed that the value of the mobility corresponding to $x^2/K = 47·8$ was that of the air-ion of mobility 1·36 cm./sec. per volt/cm. This is the mean of the values obtained by a great number of workers between whom there is fairly good agreement. (See Landolt-Börnstein Tabellen.) This value was assumed because it was difficult to measure the quantity x, which has to be measured twice as accurately as the other quantities, with the necessary precision. Further, with the

distance between the plates of the ionization vessel (*i. e.* approximately 8 cm.) there is reason to doubt that the potential gradient would be uniform throughout.

TABLE I.

Mobilities of Positive Ions in Dry Air.

Life of Ion (sec.).	Press. (mm. Hg.).	Rotation. Time for 100 revs. (sec.).	Reduction Factor.	Intercept (volts).	a^2/K.	Mean.	Mobility (K).
·1381	152	6·25	·461	70	48·3		
·0981	23·0	22·0	·446	15	48·3		
·0814	90	17·6	·461	68	46·9		
·0681	23	22·0	·310	20·7	46·7		
·0599	98	13·0	·461	106	49·3		
·0466	62	10·10	·461	83	48·1		
·0373	70·5	10·35	·348	117	46·8		
·0288	42·5	6·25	·461	95	49·0		
·0263	70·5	7·30	·348	164	46·5	47·8	1·36 cm./sec./volt/cm. (Value assumed.)
·0219	22·0	7·04	·310	64	48·5		
·0178	45	5·04	·352	157	47·0		
·0178	23·0	4·00	·446	79	46·7		
·0176	42·5	3·82	·461	147	46·3		
·0173	22·0	5·88	·310	76	48·1		
·0158	22·0	5·10	·310	89	48·7		
·0139	22·0	4·50	·310	102	49·3		
·00947	21·5	3·06	·310	132	44·3		
·00939	27·5	3·03	·310	171	44·3		
·00676	22·0	3·10	·218	184	43·0	44·2	1·47
·00675	15·5	3·26	·207	136	45·0		
·00428	14·0	4·00	·107	169	39·3		
·00404	11·5	2·50	·169	138	38·7		
·00297	9·0	2·77	·107	162	40·2	39·5	1·65
·00229	8·2	2·78	·0824	188	39·8		

Note.—In each of Tables I., II., and III. the values underlined in the sixth column with full lines were those obtained with air-gap of ·16 mm. between central segments of commutator; those underlined with dotted lines, with mica insulation ·17 cm. wide between segments; and all others with bakerlite insulation 1·2 cm. wide.

(ii.) *Hydrogen.*—The results are set out in Table II. In the first reading the ions were examined at a longer life than in the other gases. This necessitated a slow rotation of the commutator, and difficulty was experienced in securing the necessary uniformity of rotation. In consequence this result is not so reliable as the others, although the intercept was obtained from a straight line. The mobility of ions of lives between ·261 and ·01363 sec. appears to be constant and has the value 5·30 ; between ·00913 and ·00644 the value 5·95 holds, while between ·00503 and ·00330 the mobility is 6·57. It will be noticed that when the life of the ion was ·01152 sec. a value of the mobility was obtained which lies between the first set of values and the second. Possibly this value should be included in the second set.

TABLE II.

Mobilities of Positive Ions in Dry Hydrogen.

Life of Ion (sec).	Press. (mm. Hg.).	Rotation, 100 revs. (sec.).	Reduction Factor.	Intercept (volts).	x^2/K.	Mean.	Mobility.
·442	340	96·0	·467	13·0	13·62	.....	4·78
·261	244	56·0	·467	15·5	12·60		
·133	307	27·5	·486	36·0	11·90		
·1285	307	27·5	·467	36·0	12·38		
·0770	209	16·75	·461	44	12·32	12·29	5·30
·0432	188·5	9·40	·472	67	12·24		
·1363	101	3·00	·453	120	12·30		
·01152	81·5	3·04	·379	106	11·45		
·00913	61·5	3·03	·301	94	11·05		
·00894	82·0	3·02	·296	130	11·00		
·00832	74·5	5·00	·166	126	10·70	10·84	5·99
·00667	74·5	4·00	·166	156	10·60		
·00503	58·0	6·10	·0824	151	9·95		
·00412	58·0	5·00	·0824	169	9·42	9·73	6·67
·00330	44·5	4·00	·0824	177	9·97		

(iii.) *Helium.*—The results are set out in Table III. The mobility remains constant for lives between ·1001 sec. and ·01095 sec., and has the value of 5·61 cm./sec. per volt/cm.

When the life of the ion varies between ·00795 and ·00679 sec. the value of the mobility is 6·12, while between ·00528 and ·00290 sec. the value is 6·72.

TABLE III.

Mobilities of Positive Ions in Helium.

Life of Ion (sec.).	Press. (mm. Hg.).	Rotation, 100 revs. (sec.).	Reduction Factor.	Intercept (volts).	x^2/K.	Mean.	Mobility.
·1001	225	22·0	·455	34	11·50		
·0470	222·5	10·50	·447	74	11·83		
·0224	222·5	5·00	·447	152	11·80		
·0154	92·5	4·00	·384	91	11·48		
·0146	97·7	3·28	·446	105	11·00	11·56	5·61
·0126	92·5	3·28	·384	110	11·40		
·01135	100	5·00	·227	125	11·05		
·01095	90·5	3·28	·333	124	11·42		
·00795	85·5	3·28	·207	152	10·79		
·00779	71·0	4·60	·169	130	10·80		
·00686	63·0	3·32	·207	128	10·60	10·62	6·12
·00679	85·5	3·28	·207	171	10·30		
·00528	46·5	4·94	·107	110	9·51		
·00375	30·5	3·50	·107	106	9·85	9·69	6·72
·00290	30·5	2·70	·107	134?	9·73?		

One of the difficulties with helium was that a limit was imposed on the negative potential gradient that this gas would withstand before it became conducting (there being no external ionizing agent present). On one occasion, with the commutator at rest and when the pressure of the helium was 90·5 mm., it was found that when the lower plate on the ionization chamber was charged to −254 volts the upper plate became charged negatively. When the negative potential was increased the rate of charge increased very rapidly. When the potential was decreased to −242 volts, there was no such current, showing that the observed currents were not due to ionization caused by external sources, but that helium "broke down" (*i. e.* conducted) under quite small negative potential gradients. At times such clear demonstration of this breakdown was not possible, for, under much lower pressures and at potentials as high as −280 volts,

the electrometer registered no negative charge. The effect was still present however, for when the negative potential was kept at −280 and the positive adjusted to 200 volts, it was found that, when the commutator was rotated, the electrometer registered a negative instead of a positive charge; the positive charge was expected, since the gas was ionized while the lower plate of the ionization chamber was charged positively, and the pressure of the gas and rate of rotation of the commutator were such as would permit the positive ions to reach the top plate. When the negative potential was decreased and the positive decreased accordingly, this negative charge disappeared and the expected positive charge made its appearance. It is probable that, in the experiments last described, there were some minute traces of impurity present in the helium. When this phenomenon was first noted the coconut charcoal through which the gas passed had been evacuated while immersed in a bath of boiling sulphur just immediately previous to its being immersed in liquid air; and the fact that the breakdown was so readily demonstrated was due to the extreme purity of the helium.

There is another indication that the helium used was very pure. Franck and Gehlhoff* stated that in pure helium the mobility of the negative ion was about 500 cm./sec. per volt/cm., while Franck and Pohl† had found that when slight traces of impurity were present this mobility was 6·31. Accordingly the sector was adjusted on the commutator so that the mobility of the negative ions could be determined. Only one determination was made and a mobility of just over 1000 cm./sec. was found. It is intended to continue this examination of the negative ions later, this experiment being undertaken to demonstrate that the helium used was reasonably pure, even when the "breakdown" of helium under negative potentials did not occur.

As in the method which has been described for finding the mobilities of positive ions, the negative potential applied to the commutator was always greater than the positive, and as helium becomes conducting under certain negative potential gradients, the positive potentials that could be used with helium were limited if the gas was investigated at low pressures. In consequence of this, the mobilities of the helium positive ions have been investigated for as short lives as are possible with the present apparatus. In fact, the last reading (life ·00290 sec.) merely shows that the mobility

* Vide *Jahr. Rad.* ix. p. 250 (1912).
† *Verh. D. Phys. Ges.* ix. p. 194 (1907).

is not less than 6·72 cm./sec. per volt/cm., as it was impossible to vary the positive potential over a wide enough range to obtain the intercept with the necessary degree of accuracy.

Discussion of Results.

Comparison with Results obtained by other Investigators.

An examination of the tables shows that, for the three gases investigated, the mobility of the positive ions depends on the life of the ion, and further that this dependence is not a continuous function of the life, but, for certain ranges of lives, the mobility remains constant. In each of the three gases investigated three different mobilities (four for hydrogen) have been found, and the change from one type to the next occurs for the three gases at very nearly the same lives. This is shown very clearly in Table IV. Probably the simplest type of ion investigated is that labelled third type, as the mobilities of these were measured in a very short time after their formation. If, however, the life of the ion is between 1/200 and 1/160 sec., the mobility of the ion in each case becomes less. There is a second change in the mobility at about 1/100 sec.

Table IV.

Collected Results for Air, Hydrogen, and Helium.

Gas.		First Type.	Second Type.	Third Type.
		Sec.	Sec.	Sec.
Air	Range of lives ...	·138–·0139	·00947–·00675	·00428–·00229
	Mobility	1·36	1·47	1·65
Hydrogen	Range	·261–·0136	·00913–·00664	00503–·00330
	Mobility	5·30	5·99	6·67
Helium	Range	·1001–·01095	·00795–·00679	·00528–·0029
	Mobility	5·61	6·12	6·72

This seems to suggest that whatever the mechanism is which causes the change from one type to another it is the same in the three gases; in other words, the ions in helium behave exactly similarly to those in the other two gases.

This investigation was undertaken originally to establish, if possible, the presence of doubly-charged helium ions. Millikan * and his co-workers have shown that no gas other than helium when ionized by α-rays showed any indication

* Millikan, Gottschalk, and Kelly, Phys. Rev. xv. p. 157 (1920).

of doubly-charged ions. As in the above experiments no difference can be found between behaviour of helium ions and those in air and hydrogen, one is forced to the conclusion that there is no evidence under the experimental conditions here described of doubly-charged ions in helium. The reason that, while Millikan and Wilkins * found evidence of doubly-charged helium ions, there is no evidence here, can be attributed to the different methods of experiment. In the method of Millikan a charged oil-drop was held suspended in the gas under examination while α-rays passed very close to the drop. The interval of time between the formation of the ion and its arrival on the oil-drop (*i. e.* the life of the ion) was stated by Millikan to be "something like a ten-thousandth of a second." This life is much shorter than the shortest reached in these experiments (1/500 sec.). One is forced to the conclusion that the doubly-charged helium ion is converted very quickly to the singly-charged, in so short a time, in fact, that its increased mobility as a doubly-charged ion cannot be demonstrated experimentally by the method here employed.

In order to compare the results obtained with those of other experimenters, each gas will be dealt with separately.

(a) *Air* †.—Experiments by Erikson ‡ and Wahlin § had previously shown that the mobility of the positive ion in air depended on the life of the ion. In both of their investigations they were unable from the nature of their apparatus to give very accurately the life of the ion. Erikson used a modification of Zeleny's method, and he showed that while the ordinary mobility of the positive ion was 1·36, the mobility was 1·87 when the life of the ion was shorter. The transition of the higher value was estimated by Erikson to occur when the ion had aged for about 1/50 sec. In the method of Wahlin the ions were produced by polonium, and were forced into the chamber in which the mobility was measured by a small auxiliary field. Their mobility was then found by Franck's method, the alternating potential being supplied by a valve-oscillating circuit. His results substantiated those of Erikson in that he found a fast ion of mobility 1·80 and a slower one of mobility 1·35, and that the first changed to the second after a time between 1/75 and 1/120 sec.

Erikson advanced the following explanation to account for

* Wilkins, Phys. Rev. xix. p. 210 (1922).

† All mobilities are expressed in cm./sec. per volt/cm.

‡ Erikson, Phys. Rev. xx. p. 117 (1922); *ibid.* xxiv. p. 502 (1924).

§ Wahlin, Phys. Rev. xx. p. 267 (1922).

his result :—The process of ionization consists in the removal of an electron from a molecule, and this electron at once attaches to a neutral molecule and forms the negative ion. The initial positive and negative ions thus both consist of a molecule, and if their mobility is at once measured it is the same for both. The negative ion remains unchanged, but the positive ion quickly attracts a neutral molecule to it. In consequence of the increased mass of the molecule its mobility decreases to the smaller value. Erikson states that his results suggest "that in any one gas the mobility is approximately proportional to the inverse square root of the mass of the ion."

There are two objections to this rather simple theory. The first is that the mobility of an ion depends on the gas in which it is measured, and the mobility of any positive ion measured in air is the same as that of the air ion (the mobility for the air ion being the lower value 1·36) *. The mobility in air has been measured for a large number of ions in which the mass of the ion has varied considerably—from hydrogen ($M = 2$) to chloroform ($M = 119$). The mass of the ion therefore does not appear to have very great effect on the mobility of the ion. The variation in the diameter of the ion, if we assume that it is composed of a single molecule, would be much less, but there should be some detectable difference between the mobilities if these depended directly on the diameter of the ion †, whereas Tyndall and Grindley find that the mobilities of the hydrogen, carbon dioxide, ether, and chloroform ions are the same to within 1 per cent. when measured in air.

The second objection is that Nolan and Wahlin (later) have obtained evidence of the presence of more than two types of positive air-ions. The experiments above have also shown three types of ions. Nolan has used two different methods ; in one he used an air-blast method and in the other the alternating field method in which ions were driven by an auxiliary field into the main chamber. In the last he took precautions to make the field, which drew back the ions which had not reached the plate connected to the electrometer, slightly greater than that of opposite sign which urged them towards the plate. The difference in the positive and

* *Vide* Blanc, *Journ. de Phys.* vii. p. 825 (1908). Wellisch, Proc. Roy Soc. lxxxii. p. 500 (1909). Tyndall and Grindley, Phil. Mag. xlviii. p. 711 (1924). Erikson, Phys. Rev. xxvi. p. 465 (1925).

† Thus in Kaye and Laby's (1921) Tables, p. 35, the diameter of the hydrogen molecule is $2{\cdot}46 \times 10^{-8}$ cm., while the diameter of the CO_2 molecule is $3{\cdot}81 \times 10^{-8}$ cm.

negative potentials, however, was of the order of two volts, and in view of fig. 2 (above) it is considered that the difference between the positive and negative potentials was inadequate for the purpose. He measured the mobilities of both the negative and positive ions. He has found more groups of mobilities than any other investigator, and, further, that the mobilities of positive and negative ions were the same throughout.

He obtained the values of the mobilities in both experiments by observed discontinuities in his ionization current-potential curves. Some of these discontinuities were very small, and the interpretation of them has been considerably criticized. Blackwood * duplicated the apparatus used by Nolan in the air-current method, but failed to obtain a repetition of Nolan's curve. Loeb † has criticized the interpretation that Nolan places on his curves, and has pointed out that the electrometer readings would have to be extremely accurate before some of the discontinuities of Nolan could be regarded as definite evidence of different groups of ions.

In Wahlin's later determinations he again used the alternating field method, and from discontinuities in the ionization current-potential curve concluded that there were at least six types of positive air-ions. It must be pointed out that Wahlin took no precautions to make his negative potentials greater than his positive, as has been found necessary in this work.

The results of Nolan, Erikson, Wahlin, and the author are set out in Table V. (In his paper in the 'Physical Review,' Nolan ‡ mentions the presence of more ions than are given in this table—the values given here are those published in the 'Proceedings of the Royal Irish Academy.')

It would appear that the three types of ions found by the author correspond to three found by Wahlin and three by Nolan. The method used by the author has, however, the following advantages :—

1. The mobility values are found from straight-line intercepts on the potential axis and not from discontinuities in the curves.

2. The ions investigated are not produced in a subsidiary chamber, but directly in the chamber in which they are at once measured.

3. The ions are not entering the measuring-chamber continuously, but only for limited times (due to the sectored wheel).

* Blackwood, Phys. Rev. xx. p. 499 (1922).
† Loeb, Journal Franklin Institute, cci. p. 537 (1923).
‡ Nolan, Phys. Rev. xxv. p. 101 (1925).

4. Adequate precautions are taken to remove those positive ions which are approaching the top plate but which fail to reach it.

TABLE V.

Mobility of Positive Air Ions.

Nolan.	Erikson.	Wahlin.	Rogers.
+ and −			
12·4			
6·6			
5·1			
4·31			
3·02			
2·04			
1·76	1·89	1·89	1·65
1·53	...	1·57	1·47
1·38	1·35	1·35	1·36
		1·20	
		1·10	
		·970	

No evidence has been found of any faster ions mentioned by Nolan, *i. e.* those of mobility (2) and greater, and if such exist they must have a life of less than 1/500 sec. Again, the curves show no evidence of any ions slower than 1·36, since there are no marked discontinuities in the curves when the ions of mobility 1·36 are being measured.

(b) *Hydrogen.*—The mobility of the positive ions in hydrogen has been previously investigated by Chattock *, by Franck and Pohl †, by Zeleny ‡, and Nolan §.

Chattock used an ingenious method in which he employed the point discharge in gases. His value of the mobility is 5·4. Although this value corresponds to that found below for ions of lives between ·261 and ·0136 sec., the life of the ions in Chattock's experiments would be very much shorter.

Franck and Pohl used a modification of the original Rutherford method in which the lower plate of their ionization chamber was connected to sinusoidal alternating potential of frequency about 55. The ions of the sign required

* Chattock, Phil. Mag. xlvii. p. 401 (1899); *ibid.* i. p. 79 (1901).
Franck and Pohl, *Verh. Deut. Phys. Ges.* ix. pp. 67, 194 (1907).
‡ Zeleny, Phil. Trans. (A), cxcv. pp. 183, 193 (1900).
§ Nolan, Proc. Roy. Irish Acad. xxxvi. p. 74 (1923).

were introduced into the main field by a small auxiliary field. The life of ions was here approximately ·009 sec. The value of the mobility obtained by them, 6·02, agrees very well with that found here, 5·99, for ions of the same life.

The method of Zeleny consisted in deflecting the charged ions by an electric field at right angles to the direction in which they were moving in a current of gas He measured the value of the mobility for a number of different lives and then extrapolated for zero life. His value was 6·70, which is in good agreement with the value found here, 6·67 for the lives of ions between ·00503 to ·00330 sec.

The method of Nolan was the alternating field method, exactly the same as used by him for air. The values that he found were 5·23, $\left.\begin{matrix}5\cdot68\\6\cdot15\end{matrix}\right\}$* (mean 5·83), 6·77, 7·93, 9·63. The first three agree fairly well with those found by the author of 5·30, 5·99, 6·67, but no evidence has been found of the latter types, and if they exist they must be of very short life.

(c) *Helium.*—The only previous determination of the mobility of the ions was by Franck and Pohl †, and by Franck and Gehlhoff ‡. In these experiments they used the same method as for the hydrogen ions. The value that they obtained for the mobility of the positive ions was 5·09 cm/sec., a value which is considerably lower than their value for hydrogen. On the other hand, the values obtained in the above experiments for hydrogen were always less than those for helium.

There is a possible explanation of their lower value. The distance between the plates of their ionization chamber was about 3·6 cm. (*vide* their diagram on page 72 of vol. ix. of the *Verh. d. D. Phys. Ges.*). On page 195 of the same journal the effective values of the potentials used in helium were given as about 320 volts, and 275 volts on page 196. The maximum values of the potentials corresponding to these would be 450 and 390 volts, and the maximum potential gradients 125 and 108 volt/cm. resp.

Now, it has been mentioned above that when the pressure of helium was 90 mm. the gas "conducted" under a negative potential gradient of 30 volt/cm. It was thus possible in Franck's experiments that the helium conducted at the highest values of the negative potential, and hence the ionization current due to the positive ions alone would appear to cease for higher values of the positive potential than they actually did. Thus lower values of the mobility

* The bracketing is that of Nolan. † *Loc. cit.* ‡ *Loc. cit*

would be recorded than were correct. (*Note.*—Although the sparking potential of helium under negative gradients has not been exhaustively examined, it does not appear to be directly proportional to the pressure, for while the negative potential could not be raised above 240 volts when the pressure was 90 mm., a negative potential of 180 volts could be used when the pressure was 30·5 mm.)

Conclusion.

There is still no theoretical equation which will give satisfactorily the mobility of ions *, but these experiments indicate that, whatever the ion is initially, after a very short time it has developed into some type of cluster. Loeb ascribes the ageing effects found by Erikson to small changes in the diameter of the ion. The ageing effects found here have probably the same explanation. The increase in the diameter can only be ascribed to neutral molecules being added to the ion as it ages. There is one property of ions which is however not explained by the increase in diameter, and this is, as illustrated by Tables I., II., and III., that the mobility does not appear to change gradually but in definite steps. If the changes in mobility were due to the gradual addition of neutral molecules, one would expect a gradual change in mobility with the life of the ion. If the ion starts as a single molecule, it will have a definite mobility, and each addition of a neutral molecule will cause a decrease in the mobility. If a series of measurements were taken on the mobility of the ion between the time of attachment (t') of one neutral molecule, the time of attachment (t'') of the next and at longer times, it is obvious that after t'' the measured mobility should gradually decrease; for, as the time exceeded t'', an increasing portion of the life of the ion would be spent in the latter state, *i. e.* that of the less mobility. There is, however, no such gradual change of mobility found either in these experiments or in those of Erikson, Wahlin, or Nolan.

This work was commenced while the writer held an 1851 Exhibition at Cavendish Laboratory, Cambridge. My thanks are due to Sir Ernest Rutherford, who suggested this method of investigation, and for his gift of helium, and also to the Australian Oxygen Company, Melbourne, for liquid air.

* *Vide* Loeb, Journ. Frank. Inst. cci. p. 279 (1926).

XCI. *The Distribution of Temperature in Alternating Current Conductors* *. *By* M. J. O. Strutt, *D.techn.Sc.*†

Abstract.

The temperature in alternating current conductors of circular cross-section and infinite length is derived as a function of the distance from the centre for the case where the electric current is flowing along the axis, and for the case where the electric current is flowing in circles round the axis (inductive heating). In both cases very small and very high frequencies are considered. It is shown in the first case that for high frequency the highest temperature (in the centre) tends to one-half of the temperature when the same effective direct current is flowing through the conductor, the temperature of the surrounding medium being supposed to be zero. Herefrom it is deduced that by raising the frequency the temperature inside the conductor is decreased under the above circumstances. In the second case it is shown that, the temperature of the surrounding medium and the magnetic field outside the conductor being constant, the temperature inside the conductor increases everywhere with frequency. Some formulas are derived in four notes. A list of symbols is added.

I. *Introduction.*

THE purpose of the present paper is to investigate the temperature in the interior of alternating current conductors of circular cross-section and of infinite length.

Two cases will be considered separately. In the first place the electric current will be supposed to flow in the direction of the axis of the conductor. This problem relates to electric cables, lines, etc. In the second place the electric current will be assumed to flow in circles round the axis of the conductor. This problem occurs in the treatment of inductive heating.

* Sections I. and II. of this paper form chapters of a thesis for the degree of Doctor in the Technical University of Delft, 1927.

† Communicated by the Author.

In both cases the temperature T is determined by the differential equation :

$$\Delta T = \frac{c}{K} \cdot \dot{T} - \frac{m_0}{K} \cdot S^2, \quad . \quad . \quad . \quad . \quad . \quad (1)$$

where

c = spec. heat per unity of volume,
K = heat conductivity,
$m_0 = \alpha \cdot \rho$,
α = constant, determined by the choice of units (with practical units equal to 0·239),
ρ = spec. electric resistance,
S = electric current density ;

and the boundary condition :

$$h \cdot (T - T_0) = -\frac{dT}{dn} \quad . \quad . \quad . \quad . \quad . \quad (2)$$

on the whole surface, where h is a constant depending on the surface of the conductor, T the temperature of the conductor surface, and T_0 the temperature of the surrounding medium at the surface of the conductor.

Throughout this paper c, K, ρ will be treated as constants.

If the axis of the conductor coincides with the z-axis, and assuming symmetrical conditions round this axis, equations (1) and (2) assume the form :

$$\frac{\partial^2 T}{\partial r^2} + \frac{1}{r} \cdot \frac{\partial T}{\partial r} = \frac{c}{K} \cdot \frac{\partial T}{\partial t} - \frac{m_0}{K} \cdot S^2, \quad . \quad . \quad . \quad (1')$$

$$h(T - T_0) = -\frac{dT}{dr}. \quad . \quad . \quad . \quad . \quad . \quad . \quad (2')$$

As the electric current density is assumed to be purely periodic with angular frequency ω, it is seen from equation (1′) that T will be a periodic function of time with frequency 2ω. Now T can be split up into a part independent of time, and a part varying with period 2ω :

$$T(r, t) = G(r) + L(r, t) \quad . \quad . \quad . \quad . \quad . \quad (3)$$

It is assumed that L is truly periodic, so that the stationary state has been arrived at.

As the conduction of heat may be compared with a process of diffusion, through which the variations of the temperature are everywhere diminished, we may expect that, already for moderate values of ω, the part L of temperature will be small compared with G. Therefore, in this paper, G only will be considered.

II. *Electric Current Flowing along the Axis.*

In the first place, S is assumed to flow in the direction of z. In this case S is given by the expression :

$$S = (\text{real part of})\ C \,.\, I_0(m \,.\, r \,.\, \sqrt{-i}) \,.\, e^{i\omega t}, \quad . \quad (4)$$

where

$$V^2 m^2 \,.\, \rho = 4 \,.\, \pi \,.\, \mu \,.\, \omega,$$

μ = permeability,

V = velocity of light,

Gauss Units having been adopted. The constant C is determined by the total current amplitude I through the conductor :

$$|\,C\,| = \frac{I \,.\, m_1}{\sqrt{2} \,.\, \pi \,.\, b \,.\, [(\text{ber}'\, mb)^2 + (\text{bei}'\, mb)^2]}, \quad . \quad (5)$$

where

$$m = m_1 \,.\, \sqrt{2},$$

b = radius of conductor.

From equations (1′) and (4) we obtain for G :

$$\frac{1}{r} \cdot \frac{d}{dr} \cdot \left(r \cdot \frac{dG}{dr} \right) = - \frac{m_0}{K} \cdot \frac{C^2}{2} [\text{ber}^2\, mr + \text{bei}^2\, mr]. \quad (6)$$

So G may be found by double integration. The first integration gives (see Note 1) :

$$\frac{dG}{dr} = \frac{\gamma}{m} \cdot [\text{ber}\, mr \,.\, \text{bei}'\, mr + \text{bei}\, mr \,.\, \text{ber}'\, mr] + A, \quad (7)$$

where

$$\gamma = - \frac{m_0}{K} \frac{C^2}{2},$$

and A is a constant of integration. As the flow of heat through the centre of the wire must be zero,

$$\left(\frac{dG}{dr} \right)_{r=0} = A = 0.$$

We now proceed to consider equation (7) for two cases :

(a) $m \,.\, b << 1$ (small frequency),

(b) $m \,.\, b >> 1$ (high frequency).

In case (*a*), equation (7) yields

$$\frac{dG}{dr} = \frac{\gamma}{m}\cdot\left(\frac{mr}{2} + \frac{(mr)^5}{2^3 \cdot 4^2}\right), \quad . \quad . \quad . \quad . \quad (7\,a)$$

and, by integrating,

$$G = \frac{\gamma}{4} r^2 \left(1 + \frac{(mr)^4}{2^4 \cdot 3 \cdot 4}\right) + B, \quad . \quad . \quad . \quad (8\,a)$$

where B is a constant of integration.

Now, supposing the temperature T_0 (equation (2)) of the medium surrounding the conductor to be zero, and the constant h (equation (2)) to be large, we get from equation (8 *a*)

$$G = \frac{m_0 \cdot I^2}{8 \cdot K \cdot \pi^2 \cdot b^4}\left[b^2\left(1 + \frac{(mb)^4}{2^4 \cdot 3 \cdot 4}\right) - r^2\left(1 + \frac{(mr)^4}{2^4 \cdot 3 \cdot 4}\right)\right], \quad . \quad . \quad . \quad (9\,a)$$

where the value of C has been inserted from equation (5). It is to be noted that, in equations (7 *a*), (8 *a*), and (9 *a*), powers of mb, and therefore of mr, higher than the fourth have been neglected.

In the case of direct current we may easily solve equation (1), and find

$$T = \frac{m_0}{K} \cdot \frac{I_1^2}{4(\pi b^2)^2}(b^2 - r^2). \quad . \quad . \quad . \quad . \quad (10)$$

Comparing equations (10) and (9 *a*), and bearing in mind that I is an amplitude which corresponds to an *effective* current $I/\sqrt{2}$, we easily verify that these equations coincide for the case that $m = 0$.

Considering case (b) :

$$mb \gg 1,$$

we may write

$$\left.\begin{aligned}
\text{ber } mr &= \frac{e^{m_1 r}}{\sqrt{2 \cdot \pi \cdot m \cdot r}} \cdot \cos\left(m_1 r - \frac{\pi}{8}\right), \\
\text{bei } mr &= \frac{e^{m_1 r}}{\sqrt{2 \cdot \pi \cdot m \cdot r}} \cdot \sin\left(m_1 r - \frac{\pi}{8}\right), \\
\text{ber}' mr &= \frac{e^{m_1 r}}{\sqrt{2 \cdot \pi \cdot m \cdot r}} \cdot \cos\left(m_1 r + \frac{\pi}{8}\right), \\
\text{bei}' mr &= \frac{e^{m_1 r}}{\sqrt{2 \cdot \pi \cdot m \cdot r}} \cdot \sin\left(m_1 r + \frac{\pi}{8}\right),
\end{aligned}\right\} \quad . \quad (11)$$

where again

$$m_1 = \frac{m}{\sqrt{2}}.$$

Inserting these values into equation (7), we get

$$\frac{dG}{dr} = \frac{\gamma}{4 \cdot \pi \cdot m \cdot m_1} \cdot \frac{e^{2m_1 r}}{r}, \quad . \quad . \quad . \quad (7\,b)$$

from which we obtain by integration (see Note 2)

$$G = -\frac{m_0}{K} \cdot \frac{C^2}{2} \cdot \frac{1}{4 \cdot \pi \cdot m_1^2 \cdot \sqrt{2}} \mathrm{Ei}\,(2m_1 r) + B, \quad . \quad (8\,b)$$

where $\mathrm{Ei}(2m_1 r)$ is the integral-logarithm of $2m_1 r$, and B a constant of integration.

Inserting the values of equation (11), we obtain from equation (5)

$$|C| = \frac{I \cdot m_1 \cdot \sqrt{m}}{\sqrt{\pi \cdot b \cdot e^{m_1 \cdot b}}}. \quad . \quad . \quad . \quad . \quad (5\,b)$$

Now again assuming the temperature T_0 (equation (2)) of the surrounding medium to be zero, and combining equations (5 *b*) and (8 *b*), we obtain

$$G = \frac{m_0}{K} \cdot \frac{I^2 \cdot (2m_1 b)}{16 \cdot \pi^2 \cdot b^2 \cdot e^{2m_1 b}} [\mathrm{Ei}\,(2m_1 b) - \mathrm{Ei}\,(2m_1 r)]. \quad (9\,b)$$

It should be noted that equation (9 *b*) is only valid for values of r, such that

$$mr >> 1.$$

In order to find the temperature for $r = 0$, we may proceed as follows. We may make r smaller and smaller, at the same time increasing m without limit:

$$r \rightarrow 0,$$

$$m \rightarrow \infty,$$

such that, during this whole process, mr retains a value large compared with unity. Carrying this out and replacing the function $\mathrm{Ei}\,(2m_1 r)$ by its values for large arguments (see Note 3), we obtain

$$G_{\substack{r \rightarrow 0 \\ m_1 \rightarrow \infty}} = \frac{m_0}{K} \cdot \frac{I^2}{16 \cdot \pi^2 \cdot b^2}. \quad . \quad . \quad . \quad . \quad (12)$$

Comparing this value with the one obtained in the case of direct current (equation (10)), we find the interesting result, that *the highest alternating current temperature of a conductor, the frequency tending towards infinity, is equal to one-half of the highest direct current temperature of the same conductor.* Here it is supposed that the *effective* currents are the same, and that the temperature of the surrounding medium is zero.

If the latter assumption is not fulfilled, we may apply our result to the differences of the temperatures in the conductor and that of the surrounding medium. Moreover, we have assumed the constant h from equation (2) to be large, which arises, *e. g.*, in the case where the conductor is surrounded by a liquid. From this result we deduce that, with constant total current and increasing frequency, the temperature decreases everywhere inside the conductor, the temperature at the boundary being kept constant.

III. *Electric Current flowing in Circles round the Axis.*

This case occurs in the theory of inductive heating, the magnetic force having the direction of z and being given in the conductor (charge) by

$$H = (\text{real part of})\ H_0 . I_0(mr\sqrt{-i}) . e^{i\omega t}, \quad . \quad (13)$$

where H_0 represents a constant determined by the uniformly distributed magnetic force outside the conductor:

$$H_0 = \frac{H_1}{I_0(mb\sqrt{-i})}, \quad . \quad . \quad . \quad . \quad . \quad (14)$$

b again being the radius of the conductor. From equation (13) the current density S is easily found to be

$$S = (\text{real part of})\ \sigma . \frac{dH}{dr}$$

$$= (\text{real part of})\ \frac{V}{4\pi} H_0 m . \sqrt{-i}\, I_0'(mr\sqrt{-i}) e^{i\omega t}, \quad (15)$$

where $\sigma = \frac{V}{4\pi}$, adopting again Gauss Units and denoting the differentiation with respect to mr by an accent, as in the case treated before. Inserting the value (15) into equation (1′), we find for G the equation

$$\frac{1}{r} . \frac{d}{dr}\left(r . \frac{dG}{dr}\right) = -\frac{m_0}{K} . \sigma^2 \frac{H_0^2}{2} m^2 . [(\text{ber}'\, mr)^2 + (\text{bei}'\, mr)^2], \quad . \quad . \quad . \quad (16)$$

so that G may be found by double integration. The first integration gives (see Note 4)

$$\frac{dG}{dr} = \sigma^2 . \frac{\gamma}{2} . m . (\text{ber}\, mr . \text{ber}'\, mr + \text{bei}\, mr . \text{bei}'\, mr), \quad (17)$$

γ denoting $-\frac{m_0}{K} . H_0^2$, the constant of integration being zero for the same reason as in equation (7).

By integrating equation (17) once again, we get

$$G = \frac{\gamma}{4}\sigma^2 (\mathrm{ber}^2 mr + \mathrm{bei}^2 rm) + B_1, \quad . \quad . \quad (18)$$

B_1 being a constant of integration, determined by the conditions at the surface of the conductor. Supposing, again, the temperature of the medium surrounding the conductor to be zero, and the constant h of equation (2) large, equation (18) yields

$$G = \frac{m_0}{K}\sigma^2 \frac{H_0^2}{4} . (\mathrm{ber}^2 mb + \mathrm{bei}^2 mb - \mathrm{ber}^2 mr - \mathrm{bei}^2 mr). \quad (19)$$

From equation (14) we get

$$|H_0| = \frac{H_1}{[\mathrm{ber}^2 mb + \mathrm{bei}^2 mb]^{\frac{1}{2}}},$$

and inserting this value into equation (19), we find

$$G = \frac{m_0}{K} . \frac{H_1^2}{4} . \sigma^2 . \left[1 - \frac{\mathrm{ber}^2 mr + \mathrm{bei}^2 mr}{\mathrm{ber}^2 mb + \mathrm{bei}^2 mb}\right]. \quad . \quad (20)$$

In the case that

$$mb \ll 1 \quad \text{(small frequency)},$$

we easily obtain from equation (20)

$$G = \frac{m_0}{K} . \frac{H_1^2}{2^3 . 4^2} . \sigma^2 . \left[\frac{(mb)^4 - (mr)^4}{1 + \frac{(mb)^4}{32}}\right], \quad . \quad (20\,a)$$

powers of mb and of mr higher than the fourth being neglected.

As is to be expected, G vanishes with m (*i. e.* becomes equal to the temperature of the surrounding medium), a stationary magnetic field outside the conductor inducing no currents in it.

If we increase the frequency (and hence m), keeping H_1 constant, we see, from equation (20), that G increases in every point of the cross-section.

Hence from equation (20) we cannot explain the well-known phenomenon that, *e. g.* a disk placed in a longitudinal alternating magnetic field assumes a higher temperature at its circumference than at its centre. This phenomenon seems to depend essentially on the finite (and in fact rather small) length of the cylinder.

If we do not suppose the constant h from equation (2) to

be very large, we find for the temperature (that of the surrounding medium being zero) from equation (18)

$$G = \frac{m_0}{K} \cdot \sigma^2 \cdot \frac{H_1^2}{2} \left[\frac{1}{2} + \frac{m}{h} \frac{(\mathrm{ber}\, mb \cdot \mathrm{ber}'\, mb + \mathrm{bei}\, mb \cdot \mathrm{bei}'\, mb)}{\mathrm{ber}^2 mb + \mathrm{bei}^2 mb} \right.$$
$$\left. - \frac{1}{2} \cdot \frac{\mathrm{ber}^2 mr + \mathrm{bei}^2 mr}{\mathrm{ber}^2 mb + \mathrm{bei}^2 mb} \right]. \quad (21)$$

If we increase the frequency without limit, at the same time keeping the energy dissipated in the conductor constant, the induced currents and hence the temperature inside the conductor tend to zero, as is easily seen by expressing H_1 in terms of the dissipated energy *.

IV. *Notes.*

Note 1.—The integral wanted is

$$\int^r r \cdot (\mathrm{ber}^2 mr + \mathrm{bei}^2 mr) \cdot dr.$$

By the aid of the formulas :

$$\mathrm{ber}\, mr = \tfrac{1}{2} [(I_0(mr \sqrt{-i}) + I_0(mr \sqrt{i})],$$

$$\mathrm{bei}\, mr = \frac{1}{2i} [I_0(mr \sqrt{-i}) - I_0(mr \sqrt{i})],$$

$$\mathrm{ber}^2 mr + \mathrm{bei}^2 mr = I_0(mr \sqrt{-i}) \cdot I_0(mr \sqrt{i}),$$

we may write for this integral

$$\int r \cdot I_0(mr \sqrt{-i}) \cdot I_0(mr \sqrt{i})\, dr.$$

Integrating by parts and denoting the differentiation with respect to mr by an accent, we get for this integral

$$\frac{r}{2im} [I_0'(mr \sqrt{-i}) \cdot I_0(mr \sqrt{i}) - I_0(mr \sqrt{-i}) \cdot I_0'(mr \sqrt{i})],$$

and by converting these functions into *ber* and *bei*, we obtain for the integral

$$\frac{r}{m} [\mathrm{ber}\, mr \cdot \mathrm{bei}'\, mr - \mathrm{bei}\, mr \cdot \mathrm{ber}'\, mr].$$

I have not succeeded in integrating equation (7) of section II. again.

* *E. g.* Burch & Davis, Phil. Mag. (7) i. p. 768 (1926).

I finally remark that the previous integration could be avoided by regarding the physical meaning of the integral, *i. e.* the energy dissipated in a conductor of radius r times a constant, if we insert zero as lower limit of integration. The expression of this energy is well known *, and thus may be used to check the above result. As the expression just mentioned may be calculated by the aid of Poynting's theorem †, the second method of evaluating the integral is, in fact, equivalent to the conversion of a surface-integral to an integral taken along a circumference, and so forms an application of Gauss's theorem.

Note 2.—The integral wanted is

$$\int^{r} \frac{e^{2m_1 r}}{r},$$

for which we find, by expansion,

$$\ln(2m_1 r) + 2m_1 r + \frac{(2m_1 r)^2}{2.2!} + \frac{(2m_1 r)^3}{3.3!} + \ldots.$$

Now, by definition ‡,

$$\begin{aligned} \mathrm{Ei}\,(2m_1 r) &= \int_{\infty}^{-2m_1 r} \frac{e^{-u}}{u}.du \\ &= \beta + \ln(2m_1 r) + 2m_1 r + \frac{(2m_1 2)^2}{2.2!} + \ldots, \end{aligned}$$

where β denotes the constant of Euler-Mascheroni :

$$\beta = 0{\cdot}57721\ldots.$$

By comparing the two expressions we easily derive equation (8) of the text.

Note 3.—Firstly, we notice that, for large values of $2m_1 b$, the expression Ei $(2m_1 r)$ in equation $(9\,b)$ becomes negligible compared with Ei $(2m_1 b)$. Now, for large values of $2m_1 b$ we may write §

$$\mathrm{Ei}\,(2m_1 b) \sim \frac{e^{2m_1 b}}{2m_1 b},$$

and with this expression we easily obtain equation (12).

* *E. g.* Jahnke & Emde, 'Funktiontafeln' p. 144.
† *E. g.* J. J. Thomson, 'Recent Researches,' p. 320.
‡ *E. g.* Jahnke-Emde, *l. c.* p. 19.
§ *E. g.* Jahnke-Emde, *l. c.* p. 9.

Note 4.—The integral wanted is

$$\int^{r} r\,[(\mathrm{ber}'\,mr)^2+(\mathrm{bei}'\,mr)^2]\,dr.$$

By the aid of the formulas given in Note 1, we may write

$$\int^{r} r.\mathrm{I}_1(mr\sqrt{-i}).\mathrm{I}_1(mr\sqrt{\bar{i}})\,dr,$$

and, integrating by parts, find

$$\frac{r}{2m}.[\mathrm{I}_0'(mr\sqrt{-i}).\mathrm{I}_0(mr\sqrt{\bar{i}})+\mathrm{I}_0(mr\sqrt{-i}).\mathrm{I}_0'(mr\sqrt{\bar{i}})],$$

from which equation (17) of the text is easily derived by inserting *ber* and *bei* functions again.

As to the evaluation of this integral, we may make the same remark as in Note 1, the integral with lower limit zero denoting the energy dissipated in a conductor of radius r times a constant. The known expression for this energy * may be used to check the result obtained above.

V. *List of Symbols.*

b radius of conductor.
C amplitude of current density (equation (4)).
c specific heat capacity per unit volume.
Ei integral logarithm (equation (8 *b*) and Note 2).
G temperature in the conductor independent of time.
H magnetic force (equation (13)).
H_0 amplitude of magnetic force (equation (13)).
H_1 magnetic force outside conductor (equation (14)).
h constant depending on the nature of the surface of the conductor and of the surrounding medium (equation (2)).
I amplitude of total alternating current (equation (5)).
I_1 total direct current (equation (10)).
K specific heat conductivity.
L temperature inside conductor varying with time.
m alternating current constant (equation (4)).
$m_\varrho = \alpha.\rho.$
$m_1 = m/\sqrt{2}.$
n normal direction at conductor surface.
r distance from centre of conductor.

* Burch and Davis, *l. c.*

S amplitude of alternating current density (equation (1)).

T temperature inside conductor.

T_0 temperature of surrounding medium as the surface of the conductor.

V velocity of light.

α constant depending on choice of units (equation 1)).

β Euler's constant (Note 2).

$\gamma = -\frac{m_0}{K} \cdot \frac{C^2}{2}$ (in section II.).

$\gamma = -\frac{m_0}{K} \cdot H_0^2$ (in section III.).

μ permeability.

ω angular frequency of alternating current.

ρ specific electric resistance.

$\sigma = \frac{V}{4\pi}$.

Physical Laboratory of
Philips's Glowlampsworks, Ltd.,
Eindhoven, Dec. 1927.

XCII. *The Problem of a Hidden Polarized Sphere.* *By* Prof. A. Petrowsky, *Hon. Member of Rori* (*The Russian Society of Radio Engineers*) *.

Contents.

§ 1. Zero curves of longitudinal electroprofiles.
§ 2. Maxima curves of longitudinal electroprofiles.
§ 3. Zero curves of transversal electroprofiles.
§ 4. Maxima curves of transversal electroprofiles.
§ 5. Zero curves of oblique electroprofiles.
§ 6. Maxima curves of oblique electroprofiles.

Part II.

Properties of Zero Curves and Maxima Curves.

IN Part I. † of this paper a general solution of differential equations was found, expressing a distribution of electric force, and general characteristics of electroprofiles were given, obtained by observations on the plane of division.

* Communicated by the Author.
† See Phil. Mag., Feb. 1928, p. 334.

In the present part we shall examine the following question :—

Let us suppose that the observer, wishing to determine the exact place of the hidden sphere, has chosen a certain arbitrary direction, has drawn in that direction a row of parallel equidistant lines, and has taken electroprofiles along each of them. As we already know, he will obtain curves, each of them having two (or one) zero points and three (or two) maxima. Marking on the plan of the section under investigation the places of the zero points and maxima, and joining all the corresponding points with smooth curves, he will get five (sometimes three) geometrical loci. We shall now consider the particularities of these loci.

§ 1. Let us begin with Case A, when the electroprofiles are taken parallel to the plane of polarization of the hidden sphere.

From formula (32), Part I., it follows that the zero points are defined by the equation :

$$3u\cos\alpha-(1+v^2-2u^2)\sin\alpha=0 \quad . \quad . \quad . \quad (1)$$

or

$$u^2-\frac{1}{2}v^2+\frac{3}{2}\cot\alpha\,.\,u-\frac{1}{2}=0. \quad . \quad . \quad . \quad (1')$$

This equation means the following :—

(*a*) In passing from one electroprofile to another (parallel to the plane of polarization) the zero points shift along the branches A′A′ and A″A″ of the hyperbola * (fig. 1).

(*b*) The centre C of this hyperbola lies in the plane of polarization behind the place of position of the hidden sphere, at a distance from the projection of its centre equal to

$$\left.\begin{aligned} x_0&=\frac{3}{4}\cot\alpha\,.\,h,\\ y_0&=0. \end{aligned}\right\} \quad . \quad . \quad . \quad . \quad . \quad . \quad (2)$$

(*c*) The real semi-axis of the hyperbola lies in the plane of polarization and has the length :

$$a\sqrt{\frac{1}{2}+\frac{9}{16}\cot^2\alpha\,.\,h}, \quad . \quad . \quad . \quad . \quad . \quad (3)$$

* In fact the invariant of the equation is equal to $+2>0$, which corresponds to the hyperbola.

and the imaginary one is directed perpendicular to this plane and has the length * :

$$b = \sqrt{2}\,.\,a. \quad . \quad . \quad . \quad . \quad . \quad . \quad . \quad (4)$$

Fig. 1.—Curves presenting geometrical locus of zero points (O-curves) of an electroprofile taken parallel to the plane of polarization (longitudinal electroprofile).

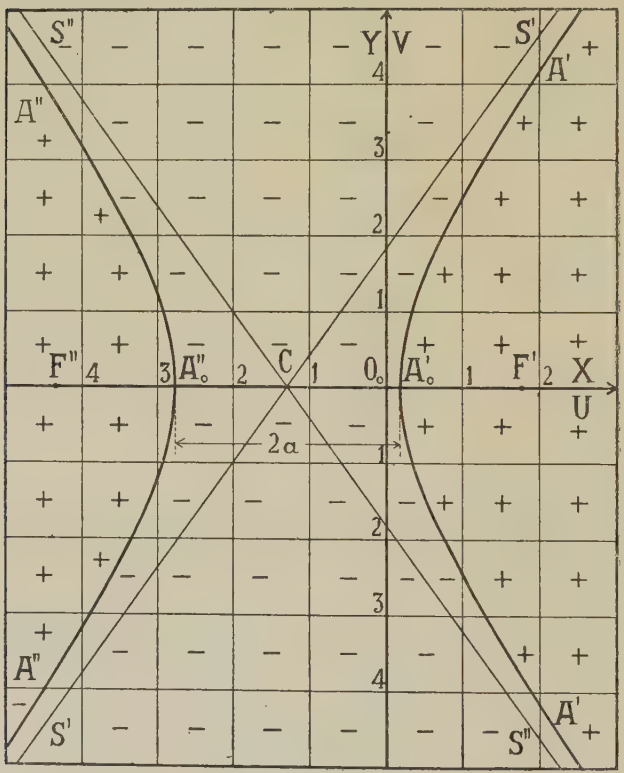

* As the equation contains neither the product uv nor the first power v, the hyperbola is symmetrical with respect to line U; the direction of this line coincides with the direction of the real axis of the hyperbola; transforming the equation of the curve to the centre and to the axis, we obtain

$$u^2 - \frac{1}{2}v^2 = \frac{1}{2} + \frac{9}{16}\cot^2 a \quad . \quad . \quad . \quad . \quad . \quad . \quad . \quad (5)$$

or

$$\frac{u^2}{\frac{1}{2} + \frac{9}{16}\cot^2 a} - \frac{v^2}{1 + \frac{9}{8}\cot^2 a} = 1, \quad . \quad . \quad . \quad . \quad . \quad (5')$$

from which follow the expressions (3) and (4).

(*d*) The foci of the hyperbola are at distances from its centre equal to

$$c = \sqrt{3}\,.\,a. \quad . \quad . \quad . \quad . \quad . \quad . \quad (6)$$

(*e*) The asymptotes S′S′ and S″S″ of the hyperbola are defined by the equations:

$$y = \sqrt{2}\,x, \quad . \quad . \quad . \quad . \quad . \quad . \quad . \quad (7')$$

$$y = -\sqrt{2}\,x; \quad . \quad . \quad . \quad . \quad . \quad . \quad (7'')$$

therefore they are inclined to the axis of abscissæ at angles equal to 54° 45′.

A group of O-curves corresponding to $\alpha = 15°$, 45°, and 90°.

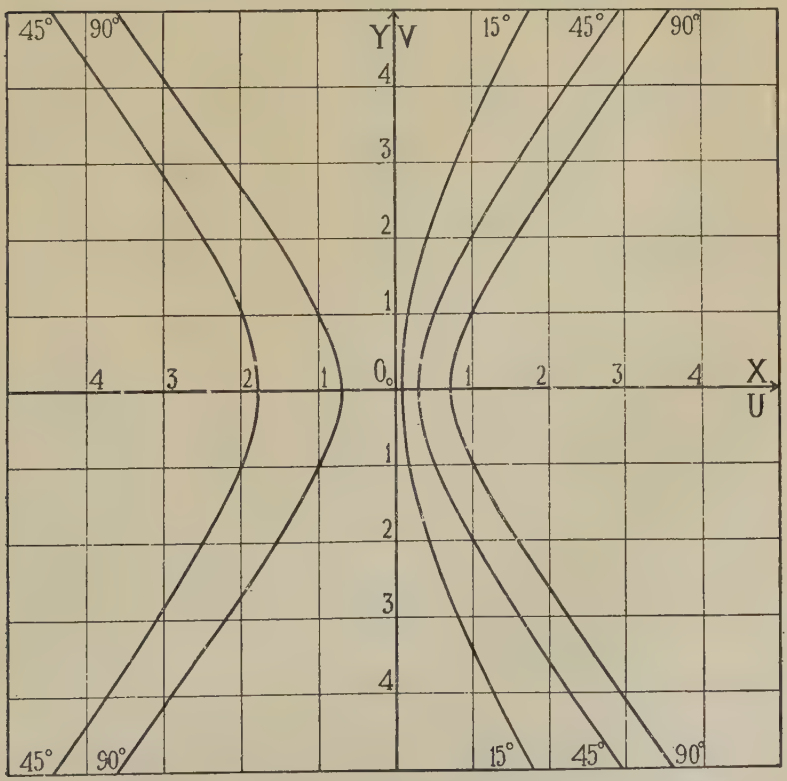

At different angles α of inclination of the axis of polarization to the vertical the position of the above-mentioned hyperbola varies ; and the differences are more marked for the front than for the rear branches, as is seen from fig. 2, on which are given hyperbolas obtained for $\alpha = 15°$, 45°,

and 90°. [The rear branch of the hyperbola, corresponding to $\alpha = 15°$, has no place already within the boundaries of the design ; when $\alpha = 0°$ the hyperbola disappears, being reduced to one general point—the origin of the coordinates O_0.]

§ 2. Differentiating the formula (32), Part I., and equating the differential coefficient to zero, we obtain an equation defining the maxima of curve F_x :

$$1 + v^2 + 3\tan\alpha \,.\, (1+v^2)u - 4u^2 - 2\tan\alpha \,.\, u^3 = 0 \quad . \quad (8)$$

or
$$1 + v^2 = \frac{2u^2(2 + \tan\alpha \,.\, u)}{1 + 3\tan\alpha \,.\, u} \quad . \quad . \quad . \quad . \quad (8')$$

This equation represents a curve of the 3rd order placed symmetrically with respect to the plane of polarization and consisting of three branches * (fig. 3). The first branch $M'M'$ is the geometrical locus of the front positive maximum, and lies between a certain value $u = u'$ and $u = +\infty$; the second branch is the geometrical locus of the middle negative maximum, and lies between $u = -\frac{\cot\alpha}{3}$ and a certain negative value $u = u'''$; it has for asymptote the straight line $T'''T'''$, perpendicular to the plane of polarization, expressed by the equation :

$$u = -\frac{\cot\alpha}{3}; \quad . \quad . \quad . \quad . \quad . \quad . \quad (10)$$

* The differential coefficient is

$$\frac{d(1+v^2)}{du} = \frac{2u}{(1+3\tan\alpha \,.\, u)^2}(4 + 9\tan\alpha \,.\, u + 6\tan^2\alpha \,.\, u^2) \,. \quad . \quad (9)$$

It remains positive with positive values of u, passes through zero when $u = 0$, and becomes negative with negative u :—

(1) By $u = -\infty$ we have $1 + v^2 = +\infty$: therefore $v = \pm\infty$; by changing u from $-\infty$ to a certain value $u''' < -2\cot\alpha$, the value $1 + v^2$ diminishes to 1 : therefore v changes till 0 ; these boundaries limit the rear branch of the M-curve.

(2) Further, $1 + v^2$ becomes less than 1 : consequently v becomes an imaginary quantity till $u = -\frac{\cot\alpha}{3}$.

(3) When $u = -\frac{\cot\alpha}{3}$ we have again $1 + v^2 = +\infty$: therefore $v = \pm\infty$. In further change of u from $-\frac{\cot\alpha}{3}$ to a certain value $u'' < 0$ the value $1 + v^2$ diminishes to 1 : therefore v again reaches 0 ; these boundaries limit the middle branch of the M-curve.

(4) Further, $1 + v^2$ becomes less than 1 : therefore v once more becomes an imaginary quantity till u, passing through zero, takes a certain positive value u'.

(5) By $u = u' > 0$ we have $1 + v^2 = 1$; by further change of u the value $1 + v^2$ increases, passing into infinity together with u : this region is occupied by the front branch of the M-curve.

the third branch $M'''M'''$ is a geometrical locus of the positive rear maximum, and lies between a certain negative

Fig. 3.—Curves representing geometrical loci of maxima (M-curves) of electroprofiles taken parallel to the plane of polarization (transversal electroprofile).

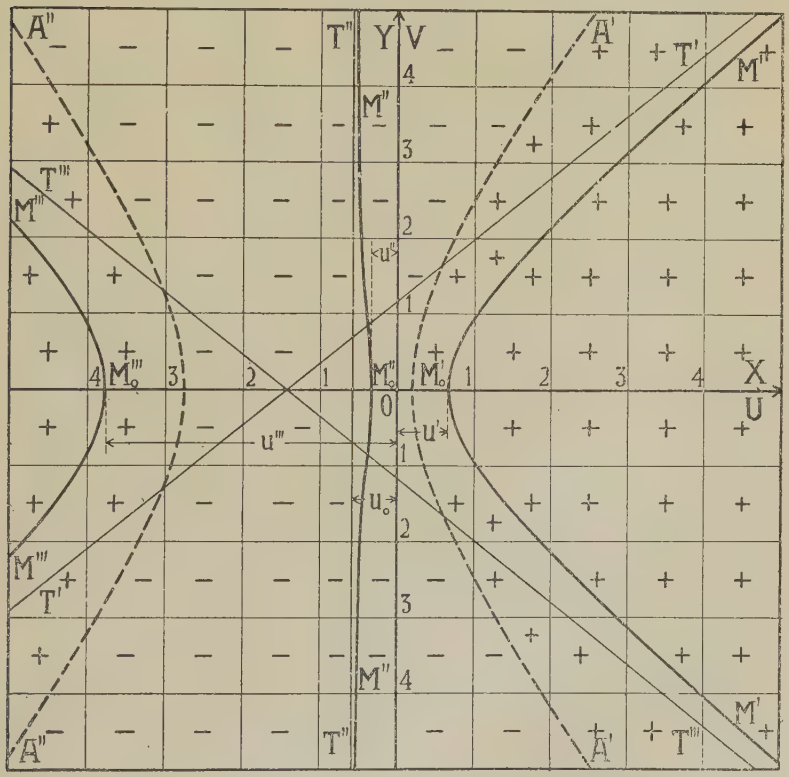

value $u=u'''$ and $u=-\infty$. The first and third branches also have asymptotes ; the last are expressed by equations :

$$v=\sqrt{\frac{2}{3}}\left[x+\frac{5}{6}\cot\alpha\right], \quad . \quad . \quad . \quad . \quad (11)$$

$$v=-\sqrt{\frac{2}{3}}\left[x+\frac{5}{6}\cot\alpha\right] . \quad . \quad . \quad . \quad (12)$$

The values u', u'', and u''', expressing in a relative degree the shortest distance of the three above-mentioned geometrical loci from the projection of the place of the centre

of the sphere, may be obtained as roots* of the cubic equation (8) by supposing $v^2=0$. Hence the equation :

$$u_m^3+2\cot\alpha\,.\,u_m^2-\frac{3}{2}u_m-\frac{\cot\alpha}{2}=0. \quad . \quad . \quad (13)$$

In view of the complexity of the functions expressing these roots, we do not state them.

We shall get the numerical value of each maximum by substituting in the expression F_x the value u_m, equal to the corresponding root of the equation (13) and the value $v=0$.

$$F_m=Q\frac{3u_m\cos\alpha-(1-2u_m^2)\sin\alpha}{(1+u_m^2)^{\frac{5}{2}}}$$

$$=Q\frac{1+2u_m^2}{(1+u_m^2)^2\sqrt{1+4u_m^4}}. \quad . \quad . \quad . \quad . \quad . \quad (14)$$

With different angles α of the inclination of the axis of polarization to the vertical, the distribution of M-curves is various : this difference is least perceptible in the middle branch M″, more so on the front branch M′, and most on the rear branch M‴.

This is well seen on fig. 4, in which are shown M-curves corresponding to $\alpha=0°$, 15°, 45°, and 90°. The rear branches of the curves corresponding to $\alpha=0°$ and 15° are not placed on the chart ; the middle branch of the curve corresponding to $\alpha=90°$ blends with the axis of ordinates.

§ 3. Let us now examine Case B ; *i. e.*, when the electro-profile is taken perpendicular to the plane of polarization of a hidden sphere.

From formula (33), Part I., it follows that the zero points are defined by the equation :

$$v=0 \quad . \quad . \quad . \quad . \quad . \quad . \quad . \quad . \quad (15)$$

which corresponds to the straight line A′A′ lying in the plane of polarization of the sphere, and by equation † :

$$\cos\alpha+u\sin\alpha=0, \quad . \quad . \quad . \quad . \quad . \quad (16)$$

corresponding to the straight line A″A″, perpendicular to the plane of polarization and intersecting the latter in the point A_0'', for which

$$u''''=-\cot\alpha. \quad . \quad . \quad . \quad . \quad . \quad (17)$$

* It is easy to ascertain that all three shown roots are real.

† The straight line defined by equation (16) is remarkable in that for points of this straight line, not only is the value F_y itself equal to zero, but also all differential coefficients of F_y by v, of any order whatever, also become zero.

§ 4. Differentiating formula (33), Part I., by v, and equating the differential coefficient to zero, we have the equation defining the geometrical locus of maxima:

$$1+u^2-4v^2=0 \quad . \quad . \quad . \quad . \quad . \quad . \quad (18)$$

or

$$4v^2-u^2=1. \quad . \quad . \quad . \quad . \quad . \quad . \quad (18')$$

Fig. 4.—Group of M-curves corresponding to $a=0°$, 15°, 45°, and 90°.

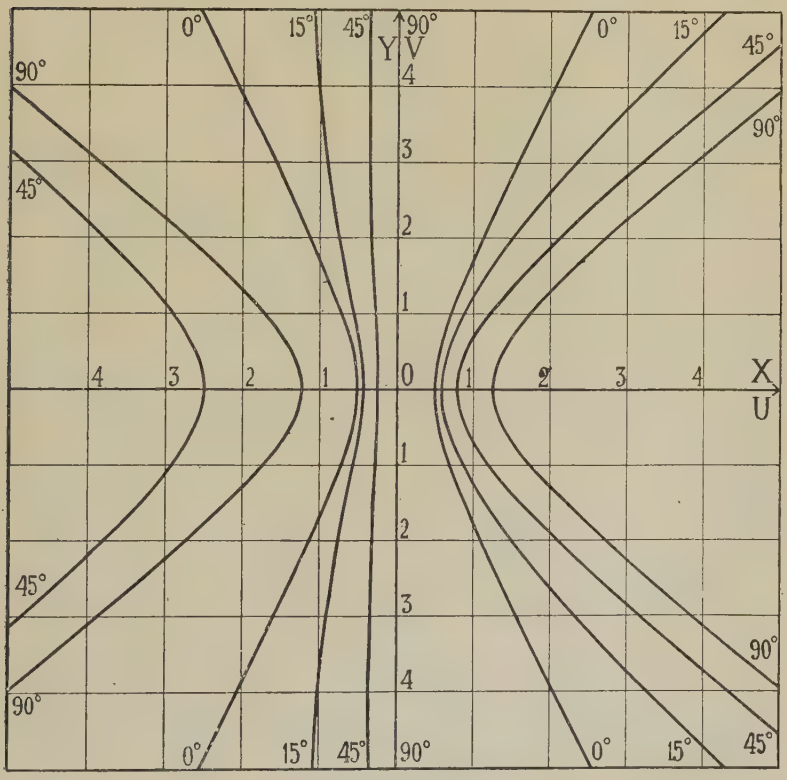

Hence we have the following :—

(*a*) According to the removal from one transversal electro-profile to another, the maxima remove along the lines of the hyperbola M′M′, M‴M‴ (fig. 5).

(*b*) The centre of this hyperbola lies exactly over the centre of the sphere.

(*c*) The real semi-axis of the hyperbola is perpendicular to

the plane of polarization, and is equal to the half depth of the centre of the hidden sphere :

$$a=\frac{h}{2}, \quad . \quad . \quad . \quad . \quad , \quad . \quad . \quad . \quad (19)$$

but the imaginary semi-axis is in the plane of polarization and has a value equal to the depth of sphere ; *i. e.*, twice as much as the preceding one,

$$b=h. \quad . \quad . \quad . \quad . \quad . \quad . \quad . \quad . \quad (20)$$

Fig. 5.—Geometrical loci of zero points and maxima of transversal electroprofiles.

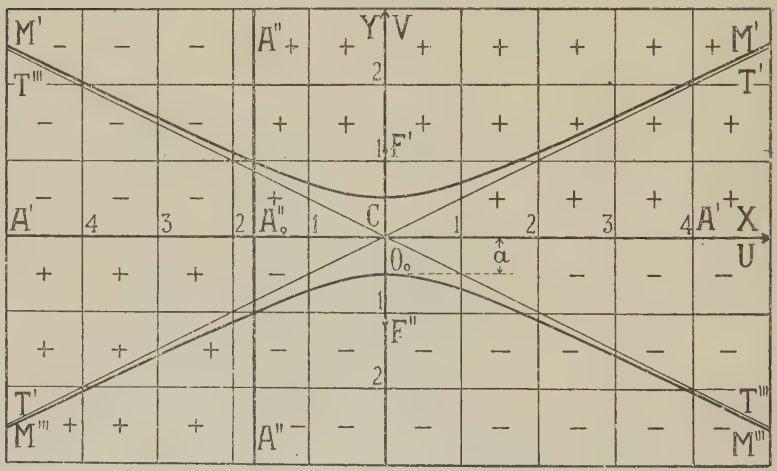

(*d*) The foci of the hyperbola F′ and F″ are at distances from the centre equal to

$$c=\frac{\sqrt{5}}{2}h. \quad . \quad . \quad . \quad . \quad . \quad . \quad . \quad (21)$$

(*c*) The asymptotes T′T′ and T‴T‴ of the hyperbola are expressed by the equations :

$$u=-2v, \quad . \quad . \quad . \quad . \quad . \quad . \quad . \quad (22')$$

$$u=+2v\,; \quad . \quad . \quad . \quad . \quad . \quad . \quad . \quad (22'')$$

i. e., are inclined to axis OX at angles of 26° 30′.

The value of the maxima is expressed by the formula :

$$(F_y)_m=\pm\frac{48Q(\cos\alpha+u\sin\alpha)}{25\sqrt{5}(1+u^2)^2} \quad . \quad . \quad . \quad . \quad . \quad (23)$$

For different values of u this value is also different:

(α) with $u = -\cot\alpha$, $(F_y)_m = 0$; . . . . . (24)

(β) with $u = -\frac{2}{3}\cot\alpha + \sqrt{\frac{4}{9}\cot^2\alpha + \frac{1}{3}}$ . . . (25)

it takes the greatest value, equal to

$$(F_y)_m = \pm\frac{48Q}{25\sqrt{5}} \cdot \frac{-\frac{1}{3}\cos\alpha + \sqrt{\frac{4}{9}\cos^2\alpha + \frac{1}{3}\sin^2\alpha}}{\left[1 + \left(-\frac{2}{3}\cot\alpha + \sqrt{\frac{4}{9}\cot^2\alpha + \frac{1}{3}}\right)^2\right]^2}; \quad \text{. . . (26)}$$

[Sign + corresponds to positive v, and sign − to negative v.]

(γ) with $u = -\frac{2}{3}\cot\alpha - \sqrt{\frac{4}{9}\cot^2\alpha + \frac{1}{3}}$, . . . (27)

it takes the greatest value, equal to

$$(F_y)_m = \mp\frac{48Q}{25\sqrt{5}} \cdot \frac{-\frac{1}{3}\cos\alpha + \sqrt{\frac{4}{9}\cos^2\alpha + \frac{1}{3}\sin^2\alpha}}{\left[1 + \left(-\frac{2}{3}\cot\alpha - \sqrt{\frac{4}{9}\cot^2\alpha + \frac{1}{3}}\right)^2\right]^2}. \quad \text{. . . (28)}$$

[Sign − corresponds to positive v, and sign + to negative v.]

§ 5. Let us examine now a general Case C, when the electroprofile is taken at a certain angle ϕ to the plane of polarization O_0X of the hidden sphere.

From formula (46), Part I., follows that zero points of the gradient of the field are defined by the equation:

$$3u'\cos\alpha - (1 + v'^2 - 2u'^2)\cos\phi \,.\, \sin\alpha - 3u'v'\sin\phi \,.\, \sin\alpha = 0 \quad \text{. . . (29)}$$

or $$u'^2 - \frac{1}{2}v'^2 - \frac{3}{2}\tan\phi \,.\, u'v' + \frac{3}{2}\frac{\cot\alpha}{\cos\phi}u' - \frac{1}{2} = 0. \quad \text{. (29')}$$

This equation shows the following:—

(α) According to the transition from one electroprofile to another inclined at the same angle ϕ to the plane of

polarization, the zero points remove along the branches A′A′ and A″A″ of the hyperbola * (fig. 6).

(*b*) The centre C of this hyperbola has the coordinates:

$$u_c' = -\frac{6\cos\phi\cot\alpha}{8+\sin^2\phi}, \quad \ldots\ldots \quad (30)$$

$$v_c' = +\frac{9\sin\phi\cot\alpha}{8+\sin^2\phi} \quad \ldots\ldots \quad (31)$$

or

$$u_c = -\frac{3(2+\sin^2\phi)\cot\alpha}{8+\sin^2\phi}, \quad \ldots\ldots \quad (30')$$

$$v_c = +\frac{3\sin\phi\cos\phi\cot\alpha}{8+\sin^2\phi}; \quad \ldots\ldots \quad (31')$$

Fig. 6.—Geometrical loci of zero points and maxima of oblique electroprofiles.

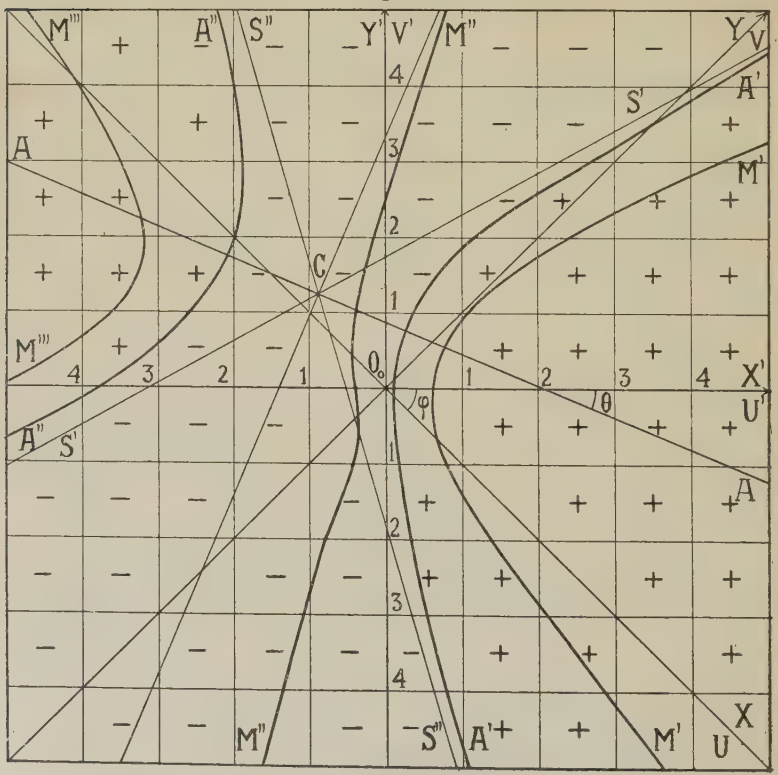

* In reality the invariant of equation (29′) is

$$\Delta = \frac{9}{16}\tan^2\phi + \frac{1}{2} > 0;$$

i. e., it presents a positive value corresponding to the hyperbola.

it does not lie any longer in the plane of polarization, and remaining behind the disposition of the centre of the sphere, removes to the same side from the plane of polarization to which the fore part of the line of survey has passed*.

(*c*) The real semi-axis ACA of the hyperbola is inclined to the line of survey at an angle θ, which is defined by the formula:

$$\tan 2\theta = -\tan\phi, \quad . \quad . \quad . \quad . \quad . \quad . \quad (33)$$

from which follows

$$2\theta = -\phi \quad . \quad . \quad . \quad . \quad . \quad . \quad . \quad (34)$$

or

$$\theta = -\frac{\phi}{2}; \quad . \quad . \quad . \quad . \quad . \quad . \quad (34')$$

in other words, the declination of the real semi-axis of the hyperbola from the line of survey takes place in a reverse direction and at half the angle.

(*d*) Transforming the equation of the hyperbola to the centre and to the axis, we obtain

$$\left(\cos^2\theta - \frac{1}{2}\sin^2\theta - \frac{3}{2}\tan\phi\sin\theta\cos\theta\right)u'''^2$$

$$-\left(\frac{1}{2}\cos^2\theta - \sin^2\theta - \frac{3}{2}\tan\phi\sin\theta\cos\theta\right)v'''^2$$

$$= \frac{1}{2} + \frac{9\cot^2\alpha}{2(8+\sin^2\phi)}, \quad . \quad . \quad . \quad (35)$$

from which one may find the values of the semi-axis and foci distances:

$$a = h\sqrt{\frac{2\cos\phi\left(1+\frac{9\cot^2\alpha}{8+\sin^2\phi}\right)}{3+\cos\phi}}, \quad . \quad . \quad (36)$$

$$b = h\sqrt{\frac{2\cos\phi\left(1+\frac{9\cot^2\alpha}{8+\sin^2\phi}\right)}{3-\cos\phi}}, \quad . \quad . \quad (37)$$

$$c = 2h\sqrt{\frac{3\cos\phi\left(1+\frac{9\cot^2\alpha}{8+\sin^2\phi}\right)}{8+\sin^2\phi}}. \quad . \quad . \quad (38)$$

* Transforming the equation of the hyperbola (29′) to the centre, we obtain

$$u''^2 - \frac{1}{2}v''^2 - \frac{3}{2}\tan\phi\,.\,u''v'' - \left(\frac{1}{2}+\frac{9\cot^2\alpha}{2(8+\sin^2\phi)}\right) = 0. \quad (32)$$

(*e*) The asymptotes S′S′ and S″S″ of the hyperbola have the equations :

$$v' = \left(-\frac{3}{2}\tan\phi + \sqrt{\frac{9}{4}\tan^2\phi + 2}\right)u' + \frac{3\cot\alpha}{\sqrt{8+\sin^2\phi}}, \quad (39)$$

$$v' = \left(-\frac{3}{2}\tan\phi - \sqrt{\frac{9}{4}\tan^2\phi + 2}\right)u' - \frac{3\cot\alpha}{\sqrt{8+\sin^2\phi}}. \quad (40)$$

The angle between the asymptotes is defined by the equation :

$$\tan\omega = -\sqrt{8+9\tan^2\phi}; \quad . \quad . \quad . \quad . \quad (41)$$

therefore it depends only upon the angle ϕ and lies between 90° and 180°.

§ 6. Differentiating the value $F_{x'}$ by u', we obtain

$$\frac{\partial F_{x'}}{\partial u'} = \frac{3Q}{\left[1+u'^2+v'^2\right]^{\frac{7}{2}}}\{\sin\alpha\left[-2\cos\phi\,.\,u'^3+4\sin\phi\,.\,u'^2v'\right.$$
$$\left.+3\cos\phi\,.\,u'v'^2-\sin\phi\,.\,v'^3+3\cos\phi\,.\,u'-\sin\phi\,.\,v'\right]$$
$$-\cos\alpha\left[4u'^2-v'^2-1\right]\}, \quad . \quad . \quad . \quad . \quad . \quad . \quad . \quad (42)$$

from which follows that the curve of maxima is expressed by the equation :

$$\sin\alpha\left[-2\cos\phi\,.\,u'^3+4\sin\phi\,.\,v'u'^2+3\cos\phi\,.\,v'^2u'-\sin\phi\,.\,v'^3\right.$$
$$\left.+3\cos\phi\,.\,u'-\sin\phi\,.\,v'\right]-\cos\alpha\left[4u'^2-v'^2-1\right]=0. \quad (43)$$

This is a curve M′M′ M″M″ M‴M‴ of the third order, which intersects the axis of abscissæ u' in three points, defined by the equation :

$$u'^3+2\frac{\cot\alpha}{\cos\phi}u'^2-\frac{3}{2}u'-\frac{\cot\alpha}{2\cos\phi}=0, \quad . \quad . \quad (44)$$

and the axis of ordinates v' in one point, defined by the formula :

$$v' = \frac{\cot\alpha}{\sin\phi}. \quad . \quad . \quad . \quad . \quad . \quad . \quad . \quad (45)$$

When $\phi=0$, it passes into a curve expressed by equation (8), and when $\phi=90°$ into the hyperbola expressed by the equation :

$$4u'^2-v'^2=1, \quad . \quad . \quad . \quad . \quad . \quad . \quad . \quad (46)$$

which corresponds entirely to formula (18′).

Examination of equation (43) shows that in observing the inequalities,

$$\left.\begin{aligned} 0<\alpha<90°, \\ 0<\phi<90°, \end{aligned}\right\} \quad . \quad . \quad . \quad . \quad . \quad . \quad (47)$$

the following hold:

(*a*) The M-curve is asymmetric with respect to the line of removal and of its perpendicular;
(*b*) the M-curve has no centre of symmetry;
(*c*) the M-curve has no axis of symmetry;
(*d*) the M-curve has asymptotes whose equation is as follows:

$$v'=pu'+q, \quad . \quad . \quad . \quad . \quad . \quad . \quad . \quad (48)$$

and the angle coefficient is the root of the equation:

$$t^3-3\cot\phi\,.\,t^2-4t+2\cot\phi=0, \quad . \quad . \quad . \quad (49)$$

and the segment q is connected with the coefficient p by the correlation:

$$q=\frac{(p^2-4)\cot\alpha}{\sin\phi(3p^2-6\cot\phi\,.\,p-4)}. \quad . \quad . \quad . \quad (50)$$

One may ascertain that the equation (49) always has three real roots, and consequently the M-curves have three asymptotes.

XCIII. *The Problem of a Hidden Polarized Sphere. By* Prof. A. Petrowsky, *Hon. Member of Rori (The Russian Society of Radio Engineers)* *.

Contents.

§ 1. An analytical calculation of elements by data obtained by studying the longitudinal electroprofiles.
§ 2. A graphical calculation.
§ 3. A calculation of elements obtained by studying transversal electroprofiles.
§ 4. A general case of calculation.

Part III.

Definition of Elements characterizing the Hidden Sphere.

STATEMENTS in the first two parts of this paper enable one to found the following method for defining elements characterizing a polarized hidden sphere by observations of electroprofiles on the surface of division.

* Communicated by the Author.

Having taken the electroprofiles, and tracing on the plan the geometrical loci of zero curves and maxima curves, the observer will have one of three following cases, which we shall examine separately.

§ 1. Case A.—The curves have the form, presented on fig. 1, characterized by the asymptote of the middle branch of the maxima curve being parallel to the imaginary axis of the zero hyperbola; hence we conclude that the profile has been taken along the lines parallel to the plane of polarization.

Further we proceed as follows.

(*a*) Drawing the asymptotes S′S′ and S″S″, we find the centre C of hyperbola A′A′, A″A″ and its axis. The direction of the real axis presents the direction of the plane of polarization. The projection O_0 of the sphere's centre is between the centre C of the hyperbola and its front branch A′A′, being at a distance from its centre equal to

$$x_c = \frac{3}{4}\cot\alpha \,.\, h. \quad . \quad . \quad . \quad . \quad . \quad . \quad (1)$$

(*b*) Let us trace the asymptote T″T″ to the curve of the second (negative) maxima. The point of intersection C_4 of this asymptote, T″T″, and the real axis of the hyperbola lies behind the projection of the sphere's centre at a distance equal to

$$x_4 = \frac{1}{3}\cot\alpha \,.\, h. \quad . \quad . \quad . \quad . \quad . \quad . \quad (2)$$

(*c*) Measure on the plan the distance CC_4. It is evidently to be equal to

$$d = \frac{5}{12}\cot\alpha \,.\, h\,; \quad . \quad . \quad . \quad . \quad . \quad . \quad (3)$$

hence we find the distance of projection of the sphere's centre O_0 from centre C of the hyperbola:

$$x_c = \frac{3}{4}\cot\alpha \,.\, h = \frac{9}{5}d. \quad . \quad . \quad . \quad . \quad . \quad (4)$$

(*d*) Let us measure on the plan the real semi-axis of the hyperbola.

According to formula (3), Part II., its square member equals

$$a^2 = \frac{h^2}{2} + \frac{9}{16}\cot^2\alpha \,.\, h^2 \quad . \quad . \quad . \quad . \quad . \quad (5)$$

or

$$a^2 = \frac{h^2}{2} + \frac{81}{25}d^2 = \frac{h^2}{2} + x_c^2\,; \quad . \quad . \quad . \quad . \quad (5')$$

whence we find the depth of the sphere:

$$h=\sqrt{2a^2-\frac{164}{25}d^2}. \quad . \quad . \quad . \quad . \quad . \quad (6)$$

(*e*) We find the angle of inclination of the axis of polarization to the vertical by formula (3), substituting in it the value h:

$$\cot\alpha=\frac{12\,d}{5h}. \quad . \quad . \quad . \quad . \quad . \quad . \quad (7)$$

(*f*) Measuring the distance x_m from the projection O_0 of the sphere's centre to the point of intersection of any of the curves maxima with the real axis of the hyperbola (*e.g.*, the distance from O_0 to M_0'), dividing it by value h, formula (6), we obtain

$$u_m=\frac{x_m}{h}. \quad . \quad . \quad . \quad . \quad . \quad . \quad . \quad (8)$$

Substituting in expression (14), Part II., this value u_m and likewise the corresponding value of maximum F_m found from experiment, we find

$$Q=\frac{(1+u_m^2)^{5/2}F_m}{3u_m\cos\alpha-(1-2u_m^2)\sin\alpha}. \quad . \quad . \quad . \quad (9)$$

(*g*) Lastly, supposing E to be the greatest value of the electromotive force which is developed by the sphere, one may find the radius of the sphere:

$$r_0=\sqrt{\frac{Qh^3}{E}}=h\sqrt{\frac{Qh}{E}}. \quad . \quad . \quad . \quad . \quad . \quad (10)$$

§2. The calculation discussed in § 1, (*c*), (*d*), (*e*) may be made graphically. This is shown on fig. 1, and consists as follows:—

(*c'*) Plot along Cv' from point C segment Ca and Cb in ratio 5 : 9, join a with C_4, and draw a line CO_0 parallel to aC_4. Point O_0 is the projection of the sphere's centre sought for.

(*d'*) Draw a line O_0O parallel to Cv' and line O_0p, bisecting the angle UO_0O; describe from point C as from a centre an arc $A_0'n$ with radius equal to the real semi-axis of hyperbola a, up to the crossing of this arc with line O_0O in some point n; then taking point O_0 for the centre, describe an arc np up to the intersection with the bisecting

line O_0p in some point p ; from point p erect perpendicular pO to the bisecting line O_0p up to intersection with line O_0O in point O.

The segment O_0O is the depth of the sphere's centre.

(e') On the line O_0C we find point q, for which $O_0q = \frac{4}{3}O_0C$; joining point q with point O and tracing Os' perpendicular to qO, obtain angle O_0Os. Angle O_0Os is α.

Fig. 1.—A graphical calculation of position, depth, and radius of the sphere (Case A).

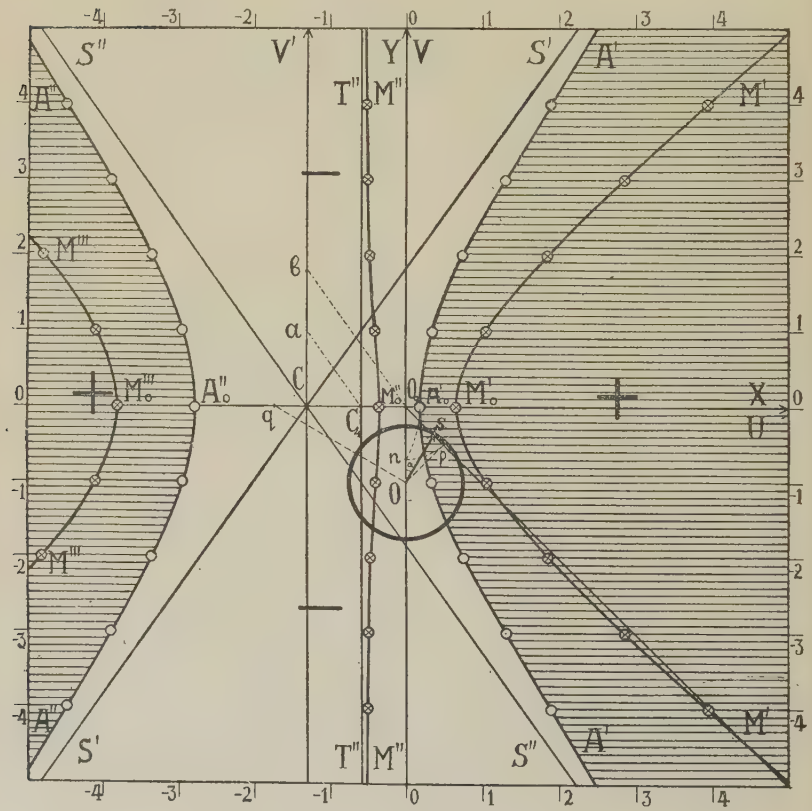

Thus, if examining all constructions as if made in a vertical section (and not in a plan), in which line CU corresponds to the dividing surface, then point O shows the position of the sphere's centre and direction Os the axis of polarization.

Fig. 3.

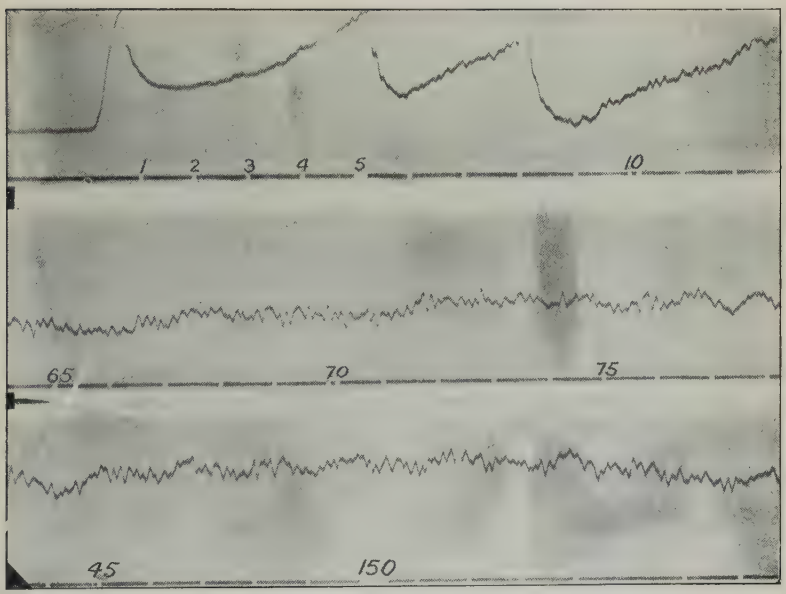

Fig. 4.

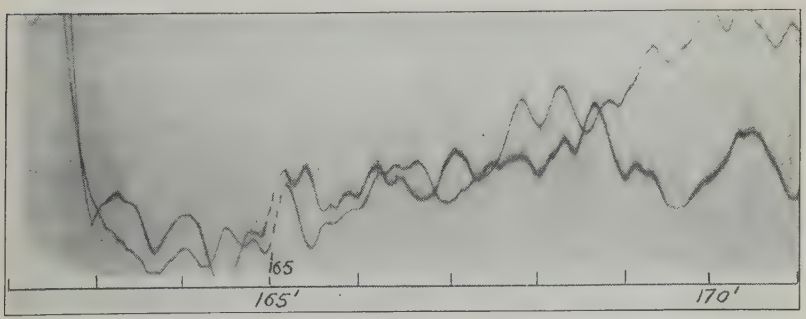

Fig. 2.

Fig. 3.

Fig. 5.

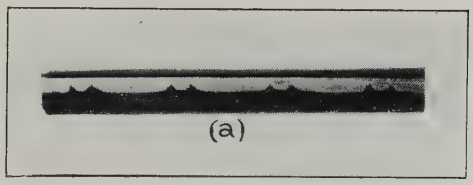

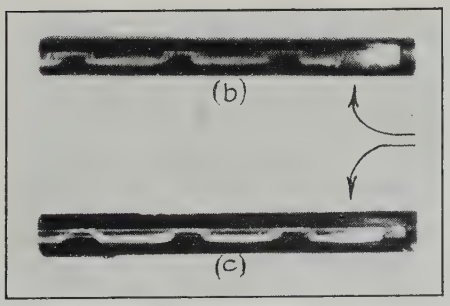

Calculating, according to the statements in (*f*) and (*g*), the value of the radius r_0 of the sphere, and tracing with this radius the periphery from centre O, we get a full graphic representation of all correlations sought for.

§ 3. Case B.—The curves have a shape represented on fig. 2, characterized by the fact that the zero lines represent two reciprocally-perpendicular straight lines A′A′ and A″A″, and the curves of maxima the hyperbola M′M′, M″M″, whose imaginary axis U coincides in direction with one of the zero straight lines A′A′. One may conclude that the profile is taken along the lines perpendicular to the plane of polarization. At the same time we act as follows :—

Tracing the asymptotes T′T′ and T‴T‴, we find the centre C of the hyperbola and its axis. The direction of its imaginary axis CU represents the projection of the plane of polarization. The projection O_0 of the sphere's centre is in the centre of the hyperbola.

(*b*) Measure the real axis of the hyperbola $2a$.

The depth of the sphere's centre is equal to

$$h=2a. \quad . \quad . \quad . \quad . \quad . \quad . \quad . \quad . \quad (11)$$

(*c*) Let us measure the distance d between the centre of the hyperbola and the point of intersection of two zero lines. The angle of inclination of the axis of polarization is defined by the equality :

$$\cot\alpha=-\frac{d}{h}=-\frac{d}{2a}. \quad . \quad . \quad . \quad . \quad . \quad . \quad (12)$$

(*d*) Substituting the value $\cos\alpha$ and the value $(F_y)_m$, found from experiment for line U=0 in the expression (23), Part II., find

$$Q=\frac{25\sqrt{5}}{48\cos\alpha}=\frac{25\sqrt{5}\sqrt{4a^2+d^2}}{48\,d}. \quad . \quad . \quad . \quad (13)$$

(*e*) Lastly, if E is the greatest value of the electromotive force developed by the sphere, one may find the radius of the sphere

$$r_0=\sqrt{\frac{Qh^3}{E}}=h\sqrt{\frac{Qh}{E}}. \quad . \quad . \quad . \quad . \quad . \quad (14)$$

The graphical design becomes in this case very simple (fig. 2), namely :

(*a*) Plotting along the line O_0O from point O_0, the segment O_0O equal to $2a$, we find the centre of the sphere.

(*b*) Joining point A_0'' with O and tracing the perpendicular O*s*, we obtain the direction of axis of polarization.

(*c*) Calculating the value r_0 and tracing the circle with this radius from centre O, we conclude the investigation of the case.

Fig. 2.—A graphical calculation of the position, depth, and radius of the sphere (Case B).

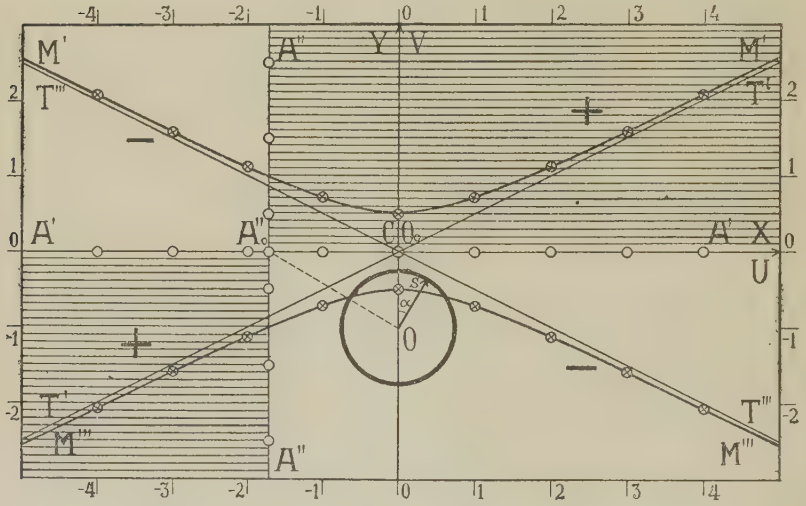

§ 4. Case C.—The curves of zeros and maxima have a shape, presented on fig. 3, characterized by the fact that both one and the other are placed non-symmetrically with respect to the direction of the survey O_0X'. The zero curves $A'A'$, $A''A''$ must at the same time present an hyperbola, whose axis ACA is inclined to the line of survey O_0X' at a certain angle θ. This denotes that the line of survey is inclined to the plane of polarization of a hidden sphere at an angle $\phi=2\theta$. Therefore we find the direction of the plane of polarization, tracing on the plan a line PCP inclined from the real axis of zero hyperbola to angle θ and withal to the opposite side of that to which is inclined the line of survey.

Fixing in this way the direction of plane of polarization,

the observer repeats once more the survey of electroprofile, taking it either parallel to the found plane or perpendicular

Fig. 3.—Graphical determination of the direction of the plane of polarization of the sphere (Case C).

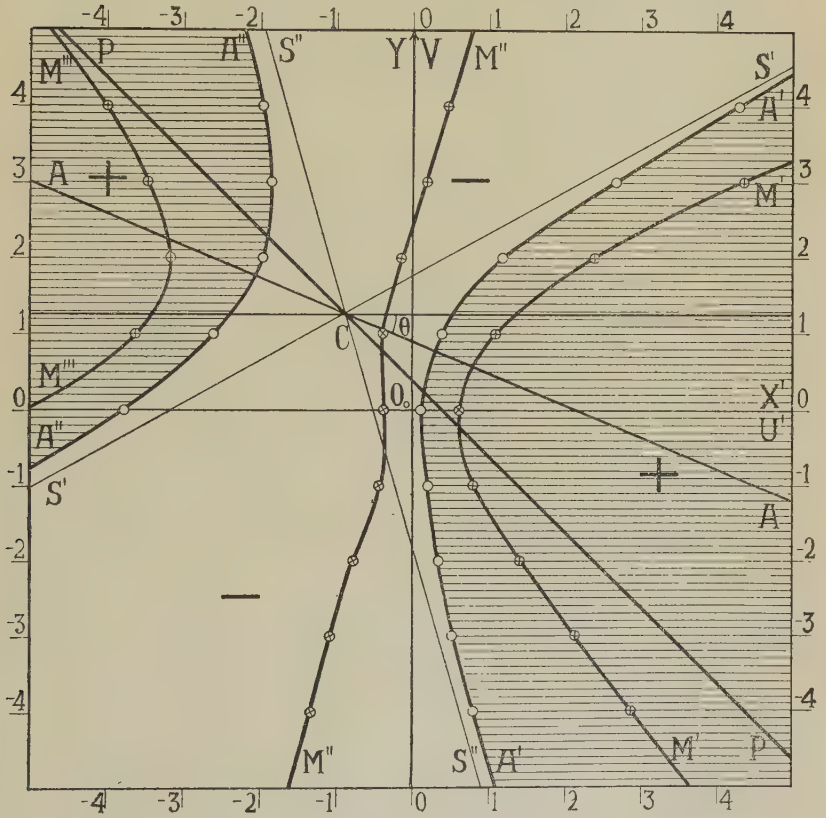

to it, which leads the solution of the problem to Case A or Case B.

XCIV. *Oscillatory Motion of a Viscous Liquid in a long straight Tube.* *By* S. F. Grace, *M.Sc.* (*University of Liverpool*) *.

§ 1. THE problem of the steady flow of a viscous liquid through a tube of circular section has been considered by Osborne Reynolds †; he finds that the critical

* Communicated by the Author.

† "On the Dynamical Theory of Incompressible Viscous Fluids and the Determination of the Criterion," Phil. Trans. A, clxxxvi. p. 123 (1895) [Papers, ii. p. 535].

velocity, beyond which the flow becomes turbulent, varies directly as the kinematic viscosity and inversely as the radius of the tube. With regard to oscillatory motions, the laminar non-turbulent oscillations of a viscous liquid between two parallel plates are dealt with by Lamb *, while in this paper the oscillations along a straight tube are considered and the velocity-distribution over a right section of a tube of uniform circular section is discussed in detail.

It is found that for very slow oscillatory motion along a uniform circular tube the velocity-distribution resembles that for steady motion along the tube, the velocity being in phase with the disturbing force. As the period of oscillation decreases, the magnitude of the velocity in the central portion of the tube tends to become uniform, the breadth of this central portion gradually increases, while the phase of the velocity tends to lag more and more behind that of the disturbing force. For comparatively short periods of oscillation, viz., less than 6 sec. for a tube of radius 1 cm., the velocity across a right section of the tube is approximately uniform, and has a phase-lag of $\frac{1}{2}\pi$ behind the disturbing force, except near the walls of the tube. Here, proceeding radially inwards, the velocity increases rapidly from zero to a maximum, and then diminishes to the neighbourhood of the uniform value; the phase-lag meanwhile gradually increases to $\frac{1}{2}\pi$.

The object of the present paper is to draw attention to the difference in the velocity-distribution in the case of the oscillatory motion of a viscous liquid as compared with that which occurs when the liquid is in steady motion, and to raise the question as to what form the Osborne Reynolds criterion will take for oscillatory motion. The great difference in velocity-distribution produced by oscillation suggests the advisability of an examination of this criterion in the case of oscillatory motion from both theoretical and experimental view-points.

The author desires to express his thanks to Prof. J. Proudman for bringing the problem of the present paper to his notice.

§ 2. *Tube of General Section.*

Consider a uniform long straight tube of any section, and take rectangular axes $Oxyz$, with O at the centroid of a right section and Oz parallel to the length of the tube. Let the tube be filled with liquid, which is made to oscillate in the

* Lamb, 'Hydrodynamics,' 5th ed., §§ 345 7.

direction of the length, and assume that the motion is everywhere axial ; thus, if u, v, w are the components of velocity at (x, y, z), then $u=v=0$, and the equation of continuity becomes

$$\partial w/\partial z=0.$$

Hence, with the usual notation, the general hydrodynamical equations for a viscous liquid * reduce to

$$\left.\begin{aligned} 0&=\mathrm{X}-\frac{1}{\rho}\frac{\partial p}{\partial x},\\ 0&=\mathrm{Y}-\frac{1}{\rho}\frac{\partial p}{\partial y},\\ \frac{\partial w}{\partial t}&=\mathrm{Z}-\frac{1}{\rho}\frac{\partial p}{\partial z}+\nu\left(\frac{\partial^2 w}{\partial x^2}+\frac{\partial^2 w}{\partial y^2}\right). \end{aligned}\right\} \quad . \quad . \quad . \quad (1)$$

Assuming that no external bodily forces act in the directions Ox and Oy, the first two equations of (1) give

$$\frac{\partial p}{\partial x}=\frac{\partial p}{\partial y}=0,$$

so that p is a function of the variables z and t only.

Now let

$$\mathrm{Z}-\frac{1}{\rho}\frac{\partial p}{\partial z}=\mathrm{C}e^{i\sigma t},$$

where C is a constant depending upon the forces producing the oscillation of the liquid, and put

$$w=f(x, y)e^{i\sigma t}.$$

The third equation of (1) now becomes

$$i\sigma f=\mathrm{C}+\nu\left(\frac{\partial^2 f}{\partial x^2}+\frac{\partial^2 f}{\partial y^2}\right)$$

or

$$\frac{\partial^2 f}{\partial x^2}+\frac{\partial^2 f}{\partial y^2}-\frac{i\sigma}{\nu}f=-\frac{\mathrm{C}}{\nu}. \quad . \quad . \quad . \quad . \quad (2)$$

§ 3. *Tube of Circular Section.*

In the case of a uniform tube of circular section, the radius of which is a, the equation (2) is transformed into cylindrical polar coordinates r, θ, z, where

$$r\cos\theta=x, \qquad r\sin\theta=y,$$

* Lamb, ' Hydrodynamics,' 5th ed., § 328.

and the function f assumed to be independent of θ. Thus

$$w=f(r)e^{i\sigma t},$$

where

$$\frac{d^2f}{dr^2}+\frac{1}{r}\frac{df}{dr}-\frac{i\sigma}{\nu}f=-\frac{C}{\nu}.$$

This is Bessel's equation of zero order, and the solution is

$$f(r)=\frac{C}{i\sigma}\left[1-\frac{J_0\{r\sqrt{(-i\sigma/\nu)}\}}{J_0\{a\sqrt{(-i\sigma/\nu)}\}}\right], \quad . \quad . \quad . \quad (3)$$

on the assumption that there is no slipping of the liquid at the surface of the tube, *i. e.*, that $f=0$ for $r=a$.

Taking σ/ν small, it is seen, neglecting squares and higher powers of σ/ν, that

$$f(r)=\frac{C}{i\sigma}\left\{1-\frac{1+\frac{1}{4}ir^2\sigma/\nu}{1+\frac{1}{4}ia^2\sigma/\nu}\right\}=\frac{C}{4\nu}(a^2-r^2).$$

This is the solution of the problem of the steady flow of liquid through the tube *.

The functions $J_0(x\sqrt{-i})$ which occur in (3) may be split up into their real and imaginary parts by means of the relations †

$$J_0(x\sqrt{-i})=I_0(x\sqrt{i})=\mathrm{ber}\,x+i\,\mathrm{bei}\,x,$$

and if $f(r)$ is written in the form v_1-iv_2, it is found that

$$\left.\begin{aligned} v_1&=\frac{C}{\sigma}\cdot\frac{\mathrm{bei}\,a\lambda\,\mathrm{ber}\,r\lambda-\mathrm{ber}\,a\lambda\,\mathrm{bei}\,r\lambda}{\mathrm{ber}^2a\lambda+\mathrm{bei}^2a\lambda},\\ v_2&=\frac{C}{\sigma}\left\{1-\frac{\mathrm{ber}\,a\lambda\,\mathrm{ber}\,r\lambda+\mathrm{bei}\,a\lambda\,\mathrm{bei}\,r\lambda}{\mathrm{ber}^2a\lambda+\mathrm{bei}^2a\lambda}\right\},\end{aligned}\right\} \quad . \quad (4)$$

where λ has been written in place of $\sqrt{(\sigma/\nu)}$.

The values of ber x and bei x are tabulated for $x=0$ to 10 at intervals of 0·1 in the British Association Report of 1912, and the values of $\mathrm{ber}^2x+\mathrm{bei}^2x$ for the same values of x in the Report of 1916. With the aid of these tables the values of v_1 and v_2 have been found for values of r/a between 0 and 1 and for values of $a\lambda$ equal to 1, 2, ..., 10 and the results exhibited graphically.

Since in practical applications one is usually concerned with an oscillation of definite magnitude rather than with the forces which produce this oscillation, the ratios v_1/V and v_2/V have been obtained and plotted against r/a, V being

* Lamb, 'Hydrodynamics,' 5th ed., § 331.
† Watson, 'Bessel Functions,' § 3·8.

the maximum velocity of the liquid along the axis of the tube—*i. e.*, $V=\sqrt{(v_1^2+v_2^2)_{r=a}}$.

In diagrams I. and II. the variations of v_1/V and v_2/V are

Diagram I.

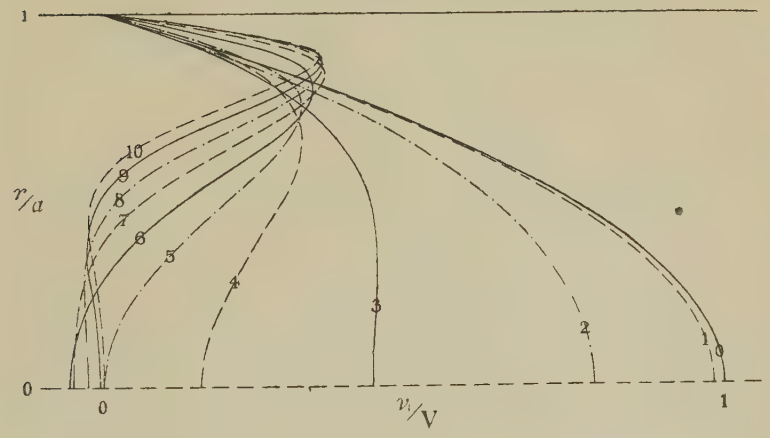

Diagram II.

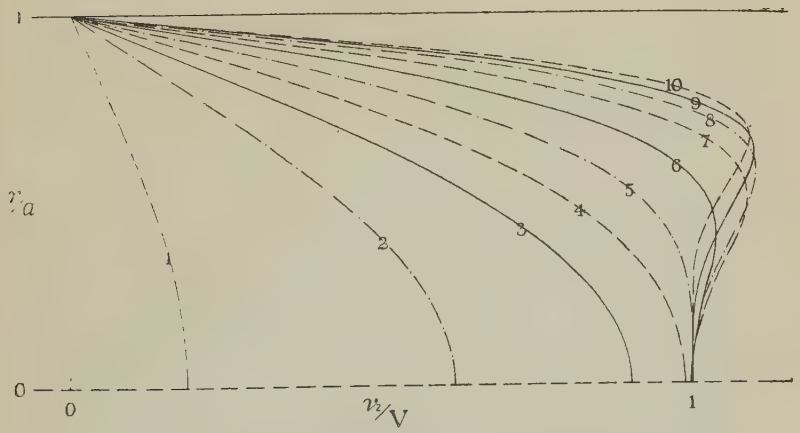

shown for periods of oscillation of the liquid given by $a\lambda=1, 2, \ldots, 10$. For water at 18° C. oscillating in a tube of radius 1 cm., taking $\nu=0{\cdot}0106$ gm./cm. sec., the periods (T) are given approximately by

$a\lambda =$ 1, 2, 3, 4, 5, 6, 7, 8, 9, 10

T = 593, 148, 66, 37, 24, 16, 12, 9, 7, 6 sec.

The curve marked 0 in diagram I. represents the velocity-distribution for steady motion along the tube.

§ 4. *Asymptotic Formulæ.*

For large values of x (real) *

$$\text{ber}\, x = (2\pi x)^{-\frac{1}{2}} e^{\alpha} \cos\beta, \qquad \text{bei}\, x = (2\pi x)^{-\frac{1}{2}} e^{\alpha} \sin\beta,$$

$$\text{ber}^2 x + \text{bei}^2 x = e^{2\alpha}/2\pi x.$$

where $\alpha = x/\sqrt{2}, \qquad \beta = x/\sqrt{2} - \pi/8.$

If these asymptotic forms be substituted in the expressions for v_1 and v_2, then, for large values of $r\lambda$, it is found that

$$\left.\begin{aligned} v_1 &= \frac{C}{\nu\lambda^2}\left(\frac{a}{r}\right)^{\frac{1}{2}} e^{-\gamma} \sin\gamma \\ v_2 &= \frac{C}{\nu\lambda^2}\left\{1 - \left(\frac{a}{r}\right)^{\frac{1}{2}} e^{-\gamma}\cos\gamma\right\}, \end{aligned}\right\} \quad . \quad . \quad (5)$$

where $\gamma = \lambda(a-r)/\sqrt{2}.$

Comparing the values of v_1/V, v_2/V obtained from these formulæ with those obtained from the expressions (4), it is found that for $a\lambda = 5$ the formulæ (5) provide a good approximation for values of r between $\frac{1}{2}a$ and a, the greatest error occurring for $r = \frac{1}{2}a$, and being here less than 1 per cent. For $a\lambda = 10$, either of the formulæ (4) and (5) may be used between $r/a = 0{\cdot}1$ and 1 for plotting the values of v_1/V, v_2/V against r/a on paper 16 in. × 10 in., as in the original diagrams I., II., since the differences between the two sets of values are inappreciable.

Consequently, for the purposes of the present problem, there is no need for further tabulation of the functions ber x and bei x; the formulæ (4) are used for values of $a\lambda$ between 0 and 10 and the formulæ (5) for larger values. Since these latter formulæ are only valid for $r\lambda$ large, it follows that they cannot apply for small values of r—i. e., for points near the axis of the tube. However, a glance at the diagrams I. and II. shows that for λ large v_1 is here approximately zero, while v_2 is approximately equal to V.

Diagram III. shows the forms of the curves v_1/V, v_2/V for large values of λ; they are drawn for $a\lambda = 20$—*i. e.*, for a period of oscillation of 1·5 sec. for water in a tube of radius 1 cm.

* Watson, ' Bessel Functions,' § 7·24.

It will be noted that for large values of $a\lambda$ and for r in the neighbourhood of a the distribution of v_1 and v_2 is

Diagram III.

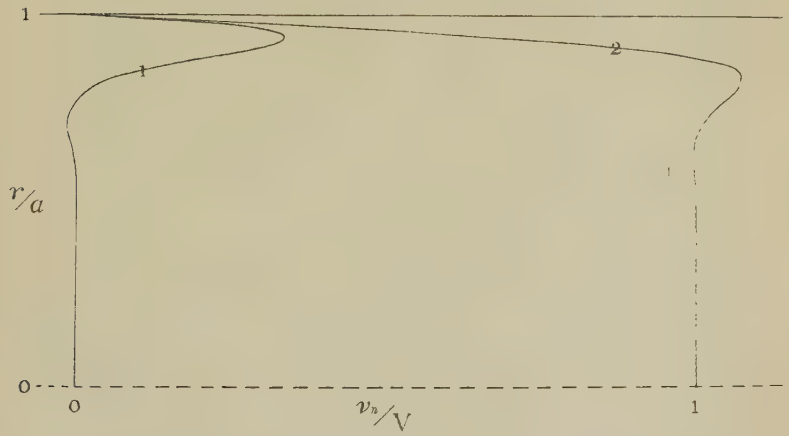

practically independent of a, since only $a-r$ and a/r occur in the expressions (5).

XCV. *A New Method of Conductivity Measurement by means of an Oscillating Valve Circuit. By* Professor E. F. Burton *and* Arnold Pitt, *B.A., Department of Physics, University of Toronto* *.

I. *Introduction.*

In the course of setting up the apparatus for the measurement of the dielectric constant of conducting liquids by the use of the oscillations of a valve circuit, remarkable effects of the conductivity of the sample of liquid on the oscillating period, when the oscillations are in a peculiarly sensitive region, came to light unexpectedly. The extreme sensitivity to small changes in the conductivity of the purest conductivity water to which minute quantities of impurities are added indicates that the method herewith described offers something useful in this field.

The lay-out of the apparatus is very simple, but it requires considerable patience to master the conditions necessary to

* Communicated by the Authors.

produce the sensitive region, but once it has been obtained it can be easily reproduced at will. Fig. 1 shows the arrangement: the left-hand portion of the figure represents an ordinary oscillating tube-circuit, for which the writers have used a Mullard tube; the coils L_1 and L have coefficients of self-induction of 0·072 and 0·250 henries respectively, the condenser C_1 has a range of 0–250 micro-microfarads, while the plate potential is 60 volts. The two L coils are placed closely end to end, and the sample, the conductivity of which is required, is inserted in the central core space; the position of maximum sensitiveness for the sample is within the core of L_1.

Fig. 1.

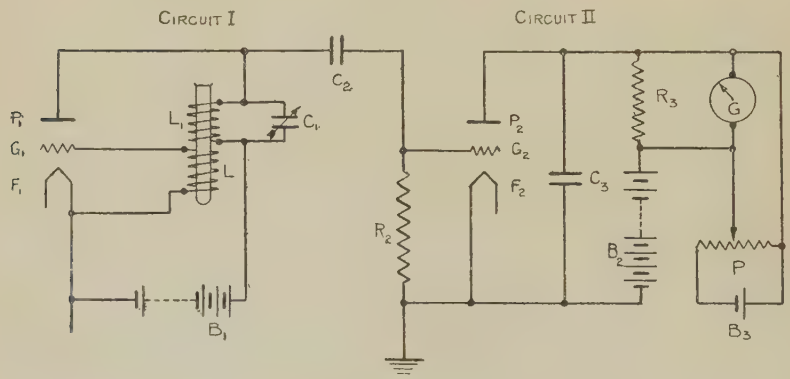

P_1, G_1, F_1, elements of tube: Mullard D.F.A. 4.
B_1, battery giving anode voltage of 60 volts.
L_1, coil of self-induction, 0·072 henries, resistance 31·8 ω.
L, coil of self-induction, 0·250 henries, resistance 124·8 ω.
C_1, variable air-condenser, up to 250 $\mu\mu$fd.
C_2 and C_3, fixed condensers, capacities 0·01 μfd. and 1·0 μfd., respectively.
G_1, a sensitive aperiodic galvanometer, 1000 ω resistance (Ayrton-Mather type).
R_2, grid leak of 3 megohms. R_3, adjustable shunt for G.
P_2, G_2, F_2, element of U.X. 201 A tube.
B_2, battery giving anode voltage of 70 volts.
B_3, P, cell and potentiometer to adjust galvanometer.

The filament current is adjusted to about 0·2 ampere, the anode potential fixed at about 60 volts, the condenser adjusted so as to produce oscillations in the circuit, and the intensities of the voltage changes due to these oscillations as

impressed on the second circuit are measured by the galvanometer attached in this second circuit. The change of potential impressed on the grid of the second tube is rectified and amplified in the ordinary manner. The details of the second tube-circuit are indicated in fig. 1. The condenser C_2 has a fixed capacity of $\cdot 01\,\mu$fd., and a grid leak of 3 megohms is inserted. The condenser, C_3, has a fixed value of $1\,\mu$fd. The filament voltage is 4 volts (current 0·21 ampere), and the anode voltage of this circuit is 70 volts.

When the circuits are operating the galvanometer is deflected off the scale owing to the steady plate current, but this deflexion is neutralized by the application of a contra-current from a potentiometer arrangement shown in the figure. Any succeeding deflexion of the galvanometer will measure the variation in plate current due to changes in the oscillating circuit caused by the insertion of the specimens in the L coils.

The sensitive region referred to in the first paragraph is obtained by adjusting the capacity of C_1 so that it is near the value for which the oscillations stop: with the values of self-inductance, filament current, and plate voltage indicated above, the oscillations cease at a value of 90 micro-microfarads for C_1. If, for example, C_1 is set at 100 micromicrofarads, the galvanometer is deflected and a zero re-established by the potentiometer voltage; the insertion of a sample of conducting material (liquid or solid) in the core of the coils L gives an additional deflexion of the galvanometer apparently due mainly to the influence of the conductivity of the material and not its magnetic permeability, as one might expect.

In the Tables which follow are shown results for the following series of substances:—(*a*) Samples of water of gradually increasing conductivities but all of quite small values; and (*b*) Samples of various organic liquids, purchased as C.P. but not specially re-purified.

(*a*) In Table I. are listed the results for measurements on aqueous solutions of very small conductivities. Beginning with doubly-distilled water of low conductivity, a series was prepared by using a standard KCl solution.

It is at once apparent that the apparatus is extremely sensitive to changes of conductivity between 2×10^{-6} and 200×10^{-6} for this setting of the condenser C_1, which was $100\,\mu\mu$fd.

(*b*) The capacity of C_1 was then changed to $95\,\mu\mu$fd.,

which made the whole much more sensitive to extremely low conductivities, and the effects of samples of various

TABLE I.

Solution	Conductivity $k \times 10^6$.	Deflexion of Galvanometer.
1.....	2·5*	18·5 cm.
2.....	10·5	32·2
3.....	11·5	33·7
4.....	15·0	38 2
5.....	24·0	45·9
6.....	47·7	51·4
7.....	76·6	55·4
8.....	222·8	58·9
9.....	255·0	60·1
10.....	502·0	60·6
11.....	1225·0	62·0

* The conductivity of this sample increased slightly, due to impurities in the experimental tube.

organic liquids were tried. These liquids were sealed hermetically into glass tubes which just fitted into the coils LL_1 projecting about 2 cm. from each end. Table II.

TABLE II.

Organic Liquids.

Liquid.	Formula.	Galvanometer Deflexion in cm. (corrected for effect of empty glass alone)
Carbon Tetrachloride ...	CCl_4	17·2
Chloroform	$CHCl_3$	42·5
Ether	$C_4H_{10}O$	32·3
Amyl Alcohol	$C_5H_{11}OH$	23·7
Butyl „	C_4H_9OH	71·4
Ethyl „	C_2H_5OH	77·2
Pentane.....	C_5H_{12}	8·8
Hexane	C_6H_{14}	6·8
Benzol	C_6H_6	18·0
Xylene (C. P.) }	C_8H_{10}	15·3
Xylol (Com.) }		11·8
Toluene (Com.) }	C_7H_8	14·0
Toluol (C. P.) }		15·1

shows the results for a series of organic liquids chosen, more or less, at random.

No attempt was made to measure the conductivity of the above liquids by any other method; these numbers are given merely to illustrate the way in which such slightly conducting liquids can be differentiated among themselves. Quantitative relations between the sensitivity of this arrangement and that used for results in Table I. were not obtained, as the purest water would have thrown the galvanometer image completely off the scale with the sensitivity used for organic liquids.

Remarks.

The purpose of the present paper is merely to draw attention to the occurrence of a rather striking phenomenon which opens out great practical possibilities in the measurement or testing of very small conductivities; along these lines further work is being carried on.

At the same time, the theoretical problems involved are very interesting, and it is hoped to prosecute this feature of the investigation. At present the writers are not in possession of sufficient data as to the influence of variation in the period of oscillations and other experimental conditions to justify embarking on this phase of the work here.

After the phenomenon noted here was first observed, the paper by Belz (Phil. Mag. (6) xliv. p. 479, 1922) on the magnetic effects of insertion of samples of various salts in coils of similar circuits was noticed. The conductivity effect seems to have escaped him, except for metallic wires, which, of course, also show a large effect in the above apparatus.

Summary.

A primary valve oscillating circuit and subsidiary measuring circuit have been developed which enable one to obtain remarkable indications of the conductivities of very dilute aqueous solutions and of various organic liquids.

The writers desire to express their thanks to the Director of the Physical Laboratory, Professor J. C. McLennan, for his generous support in the course of this work.

Department of Physics,
University of Toronto,
Toronto, Canada.

XCVI. *The Ultra-violet Absorption Spectrum of Cod-Liver Oil.* *By* Jay W. Woodrow, *Ph.D.**

SCHULTZ and his co-workers † have found absorption bands for a thin film of cod-liver oil at about 328 $\mu\mu$ and 279 $\mu\mu$. Heilbron, Kamm, and Morton ‡, using a quartz spectrograph and rotating sector photometer, found three regions of abnormal absorption in the ultra-violet spectrum with a film of cod-liver oil about 0·1 mm thick. Almost complete absorption occurred for wave-lengths less than 260 $\mu\mu$, while a band was observed with its maximum at 320 $\mu\mu$, and another in the region from 270 $\mu\mu$ to 290 $\mu\mu$. The latter was attributed to the small amount of ergosterol present. R. Pohl §, using a special type of photoelectric photometer has observed an absorption band at 280 $\mu\mu$ for chloresterol dissolved in alcohol.

In the experiments to be described briefly here, a photoelectric spectrophotometer was used to investigate the absorption spectrum of cod-liver oil between the wave-lengths 255 $\mu\mu$ and 320 $\mu\mu$.

The photoelectric cell was made of pyrex glass with a quartz window sealed in by means of a graded quartz-to-pyrex seal. The cathode consisted of an aluminium cylinder with an opening immediately back of the quartz window, while the anode was a silver wire at the centre of this cylinder. The air-pressure within the cell was reduced until the maximum photoelectric current was obtained with a potential difference of about 350 volts between the wire and the cylinder. This gave a high sensitivity, as the current was large, due to ionization by collision. The current was measured by means of a quadrant electrometer, using an electrostatic balance with a potentiometer and a condenser.

The spectrometer was specially constructed in the laboratory for these experiments. It had a large quartz prism and a pair of large quartz lenses of long focal length, giving rather large dispersion in the utra-violet. It was calibrated by means of a small direct-reading ultra-violet spectrometer. A spark between molybdenum terminals was used as the source of light, since this arrangement gave very strong

* Communicated by Prof. J. S. Townsend, F.R.S.

† Schultz & Morse, Amer. J. Dis. Child. xxx. p. 199 (1925); Schultz & Ziegler, J. Biol. Chem. lxix. p. 415 (1926).

‡ Heilbron, Kamm, & Morton, Biochem. J. xxi. pp. 78 & 1279 (1927).

§ R. Pohl, *Nachrichten der Gesellschaft der Wissenschaften zu Göttingen, Mathematische-Physikalische Klasse*, 1926, Hefte 2, p. 142.

illumination in the region to be studied and remained very constant for the time necessary to take the readings.

The absorption cell consisted of two thin fused quartz plates separated by strips of metal foil about 0·04 mm. in thickness. After considerable difficulty at first, it was finally found possible to fill such a cell with the oil and have it free from air-bubbles. In all the readings, the absorption due to this cell was compared with that of another cell made in exactly the same way except that it contained no oil. These two cells were mounted together in such a way that either one could be brought accurately into place before the slit of the photoelectric cell. Trials were also made with the absorption cells in front of the slit of the spectrometer, giving the same results as in the other position.

Fig. 1.

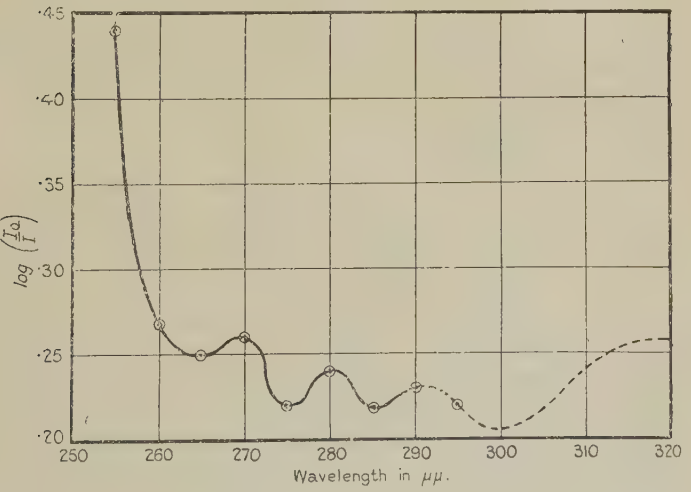

The results of the experiments are given by the curve in the accompanying figure, where I and I_0 represent the currents obtained for the cod-liver oil and the empty absorption cells respectively. It is seen that almost complete absorption occurred for wave-lengths less than 250 $\mu\mu$. As the photoelectric cell was not very sensitive for wave-lengths greater than 290 $\mu\mu$, the measurements were not so accurate in this region, and this part of the curve is shown by a broken line. However, the experiments indicated very definitely rather strong absorption in the neighbourhood of 320 $\mu\mu$. There are also three narrow absorption bands with

maxima near 270, 280, and 290 $\mu\mu$ respectively. These coincide almost exactly with the absorption bands of ergosterol which Heilbron * and his co-workers place at 270, 281·5, and 293·5 $\mu\mu$. The magnitude of these absorption bands is not great, as is to be expected, since the amount of ergosterol present is small, but its effects are much larger than the experimental errors for the apparatus used.

Absorption cells of greater thickness were also tried, but it was found that the experimental errors were too great with the larger values of the ratio I_0/I for the absorption bands to show up clearly.

Summary.

It has been shown that the characteristic ergosterol absorption bands can be observed in a thin film of cod-liver oil by means of a sensitive photoelectric spectrophotometer.

In conclusion, I wish to express my gratitude to Professor J. S. E. Townsend for furnishing the equipment for this investigation and for many helpful suggestions made during the progress of the work.

Electrical Laboratory,
Oxford University,
Oxford.

XCVII. *Multiple Reactive Gears.* *By* E. K. Sandeman, *Ph.D.* (*London*), *B.Sc.*, *A.C.G.I.*†

THE Multiple Reactive Gear follows as a logical outcome of the particular "Theory of the Torque Converter," which appeared in the October number of the Philosophical Magazine. In explaining the present modification of the principles, the same conventions and notation will be employed. It was there mentioned that certain advantages might result from employing, instead of a single mass, a mechanical reactive network containing a number of elements of mass or stiffness. Such a network can be made to have a reactance which changes with frequency (*e. g.* engine speed), in a much more flexible manner than the reactance of a pure mass ; the use of a multiplicity of elements enables several performance conditions to be satisfied in the same gear.

In fig. 1 *a* are shown two mechanical networks of the

* Heilbron, Kamm, & Morton, Biochem. J. xxi. pp. 78 & 1279 (1927).
† Communicated by the Author.

Fig. 1 *a*.

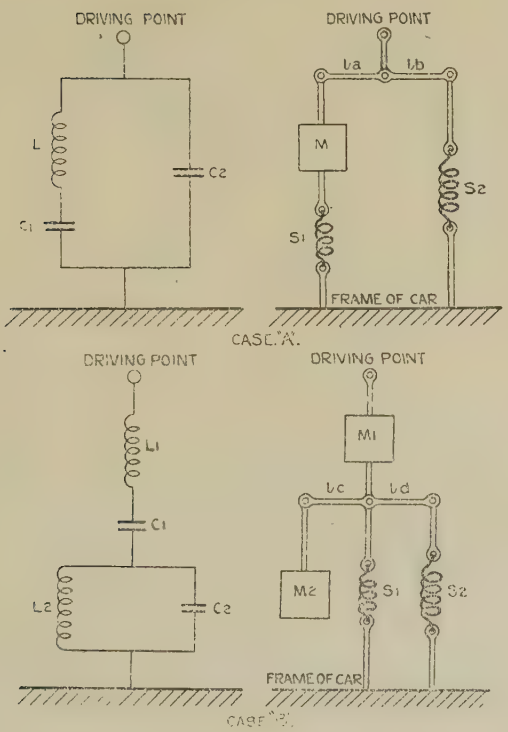

Fig. 1 *b*.

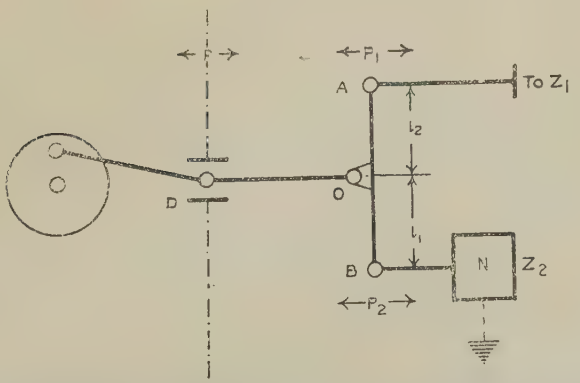

type contemplated, together with their equivalent electrical circuits. These networks are intended to have their driving-points connected to B (fig. 1 *b*). If $l_a = l_b$ and $l_c = l_d$, then

in order that the impedances of the mechanical networks in pounds per foot per second shall be represented by the same numbers as the impedances of the electrical networks expressed in ohms, the equations relating the equivalent elements must be as below, where masses are expressed in pounds, stiffnesses in pounds per foot, inductances in henrys, and capacities in farads.

Case A: $M=\frac{g\mathrm{L}}{4}$, $S_1=\frac{1}{4\mathrm{C}_1}$, $S_2=\frac{1}{4\mathrm{C}_2}$,

Case B: $M_1=g\mathrm{L}_1$, $M_2=\frac{g\mathrm{L}_2}{4}$, $S_2=\frac{1}{4\mathrm{C}_2}$, $S_1=\frac{1}{\mathrm{C}_1}$,

where g = the acceleration of gravity in feet per second per second.

The networks in fig. 1 are only types, it being possible to construct 2 two-element networks, 4 three-element networks, 11 four-element networks, etc. The values of the elements constituting one of these networks may be determined as follows :—

In equations (1), (11), and (13) of the above-mentioned paper the required resistance towards the engine is

$$\mathrm{R}_e = \text{the real part of } \frac{1}{\left(\frac{l_1}{l_1 \pm l_2}\right)^2 \frac{1}{\mathrm{Z}_a} + \left(\frac{l^2}{l_1 \pm l_2}\right)^2 \frac{1}{\mathrm{Z}_b}}, \quad \ldots \quad (1)$$

where Z_a is the load impedance and Z_b is the impedance presented by the network N at B (fig. 1).

Putting

$$\left(\frac{l_1}{l_1 \pm l_2}\right)^2 = \mathrm{A}, \qquad \left(\frac{l_2}{l_1 \pm l_2}\right)^2 = \mathrm{B}, \quad \ldots \quad (2)$$

let

$$\mathrm{Z}_a = \mathrm{C} + j\mathrm{D}, \quad \ldots \quad (3)$$

since the load resistance may be complex owing to the shunt stiffness ; and let

$$\mathrm{Z}_b = j\mathrm{X}, \quad \ldots \quad (4)$$

since the network impedance is a pure reactance ; then

$$R_e = \text{real part of } \frac{1}{\frac{A}{C+jD}+\frac{B}{jX}} \quad . \quad . \quad . \quad . \quad . \quad . \quad . \quad (5)$$

$$= \text{real part of } \frac{jCX-DX}{jAX+BC-jBD}$$

$$= \text{real part of } \frac{(jCX-DX)(BC-jAX-jBD)}{B^2C^2+(AX+BD)^2}$$

$$= \frac{CAX^2}{B^2C^2+A^2X^2+B^2D^2+2ABDX} \quad . \quad . \quad . \quad . \quad . \quad (5\,a)$$

$$\therefore (CA-R_eA^2)X^2-2R_eABDX-R_eB^2(C^2+D^2)=0.$$

$$\therefore X=\frac{2R_eABD \pm \sqrt{4R_e^2A^2B^2D^2+4R_eB^2(C^2+D^2)(CA-R_eA^2)}}{2(CA-R_eA^2)}.$$

$$. \quad . \quad . \quad (6)$$

If $R_e > Z_a$, then O must divide AB (fig. 1 *b*) internally, and the + signs in equation (2) are applicable. If $R_e < Z_a$, then O divides AB externally, and the — signs in equation (2) are applicable.

If $R_e > Z_a$, then

$$B=1-A. \quad . \quad . \quad . \quad . \quad . \quad . \quad (7)$$

Then from equation (5 *a*)

$$R_e=\frac{CAX^2}{(1-A)^2C^2+A^2X^2+(1-A)^2D^2+2A(1-A)DX}.$$

$$\therefore (1-2A+A^2)C^2+A^2X^2+(1-2A+A^2)D^2$$
$$+(2A-2A^2)DX=\frac{1}{R}CAX^2.$$

$$\therefore C^2-2AC^2+A^2C^2+A^2X^2+D^2-2AD^2$$
$$+A^2D^2+2ADX-2A^2DX-\frac{1}{R_e}CAX^2=0$$

$$\therefore (C^2+D^2+X^2-2DX)A^2$$
$$+\left(2DX-2C^2-2D^2-\frac{1}{R_e}CX^2\right)A+C^2+D^2=0.$$

$$2C^2+2D^2+\frac{CX^2}{R_e}-2DX$$

$$\therefore A=\frac{\pm\sqrt{\left(2DX-2C^2-2D^2-\frac{CX^2}{R_e}\right)^2-4(C^2+D^2)(C^2+D^2+X^2-2DX)}}{2C^2+2D^2+2X^2-4DX}. \quad . \quad . \quad . \quad (8)$$

Similarly, if $R_e > Z_a$, then

$$B=A-1 \quad . \quad . \quad . \quad . \quad . \quad . \quad . \quad (9)$$

and

$$2C^2+2D^2+\frac{CX^2}{R_e}+2DX$$

$$A=\frac{\pm\sqrt{\left(2DX+2C^2+2D^2+\frac{CX^2}{R_e}\right)-4(C^2+D^2)(C^2+D^2+X^2+2DX)}}{2C^2+2D^2+2X^2+4DX}. \quad . \quad . \quad . \quad (10)$$

For the present purpose the positive value of the root will be taken.

Equation (6) gives the value of the impedance of the reactive network at any one power in order that a load resistance Z_a shall present a required impedance R_e towards the engine.

At any one power the values of R_e and Z_a are read respectively from the engine and load-resistance diagrams (figs. 2 and 3).

The value of R_e at each power is, on the engine diagram, the resistance corresponding to the point of intersection of the power line for the power concerned, with alternatively—

(*a*) The upper curve of the limit of commercial performance when maximum car speed is required (*i. e.*, the engine delivers maximum power).

(*b*) The curve of maximum economy when maximum economy is required.

The value of Z_a * at each power is, on the load diagram, the resistance corresponding to the point of intersection of

* In the presence of shunt stiffness Z_a will be modified, as in equation (18) of previous article.

the power line for the power concerned, with alternatively—

(*c*) The maximum gradient curve if maximum efficiency on hills is required.

(*d*) The average resistance curve if the best average performance is required.

Fig. 2.

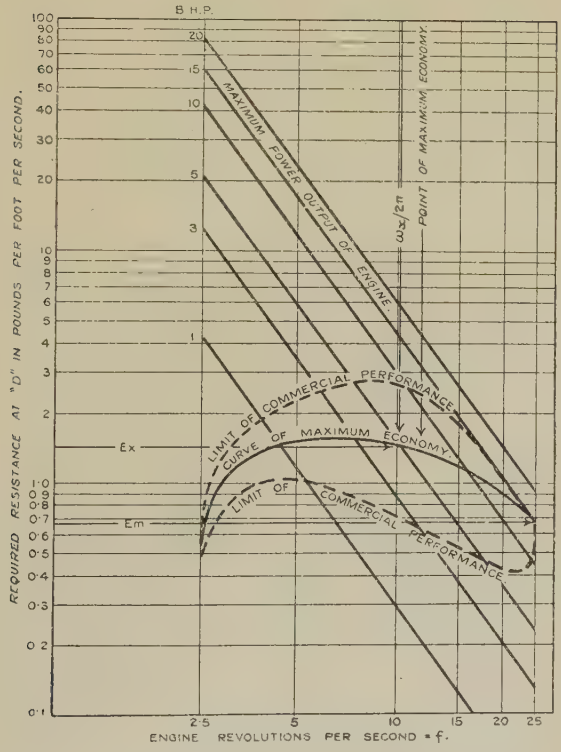

The above are chosen as examples of the type of criteria of performance which might be chosen, but other types can be chosen if desired.

Having chosen the type of engine performance required and the type of car performance (load performance) required, it is only necessary to adjust the lever ratio l_1/l_2 and the reactance X so that at a number of chosen powers under load conditions specified by (*c*) or (*d*) the engine shall give a performance as specified by (*a*) or (*b*).

The value of l_1/l_2 may be determined as follows :—

Let $\hat{R}_e$ and $\hat{Z}_a = \hat{C} + j\hat{D}$ be the values of R_e and Z_a at power p when the value of $\frac{R_e}{Z_a}$ is a maximum. The shunt network is arbitrarily given a value which is as large as is practicably possible ; let this value be $\hat{X}$. The corresponding

Fig. 3.

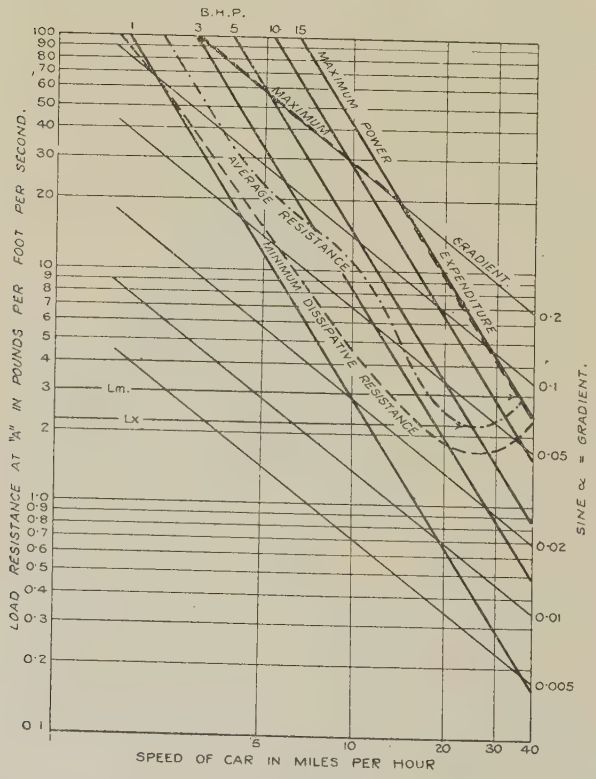

value of $A = \frac{l_1}{l_1 \pm l_2}$ is given by substituting $\hat{R}_e$, $\hat{Z}_a$, and $\hat{X}$ in equations (8) or (10), according to whether $\frac{R_e}{Z_a}$ is greater or less than unity. The value of B then follows from equation (9). Then by choosing suitable finite values of X at suitable powers other than p, exact impedance matching

at these powers may be obtained for conditions of load and engine performance corresponding alternatively to (*a*) or (*b*) and (*c*) or (*d*) above. The necessary value of X is given at each power by inserting the value of Z_a and R_e at that power, together with the values of A and B, in equation (6). The frequencies (engine speeds in revolutions per minute $\times 60$) at which these powers are delivered are the frequencies corresponding to the points of intersection of the power-lines on the engine diagram with the curve of maximum economy, or the limit of commercial performance curve.

It is therefore required to construct a mechanical network which shall have certain known values of reactance X at a number of known frequencies. Formulæ for constructing an electrical network to accomplish this are given in 'Transmission Circuits for Telephone Communication,' by K. S. Johnson (van Nostrand Company), Appendix E, p. 296.

If the values of X calculated from equation (6), which are actually in pounds per foot per second, are imagined to be electrical ohms, then the Johnson formulæ will give a solution in terms of inductance L henrys and capacity C farads.

The type of formulæ to be used for conversion to masses in pounds, and to stiffnesses in pounds per foot, were given at the beginning of the present article.

In general, the network must be so constructed that while one effective network anti-resonance may occur at the limit of the range of frequencies (*i. e.* engine speeds) of importance, no resonance must occur in that range, or the load will be completely short-circuited. In particular cases this condition may be violated, since in practice, with the throttle open, the engine will rapidly accelerate from a speed at which network resonance occurs.

The networks shown are intended to have the driving-point connected to B (fig. 1) and the other end to the frame of the car, but networks may be used where no connexion is made to the frame of the car.

Conclusion.

The Multiple Reactive Gear affords, among others, the following possibilities:—

If n elements are used in the network, by suitable adjustment of the fixed gear ratio (including the lever ratio), when the throttle is suitably adjusted, the engine may be made to give its most economical performance under average load conditions at $(n+1)$ chosen powers; or the engine may

be made to give its most economical performance under average load conditions at n chosen powers, and to deliver its maximum possible power on the heaviest gradient, or the engine may be made to give its maximum power under average load conditions at $(n+1)$ chosen engine speeds; or the engine may be made to attain any predetermined speed before it begins to exert an appreciable torque on the load. This last performance condition can be realized very simply by making the network anti-resonant at an engine speed just above the speed at which the engine is required to run. It is evident that the number of performance conditions may be multiplied indefinitely.

A number of modifications naturally suggest themselves which enable the impedance of the load to be further modified. Among these are the use of non-linear stiffnesses, *i. e.* springs whose stiffness increases as they are compressed; by this means the increasing stiffness brought into play by the large velocities flowing, as resonance is approached, may be made to prevent a condition of resonance ever being reached. Another device is a mechanical network presenting an impedance in series with the load.

Appendix.

Solution of the Impedance looking into the Double-acting Ratchet.

In the "Theory of the Torque Converter," published in the October number of the Philosophical Magazine, it was shown that R_E, the real part of the impedance looking into the double-acting ratchet, is approximately a pure resistance equal to the resistance looking into the ratchet-driven rotor.

It will now be shown how, in practice, an exact solution may be obtained. As a preliminary the case will be considered where a special type of ratchet is employed which is double-acting, and which maintains contact at each stroke during the whole time that the force in the rod between A (fig. 1) and the ratchet, *e. g.* compression or tension, is in the same sense. This is equivalent to a synchronous commutator in which commutation occurs at the time when the voltage has fallen to zero. In practice such a condition would be hard to realize exactly, but the results obtained from such an assumption indicate the magnitude and the type of the effect to be expected in the practical case, and, what is more important, it indicates how certain simple measurements can be made in practice to determine exactly the resistance to be

expected looking into any type of ratchet used, whether automatic or clutch-controlled.

It will now be shown that under the above conditions if R_L is the continuous velocity resistance of the ratchet-driven rotor then the resistance looking into the ratchet is practically given by

$$R_E = \frac{\pi^2}{8} R_L,$$

and that other effects introduced by the non-harmonic nature of the load are negligible.

In fig. 1*b* is shown the general arrangement of the multiple reactive gear, which is identical in principle with the torque converter except that the mass M attached to B is replaced by the network N.

In fig. 4 is shown an equivalent electrical circuit for the

Fig. 4.

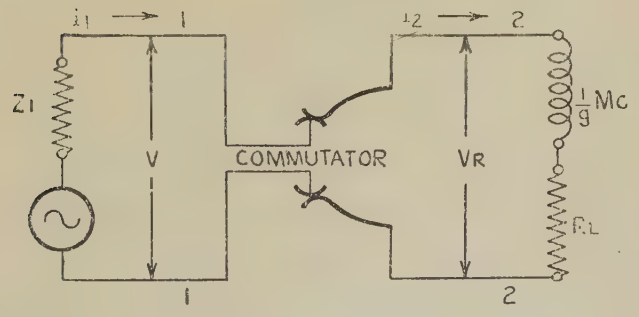

Fig. 5.

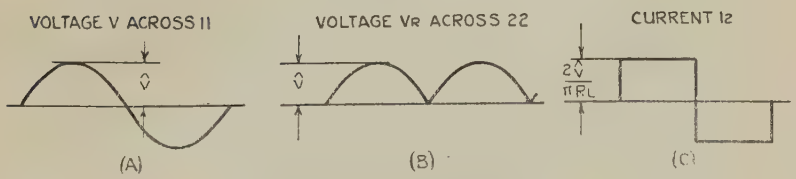

part of the gear to the right of A. Z_1 is the impedance looking back from A towards the engine, M_C is the mass of the car in pounds, and R_L is the load resistance.

An e.m.f., as at A in fig. 5, occurring across 1, 1, therefore gives rise to an e.m.f. V_R, as at B in fig. 4, occurring

across 2, 2. By means of a Fourier expansion it may be shown that

$$V_R = \frac{2\hat{V}}{\pi} - \frac{4}{3}\frac{\hat{V}}{\pi}\cos\omega t - \frac{4}{15}\frac{\hat{V}}{\pi}\cos 4\omega t - \text{etc.}$$

If Z_2 has a very large impedance to alternating currents, as is the case in practice, then no alternating current flows through Z_2, but only direct current of magnitude

$$I_2 = \frac{2\hat{V}}{\pi R_L},$$

where R_L is the resistance component of the load defined by $\frac{550\,W}{\dot{x}^2}$, W being the transmitted horse-power and $\dot{x}$ the peripheral speed of the ratchet-driven rotor.

The current through Z_1 is therefore of the form shown at C in fig. 5. This is of the form

$$I_1 = A\sin\omega t + \tfrac{1}{3}A\sin 3\omega t + \tfrac{1}{5}A\sin 5\omega t + \text{etc.},$$

where

$$A = \frac{4}{\pi} \times \frac{2\hat{V}}{\pi R_L} = \frac{8}{\pi^2}\frac{\hat{V}}{R_L}$$

= the amplitude of the current of fundamental frequency.

The resistance, looking into the ratchet, is therefore

$$\frac{\pi^2}{8} R_L.$$

It is necessary here to show how the above condition of affairs (in Z_1) can be imitated ; in particular is this desirable in order to justify the use of an initial fictitious assumption of a sinusoidal voltage V across the output of Z_1.

If a circuit is set up, as in fig. 6, with two generators of e.m.f. as shown, the current in Z_1 will be I_1 as above, where the voltage of fundamental frequency across Z_1 will be

$$V = \frac{R_E}{Z_1 + R_E} e_1 = \hat{V}\sin\omega t.$$

There will be a series of voltages of multiple frequency across Z_1, but since Z_1 is a pure reactance, no power will be delivered to it, and all the power generated by e will be absorbed in R_E. It can be imagined that part of the power delivered to R_E is used to drive a generator of e.m.f. e_2.

It therefore follows that one effect of the double-acting rectifier is to increase the effective load resistance presented towards the engine by the factor $\frac{\pi^2}{8}$. This follows from consideration of the forces of fundamental frequency.

The multiple frequency forces produce velocities which flow through the two alternative paths provided by the engine and the shunt network. In order that the engine speed shall not be appreciably altered by these velocities, and the wave-form of the velocity of the point D caused to depart very much from a sine-wave, the impedance looking into the engine must be large compared with the reactance network. In

Fig. 6.

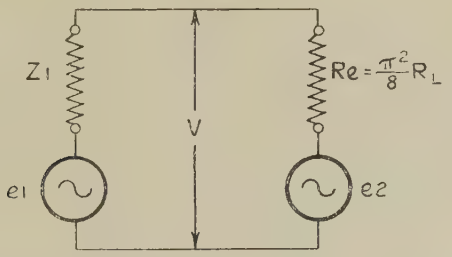

$$e_1 = \frac{1}{R_e}(Z_1 = R_e)\,\hat{V}\sin\omega t,$$

$$e_2 = \frac{1}{R_e}(Z_1 + R_e)\,\frac{\hat{V}}{3}\sin 3\omega t + \frac{\hat{V}}{5}\sin 5\omega t + \text{etc.}$$

practice this condition must also be satisfied in order that the reactive forces due to the network do not introduce undue fluctuations in engine speed. It is therefore true to say that the only appreciable effect of the forces of multiple frequency due to the ratchet is to cause relatively small velocities of multiple frequency to flow through the network.

Measurements to be made in Practice.

If it was not previously apparent, it is evident from the foregoing that by measuring at A (fig. 1) the force-wave in pounds and the velocity-wave in feet per second as functions of time, the impedance looking into the ratchet follows as the ratio

$$\frac{\text{Force component of fundamental frequency}}{\text{Velocity component of fundamental frequency}}.$$

Fortunately, the measurement of both these quantities is very simple. Two moving coils situated in radial magnetic fields are coupled through suitable mechanical reducing mechanisms, the one to the point A (fig. 1) and the other to point B (fig. 1). The two coils are connected through two resistance coupled amplifiers to the two ribbons of a twin oscillograph. The coils, amplifiers, and oscillographs are previously calibrated for velocity by being connected to a reciprocating part of known velocity. In this way the velocities of the points A and B are measured.

If at any frequency the reactance of the network is positive and $= M\omega$,

$$\text{the force at B} = \frac{M}{g}\ddot{x}_b,$$

$$\text{the force at A} = \frac{l_1}{l_2} \times \text{the force at B}.$$

Hence by multiplying the slope of the velocity-curve for B by $\frac{l_1 M}{l_2 g}$ the force-curve for A may be obtained. When the network reactance is elastic it may similarly be shown that the force is given by the product of the effective stiffness and the integral of the velocity-curve.

Fourier analysis then gives the force and velocity amplitudes of fundamental frequency. An alternative method, which is only practicable at high engine speeds (circa 2000 r.p.m.), is the use of amplifiers containing low pass filters to suppress all forces except those of fundamental frequency. This obviates the use of Fourier analysis.

It is evidently not practicable to make such measurements on a running car, but the inertia of the load may be simulated by a heavy flywheel and its energy dissipation by brake bands, or, better still, by the use of an hydraulic accumulator.

XCVIII. *On the Capillary Action of Mercury in the Absence of Gas-Grown Skins.* *By* J. J. Manley, *M.A.* (*Research Fellow, Magdalen College, Oxford*) *.

[Plates XII.–XIV.]

WHILST removing the gas-grown skin from within a charged barometric tube, it was found that the curvature of the mercury lessened. First the normal

* Communicated by the Author.

convexity dwindled until the surface appeared as a perfect plane: then as the skin became highly attenuated, the plane surface gradually gave place to one purely concave. Photographs of the unaided mercurial surface fail to show this progressive change with the requisite clearness. This difficulty was met by first attaching a strip of paper p to the posterior surface of the tube and directing the camera obliquely. As p was thus seen by reflexion, the form of its image at once revealed the form of the mercurial surface. The initial or normal curvature of the surface together with three successive phases in the transition, are respectively shown in α, β, γ, and δ of fig. 1 (Pl. XII.)*. The experiment by which this complete inversion of curvature was effected was as follows:—

Experiment A.—First, the barometric tube was made chemically clean and dry and then highly evacuated. Next, its lower and sealed end was opened under pure mercury contained in a deep cistern and the tube thus charged. The tube was then set up between rotatable guides and rapidly driven up and down by a motor. During the ascent of the tube a feeble electric glow was produced within, and this was accompanied by a slow destruction of the gas-grown skin. At the conclusion of the experiment, when the mercurial surface was concave, the tube was inclined and a very small but quite appreciable bubble of gas representative of the destroyed and normal skin discovered. Other methods successfully used for the destruction of a gas-grown skin were the following:—

Experiment B.—The first additional experiment was made with a stationary barometric tube prepared and charged as for experiment A. Upon the upper portion of this tube was wound a spiral of wire the free end of which was joined to a coil yielding a 1 inch spark. The second terminal of the coil communicated with the mercury in the cistern. On activating the apparatus the vacuous space at first remained dark; but

* These changes in curvature were, as will be seen from the following quotation, known to Young, who wrote:—"Professor Casbois, of Metz, has shown that the depression of mercury in glass tubes depends on the imperfection of the contact, and when it has been boiled in the tube long enough to expel all foreign particles, the surface becomes concave and the depression becomes an elevation. Perhaps this change may be the effect of the commencement of chemical action between the mercury and the component parts of the glass." (Thomas Young's Collected Works, vol. i. p. 425.) For this extract I am indebted to Prof. W. Ramsden. Since Young's day others have doubtless observed the same phenomena: but the explanation offered in this paper has not, I believe, been previously given.

after a short time a dull thud * was heard, and this was instantly followed by a glow-discharge of the usual intensity. The discharge having been established, the mercurial surface soon lost its convexity, first becoming flat and then concave. The change in form was complete within 20 minutes. As in experiment A, free gas appeared in the tube; but in this instance the bubble was distinctly larger.

Experiment C.—The next experiment, C, was made with the apparatus shown in fig. 2 (Pl. XII.). The unseen portion of the barometric tube T was narrow; but the attached cylindrical vessel V had a diameter approximating 28 mm. After the latter had been more than half filled with pure mercury, it was placed in a sand-bath and enclosed with asbestos; the mercury was then boiled and so distilled. During the distillation, the apparatus functioned as a Sprengel pump and quickly produced a high vacuum. When but little mercury remained, the distillation was arrested and V allowed to cool. Finally, the mercurial surface was photographed, the result being that shown in θ_1 (fig. 2). For illustrating the entire reversal of the curvature of the surface, a photograph of a second tube θ_2 having the same diameter as θ_1, but containing mercury in the presence of air, is also shown in fig. 2.

Experiment D.—The final experiment, D, was made to determine what effect the removal of the gas-grown skin might have upon the capillary height of the mercury. Accordingly the apparatus shown in fig. 3 (Pl. XIII.) was constructed. It differed from that of fig. 2 in that it possessed a narrow side-tube *t*. As for the preceding experiment C, so here pure mercury was introduced into the chemically clean and dry apparatus and then photographed (λ_1, fig. 3). Next the mercury was for a time rapidly distilled and a high vacuum produced. This done the flame was removed, the apparatus allowed to cool and a second photograph (λ_2, fig. 3) obtained. In λ_1 we note the usual capillary depression of the mercury in the side-tube *t*. The internal diameter of *t* was 3 mm., and the measured depression 1·8 mm. After the distillation, both the wide and the narrow mercurial surfaces had, according to cathetometer measurements, one and the same level, the mercury in *t* being, as is clearly shown in λ_2, fig. 3, neither depressed nor elevated. The concavity of the surface of the residual mercury is demonstrated in fig. 4 (Pl. XIV.). A numerical value for the actual capillary effect

* It would appear that the thud indicated a sudden and more or less complete rupture of the normal and resistant gas-grown skin.

common to both limbs of the apparatus was found by comparing the corrected length of the mobile mercurial column in the tube T with the mean of the reduced readings of two standard barometers. It was thus found that the mean standard barometer reading differed from that of the tube T by −3·12 mm. Hence the ordinary and negative capillary effect of 1·8 mm. for the narrow limb *t* became, on the removal of the gas-grown skin, a positive one of 3·1 mm., a change totalling 4·9 mm. We conclude with some remarks upon the results obtained in the several experiments.

Remarks.—Elsewhere * I have shown that at air-temperature a glass cylinder, even when maintained in a highly exhausted state for prolonged periods, still retains a gas-grown skin of unchanging density. Such a skin, which may quite appropriately be termed normal and permanent, is equivalent to an infinitely thin-walled tube which, as in the case of a standard barometric column, is interposed between the glass and the mercury. From the experiments A–C (*vide supra*), it seems abundantly clear that this barrier skin or film is initially responsible for the usual capillary depression of mercury. In general, liquids other than mercury instantly dissolve the skin and so come into intimate contact with and wet the glass: hence the familiar capillary elevation. Mercury, as we have seen, exhibits the same phenomenon so soon as the barrier skin has been either electrically erupted (exps. A & B), or destroyed by heat (exps. C & D). It will, however, be observed that the "wetting" of glass by mercury differs from that produced by other liquids: for on raising the tube δ of fig. 1, the mercury drains completely from off the receding surface; with other liquids the glass retains a covering film.

The destruction of a gas-grown skin is gradual rather than instantaneous. This fact may be viewed in two ways:—

(1) If, as Langmuir and others have contended, the depth of the skin is represented by one molecule only, we reach the conclusion that upon the eruption of some of the molecules those remaining are re-arranged and form a more open type of skin or network. As the eruptive action progresses, the meshes of the molecularly constituted net continue to expand until, finally, the whole of the surface under consideration is left utterly bare.

(2) In opposition to Langmuir's views regarding the depth of the skin, we have the result of the preliminary measurement of a normal gas-grown skin alluded to above. That measurement appears to show quite conclusively that the

* Proc. Phy. Soc. vol. xxxvi. pp. 288–290.

depth of a skin permanent at air-temperature and persisting in a high vacuum for nearly three years is most nearly represented by at least twenty strata of molecules. Under these circumstances it is reasonable to suppose that the destruction of the skin is commenced by the ejection of the upper stratum, and that the gradual attenuation is accomplished by the eruption of successive strata, the last to be thrown off being that nearest the glass. But, whatever view be accepted, the variations in curvature and also the growth in the capillary attraction of mercury observed during our experiments, are evidently largely dependent upon the mean thickness of the skin covering the glass.

The positive capillary attraction of 3·1 mm. obtained for mercury in experiment D is, when expressed in terms of water, approximately equal to 42 mm. This height is four times greater than that actually attained by water in a tube having a bore of 3 mm.

In conclusion, it may be stated that, with the object of still further testing the influence of a gas-grown skin, some measurements were made of the capillary attraction of "conductivity" water—(*a*) under usual conditions and (*b*) with tubes freed from gas-grown skins and situated within the highest attainable vacua. The differences noted in the two sets of data were negligible. Whence it appears that for liquids capable of dissolving gas-grown skins positive capillary attractions must invariably obtain.

XCIX. *Apparent Irregularities in Experiments with heterogeneous X-ray Beams, with special reference to the J-Phenomenon.* *By* R. T. Dunbar, *M.A., Ph.D.**

Introduction.

1. SINCE 1916, a number of papers have been published by Barkla and his collaborators, dealing with the results of their experimental researches on the properties of heterogeneous X-ray beams †. These papers deal with

* Communicated by the Author.

† (1) Barkla & Janette Dunlop, Phil. Mag., Mar. 1916.
(2) C. G. Barkla, 'Bakerian Lecture,' 1916.
(3) Barkla & Margaret White, Phil. Mag., Oct. 1917.
(4) Barkla & Rhoda Sale, Phil. Mag., April 1923.
(5) C. G. Barkla, 'Nature,' Nov. 17th, 1923.
(6) " " Nov. 22nd, 1924.
(7) Barkla & Khastgir, Phil. Mag., Jan. 1925.

anomalies which the authors attribute to the existence of a new group of phenomena, to which they have given the name "J-Phenomena." For a full account of these the original papers must be consulted. For the present it will be sufficient to indicate their nature. They possess one remarkable property, that of appearing or not appearing under precisely the same physical conditions, so far as the observers have been able to discover. For example, Barkla writes [(8) p. 1036] : "We do not propose to give a description of the apparatus used in all experiments—they are far too numerous. And it is not easy to see that much would be gained, for the apparatus and arrangement used in experiments showing the J-phenomenon are identical with those in which the J-phenomenon did not occur." In one case, no fewer than three alternative results are to be expected : the experiment consists in comparing the X-radiations scattered at two different angles, by the method of observing the relative ionizations produced by the beams when successive equal sheets of Al (or other absorbing substance) are placed in their path. [(13) p. 550] "We have more recently obtained series of experimental results of both kinds—those showing a difference between the two beams by discontinuities and those showing a difference continuously, in addition to those showing no difference whatever between the two scattered beams."

2. To explain the phenomena, X-radiation is invested with certain new properties : heterogeneous beams are no longer to be looked upon as mere sums of harmonic constituents—they must be regarded as possessing other *additional* properties, which do not belong to any particular constituent or constituents, but to the beam as a whole. The beam is capable of suffering absorptions (additional to those associated with the photoelectric effect, and with scattering) in which every constituent loses the same fraction of its intensity. Such an absorption, it is clear, would

(8) C. G. Barkla, Phil. Mag., May 1925.
(9) Barkla & Gladys Mackenzie, 'Nature,' June 20th, 1925.
(10) Barkla & Khastgir, Phil. Mag., Nov. 1925.
(11) „ „ „ 'Nature,' Feb. 13th, 1926.
(12) C. G. Barkla, 'Nature,' March 27th, 1926.
(13) Barkla & Gladys Mackenzie, Phil. Mag., Feb. 1926.
(14) Barkla & Khastgir, Phil. Mag., Sept. 1926.
(15) Barkla & Gladys Mackenzie, Phil. Mag., Nov. 1926.
(16) Barkla & Watson, Phil. Mag., Nov. 1926.
(17) C. G. Barkla, 'Nature,' May 28th, 1927.
(18) Barkla & Khastgir, Phil. Mag., Oct. 1927.

not modify the relative intensities of the components. Further, this J absorption, as they call it, *may* or *may not* take place—the deciding conditions have not been discovered, —and if it does, it may take place *continuously* or *discontinuously*, the total absorption in a sufficiently thick layer being the same in either case. The discontinuous condensations of energy are considerable, amounting to about 5 or 10 per cent. of the incident intensity, the thickness of the layer receiving the energy being, in the case of aluminium, probably considerably less than one-tenth of a millimetre.

3. To discuss whether these new hypotheses will fulfil their purpose, explaining the many irregularities and apparent inconsistencies observed, would be premature ; for it is not yet clear, as it is hoped in this paper to show, that any modification of the well-established theories is required : much that has been described as conflicting with the existing theories is actually demanded by them. For the purpose of specifying the "quality" of a heterogeneous beam, the half-value mass-absorption coefficient *, invariably used by experimenters in this field, must be described as quite inadequate and misleading, unless the radiations are well filtered ; for, as will be illustrated in the sequel, different heterogeneous beams possessing the same $\bar{\mu}/\rho$ will, according to the accepted theories, not necessarily give anything like the same experimental results when examined by Barkla's methods. Consequently, such experiments are not only incapable of testing existing theory, but are liable to produce results which disagree among themselves. Barkla's standpoint is different : the "irregularities" observed by him, assuming that $\bar{\mu}/\rho$ defines the properties of the beam, have exhibited so pronounced a *regularity* that he has been led to conclude that he has been observing phenomena which depend only upon $\bar{\mu}/\rho$ (rate of absorption as a whole), and not upon the constituent frequencies [(8) p. 1055]. The question of the existence of the J-phenomena is seen, therefore, to be concerned, not so much with the fact that discontinuities have been met with, but with the fact that the discontinuities have consistently appeared at the same points, and have exhibited other regularities.

4. The present paper contains an account of two experiments carried out by the author since his previous paper on

* By trial a thickness x of substance, usually aluminium, is found which, when placed in the path of the radiation, absorbs 50 per cent. If I_0 is the incident intensity, and I the transmitted intensity ($I = 0{\cdot}5\, I_0$ approx.), μ is calculated from $I = I_0 e^{-\mu x}$, and if ρ is the density of the aluminium, $\bar{\mu}/\rho$ is called the half-value mass-absorption coefficient of the heterogeneous beam in aluminium.

the J-phenomenon *. Following this, an attempt is made to derive from theory the types of irregularity which are to be expected when working with heterogeneous beams as if they were nearly homogeneous; these show some resemblance to results which have been described as J-phenomena.

Experiments.

5. The writer's experiments on the J-phenomenon commenced under the direction of Professor Barkla at Edinburgh, in 1919. At that time [see (2) and (3)], the anomalies were attributed to the existence of a J-series of characteristic radiations, for all the evidence was, without exception, in good agreement with this view. Experiments of another kind, conducted elsewhere, however, had begun to throw some doubt on Professor Barkla's interpretation of the results. Duane and Shimizu †, for example, were unable to find any evidence for the existence of J-characteristic rays using an anticathode of aluminium. The writer's experiments were therefore directed to extending the evidence already obtained for the existence of the J-series.

6. In these early experiments of the author's, the X-ray outfit provided consisted of a gas-filled tube, a 10 in. induction coil, and a mercury-gas interrupter. The tube was (apparently) self-rectifying, and the gas pressure within it was regulated by adjustment of the wires leading to the "softening" side-tube. Ionizations were measured by means of gold-leaf electroscopes of the well-known cubical box type. All the experiments which so far had given J-effects in the laboratory were performed with similar apparatus, except that the hammer-break replaced the mercury interrupter. After several months' experience with this simple apparatus, I had failed to obtain any reliable or satisfactory results from it. Irregularities were found, but could not be found consistently. The observational points when plotted had the appearance of being subject to an experimental error decidedly larger than could be accounted for by errors in reading the electroscopes. I suspected that the cause of the trouble was either that the rays were insufficiently filtered (*i. e.*, too heterogeneous) or that the tube's variations were more rapid than could be followed by the means at my disposal. To remove the latter possibility, the gas tube was replaced

* R. T. Dunbar, Phil. Mag., Jan. 1925.

† Duane and Shimizu, Phys. Rev. xiii. p. 288 (1919), and xiv. p. 389 (1919).

by a Coolidge tube, with tungsten anticathode ; but the trouble persisted, suggesting that it arose from the radiations being too heterogeneous. The amount of filtering possible is limited in practice by the intensity of the rays and the sensitivity of the electroscopes. It was necessary, therefore, to increase one or both of these if comparatively homogeneous beams over the desired range of hardnesses were to be obtainable. The intensity was multiplied many times by the substitution of a Mammoth 16 in. coil for the small 10 in. one. With this apparatus consistency appeared for the first time. With the disappearance of inconsistency, however, all evidence of J-effects disappeared also, showing that the conditions necessary for the appearance of J-effects were removed by filtering in this particular set of experiments, and that it would be necessary to revert to the use of thin filters. I preferred to persist with the well-filtered beams, as more likely to give definite results, and with a view to finding whether any irregularities of any kind could be found with them. Some were found in ionization and scattering experiments, but they subsequently received a very satisfactory explanation when the Compton effect was discovered. These later experiments have already been described and discussed *. That Barkla required heterogeneous beams to obtain his J-effects is indicated by the following quotation [(8) p. 1038]: "In many of the following experiments no attempt was therefore made to produce even approximately homogeneous beams, for these heterogeneous radiations provided us with the phenomenon which we wished to examine." It is to be noted that the facts mentioned in this paragraph are not inconsistent with the view that the effects arise from an inadequate description of the heterogeneous beam, for (1) *only well-filtered* beams with the same μ/ρ are sufficiently nearly alike to make a knowledge of the intensity distribution among the wave-lengths, for most practical purposes, superfluous, and (2) it is only with well-filtered beams that the J is definitely absent. So far as the writer's own experience is concerned, every shred of evidence favours this view ; at no time has the radiation ever evinced any of the properties mentioned in § 2.

7. The last experiment carried out in Professor Barkla's laboratory by the author was a scattering experiment. This has been described elsewhere (*loc. cit.* p. 228 et seq.). In this experiment some 5 or 6 observations showed a departure from Compton's theory sufficient to indicate the possibility

* *Loc. cit.*

of some J or other unrecognized effect being present. The indication was so slight that in ordinary circumstances it would probably have been either unobserved or put down to a result of some slight imperfection in the apparatus or method of measurement. Its possible association with the J-phenomenon was the only reason for drawing attention to it. The curve is reproduced here (fig. 1). The feature of the curve is an apparent "step" form, unduly emphasized by the drawing of lines through the observations. Without the lines (as frequently elsewhere) the pattern disappears.

Fig. 1.

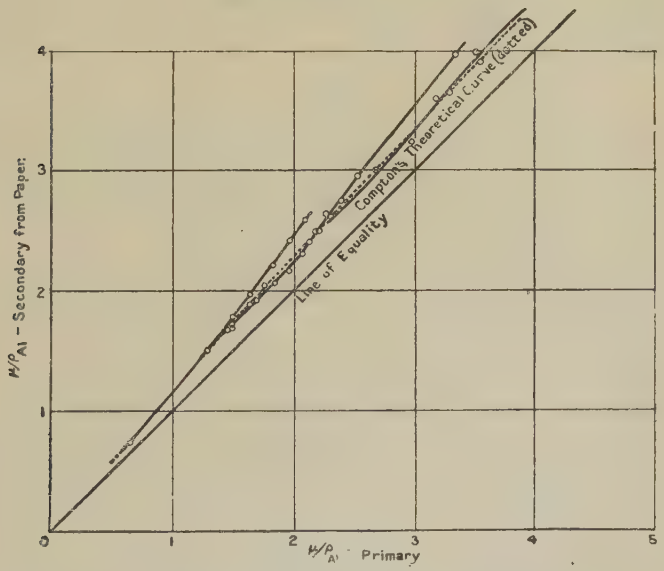

These steps are, according to Barkla and Watson *, J-discontinuities. "In Dunbar's experiments . . . . the discontinuities certainly appeared, but the conditions were not sufficiently controllable, nor was the experiment itself of the kind which was later found most suitable to exhibit the phenomenon." The two experiments about to be described consist of (I.) a repetition of the above experiment under much improved conditions, (II.) an experiment of the kind which in Barkla and Watson's opinion is more suitable for exhibiting the J-phenomenon.

* (16) p. 1122.

Experiment I.

8. Owing to the discrepancies which have appeared between the results of different observers, and even between the results of the same observer with the same apparatus, in experiments upon the J-phenomenon, rather a detailed description of the apparatus and procedure will be expected, and will therefore be given without apology. As the first experiment is merely a repetition of a previous one, and the latter has already been fully treated, it will be necessary to give only the points of difference between the two. For convenience the two experiments will be referred to as A and B, A being the one carried out at Edinburgh in 1923–24, and B recently at Cardiff. The changes adopted, which are for the most part refinements, are given in Table I.

TABLE I.

Experiment A.	Experiment B.
Coolidge tube without rectifier.	Coolidge tube with mechanical rectifier on interrupter.
"Sanax" mercury - paraffin interrupter.	Gas-mercury jet interrupter.
Simple, untilted, gold-leaf electroscope on Secondary.	String electrometer on Secondary.
Secondary X-ray pencil about 4 cm. diameter.	Diameter reduced to 2 cm.
Diameter of ionization - chambers, 10 cm.	Diameter increased to 12·5 cm.
Saturation potential on Primary ion.-chr. 200 volts.	Increased potential to 350 volts.
Runs of tube from 3 to 15 minutes' duration.	Runs were from 2 to 9 minutes.
Recovery interval between readings (allowing tube to cool), 3 to 5 minutes.	Recovery interval 5 to 10 minutes.
Readings were seldom repeated.	Initial reading was, as a rule, repeated after every third or fourth reading, the absolute as well as the relative rates of leak being determined.

9. The method of measuring the relative ionizations in the primary and secondary ionization chambers in the repeated experiment (Expt. B) demands a more extended description. The feeble secondary requires a really sensitive electrometer. Also, the use of deflexion methods for *both* primary and

secondary is not to be recommended, for obvious reasons, if accuracy is aimed at. A string electrometer was used on the secondary, the connexions being depicted in fig. 2 (the Townsend method). The leak is determined in terms of a potentiometer reading. The insulated system of the secondary ionization chamber is connected to one plate of a small air-condenser of capacity 1 cm., approx., the other plate of which is connected to a Varley-Thomson potentio-

Fig. 2.

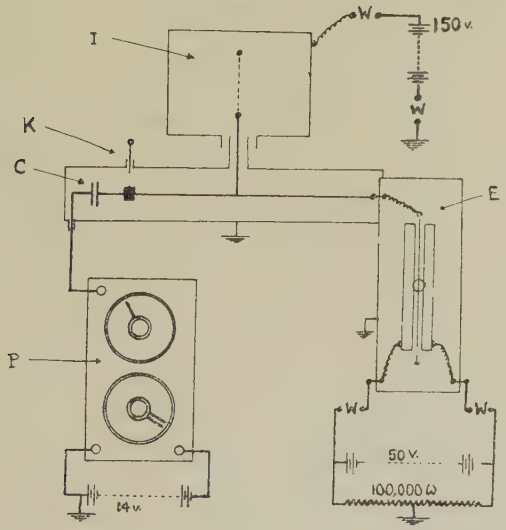

C - Air-Condenser, Capacity about 1 cm.
E - String Electrometer.
I - Secondary Ionisation Chamber.
K - Earthing Key.
P - Varley-Thomson Potentiometer.
W - Water Resistance.

meter. During the incidence of the X-rays, the string of the electrometer is kept on the zero mark (zero potential) by adjusting the potentiometer. Thus, an equal charge to that picked up by the electrode is attracted into the condenser, and its magnitude, being accurately proportional to the change of potential of the other plate, is obtained from the initial and final readings of the potentiometer in arbitrary units. The arrangement was found to be remarkably simple to manipulate, and both sensitive and accurate. It possesses

all the advantages of a null method : (*a*) the readings are independent of the sensitivity and calibration curve of the electrometer: consequently, errors due to accidental variations in the field battery, tension of the fibre, etc., do not come in ; (*b*) the sensitivity (*i. e.*, deflexion sensitivity) can be increased up to the limit of stability without in the least impairing the accuracy ; (*c*) the insulated system is maintained, as nearly as may be, at zero potential, and leaks over insulating supports are therefore negligible ; (*d*) the accuracy is much higher and the readings are dependent on the steadiness of fewer factors than in any deflexion method. In the actual experiment, the readings were estimated to be correct to at least one part in 1000. The error in measuring S/P (*i. e.*, secondary ionization/primary ionization) arose almost entirely from the reading of the primary ionization, for which a less accurate instrument was used.

10. A gold-leaf electroscope of the 3 in. cube type, carefully mounted and shielded from temperature changes, was connected to the primary ionization chamber. The reading microscope was mounted on a travelling carriage, which permitted an exact coincidence of the edge of the leaf with a scale division at the beginning of each run ; the X-rays were switched off when the leaf was exactly coincident with another scale division, 12 removed from the first ; the same pair of scale divisions was used for every run of the tube. This procedure entirely avoided errors due to (*a*) estimation of fractions of a division, (*b*) calibration of the eye-piece scale. The error in measuring the ratio S/P was calculated from some 40 determinations of the ratio with unintercepted radiations. By the method of least squares the probable error of a single determination was found to be one in 350. This accuracy is distinctly better than in Expt. A, in which two simple electroscopes were used, and the ratios determined by timing the "transits" of the leaf-edges across the scale divisions, using a split-seconds stop-watch. The accuracy in the corresponding experiments carried out by Professor Barkla's observers does not appear to have been stated, but from the graphs, and particularly from the information given by Barkla and Khastgir [(10) pp. 1131–2], the accuracy of measurement of ratios of ionizations in single experiments appear to have been approximately the same as in the author's present experiments.

11. The results of the experiment are shown in Table II. and in fig. 3. A comparison of figs. 1 and 3 will show that what has been described as a J-effect has been eliminated.

Table II.

Observed differences in the half-value mass-absorption coefficients for Aluminium, between Primary X-rays and the Secondary at 90° from Filter-paper.

	Filter-paper radiator.	Aluminium filtering incident beam.	Per cent. absorption for next columns.	Primary $\bar{\mu}/\rho$ (Al).	Observed $\delta\bar{\mu}/\rho$ (Al).	Theoretical $\delta\mu/\rho$ (Al) (maximum).
	sheets.	mm.				
1	100	0·5	47	1·61	0·24	0·22
2	,,	0·5	46	1·80	0·23	0·24
3	,,	none	51	2·07	0 26	0·27
4	,,	,,	51	2·10	0 26	0·27
5	,,	,,	42	2·26	0·34	0·29
6	,,	,,	54	2·27	0·27	0·29
7	,,	,,	57	2·34	0 34	0·30
8	50	0·5	50	1·76	0·25	0·24
9	,,	0·5	54	1·95	0·31	0·26
10	,,	0·9	40	2·05	0·23	0·27
11	,,	none	50	2·29	0·30	0·29
12	,,	,,	57	2·30	0·30	0·29
13	,,	,,	45	2·42	0·30	0·30
14	,,	,,	56	2·62	0·26	0·32
15	,,	,,	52	2·67	0·30	0·33
16	,,	,,	51	2·84	0·35	0·34
17	,,	,,	41	2·90	0·32	0·35
18	,,	,,	52	2·95	0·36	0·36
19	,,	,,	43	3·20	0·40	0·38
20	,,	,,	54	3·39	0·35	0·39
21	,,	,,	45	3·42	0·34	0·40
22	,,	,,	46	3·50	0·38	0·40
23	,,	,,	43	3·58	0·33	0·40
24	,,	,,	42	3·63	0·40	0·41
25	,,	,,	61	3·80	0·39	0·42
26	,,	,,	61	3·86	0·38	0·43
27	,,	,,	55	3·97	0·39	0·44
28	,,	,,	51	4·02	0·47	0·44
29	,,	,,	46	4·12	0·46	0·45
30	,,	,,	57	4·15	0·39	0·45
31	,,	,,	41	4·25	0·39	0·46
32	,,	,,	54	4·39	0·36	0·47
33	,,	,,	42	4·43	0·42	0·47
34	,,	,,	52	4·66	0·43	0·49
35	,,	,,	45	4·82	0·43	0·50
36	,,	,,	40	4·92	0·53	0·51
37	,,	,,	53	5·06	0·43	0·52

An examination of the differences between the two experiments, however, does not bring us any nearer to the origin of the J-phenomenon ; it merely indicates that the effects, whatever they are, are removed by refining the measurements and the experimental procedure. The radiations were apparently quite as heterogeneous in the second as in the first case, judging by the thickness of the filters and of the scatterer. The whole point of repeating the experiment

Fig. 3.

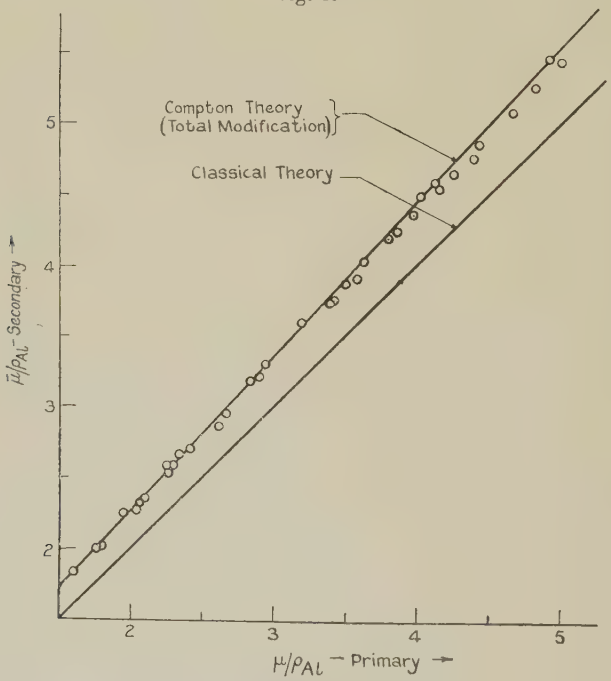

Primary heterogeneous.
Secondary from paper.
Secondary at 90° from Primary.

was to verify the existence of the irregularities, which, if found again, would be a definite starting-point for an investigation of J-effects. Refinement was aimed at, without altering the conditions except in so far as to make them less variable. The negative result very strongly favours the view that the effects in the previous experiment were not fundamental. In the writer's opinion they arose from prolonged exposures and the presence of inverse current.

Experiment II.

12. The second experiment, which is now about to be described, is one in which the two radiations, primary and secondary, are compared with each other, not by observing their half-value coefficients of absorption as in Experiment I. (which is done by intercepting the radiations with a single sheet), but by what would appear to be a more thorough method, namely, by observing the *relative* rates of extinction of the beams as a result of interposing a gradually-increased thickness of filter. This method was introduced by Barkla, and the experiment is one which has been repeated so often in his laboratory (altering the radiator, material of the absorbing sheets, angle of scattering, etc.) that it appears to represent something like half of the published experimental work on the J-phenomenon. It is the method which Barkla and Watson consider the most suitable for exhibiting the J-phenomenon.

13. The procedure is obvious and the theory (for homogeneous radiations) simple. Let S_0 and P_0 be the intensities of the unintercepted secondary and primary radiations, as measured (the only convenient way, though liable to misinterpretation) by ionization. If the same gas is used in the two ionization chambers, and they are identical in every respect and placed at the same distance from the scatterer, if, also, the gas has no characteristic radiation of wave-length in the neighbourhood of the wave-lengths used, nor any very appreciable amount of "recoil" ionization, it has been shown both by Compton's theory and by experiment (see, for instance, Dunbar, *loc. cit.* p. 233) that S_0/P_0 is a constant, independent of the wave-length *. If S and P are the intensities (ionizations) when a thickness of aluminium or other substance, equal to x, intercepts both beams, we have at once, assuming exponential absorption and that the radiation is completely modified in scattering,

$$\frac{S}{P} = \frac{S_0}{P_0} \cdot e^{-\delta\mu \cdot x} \quad . \quad . \quad . \quad . \quad . \quad . \quad (1)$$

for a single frequency constituent, the increase of whose absorption coefficient in the aluminium or other substance associated with the Compton effect is $\delta\mu$. For a continuous

* To the first order of small quantities.
Consider only the radiation scattered at 90° here as elsewhere throughout the paper.

heterogeneous beam, it can be easily shown that the result is

$$\frac{S}{P} = \frac{S_0}{P_0} \cdot \frac{\int_0^\infty i(\lambda)\, e^{-(\mu+\delta\mu)\cdot x}\, d\lambda}{\int_0^\infty i(\lambda)\, e^{-\mu\cdot x}\, d\lambda}, \quad \ldots \quad (2)$$

where $i(\lambda)\, d\lambda$ is the intensity distribution of the primary beam and μ is the absorption coefficient in Al of radiation of wave-length λ. For a beam consisting of lines of wave-lengths $\lambda_1, \lambda_2, \ldots$, of intensities $i_1, i_2 \ldots$, respectively, the corresponding result is

$$\frac{S}{P} = \frac{S_0}{P_0} \cdot \frac{\Sigma i_r\, e^{-(\mu_r+\delta\mu_r)x}}{\Sigma i_r\, e^{-\mu_r x}} \cdot \quad \ldots \quad (3)$$

For unmodified scattered radiation—that is, if the radiation is scattered according to the classical theory—the relation between S/P and x degenerates into

$$\frac{S}{P} = \frac{S_0}{P_0} \cdot \quad \ldots \quad (4)$$

14. The curves obtained by experiment are to be compared with the above four theoretical relations. (1) is evidently a ratio which falls steadily (exponentially) with increasing x; (4) will give a constant ratio—that is to say, a horizontal straight line—if the ratio is taken as ordinate and x as abscissa. The relation (2) I have been unable to work out, even for simple laws of distribution. (3), which is for a line-spectrum, is simple but lengthy in calculation, and a few examples have been worked out with a view to obtaining *first approximations* to the solutions for continuous distributions, which are, of course, the type of radiations we experiment upon. Rough solutions of the relation (2) have been arrived at in this way. These calculations will be discussed later.

15. The results obtained in Professor Barkla's laboratory are of three types, those in which S/P is constant for all values of x, indicating, as the authors presume, *unmodified* scattering; those in which the ratio falls steadily with increasing x, resembling relation (1), which is for homogeneous beams and Compton scattering; and, finally, an apparent combination of these two—the ratio is constant up to a certain value of x and then suddenly makes up for lost time, as it were, by falling to a lower value, at which it

remains constant for further increases of x, and so on [see fig. 4, reproduced from (16)]. The discontinuous changes in the third type are of the order of 5 to 10 per cent.

16. The first and second types (continuously constant and continuously falling) will be shown later to be *both* in conformity with the Compton effect, although the former has been very naturally interpreted as evincing unmodified scattering. It will appear that when the heterogeneous beam contains both very hard and very soft radiations of approximately equal intensities, the relation (2) (or more accurately (3)) shows that the ratio is almost accurately constant over a considerable range of values of x, in spite of the full Compton change of wave-length. The unexpected result is accounted for by the fact that filtering, which invariably transmits a more penetrating beam hardens up the secondary

Ionization by scattered radiation
Ionization by primary radiation

Fig. 4.

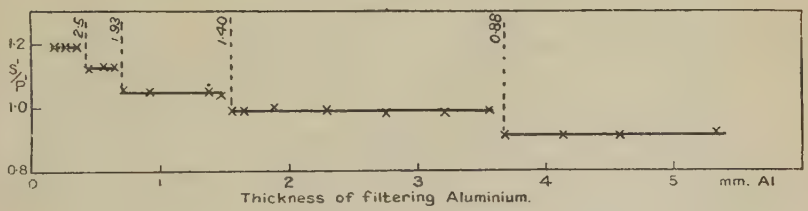

W target: 60 kv. peak.

(with heterogeneous rays) more rapidly than the primary, till, with certain beams at least, the secondary, originally the more absorbable, is more penetrating than the primary: this state of affairs does not persist however, for the primary in the long run is the more penetrating. For a considerable range of values of x, the two beams are almost exactly of the same penetrating power (though differently constituted). The third (discontinuous) type of result is in quite a different category. Discontinuous absorption of a heterogeneous beam cannot be accounted for on any theory which assumes that the beam is merely the sum of its constituents. This type will be considered later.

17. The author's experiment was carried out with exactly the same apparatus as in Experiment I. The procedure in taking the observations is the only point of difference. The interpretation of the results is not, however, quite so simple as would at first sight appear. The following

points are evidently to be considered before observations are taken :—

(1) The assumption is made that the same heterogeneous beam can be maintained unvaried for an hour or two. The 21 observations in fig. 4, for instance, taken from Barkla and Watson's paper, must have required from one to two hours of actual running of the tube. The intensity distribution in the X-ray beam depends on the temperature of the cathode if a Coolidge tube is used, and on the temperature of the tube itself if a gas-tube. It varies to a certain extent also as the coils of the transformer become warm. Variations are therefore to be expected, and some method of watching for changes devised. In the author's experiment, each reading was timed with an accurate stop-watch, and certain readings were repeated at intervals. Column 2, in Table III., gives the time in seconds for a leak of one division on the primary.

(2) The gas must be the same in both ionization chambers, and conform to the conditions stated in para. 13. Air must be ruled out as unsuitable, for this gas has been observed by the author to be subject to a marked increase of ionization relative to intensity of X-rays when the radiation is shortened in wave-length through the region of 0·4 Å (*loc. cit.* p. 227), the increase being due to the recoil electrons. Such a characteristic would naturally produce a fold on the curve for S/P if the Compton modification were present—a fold, in fact, should appear for both oxygen and nitrogen, but the two would probably run into one. Sulphur dioxide would give a similar result on account of the *oxygen* it contains, but, as the latter gives only some 8 per cent. of the ionization of SO_2, the effect is negligible. The recoil ionization from *sulphur* does not appreciably affect the results within the range of these experiments, consequently SO_2 was selected. That this selection was justified was proved by a control experiment in which the secondary from copper (almost entirely copper K, as tested by absorption in Al) was compared with the primary over the whole range of radiations to be used, the intensity being measured by SO_2 ionization. The curve was smooth and only slightly sloped, showing that the primary (in which alone the wave-length was changing) was smoothly represented in intensity by the ionization it produced in SO_2.

(3) If any irregularity in the ratio S/P is observed, it must be possible to say whether it arises from a change in S, or in P, or in both. This can only be provided for by timing all observations. This was done. Actually no irregularities were observed which would not be covered by observational error and slight variations in the radiation.

In Barkla's experiments all irregularity is ascribed to the secondary, but it is not clear how this conclusion was arrived at. The point is of considerable consequence, for if the observations were timed, and the secondary was found to vary suddenly by some 5 to 10 per cent., *by time*, while the primary remained perfectly regular, the origin of the 5 to 10 per cent. J-discontinuity would justifiably be ascribed to some "post-scattering" process. Without the experimental data, however, the possibility must still remain that the irregularities arose from the source of most irregularities in X-ray work, the X-ray tube. A change in the incident X-rays would affect both P and S, but in general to different degrees. Such changes could be detected at once from the *absolute* rates of leak.

18. Table III. and fig. 5 contain the result of the author's experiment. The curves exhibit no discontinuities such as have been found in Barkla's experiments. There are minor irregularities in curvature, but these will be seen to be

TABLE III.

Comparison of Primary and Scattered (90°) by progressive absorption with aluminium sheets.

	Time per div. (P).	x (Filter).	S/P.
	sec.	mm.	
	17·1	nil	1·000
1.	46·2	(0·38)*	1·000
$\bar{\mu}/\rho$	?	0·19	·971
(Al)	28·5	0·39	·946
4·7	35·4	0·58	·935
	17·0	nil	1·000
	13·2	nil	1·000
	22·5	0·46	·950
2.	34·0	0·91	·905
$\bar{\mu}/\rho$			
(Al)	34·6	(0·91)	·990
4·2	34·5	0·91	·907
	22·5	0·46	·940
	13·5	nil	1·000

	Time per div. (P).	x (Filter).	S/P.
	13·3	nil	1·000
	23·0	0·46	·948
	24·6	0·55	·933
3.	13·0	nil	1·000
$\bar{\mu}/\rho$	27·0	0·65	·920
(Al)			
4·2	29·7	0·75	·923
	13·6	nil	·998
	30·8	0·75	·923
	28·8	0·65	·938
	19·3	nil	1·000
	21·5	0·10	·978
4.	23·4	0·19	·965
μ/ρ	25·8	0·29	·962
(Al)	28·2	0·39	·954
3·7			
	18·5	nil	1·002

* Filters in brackets were placed in the path of the incident beam, otherwise they were in the paths of secondary and primary after incidence on the radiator, which consisted of 50 sheets of filter-paper.

TABLE III. (*continued*).

Comparison of Primary and Scattered (90°) by progressive absorption wtth aluminium sheets.

	Time per div (P).	x (Filter).	S/P.
	sec.	mm.	
	14·0	nil	1·000
	16·8	0·19	·994
	?.	0·39	·966
5. μ/ρ (Al) 3·4	24·1	0·58	·958
	13·6	nil	1·003
	23·7	0·58	·947
	19·3	0·39	·967
	16·3	0·19	·978
	13·5	nil	1·003
6. μ/ρ (Al) 3·4	?	nil	1·000
	18·8	0·46	·942
	11·7	nil	·990
	19·5	(0·46)	·987
	20·4	0·55	·934
	21·9	0·65	·929
	23·3	0·75	·921
	12·0	nil	·995
	27·5	0·91	·914
	30·5	1·10	·898
	29·8	(1·10)	·992
7. $\bar{\mu}/\rho$ (Al) 3·0	12·8	nil	1·000
	19·3	0·46	·953
	12·7	nil	·988
	21·8	0·65	·929
	26·2	0·91	·908
	30·4	1·10	·903
	12·7	nil	·990
	30·2	(1·10)	·990
	35·1	1·36	·896
	?	nil	·993
8. μ/ρ (Al) 3·0	10·5	nil	1·000
	17·7	0·46	·960
	19·6	0·65	·945
	21·9	0·91	·928
	10·6	nil	1·017
	23·3	1·10	·924
	26·8	1·36	·925
	27·4	(1·36)	1·008
	11·0	nil	1·008

	Time per div. (P).	x (Filter).	S/P.
	sec.	mm.	
	10·4	nil	·997
	15·4	0·46	·945
	9·7	nil	·997
9. $\bar{\mu}/\rho$ (Al) 3·0	19·5	0·91	·905
	25·6	1·36	·868
	32·8	1·82	·845
	9·7	nil	1·006
	35·4	1·82	·859
	28·9	1·36	·890
	22·7	0·91	·914
10. μ/ρ (Al) 2·9	12·0	nil	1·000
	16·7	0·46	·960
	20·5	0·65	·946
	17·7	0·46	·965
	24·7	0·91	·920
	10·9	nil	1·008
	21·4	0·91	·923
	27·3	1·36	·908
11. $\bar{\mu}/\rho$ (Al) 2·3	11·8	nil	1·000
	27·2	(1·36)	·998
	25·4	1·36	·884
	22·3	1·10	·910
	20·4	0·91	·924
	17·5	0·65	·936
	15·2	0·46	·935
	26·4	1·36	·896
	10·8	nil	·989

perfectly accounted for by the Compton theory in a later paragraph. Curves such as these are found amongst Barkla's results, and are not excluded by his "laws of the J-Phenomenon." Barkla, however, has hinted that where continuity is observed it is probable that the result is a statistical mean of discontinuities. Thus [(16), p. 1126], ". . . . it would be expected that under variable conditions these

Fig. 5.

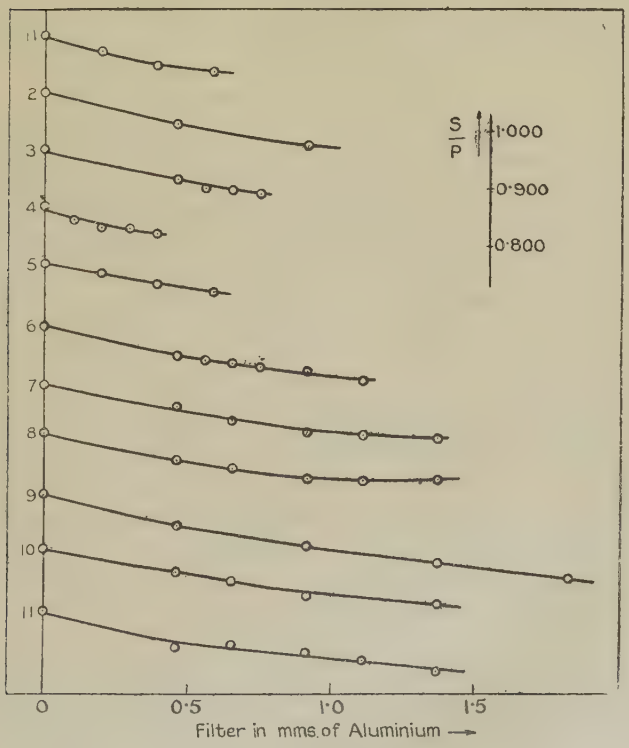

P'_s = Ionization by Primary (heterogeneous).
S = Ionization by Secondary from paper, 90° from Primary.
The radiations are compared by progressive absorption.

discontinuities would be spread out and would show an apparently steady higher absorption of the scattered than of the primary radiation, such as has frequently been found in experiments on the progressive absorption of both beams. This suggests that all the apparent differences between scattered and primary radiations as shown by some absorption

experiments may be fundamentally made up of such discontinuities." A comprehensive survey of the results obtained by all his observers, however, shows, on the average, a pronounced tendency for the results to be either *a* or *b*—*i. e.*, either obviously smooth or obviously discontinuous. We cannot suppose that the conditions of running may be so neatly divided into two—that the steady can be differentiated from the unsteady with such certainty. In the author's curves, Nos. 1 to 7, fig. 5, the average difference between repeated readings in the rate of leak was only about two and one-half per cent., although the set of readings in each case was spread over a period of about two hours. It is hardly credible that there was sufficient unsteadiness present to mask so completely what with steady conditions would have been a set of "stepped" patterns, like (Barkla and Watson's) fig. 4. Curves 8, 9, 10, and 11, fig. 5, were obtained under much less steady conditions, the time variations between some of the repeated readings being as great as 15 per cent. The curves are arranged in the order of the absorbabilities, not in the order of observation. The unsteadiness is to be attributed therefore to some effect which appears when the penetrating power of the radiation exceeds a certain value. It will be shown later that there is some evidence that the tungsten K-lines were excited to an appreciable extent in these unsteady radiations, but not in the other cases. This would account quite naturally for the instability. It is worthy of remark that the curves include examples for both very steady and very unsteady conditions; nevertheless, there is little if anything to distinguish the smoothness of one set of curves from that of the other. It appears to be clear that the step pattern was not simply obscured—it was entirely absent.

19. The only other published results, outside of Professor Barkla's laboratory, on the examination of scattered radiations by the method of progressive absorption are, so far as I have been able to find, those of B. L. Worsnop*, at King's College, London, and those of O. Gaertner †, at the Röntgen-Forschungsinstitut der Universität, Bonn. In both cases, in spite of the care and skill with which the experiments were evidently carried out, the discontinuities failed to appear. The fact that with Barkla's observers the search for J-effects has, more often than not, been successful while others have

* B. L. Worsnop, Proc. Phys. Soc. xxxix. p. 305.
† O. Gaertner, *Phys. Zeit.*, 15th July, 1927.

consistently failed, is one for which a simple explanation ought to be forthcoming. Barkla has suggested that, if the J does not appear, one ought to keep on modifying the apparatus till it does appear (Brit. Assoc. 1927). Considering that his observers have found the J with almost every conceivable combination of apparatus, and that others have used transformers, induction-coils, and hot cathode tubes of different kinds without success, the necessary modifications would appear to be in the lesser details of apparatus regarding which we have so far received little information.

Theoretical.

20. The comparison of scattered and primary radiations by the method of progressive absorption gives a relation between the ratio, S/P, and the thickness of filter, x, placed in the path of both beams. If the object of the experiment is to find out which of the two processes of scattering is operating, the classical or the quantum, the theoretical consequences of both theories have to be calculated and the observed results compared with the theoretical. The method breaks down if the observed result is in agreement with *both* theories; and this appears to happen if the very absorbable components in the heterogeneous beams are incident upon the radiator and form an important part of the scattered intensity (as measured by ionization).

21. The theoretical result for heterogeneous beams in the case of classical scattering is simple; the ratio S/P is a constant independent of x, so long as the scattering coefficient of the material of the radiator is the same for all the wave-length constituents. The quantum theory (Compton) has been shown to give the results expressed in the relations (1), (2), and (3), in para. 13. Before applying these it has to be remembered that a certain amount of absorption subsequent to scattering is present even when x is zero—absorption by the radiator itself, by the atmosphere, and by the windows of the electroscopes. Allowance has to be made for this in calculating the $\bar{\mu}/\rho$ which would be observed for the unintercepted radiation—the effect on the S/P curve is merely a slight shift of origin. It has been assumed in the following that the *equivalent* thickness of aluminium absorbing the P and S radiations, additional to the sheets, x, is 0·2 mm.

22. Assuming the relation $\mu=\sigma+a\lambda^3$, where σ is independent of λ, and a is a constant for the absorbing

material, σ, equal to about 38·34 cm.$^{-4}$ for aluminium if the wave-lengths are in Ångström Units, I have calculated results for six cases, with each of which the μ/ρ to be observed is exactly the same, making a comparison of the results all the more easy to interpret. The constituent radiations and their relative intensities are given in Table IV. and the curves for S/P appear in fig. 6. With each of these beams the $\overline{\mu}/\rho$ to be

TABLE IV.

Wave-length Components and their Relative Intensities, from which the curves in fig. 6 were calculated.

No. of Curve.	0·20 Å.	0·35 Å.	0·50 Å.	0·70 Å.	0·85 Å.	1·00 Å.
	per cent.	per cent.	per cent.	per cent.	per cent.	per cent.
1	32·9	—	—	—	—	67·1
2	—	39·7	—	—	60·3	—
3	—	—	46·5	53·5	—	—
4	22·25	—	—	77·75	—	—
5	—	—	59·8	—	—	40·2
6	30	—	—	25	—	45

observed (with Al) is 3·2, which is the mass-absorption coefficient of homogeneous radiation of wave-length 0·6 Å. The results are obtained by using relation (3) in para. 13. They show at once that the result to be expected on Compton's theory depends very much on how the intensity is distributed amongst the wave-lengths. Curves 1, 2, and 3 give a first approximation to results for beams which are very broad, broad, and fairly narrow, respectively, for the wave-lengths they contain are far separated, well separated, and rather close together, respectively. The curves are seen to be intermediate between the classical and the Compton results for *homogeneous* radiation—1 is scarcely distinguishable from the classical result over a considerable range, while 3 is very nearly the Compton result for a *single* constituent. Curve 4 is for a beam with one constituent slightly more absorbable, and the other considerably more penetrating, than the pair together, while curve 5 is for the converse, one component slightly more penetrating and the other very absorbable. The latter is scarcely distinguishable from 3 and the curve

for homogeneous radiation. 4, however, after dropping regularly, rather suddenly changes its direction and runs horizontally. [This feature can be observed in some of the author's experimental curves in fig. 5. It possibly arises from the presence of K-tungsten radiation, from the anti-cathode, superposed on the general radiation. That the ratio S/P should tend to become constant after falling steadily was so unexpected a result that it caused considerable trouble at the time, repeating observations, and testing to see if anything had altered. It was only after these calculations

Fig. 6.

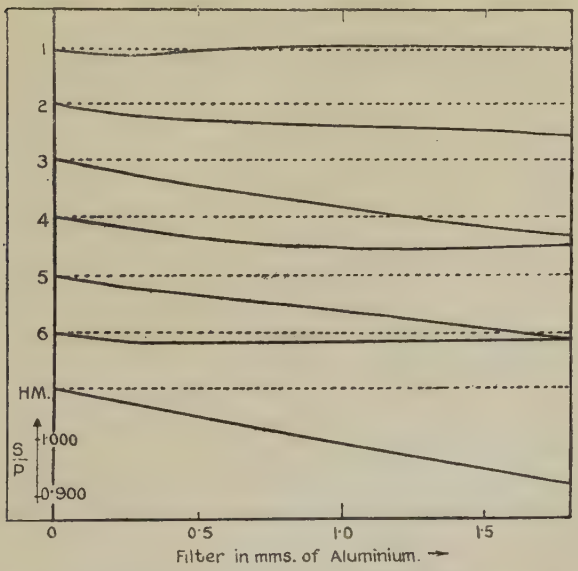

Theoretical curves to be compared with fig. 5. (The broken lines are merely horizontal rulings to aid the eye.)

Each beam has the same $\bar{\mu}/\rho$ for Al (see Table IV.), the curve marked "HM." being for a homogeneous beam.

had been completed that it was seen that the result was quite in keeping with theory.]

23. It must be clear that by a proper selection of wave-lengths and intensities, not restricted to two components only, it is possible to build up synthetically any curve whatever, within reason, lying between the classical and the quantum result for homogeneous rays. Curve 6 is a simple example.

It consists of three components: 0·2, 0·7, and 1·0 Å, with intensities in the ratio 6 : 5 : 9. It is a combination of curves 1 and 4 in the proportion of 2 : 1, very nearly. The values of S/P to be observed, as the thickness of absorbing aluminium is increased by steps of 0·2 mm. up to 3 8 mm., are, respectively: 0·975, 0·963, 0·959, 0·959, 0·959, 0·960, 0·961, 0·961, 0·962, 0·962, 0·961, 0·961, 0·960, 0·959, 0·958, 0·956, 0·954, 0·953, 0·951, 0·949. This constancy of ratio must be described as remarkable, for the rates of absorption of the corresponding constituents are very different, and it is only by a complicated process of *compensation* that the rates of absorption of the beams as a whole are so very nearly indistinguishable. Further, by adding more constituents in the proper proportion, the result may clearly be indefinitely improved upon. It seems possible that for a *continuous* beam, sufficiently broad, the result would be so perfect that absorption by aluminium subsequent to scattering would be quite incapable of distinguishing between classical and quantum scattering. [If this is true, and it has the appearance of being approximately so, it seems worthy of remark that this is a second, and independent, respect in which *compensation* appears to prevent absorption from distinguishing between quantum theory and classical theory; for, as pointed out originally by A. H. Compton, and frequently verified by experiment, the ratio of primary to secondary ionizations (for 90°, at least), with unintercepted radiations, is independent of wave-length whether the scattering is classical or quantum, the falling off of the *absolute* intensity of the secondary beam in the latter case with decrease of wave-length being, to the first order, exactly compensated for by the increased absorption by the gas, arising from the Compton increase in wave-length.]

24. The general conclusions to be drawn from fig. 6 are:

(*a*) The Compton effect, which requires an exponential fall in S/P with increasing x, for homogeneous beams, does not require such a fall if the beam is heterogeneous.

(*b*) The more widely the intensity is spread through the scale of absorbabilities—that is, the more heterogeneous the beam in the sense of absorbability (not necessarily in that of wave-length)—the closer apparently will the curve resemble that for classical scattering, a horizontal straight line.

(*c*) Very absorbable elements of the beam tend to produce an early flattening out of the curve, less absorbable elements produce the same effect later, while the presence of elements of all absorbabilities over an extended range, in the proper

proportion, would seem to give a horizontal curve over a correspondingly large range of values of x.

(*d*) The rate of fall of the curve is, on Compton's theory, influenced more by the degree of heterogeneity (in the absorbability sense) of the beam than by the half-value absorption-coefficient.

25. These conclusions invalidate a good deal of evidence that has been cited as disproving the existence of the Compton effect. For example ((17) paragraph 3), a systematic examination of the radiations scattered by different thicknesses of radiator showed that the difference in absorbability between secondary and primary was *steadily* diminished as the radiator was made gradually thinner. From this it was inferred that the change in absorbability was a gradual one brought about by the passage of the radiation through matter (the material of the radiator), and not a sudden one as visualised in the Compton effect. This, however, is exactly the result which the considerations above would lead us to expect. The incident radiation is, on the average, filtered by half the thickness of the radiator before it is scattered; consequently, a thick radiator would be expected to give a curve like 3, fig. 6, a thinner one a curve like 2, while a very thin radiator would give rise to a curve resembling 1, provided the X-ray beam in each case contained a considerable proportion of very soft elements. If for some reason the soft elements were absent—as, for instance, by wandering of the focal spot from an excrescence to a pit, and consequent filtering by the target—the Compton modification would appear to approximately the same extent, independent of the particular thickness of the radiator. This effect was observed by the same author, but was accounted for in a different way (*loc. cit.*).

26. A further illustration of how heterogeneous beams may give results which at first glance appear to contradict theory is afforded by the experiments described in (18), p. 738. A scattered radiation when tested by aluminium, copper, or gold was found to be a "modified" radiation, while the same scattered beam when tested by silver or tin (both of which substances have their K-absorption edge within the limits of the spectrum of rays tested) was found to be "unmodified"; that is, the former elements perceived a Compton change in the scattered beam, while the latter (silver and tin) found the scattered and primary radiations equally absorbable. This interesting

observation turns out to be a natural consequence of conclusion (*b*) arrived at above (paragraph 24), and is readily understood so soon as we perceive that the heterogeneity which masks the Compton effect is a heterogeneity in the sense of *absorbability* with respect to the testing substance, not necessarily in the sense of wave-length. What would be a comparatively homogeneous beam to Al, Cu, and Au, might well contain *extremes* of absorbability with Ag or Sn, if the bulk of the intensity were situated in the region of the K-absorption edge. In such a case, Compton's theory would predict that Al, Cu, and Au would find full modification, while Ag or Sn would show little if any evidence of modification. Now, let the intensity distribution be disturbed slightly—the proportion of intensity on the two sides of the absorption edge may well be sufficiently upset to give a "modified" curve with silver or tin. Such a change was observed by these authors.

27. The stepped curves obtained by Barkla and his observers will now be considered. A typical example is reproduced in fig. 4. The steps are from 10 to 20 times the probable error of experiment. This is not an isolated case : a considerable number of similar curves will be found in the works cited at the beginning of this paper. It must be clear that, although the curves in fig. 6 could account for irregularity in an observational curve as arising from slight variations in the X-rays delivered by the tube, the regularity exhibited by fig. 4 is not to be explained by such a fortuitous source of change. There can be but two possible explanations—either systematic error, arising from apparatus or procedure, or the existence of a new phenomenon ; no very obvious explanation in terms of systematic error seems to offer itself : an interpretation in terms of a phenomenon seems to present considerable difficulty also. Barkla's hypothesis of sudden condensations of radiant energy upon the absorbing sheets in the case of the scattered radiation seems to disregard the fact that the gas in the ionization chamber is also a "thin absorbing sheet," and that, according to his own observation in other experiments, the ratio S/P ought, therefore, to exhibit rising as well as falling steps on account of "sudden increases in ionization," associated with J-absorption by the gas ((12) para. 3). For this reason, an explanation in terms of an absorption process, subsequent to scattering, seems to be ruled out.

28. Finally, attention must be briefly directed to the

original J-experiments—those which indicated that there was a new series of characteristic radiations. It appears more than likely that the ionization irregularities [(2) p. 350] arose from "recoil" ionization, associated with the Compton effect. The results of the scattering experiments need not be considered [see (2) pp. 355–6]. The absorption experiments [see (3)] have been interpreted without taking into account the fact that the beams were not homogeneous. A 50 per cent. absorption of a heterogeneous beam by a light substance, such as aluminium or paper, gives a transmitted beam different to that which would be obtained by a 50 per cent. absorption by copper, for in the previous case a great part of the absorption is by *scattering*, which has little effect in quenching the longer wave-length constituents. In other words, *the lighter substance collects its 50 per cent. in a different way from the constituents to copper, and therefore the absorptions are not comparable.* In the case of homogeneous beams this objection does not arise. The magnitude of the error arising when absorption coefficients are compared, using heterogeneous beams and Barkla's 50 per cent. test, will depend on how heterogeneous the beams are, and the disparity between the two absorbing substances as regards the relative values of scattering and true absorption. The error is invariably in the direction of giving the lighter relatively too high an absorption coefficient. The following calculated examples, using, as in a previous section, two wave-lengths instead of a continuous beam, will show that the error in practice is not one which may be ignored unless the radiations are well filtered. Here, as elsewhere, irregularities are to be expected, if the radiations are not well filtered. Irregularities have been found by Barkla, using lightly filtered beams; no irregularities were found by the author when thick filters were used (Dunbar, *loc. cit.* p. 217).

29. Each of the following pairs of wave-lengths, when taken in the proportions given, will, as a combined beam, have the half-value mass-absorption coefficient in copper, 6·0 *. If heterogeneity did not matter, the corresponding $\bar{\mu}/\rho$ to be observed for aluminium would be 0·673 in each case. Calculation on the accepted views, that the phenomena of scattering and fluorescent absorption are concerned with the harmonic constituents only, and not

* For these calculations, the numerical values have been taken from A. H. Compton's 'X-rays and Electrons,' 1927, p. 185.

with the beam as a whole, gives the following very different values for $\bar{\mu}/\rho$ in Al :—

43·2 per cent. of 1·1 Å with 56·8 „ „ 0·175	gives $\bar{\mu}/\rho$, Cu = 6·0 ; $\bar{\mu}/\rho$, Al = 1·26	
31·3 per cent. of 0·9 Å with 68·7 „ „ 0·25	„ „ „	0·807
31·45 per cent. of 0·7 Å with 68·55 „ „ 0·25	„ „ „	0·798
32·45 per cent. of 0·60 Å with 67·55 „ „ 0·25	„ „ „	0·759
54·69 per cent. of 0·40 Å with 45·31 „ „ 0·25	„ „ „	0·684

Now, the value 6·0 for the μ/ρ, Cu, was selected because it was at this point that Barkla and Miss White (3) observed a step in the curve, comparing the coefficients of Cu and Al. The extreme values of μ/ρ, Al, observed by them were 0·707 and 0·766. It is suggested that the step corresponds simply to a marked difference in the degree of heterogeneity in the two cases, and that the irregularities in all the absorption-coefficient curves, ascribed by Barkla to the existence of a J-series at one time and to a J-transformation later, are intimately bound up with the fact that a heterogeneous beam is insufficiently specified by the half-value absorption coefficient.

Summary.

(1) Two experiments are described which aimed at discovering the J-discontinuities in the absorption of scattered X-radiation (heterogeneous). The results were negative.

(2) The results obtained by Barkla and his collaborators are discussed. It is shown that much of the irregularity they observe is only apparent, that it possibly arises largely, if not altogether, from the assumption that a heterogeneous beam should give sufficiently nearly the same results as a homogeneous beam, the latter having an absorption-coefficient equal to the half-value absorption-coefficient of the former. The progressive absorption method, for instance, frequently used by them to test for the Compton effect, is not suitable

unless the radiation is homogeneous, or nearly so ; for very heterogeneous beams it is unable to distinguish between classical and Compton scattering. It is suggested that the pronounced irregularities observed by the above authors are associated with the varying amounts of extremely soft radiation which may succeed in reaching the electroscopes.

In conclusion, I wish to thank the Royal Society for a grant towards the purchase of apparatus required for the experiments. I gladly take this opportunity also for expressing my great indebtedness to Professor H. Robinson, who has been keenly interested in this research and has been most helpful in many ways.

Viriamu Jones Laboratory,
University College, Cardiff.

C. *On the Cause of the Loss of Thermionic Activity of Thoriated Tungsten Filaments under certain Voltage Conditions.* *By* Ann Catherine Davies, *D.Sc.*, *and* Rhoda N. Moss, *M.Sc.**

EXTENSIVE investigations of the thermionic emission from thoriated tungsten filaments have been carried out by Langmuir †, whose conclusions in regard to the behaviour of such filaments may be briefly summarized as follows :—

The electron emission from a tungsten filament which contains a small amount of thoria and which has not been heated above a temperature of about 2600° K, is almost identical with that of a pure tungsten filament under similar conditions. Heating at temperatures above about 2600° K, however, reduces some of the oxide, and when the filament is subsequently maintained at lower temperatures the reduced thorium diffuses to the surface and, provided the temperature is not so high that the rate of evaporation of thorium from the surface exceeds the rate at which it diffuses to the surface, it accumulates until there is a complete layer of thorium of atomic thickness.

The thermionic emission at any temperature from such a filament is greater the greater the fraction of the surface covered with thorium, and when the emission at any

* Communicated by Prof. Frank Horton, F.R.S.
† I. Langmuir, Phys. Rev. xxii. p. 360 (1923).

temperature has reached the steady state, there is a balance between the number of thorium atoms arriving at the surface per second from the interior (which depends on the coefficient of diffusion, and the radial concentration gradient of thorium in the wire), and the number of thorium atoms leaving the surface per second by evaporation. Langmuir distinguishes two types of evaporation, namely, ordinary temperature evaporation and "induced" evaporation. The latter type is explained as occurring because the thorium atoms in the surface are more loosely held by underlying thorium atoms than by tungsten atoms, so that a thorium atom diffusing from the interior and arriving just under a surface thorium atom causes the latter to leave the surface. He has shown that, in general, the condition of a thoriated tungsten filament can be expressed by the relation

$$N_0 \frac{d\theta}{dt} = DGf(\theta) - E \quad . \quad . \quad . \quad . \quad . \quad (1)$$

where θ is the fraction of the filament surface which is thorium covered, N_0 is the number of thorium atoms per cm.^{2} in a complete monatomic adsorbed film ($\theta = 1$), t denotes time in seconds, D is the diffusion coefficient of thorium through tungsten at the particular temperature of the filament at any stage, G is the radial concentration gradient of thorium, E denotes the number of thorium atoms leaving a square centimetre of the surface per second, at the existing temperature of the filament, due to ordinary temperature evaporation, and $f(\theta)$ is equal to $1 - 0{\cdot}82\,\theta - 0{\cdot}18\,\theta^3$. The last two terms in this expression represent the effect of induced evaporation. At temperatures above about 2200° K the rate of evaporation of thorium from a nearly completely covered surface exceeds the rate at which thorium atoms arrive at the surface, and the equilibrium condition corresponds to a surface only partially covered with thorium—*i. e.*, not fully activated. For this reason temperatures above about 2200° K are referred to as deactivating temperatures, while temperatures between 1900° K and 2200° K, at which for most values of θ $DGf(\theta)$ exceeds E, are known as activating temperatures. It is clear from equation (1) that, since D and E vary in a definite manner with temperature, while G depends on the previous history of the filament, there is some indefiniteness as to the dividing line between activating and deactivating temperatures.

Langmuir found that the large emission of an activated thoriated tungsten filament could only be maintained, at

any particular temperature, in a high vacuum. The presence of oxidising gases destroyed the activity, and in the presence of inert gases the application of large voltages caused the emission to fall off. This was attributed to the removal of thorium atoms from the surface through bombardment of the filament by positive ions *.

In the use of thoriated tungsten for the filaments of dull-emitter valves it has been observed that the filaments only behave satisfactorily provided the voltage between the various electrodes, encouraging emission from the filament, is not made too large. The maximum safe voltage in each case differs in different types of valve, but four or five hundred volts or less applied for a few minutes at any of the ordinary working temperatures is, in general, sufficient to cause a considerable decrease in the maximum emission obtainable at such temperatures. The emission can, however, be restored to its normal value (corresponding to a completely thorium covered surface) by subjecting the filament to the usual heat treatment described by Langmuir, namely, by maintaining it for about half an hour or more at an activating temperature, *i.e.*, between 1900° K and 2200° K.

The object of the present investigation was to inquire more closely into the cause of the deactivation of thoriated tungsten filaments, in a high vacuum, by the application of voltage encouraging emission, at temperatures well below the minimum necessary to cause any decrease of emission due to the temperature alone. To this end a thorough investigation was first made of the way in which the emission from an activated thoriated tungsten filament varied with time during the application of various different arrangements of electric fields, at a series of different filament temperatures and concentration gradients of thorium in the filament. Valves of the type V. S. 8 B. were employed for this purpose. These are triode valves with cylindrical electrodes, the filament being enclosed by an open spiral grid of about 3 mm. diameter, and a cylindrical anode of about 1 cm. diameter and 2 cm. length.

Method of estimating filament temperatures and relative concentration gradients.

For many of the experiments accurate determinations of the actual temperature of the filament were not essential,

* K. H. Kingdon & I. Langmuir, Phys. Rev. xx. p. 108 (1922); *ibid.* xxii. p. 148 (1923).

and it was sufficient to ascertain by trial what ranges of heating current corresponded to Langmuir's "activating," "deactivating" and "reducing" temperatures. The re-attainment of any particular temperature was effected by adjusting the heating current to the particular reading on a sensitive ammeter, the necessary fine adjustment being made by means of a suitable arrangement of rheostats in parallel. In some of the later work, however, it was necessary to have a fairly accurate estimate of the temperatures corresponding to particular heating currents. This was achieved by measuring its resistance when various heating currents were passing through the filament in question, and estimating the corresponding temperatures by reference to the results given by Jones* showing how the resistance of a tungsten filament varies with temperature. This was done most satisfactorily by using the preliminary tests of activation, deactivation, and reducing heating current ranges, to locate approximately the correspondence between heating current and temperature for two or three definite temperatures. A check on these estimates was then obtained by comparing the ratio of the resistances at the heating currents corresponding to these temperatures, with the ratio of the resistances at the same temperatures in Jones's tables. At these relatively high temperatures the effect of the resistance of the leads to the filament was comparatively negligible, and sufficiently accurate estimates of corresponding temperatures and heating currents could be made without taking this into account. Though it is not claimed that the temperatures corresponding to different heating currents, thus estimated, have an accuracy greater than about $\pm$ 20°, the authors believe that the increment of temperature increase, produced by a given increment of heating current, cannot differ by more than a few per cent. from the values stated in the course of the paper.

A measure of the radial concentration gradient of thorium was obtained from observations of the rate at which the emission increased during the process of activation at the standard activating temperature employed in these experiments (1900° K). According to Langmuir, if i is the emission at any temperature when a fraction θ of the surface is thorium covered, i_1 the emission at the same temperature from a fully activated surface, and i_0 the

* H. A. Jones, Phys. Rev. xxviii. p. 202 (1926).

corresponding emission from a pure tungsten surface, then

$$\theta = \frac{\log i - \log i_0}{\log i_1 - \log i_0},$$

whence $$1-\theta = \log\left(\frac{i_1}{i}\right) . \log\left(\frac{i_0}{i_1}\right).$$

The value of $\log\left(\frac{i_1}{i_0}\right)$ at 1900° K is 3·7275 *. Langmuir found that the activation curves fitted a formula of the type $\log(1-\theta) = -kt$, and he showed that the constant k is directly proportional to the concentration gradient. Hence by plotting $\log\left[\log\frac{i_1}{i}\right]$ against the time a straight line is obtained, the slope of which to the time axis is proportional to the concentration gradient, if the activation observations are always taken at the same temperature. The relative values of the different concentration gradients employed in our experiments have been determined in this way, and similarity of the curves of emission against time, during activation, has been taken as the criterion for equal concentration gradients at different times.

Statement and Discussion of Results of Preliminary Experiments.

Most of the tests of the effects of the application of electric fields between the filament and the other electrodes were carried out at temperatures too low for any appreciable activation to occur. The condition of the filament after being subjected to any particular treatment was determined by measuring the emission which was obtained under arbitrary standard test conditions, namely, with a heating current corresponding to about 1700° K and with 40 volts applied between the filament and the other two electrodes joined together. The results of these preliminary experiments may be stated briefly as follows :—

1. The application of a potential difference of a few hundred volts between the filament as negative electrode, and either of the other electrodes, causes partial deactivation of the filament, the emission at once beginning to

* This value is calculated from the values of the constants A and b of the equation $i = AT^2 e^{-b/T}$ for pure tungsten, and for a fully activated thoriated tungsten surface, given by Dushman & Ewald, Phys. Rev. xxix. p. 857 (1927).

fall, and eventually becoming constant at some lower value than that obtained at the instant of application of the voltage. The emission under the test conditions falls also.

2. The extent of the deactivation, and the rate at which it occurs, for a given temperature and concentration gradient, increase with increase of applied voltage.

3. The extent of the deactivation, and the rate at which it occurs at a given voltage, increase as the temperature of the filament increases.

4. For a given voltage and a given temperature, the extent of the deactivation and the rate at which it occurs increase as the concentration gradient decreases.

5. For a given total electron emission, the extent of the deactivation for a given plate voltage is less the lower the grid voltage.

These results are in accord with equation (1) if we take into account an additional deactivating factor dependent on the number and energy of the thermionic electrons. If we assume that this factor causes P thorium atoms to be removed per second, per cm.^{2}, the equation becomes :—

$$N_0 \frac{d\theta}{dt} = DGf(\theta) - E - P. \quad . \quad . \quad . \quad . \quad (2)$$

At the temperatures at which the experiments were carried out, $DGf(\theta) - E$, for a fully activated surface, is zero, and for a partially activated surface is very low. Hence P would be the main factor controlling $\frac{d\theta}{dt}$. Starting with the filament at any particular degree of activation, the emission continues to increase slightly as the potential difference increases, owing to the Schottky effect, and the energy of each electron increases also. Hence any factor to which the electron current gives rise, and consequently the deactivation caused by this factor, would be expected to increase as the voltage increased. Hence results 1 and 2 would follow immediately as soon as P became appreciable. So long as $DGf(\theta) - E$ is very small it is clear that, in accordance with equation (2), the extent and rate of any deactivation caused by the extra factor must increase as the temperature increases owing to the increase in the thermionic current itself. Hence result 3 is accounted for. The fact that in these deactivation experiments the emission ultimately becomes constant and does not continue to fall until the pure tungsten value is reached, is accounted for because, as the emission decreases, P also decreases, and

$DGf(\theta)$ increases slightly, while E tends to decrease as θ decreases. For high concentration gradients, an appreciable rate of activation occurs at temperatures which are not normally considered to be activating temperatures. This follows at once from equation (1) since the value of $DGf(\theta) - E$ for given values of θ and the temperature must depend upon G the concentration gradient. Bearing this in mind it becomes at once clear that result 4 quoted above is in accord with equation (2).

As regards the influence of grid-voltage upon deactivation, this is readily explained if we suppose the deactivating factor to be positive ion bombardment of the filament, for it follows that the lower the grid-voltage the greater the proportion of any positive ion current which must originate on the side of the grid remote from the filament, and the greater the proportion of this which will be stopped by the grid from reaching the filament. Hence the results of all the preliminary experiments on deactivation by voltage admit of explanation on the view that the thermionic electrons give rise to positive ions which in their turn bombard the filament, thereby removing thorium atoms and decreasing the fraction θ of the filament surface which is thorium covered.

Positive Ion Currents and the Setting in of Deactivation.

It seemed desirable to make a direct determination of the order of magnitude of any positive ion currents which might be produced in the valves in circumstances similar to those in which deactivation tests had been made. This was done in the two following ways :—

(*a*) By making the plate sufficiently negative to the filament to prevent any thermions from reaching it, thus causing it to collect any positive ions produced in the space between it and the grid.

(*b*) By making the plate positive to the filament so as to cause a considerable thermionic current to flow, at the same time making the grid sufficiently negative to prevent any of the electrons from being collected by it, and enabling it to collect only positive ions.

The positive currents were measured on a sensitive galvanometer, and by measuring the thermionic current simultaneously as the applied voltage was varied, it was possible to study the behaviour of the positive ion current at the stage when deactivation commenced; in this way some interesting points were revealed. With the fields

arranged as in (*a*) a positive current was first detected when the grid potential was between 30 and 40 volts, and this increased as the voltage was increased. Ultimately a stage was reached when the rate at which the positive current increased with the voltage became much larger (fig. 1, curve A), and a few volts beyond this stage both the emission current and the positive ion current began to fall off rapidly with time (fig. 2, A). With this arrangement, when the grid-potential had reached about 90 volts, and the emission current was 26 milliamperes, the positive ion current was of the order of 10^{-7} amp. This is of about the same magnitude as the positive ion currents employed by Kingdon and Langmuir in their experiments.

With the fields arranged as in (*b*) much larger voltages

Fig. 1.

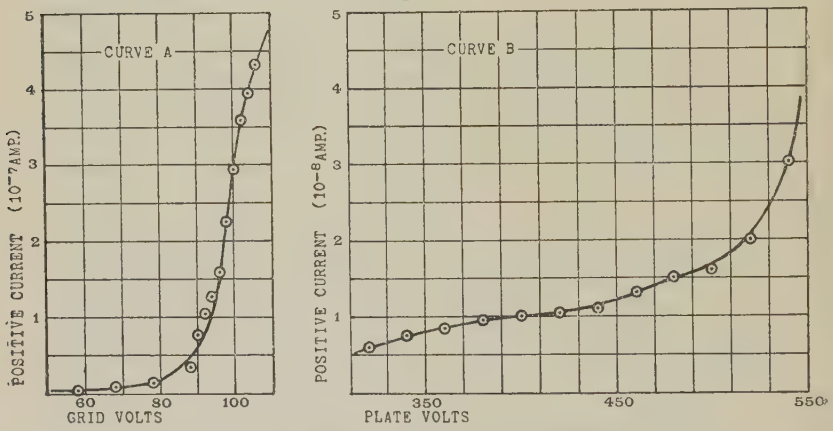

had, of course, to be employed to obtain thermionic currents of the same order of magnitude, and deactivation did not begin to be appreciable until much higher voltages than with the other arrangement, on account of the negative grid-potential. The positive ion currents were rather smaller in this case and increased much less rapidly with increasing potential difference, though the occurrence of a much augmented rate of increase of positive current just preceding the stage at which deactivation commenced was again consistently observed (fig. 1, curve B). With either arrangement, if the conditions corresponding to any stage beyond the bend in the positive ion current curve are established straight away, and readings of positive and negative currents taken at successive intervals, it is found that a certain

amount of deactivation occurs, a decrease in both currents taking place (fig. 2, A and B).

The question of the origin of the positive ions arises at this stage, and whether they can be accounted for by the ionization of residual gas distributed throughout the volume of the valves. The final stage of evacuation of the valves employed had been accomplished by using a magnesium getter, and under such conditions a pressure permanently less than 10^{-7} mm. can be maintained *. Some idea of the order of magnitude of the positive ion current to be expected

Fig. 2.

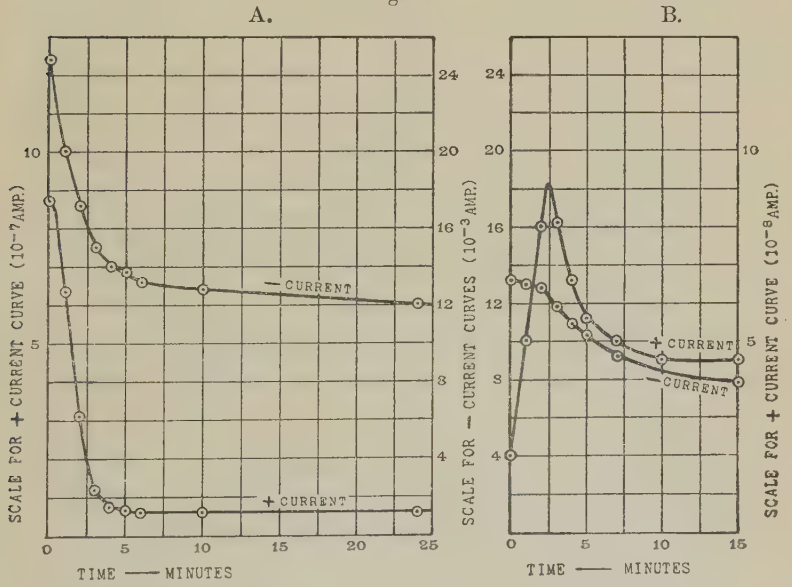

at such a pressure in valves of the type employed can be obtained from a consideration of the results yielded by certain forms of ionization gauge †, in which the dimensions of the electrodes and containers were comparable with those of the valves used in this research. It has been found that with an electron current of about 25 milliamps., with an anode voltage of 250, a positive ion current of about 10^{-8} amp. can be obtained in argon when the pressure is $7{\cdot}5 \times 10^{-8}$ mm. of mercury, whence for pressures less then 10^{-7} mm. the positive current for the same emission and the same voltage

* N. R. Campbell, Phil. Mag. vol. ii. p. 369 (1926).

† S. Dushman & C. G. Found, Phys. Rev. vol. xvii. p. 7 (1921).

would be $1{\cdot}33 \times 10^{-8}$ amp. If the residual gas were air or carbon dioxide, the ionization current at this pressure would be correspondingly lower. In our experiments with an electron current of 24 milliamps. and an anode voltage of 200, a positive ion current of $2{\cdot}1 \times 10^{-6}$ amp. was measured. Hence we cannot straight away attribute the observed effects to the presence of residual gas distributed throughout the volume of the bulb.

The variation of the positive ion current obtained in the present experiments, with variation of electron current at a constant anode voltage, and with variation of the anode voltage for a constant electron current, was investigated to see if it were in accordance with the variations to be

Fig. 3.

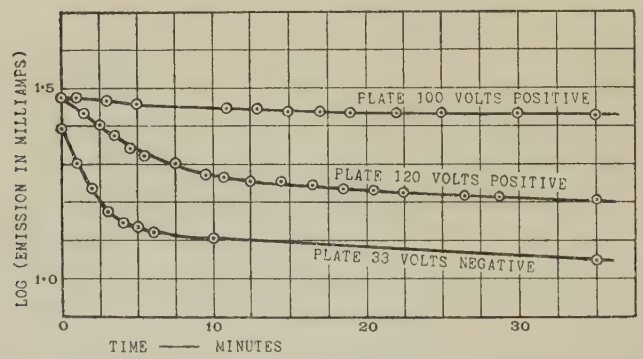

The curve for the plate 33 volts positive to the filament so nearly coincides with that for 120 volts, that to avoid confusion it has not been included in the figure.

The grid was 120 volts positive to the filament throughout the series.

expected if the positive current were due to ionization of residual gas. This was found not to be the case, the ionization current for a given emission increasing at a gradually increasing rate with increase of voltage, while the ratio of the positive current to the thermionic current increased steadily with increase of the latter instead of remaining constant, thus suggesting that there is some source of positive ions other than residual gas. This view obtains support from a consideration of the results represented in fig. 3. These curves show the variation with time of the logarithm of the emission current from a filament at a definite temperature, and concentration gradient of thorium, with a potential difference of 120 volts between the grid and the

filament, but with different voltages on the plate. The curves in the figure are typical of those obtained in several series of investigations of this kind. The potential difference of 120 volts between grid and filament was about the minimum voltage which produced appreciable deactivation in these valves. The logarithm of the emission current is plotted because, as has already been shown, this bears a linear relation to the fraction θ of the filament surface which is thorium covered *. The plate voltages employed in the investigations represented were such that in one case the grid and plate were at the same potential, in another the plate was negative to the filament, while in the third it was positive to the filament but negative to the grid. If positive ion bombardment of the filament is the sole cause of deactivation, and if residual gas distributed throughout the whole space between the electrodes were the main source of positive ions, one would expect the curves to be much the same for all cases in which the plate was at a negative potential with respect to the grid, because in these circumstances the positive ion current to the filament would be due to ionization of gas between the filament and the grid only, as all the positive ions produced between the grid and the plate would be urged by the electric field towards the plate. It is clear from fig. 3, however, that this is not the case, the deactivation being greatest when the plate is negative to the filament, and least when the plate is at a little lower potential than the grid.

Such a result can readily be explained if we assume that the positive ions, instead of being due mainly to residual gas, originate at the surfaces of the bombarded electrodes. In such a case one would expect the positive ion bombardment of the filament to be greatest when the largest proportion of the thermionic stream hits the inner surface of the grid, for the positive ions resulting from these impacts will travel directly to the filament. This occurs when the plate is negative to the filament. When the grid and plate are at the same potential, or when the plate is positive to the grid, the greater part of the electron current is to the plate, and of the positive ions originating from the bombardment of this, a certain proportion, depending on the grid potential, will be stopped by the grid. We have, therefore, to consider the factor P as consisting of $P_g + P_A$ where P_g denotes the part of P which is due to positive ions originating at the surface of the grid, and P_A that part of P which is due to

* The corresponding logarithm for pure tungsten ($\theta=0$) is $-2{\cdot}0$.

positive ions originating at the surface of the plate. When the plate is negative to the grid P_A becomes zero, since the electric field would draw positive ions back to the plate. We have seen that we should expect P_g to be greater the lower the plate potential. Hence we should expect least deactivation when the plate potential is less than that of the grid, but is considerably positive to the filament, and greatest deactivation when the plate is negative to the filament. The curves in fig. 3 show this to be the case and thus afford a certain amount of evidence in favour of the suggestion that positive ions are produced which have their origin in the bombardment of the surfaces of the electrodes.

The question now arises as to whether what occurs is a liberation of occluded gas due to heating up of the electrodes, under bombardment, or some more fundamental action. Suppose for a moment that liberation of occluded gas occurs. One would expect the amount of gas liberated to increase as the energy of bombardment of the electrode increased, *i. e.* to increase with the voltage for a given emission, and with the emission for a given voltage. Since the amount of ionization produced from a given quantity of gas will increase as the voltage increases, and also as the emission increases, it is clear that if liberation and subsequent ionization of occluded gas takes place under the electron bombardment, the positive current for a given voltage will increase more rapidly than in proportion to the emission, while the current for a given emission will increase more rapidly than in proportion to the voltage, *i. e.* the current will be expected to vary with these factors in much the manner it has been observed to do in practice. As the filament can be restored to give its original emission without difficulty, any gas evolved under bombardment of the electrodes can have no deactivating influence except when it exists in the form of positive ions which bombard the filament surface. When the emission has been restored the variation of positive ion current with voltage is found to agree with the variation obtained in the first place, showing that no permanent increase in residual gas pressure has taken place.

In connexion with the increased positive ion current at the deactivation stage the following considerations are of interest. If with the filament hot a voltage large enough to cause considerable deactivation is applied suddenly, the positive current obtained immediately is not as large as it eventually becomes, though the emission current at once attains a large value. It is found that 20 or more seconds after the voltage

has been applied, the positive ion current increases very considerably—up to 4 or 5 times its initial value—and either simultaneously, or immediately afterwards, the emission falls off rapidly, and the positive current then decreases rapidly too. This admits of explanation if the warming up of the electrodes under bombardment in any way facilitates the liberation of positive ions. That something of this kind occurs is borne out by the fact that if the voltage is switched off and on alternately, at suitably short intervals, even over such a period that the total time of application exceeds that in which very extensive deactivation occurs with continuous application, it is possible to maintain the large emission from the filament undiminished, while the positive current remains at a value comparable with that obtained when the voltage was first applied. If the electrons are being collected mainly on the grid, and if a sufficient voltage is applied between the filament and the grid to give, temporarily, a reasonably augmented positive current, the final equilibrium emission of the heated filament is fairly low and the ultimate positive ion current is always fairly small. If, however, the grid is made negative, and the plate 600 or 700 volts positive, the processes occur much more slowly and it is possible to maintain an augmented positive ion current for an appreciable interval. This is illustrated by the values given in Table I. below, in which the emission current and the

Table I.

Plate voltage.	Thermionic current 10^{-3} amp.	Positive current 10^{-9} amp.	Time Minutes.	Thermionic current 10^{-3} amp.	Positive current 10^{-9} amp.
580	7·4	12·5	0	12·0	25·0
600	8·8	14·5	1	11·8	32·5
620	9·6	16·0	2	11·6	50·0
640	10·0	19·0	4	11·0	60·0
660	10·7	20·0	6	10·1	55·0
680	11·3	21·0	8	9·2	50·0
700	12·0	25·0	10	8·2	50·0
			15	7·9	49·0
			20	7·2	45·0

positive ion current for gradually increased plate voltages are set out. When the applied voltage reached 700, it was observed that the emission current began to decrease. The

conditions were therefore kept constant and readings of the currents taken at regular time intervals. It will be seen that the positive ion current in these circumstances continued to increase for some time after the emission had begun to fall off. It would appear that the beginning of deactivation is to be attributed to the positive ions produced before the warming up of the electrodes had had time to augment the positive ion current, and that the subsequent increased rate of deactivation is to be attributed to the influence of the warming up of the electrodes in making possible the production of a larger positive ion current in spite of a smaller emission.

The possibility must, however, be borne in mind that positive ion bombardment may not be the main cause of deactivation of the filament, and that the peculiarities observed in the behaviour of the positive ion current at the stage when deactivation sets in may be merely the accompaniment of some other occurrence and not the primary cause of the reduced emission from the filament. A suggestion has been made that the reduced emission at large voltages is to be traced to an increased rate of evaporation of thorium from the surface of the filament, brought about in some way by the action of the electric field, this increased rate of evaporation causing the steady state of the filament to correspond to a surface less completely covered with thorium. Such an effect, if it occurred, would be expected to vary with different arrangements of electric fields in very much the manner in which the observed deactivation has been found to vary, and in many cases would account for the observed results equally well with the positive ion bombardment view, though it is difficult to see how the differences in the curves of fig. 3 could be explained on this view. However, if such an effect occurred, the increase of positive ion current immediately preceding deactivation might conceivably be a secondary consideration.

Experiments with Two Filament Valves.

To test the possibility of such an effect as this contributing to the observed deactivation, we had some valves specially constructed to be as nearly as possible the same as those hitherto employed, except that they contained two thoriated tungsten filaments instead of one, these being placed as close together as was consistent with there being no risk of contact between them, and as near as possible to the axis of the concentric grid and plate. In many of the experiments with these valves, the grid and plate were connected together

and various differences of potential were applied between this combined electrode and the filament which was heated to give the emission, the other filament being left unheated. Various electric fields were applied between the two filaments, the cold one being always negative, and the emission from each filament under the standard test conditions was measured at intervals during the application of the other electric fields. It was found that it was possible to arrange either so that both filaments became deactivated, or so that the cold one alone became deactivated while the hot one was unaffected. If the two filaments were at nearly the same potential, and if three or four hundred volts were applied

Fig. 4.

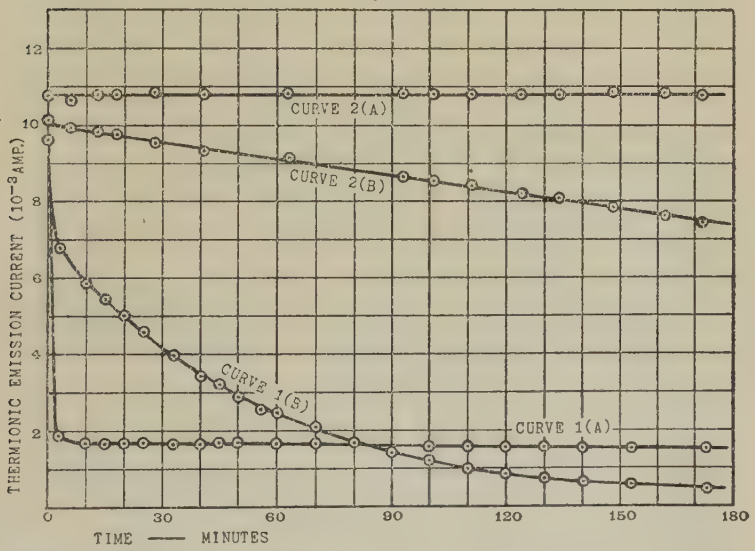

between the emitting filament and the grid and plate, the filament being negative, a reduction in the emission obtained from either under test conditions took place, the deactivation of the hot filament being more rapid and more extensive than that of the cold filament during the first few moments, though, eventually, an equilibrium condition was attained for the hot filament emission corresponding to a rather less completely covered surface, whereas the deactivation of the cold filament continued, the emission from it approaching more and more to the pure tungsten value. This is well illustrated by the curves 1 (A) and 1 (B), respectively of fig. 4. By having a potential difference of 150 volts or

more between the two filaments, and a potential difference not exceeding 120 volts between the emitting filament and the other two electrodes, it was possible to arrange so that the emission from the hot filament under working conditions, or under test conditions, remained unaffected, while the emission from the cold filament gradually fell off. This is illustrated by curves 2 (A) and 2 (B), respectively, of fig. 4. By a judicious selection of the electric fields any of the intermediate stages could be attained.

Observations were taken of the variation of the emission from the cold filament under test conditions, at intervals during the application of 120 volts between the hot filament and the grid, with the cold filament 320 volts negative to the hot filament, for the two following cases:—(*a*) with the plate at the same potential as the grid, (*b*) with the plate at the same potential as the cold filament. The total thermionic current was the same in the two cases, but in case (*b*) more electrons would strike the inner surface of the grid. The observations showed that the deactivation of the cold filament was very much more rapid in case (*b*) than in case (*a*), which agrees with the results obtained with the single filament valves, and therefore suggests that the main factor operative in causing deactivation is the same whether the filament is hot or cold.

It is clear that in these circumstances the deactivation of the cold filament cannot be due to an increased evaporation from the surface of the filament caused by a redistribution of the thorium vapour round it, brought about by the electric field, because the rate of evaporation is quite negligible in these circumstances. Hence the variation of the condition of the cold filament in these circumstances gives us a measure of the effect which can be definitely attributed to positive ion bombardment. The curves 1 (A) and 1 (B) of fig. 4 at first sight suggest that some other factor is operative as well, in the case of the hot filament, but it must be borne in mind that we do not know how the positive ion current directed towards the filaments divides itself between the two. It is quite possible, and even probable, that the hot filament receives more positive ions in these circumstances than the cold one does. Moreover, there exists the possibility that a given positive ion bombardment of a hot filament is more efficient in removing thorium atoms than the same positive ion bombardment of a similar cold filament.

Filament Temperature and the Deactivation Efficiency of Positive Ion Bombardment.

It was possible to make a test of this point by taking

series of observations for arrangements similar to those of curves 1 (A) and 1 (B) of fig. 4, for different temperatures of the hot filament. It was found that the ultimate steady value of the hot filament emission was lower, and that the deactivation of the cold filament occurred more rapidly, the higher the temperature of the hot filament. The following considerations show how the observations obtained from these experiments were utilized to test the point in question :—The condition of the filament at any instant is given by equation (2). The temperatures corresponding to the various heating currents employed were estimated in the manner already outlined as 1800° K, 1850° K, 1900° K, and 1950° K. At these temperatures E can be considered as negligible in comparison with DG*, and with $DGf'(\theta)$, so that the equation becomes

$$N_0 \frac{d\theta}{dt} = DGf(\theta) - P \quad . \quad . \quad . \quad . \quad . \quad (3)$$

When the steady state under positive ion bombardment is reached, $P = DGf'(\theta)$, and using the observed final steady value of the hot filament emission under test conditions to calculate θ, the final value of P can be obtained in terms of DG for the particular temperature and state in question. By taking observations of the rate of increase of the emission at a standard activating temperature, immediately after the completion of the particular deactivation observations in question, the value of $\frac{DG}{N_0}$ corresponding to the state

* From data given in Langmuir's paper (*loc. cit.*) we have the following relations :—

$$\log_{10} E = 31{\cdot}434 - \frac{44{,}500}{T},$$

and

$$\log_{10} D = {\cdot}044 - \frac{20{,}540}{T},$$

$$\therefore \log_{10} \frac{E}{D} = 31{\cdot}39 - \frac{23{,}960}{T},$$

from which we obtain the following :—

at 1800° K, $\log_{10} \frac{E}{D} = 18{\cdot}08$,

at 1900° K, $\log_{10} \frac{E}{D} = 18{\cdot}78$,

at 2000° K, $\log_{10} \frac{E}{D} = 19{\cdot}41$.

Now G is the order of 10^{21}. Hence $\frac{E}{DG}$ at temperatures from 1800° K—1950° K is negligible.

of the filament at the activating temperature can be calculated, and by using Langmuir's equation $\log_{10} D = \cdot 044 - \frac{20540}{T}$ the value of $\frac{DG}{N_0}$ in the actual deactivation experiment can be obtained. Hence the value of $\frac{P}{N_0}$ at the final stage of the hot filament is known, and the value at any stage during the decrease can be calculated from equation (3) using the relation

$$\frac{d\theta}{dt} = \log \frac{i_0}{i_1} \cdot \frac{d}{dt} (\log i),$$

and obtaining $\frac{d}{dt}(\log i)$ from the slope of the deactivation curve at the stage in question. For the cold filament, since DG and E are both negligible, $P = N_0 \frac{d\theta}{dt}$, and hence $\frac{P}{N_0}$ for any stage in the deactivation of the cold filament can be found from the slope of the curve for this filament. The actual observations obtained showed that by the time the emission from the cold filament under test conditions had reached the same value as the final emission from the hot filament under test conditions, the actual working emission from the hot filament in the deactivating experiment had reached a constant value. $\frac{P}{N_0}$ was therefore worked out for both filaments for this stage in each of the series of observations at different heating currents. The results of the calculations are given in Table II. The final column gives the values of $\frac{P}{N_0}$ for the hot filament divided by the actual working emission. The numbers show that in the

Table II.

Temperature during deactivation. Degrees K.	$\frac{P}{N_0}$ for hot filament.	$\frac{P}{N_0}$ for cold filament.	Thermionic current i. 10^{-3} amp.	$\frac{P}{N_0 i}$ for hot filament.
1800	$1{\cdot}97 \times 10^{-5}$	$1{\cdot}98 \times 10^{-6}$	7·6	$2{\cdot}59 \times 10^{-9}$
1850	$2{\cdot}88 \times 10^{-5}$	$5{\cdot}75 \times 10^{-6}$	8·8	$3{\cdot}27 \times 10^{-9}$
1900	$4{\cdot}44 \times 10^{-5}$	$5{\cdot}47 \times 10^{-6}$	8·7	$5{\cdot}11 \times 10^{-9}$
1950	$9{\cdot}86 \times 10^{-5}$	$17{\cdot}09 \times 10^{-6}$	10·0	$9{\cdot}86 \times 10^{-9}$

temperature region investigated, there is a rapid increase in the number of thorium atoms removed per unit emission as the temperature increases. The fact that the effects at 1850° K and 1900° K are as 3 : 5, although the thermionic currents are the same, shows that the increased effect with increasing temperature is not due mainly to the fact that the positive ion current increases more rapidly than in direct proportion to the thermionic current. In these two cases, the observations showed that the final rates of deactivation of the cold filament were practically the same, whence it may be concluded that the positive ion bombardment of the cold filament was the same in the two cases. As the actual final emission during the deactivation was the same for both, it is reasonable to suppose that the total positive ion current to the two filaments was equal in the two cases, and hence that the hot filament received the same final positive ion bombardment in these two cases. It therefore seems justifiable to conclude that the greater rate of removal of thorium atoms from the surface of the hot filament at 1900° K was due to its higher temperature. This may mean either that a given positive ion bombardment is more effective in removing thorium atoms the higher the temperature, or that there is some other factor contributing to the deactivation which increases with temperature, while the positive ion effect remains more or less constant.

Some evidence, which seems to show that the first-mentioned alternative cannot be ruled out, was obtained from experiments in which the cold filament was subjected to a definite treatment—first, with no current passing through it (the temperature therefore not being very different from, say, 350° K), and then with a current passing through it such as would raise it to a temperature of about 900° K. In every such case it was found that the rate of removal of thorium atoms at the higher temperature was about twice as great as at the lower temperature. At neither of these temperatures does any appreciable evaporation occur. Considering these results in conjunction with the variation of $\frac{P}{N_0 i}$ in the region 1800° K – 1950° K, and the relative magnitudes of $\frac{P}{N_0}$ for the hot and cold filaments set out in Table II., it seems reasonable to conclude that all the observed deactivation could be accounted for on the theory of positive ion bombardment.

The objection might be raised that the comparison of $\frac{P}{N_0 i}$ at different temperatures has been made for the final

equilibrium condition of the hot filament, *i.e.* the state after deactivation has taken place, and that the arguments put forward do not therefore prove that no other factor contributes to the deactivation of the hot filament which occurs in the first few moments of application of the voltage. By carrying out certain experiments with the two filament valves, it was possible to obtain information which enables this contention to be met. The experiments referred to were based upon the fact that it was possible to arrange so that during the intervals when the deactivating factor was operative upon the cold filament, the positive ion current to this filament was measured. Then by switching over to test conditions at definite time intervals it was possible to observe

Fig. 5.

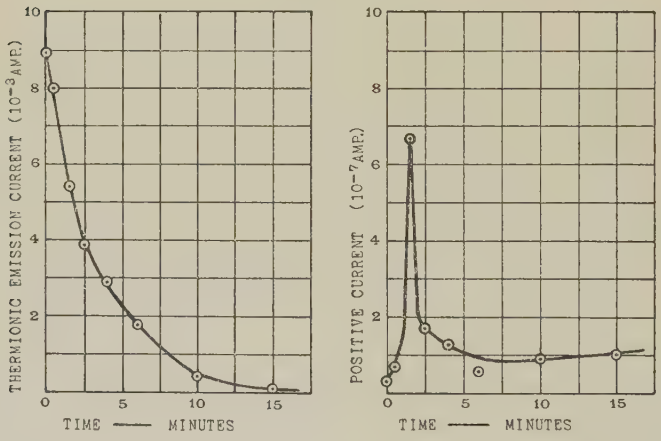

directly the effect of a known positive ion bombardment. With 120 volts applied between the grid and the plate joined and the hot filament, and with 200 volts between the two filaments, no deactivation of the hot filament occurred, and a steady positive ion current to the cold filament of 10^{-8} amp. was measured. The resulting deactivation curve for the cold filament showed that this positive ion current gave a value of $\frac{P}{N_0}$ of about 3×10^{-5}.

With the electric fields arranged a little differently, and with a larger thermionic current, deactivation of both filaments took place, and the curves in fig. 5 show the variation with time, of the positive ion current to the cold

filament, and the variation in the cold filament emission under test conditions. It may be observed that the positive ion current shows the initial increase to a larger value (about 7×10^{-7} amp.) which we associate with considerable deactivation of the hot filament. In many experiments the plate, instead of being connected to the grid, was maintained at the same potential as the cold filament, and the positive ion current to each was measured simultaneously. It was always observed that the two currents varied in a similar fashion, and the current to the cold filament was of the same order of magnitude as that to the plate, but was generally slightly smaller.

The mean values of $\frac{P}{N_0}$ for the hot and cold filaments during the first minute of application of the deactivating conditions in each of the series of observations at the four temperatures, 1800° K, 1850° K, 1900° K, and 1950° K, have been calculated, and are tabulated in Table III. The values are calculated from $\frac{d\theta}{dt}$, *i.e.* $\log \frac{i_0}{i_1} \frac{d}{dt} (\log i)$, the values $\frac{DG f(\theta)}{N_0}$ being negligible in comparison at this stage.

Table III.

Temperature during deactivation.	$\frac{P}{N_0}$ for cold filament.	$\frac{P}{N_0}$ for hot filament.
1800° K	$5{\cdot}55 \times 10^{-5}$	$9{\cdot}56 \times 10^{-4}$
1850° K	$4{\cdot}90 \times 10^{-4}$	$27{\cdot}43 \times 10^{-4}$
1900° K	$10{\cdot}09 \times 10^{-}$	$25{\cdot}78 \times 10^{-4}$
1950° K	$8{\cdot}52 \times 10^{-4}$	$39{\cdot}36 \times 10^{-4}$

If we assume, as seems justified by Langmuir's experiments, that the rate of removal of thorium atoms is proportional to the bombarding positive ion current, we see that since 10^{-8} amp. gives $\frac{P}{N_0} = 3 \times 10^{-5}$, the maximum value of positive ion current required to account for any of the above effects is about $1{\cdot}3 \times 10^{-6}$ amp. The curve in fig. 5 shows that it is not unreasonable to suppose that a current of this order of magnitude occurs for a short interval of time. Hence, bearing in mind the evidence already produced of the greater efficiency of a given positive ion bombardment of a hot filament, it seems clear that the positive ion currents

to the filaments are sufficient to account for all the observed deactivation, and that the agency of no other factor need be evoked.

Tests for other Deactivating Factors.

A direct attempt to test the extent to which any other factor might be operative in causing deactivation was made by arranging so that the positive ion current should be as small as possible, so as to reduce the removal of thorium atoms brought about in this way. This was done by arranging the electric fields so that the thermionic current from the hot filament could flow to the cold filament only. This being of much smaller surface area, and having previously been made very hot, it seemed likely that the yield of positive ions from it for a given electron bombardment would be much smaller than that obtained from the grid for the same bombardment. The actual thermionic current measured for a given applied accelerating potential difference was much smaller in these circumstances, doubtless on account of the repelling action of the field between the grid and the hot filament. Nevertheless, between the two filaments there should exist an electric field at least as intense as any existing with the other arrangements, and if this caused any increased evaporation of thorium to occur from the part of the filament subjected to it, one would expect to be able to detect it by a decrease with time in the emission measured in these circumstances. No such effect was observed, however, and the emission from each filament under test conditions remained unaffected even after the filaments had been subjected to this treatment for prolonged periods. There does not, therefore, appear to be any necessity for attributing any appreciable part of the observed deactivation to any factor other than bombardment of the filament by positive ions which originate in their turn from the electron bombardment of the grid and plate.

The authors desire to express their thanks to Professor F. Horton for his kind interest and advice throughout the course of this investigation, and to the Department of Scientific and Industrial Research for permission to publish this account of work which was carried out as part of the programme of the Radio Research Board.

CI. *Notices respecting New Books.*

X-rays and Electrons—An Outline of Recent X-ray Theory. By A. H. Compton, Professor of Physics in the University of Chicago. (Macmillan & Co., St. Martin's Street, London. Price 25*s.*)

NUMEROUS books on the subject of X-rays and atomic structure have appeared in recent years. Prof. Compton's work deals specifically with those aspects of the subject related to his own researches—the structure of the atom as deduced from the study of X-rays, their nature and properties. Evidence of this can be found in many of the chapters of the book; the investigations of other workers in this branch of physics are also recorded. 'X-rays and Electrons' gives a comprehensive and up-to-date account of the subject in two sections: the first dealing with X-rays and Electrodynamics, X-ray scattering, reflexion, refraction, and absorption; the second with X rays and the Quantum theory, including the Photo electric effect, X-ray spectra, and the Quantum theory of X-ray scattering, diffraction, and absorption. There are many valuable tables of indices of refraction and other data, and several appendices giving the results of the special theory of relativity, tables of wave-lengths of X-ray spectrum lines, and atomic and electronic constants.

Kinetic Theory of Gases. By L. B. Loeb. (McGraw Hill Publishing Co., 6–8 Bouverie Street, London, E.C. 4. Price 27*s.* 6*d.*)

Prof. Loeb has rendered signal service in placing his volume on this important branch of physics in the hands of students both elementary and advanced, serving the purpose of an introduction to the subject and a preparation for the study of the more advanced treatises and original papers.

The greater part of the volume gives a very complete and clear account of the Kinetic Theory: the equations of van der Waals, Dieterici and Reinganum; the relation of the theory to coefficients of viscosity, heat conduction and other problems; low-pressure phenomena and specific heats. Perhaps the two most important and interesting chapters are those having reference to the application of the Kinetic Theory of Gases to electrical and magnetic properties of molecules, especially the beautiful theory of Debye on the temperature variation of the dielectric constant with its experimental verification, the Bohr magneton and the classical experiments of Gerlach and Stern, and, finally, the relation to the conduction of electricity in gases, with Prof. Loeb's own contributions. At the end of each chapter there are references to original papers and treatises dealing with the special section of the subject: two useful indexes of authors and subjects are also given. Like Prof. Jellineck's 'Lehrbuch,' Prof. Loeb's volume is a mine of information and one likely to be accepted as a work of first-rate importance.

CII. *Proceedings of Learned Societies.*

GEOLOGICAL SOCIETY.

[Continued from p. 672.]

December 14th, 1927.—Prof. E. J. Garwood, Sc.D., F.R.S., Vice-President, in the Chair.

THE following communication was read:—

'The Lower Carboniferous Rocks of the Menaian Region of Carnarvonshire: their Petrology, Succession, and Physiography.' By Dr. Edward Greenly, V.P.G.S.; with Palæontological Notes by Dr. Stanley Smith, M.A., F.G.S.

The term Arvon is a convenient designation for the Menaian region of Carnarvonshire.

The Lower Carboniferous rocks of Arvon, like those of Anglesey, consist in the main of a limestone series with many beds of sandstone and shale. At the top of the series there is, as in Anglesey a series of bedded cherts; but the Millstone Grit and Coal Measures are absent, being cut out by the unconformity at the base of the Red Measures. There is a Basement Conglomerate of the normal type, with rolled pebbles of the Mona Complex.

In Arvon, however, this is underlain by a singular formation, composed of yellow and red loams and breccias, which are studded with pisolites of göthite and kaolinite. The blocks in the breccias are angular, and the loams are unstratified. The loams are of alien, the blocks of local, derivation, the blocks not being derived from the same horizon of the Mona Complex as those in the overlying conglomerate. The extent of this formation seems to have been less than 6 square miles.

The limestones are rich in corals and brachiopoda, and are all in the Zone of *Dibunophyllum*, every division of which is present. The sandstones and shales of the Basement Series have yielded plants.

The structure is that of an asymmetrical synclinal infold, truncated by a great boundary-fault.

The Series rests with complete unconformity upon the Mona Complex and the Ordovician rocks; and there is rapid overlap in a west-north-westerly direction. From the direction of the overlap, and from the contents of the conglomerates, it is inferred that the region which is now Snowdonia was completely submerged in Lower Carboniferous times. The pre-Carboniferous land, which was a branch of the ancient uplands of Anglesey, was lofty. On its south-eastern slope, it steepened into a crag, against which the breccias accumulated. This ancient upland was largely composed of Ordovician shales, with a large inlier of rocks of the Mona Complex. Owing, however, to its height, combined with the effects of the tectonics of the Complex, the outcrops on the inlier were quite different from those on the Menaian Platform of the present day. During the subsidence, different horizons were presented to waste, thus accounting for the contrast between the breccias and the conglomerates.

At first, the climate seems to have been arid, with a large diurnal range of temperature; but, as the subsidence advanced, moist and genial conditions began to set in, persisting throughout the remainder of the period represented by the limestone series.

January 11th, 1928.—Dr. F. A. Bather, M.A., F.R.S., President, in the Chair.

The following communication was read:—

'The Geology of South-Eastern Arabia.' By George Martin Lees, M.C., D.F.C., F.G.S.

South-Eastern Arabia consists of two separate tectonic and stratigraphic provinces:—(1) A foreland where, as at Dhofar, ancient gneiss is overlain by a 'Nubian' type of desert-sandstone. The first marine transgression took place in the Cenomanian; (2) An orogenetic zone of typical Alpine character. The presence of nappes is indicated by great overthrusts, klippen, and by the stratigraphic differences between adjacent units. The movement is of pre-Gosau age. Upper Cretaceous and Tertiary strata lie with strong, often vertical, unconformity on the older Mesozoic and Palæozoic rocks.

The stratigraphy of the orogenetic zone consists of:

(i) A series of pre-Permian formations of unknown age.
(ii) Permian dark-blue and black fossiliferous limestones. Near Jebel Rais limestones of a different facies appear as tectonic klippen; they are Crinoidal, Coral, Bryozoonal, and *Neoschwagerina* limestones.
(iii) Upper Triassic limestones, sandstones, and shales. The fauna consists of lamellibranchs and gasteropods; no ammonites have been found.
(iv) Jurassic to Lower Cretaceous massive limestones.
(v) ? Upper Jurassic to Lower Cretaceous shales, sandstones, and red and green radiolarites. This group probably belongs to a different tectonic unit from (iv).
(vi) Hatat Schists. A series of calc- and sericite-phyllites of unknown age, probably Mesozoic, which appear as a tectonic window at Saih Hatat.
(vii) Basic igneous series—lavas and intrusive rocks.
(viii) Unconformable Upper Cretaceous to Miocene conglomerates, limestones, and marls. The Maestrichtian is exceptionally fossiliferous.

The relation of Oman to the Zagros arc is discussed. The characteristic zone with red and green radiolarites and shales and basic igneous rocks occurs again in Persia, and forms great tracts of country south-west of Kerman. Here also Upper Cretaceous rocks are strongly unconformable. One great branch of the Cretaceous orogenetic zone of Central Persia must, therefore, have passed southwards into Oman. The Upper Cretaceous-Tertiary geosyncline broke down across the older strike, and pursued an independent direction parallel to the present Persian Gulf–Mekran coast. The late Pliocene movements also followed this trend, the influence of the older tectonics only being shown in the marked swing of the strike between Bandar Abbas and Jashk. Such a complete independence of these two phases of Alpine movement is unique.

The Oman orogenetic zone may be followed through Masirah Island to Ras Madhraka, where it passes southwards into the

Arabian Sea. The Kuria Muria Islands belong already to the foreland.

A further movement, though of much less intensity, took place in Oman in post-Miocene time. South of Sur these folds strike north-west and south-east, and appear to pass out to sea at Ras al Hadd, independent of, and across, the older structures. Perhaps these folds form a continuous loop with the Kirthar Range of Sind, but no connexion can have existed between the latter and the Cretaceous orogen of Oman.

The Triassic, Lower, and Upper Cretaceous fossils are described. They include twelve new species.

January 25th, 1928.—Dr. F. A. Bather, M.A., F.R.S., President, in the Chair.

The following communication was read :—

'The Glacial Retreat from Central and Southern Ireland.' By Prof. John Kaye Charlesworth, D.Sc., Ph.D., M.R.I.A., F.G.S.

The Newer Drift of Ireland is bounded on the south by a broad and well-developed kettle-moraine—the 'South Irish End-moraine'—which runs from the vicinity of Wexford round the northern flanks of the Dublin hills and by way of Baltinglass, Bennettsbridge, Cahir, Tipperary, Charleville, and Newcastle West to the mouth of the Shannon, a distance of 310 miles from coast to coast.

Contemporaneous with this stage of the Ivernian Ice and the Irish-Sea Ice were the independent ice-centres in the Kerry and Wicklow Hills, the Comeraghs, Galtees, Knockmealdown, and other mountain-clusters of the south. Their extent is likewise indicated by well-marked outer moraines, and corresponds to a snow-line on northern and eastern slopes of about 1000 feet and on other slopes of approximately twice that altitude.

The Irish glacial fauna is restricted, with but few exceptions, to the region outside these moraines.

The ice-recession from the Dublin and Wicklow Hills is clearly shown by moraines and marginal drainage-features. These prove a pivoting of the ice on the northern slopes of the hills, immediately south of Dublin, and the sweeping of the ice-fronts to east and west, at successive stages of the retreat, in a series of curves which swing out of each other tangentially and northwards.

The dissolution of the Ivernian Ice-sheet caused the emergence of the higher hills, such as the Castlecomer Plateau, the Slieve Bloom and Keeper Hills, and the formation of large lobes protruded southwards down the intervening valleys. The moraines of the Barrow, Nore, Suir, Shannon, and other lobes are magnificently displayed, making possible the correlation from lobe to lobe and the delineation of the successive positions of the ice-margin across the country from coast to coast. The festooning of the moraines in the southern part of the country is governed by the relief, while their sinuous form in the northern region is to be ascribed to the break-up of the ice-sheet into separate lobes, flowing on roughly parallel lines.

The ice-sheet in its recession over Southern Ireland remained pivoted on the Dublin hills, and retreated over ever-widening strips of country as the ice-front is followed westwards; a withdrawal of 65 miles in the west is represented south of Dublin by but a few hundred yards.

The ice retreating over the Central Plain was dissected into three perfectly distinct lobes, which centred upon the mountains of Donegal, Leitrim, and Galway respectively. Their stages of recession are indicated by countless moraines, the 'eskers' of Irish Glacial literature. True osar occur subordinately, transversely within, and as integral parts of, the kettle-moraines.

February 22nd.—Prof. J. W. Gregory, D.Sc., President, in the Chair.

The following communication was read:—

'The Pre-Cambrian Complex and Associated Rocks of South-Western Lleyn (Carnarvonshire).' By Charles Alfred Matley, D.Sc., F.G.S. With a Chapter on the Petrology of the Complex, by Edward Greenly, D.Sc., F.G.S.

The pre-Cambrian Complex of Lleyn occupies the coastal strip from Nevin to Aberdaron and Bardsey Island, the geology of which was described by the Author in 1913, and is a detached 'region' (the Mainland Region) of the Mona Complex of Anglesey. Its age is definitely pre-Cambrian, and its special structures and metamorphism were impressed on it before Cambrian times. It is bounded on the east by a great thrust which has driven it over Ordovician strata and the Sarn granite.

Its members are now correlated with those of Anglesey. The Gneisses, several members of the Bedded Succession, the Plutonic Intrusions, and the 'Penmynydd Zone of Metamorphism' are all represented. The Holyhead Group is absent.

The Gneisses are always found near the boundary-thrust. Both their basic and their acid members are almost identical with those of Anglesey. Their crystallization and foliation are older than the deposition of the Bedded Succession.

Most of the region is occupied by the Gwna Group. On a low horizon of this are the laminated Abergeirch Phyllites, above which come alternating grit and phyllite, quartzites, and limestones. There is a strong development of ellipsoidal spilitic lavas, with tuffs, limestone, and jasper, and sills of albite-dolerite. All members of the group, except the Abergeirch Phyllites, are mostly in the condition of a schistose autoclastic mélange. Part of the group is in the anamorphic condition known in Anglesey as the Penmynydd Zone of Metamorphism, being now mica-schists, some of which may, however, be metamorphosed Fydlyn Beds.

Resting on the Gwna Beds are some 300 feet of quartz-albite dust-rocks (Gwyddel Beds). They may be a special facies of the Skerries Group of Anglesey, with a representative of the Tyfry Beds at their base.

The gabbros are akin to those of Anglesey, and are regarded as plutonic intrusions belonging to the Complex.

The tectonics and foliation of the Complex resemble in almost every detail those of the Complex in Anglesey. On the working hypothesis of recumbent folding adopted for Anglesey, Dr. Greenly is inclined to regard the Mainland Region as the lower uninverted limb of a recumbent fold (a Lleyn Fold) belonging to a higher tectonic horizon than those now found in Anglesey.

The Arenig rocks at Aberdaron form a faulted syncline overridden on the west and north by the Complex, and faulted against it on the east. They probably occur as a 'window'. About 1000 feet of sediments belonging to the *D.-extensus* Zone and 200 feet of *D.-hirundo* Beds are exposed. They contain a thick sill of albite-dolerite, which transgresses a zone of fine-textured pyroclastic cherts containing abundant sponge-spicules.

Many basic dykes are exposed in the Complex, of which the great majority are Palæozoic (post-Llandovery and probably post-Silurian), but earlier than the great thrusting movements which took place after the close of Silurian time. Three Tertiary dykes have been found.

Many thrusts and shear-planes later than the Complex are found in the Complex itself, cutting across the foliation and the autoclastic mélange, and disrupting the Palæozoic dykes. They were produced by minor movements during the general movement which drove the Complex of Lleyn over the Ordovician strata. The boundary-thrust is certainly a great rupture, which shows no sign of dying out at either end of the exposed part of the Complex. The extent of its overdrive cannot be determined, but it should probably be measured in terms of miles, and may have been sufficient to sever the whole plexus of Palæozoic dykes in the Complex from their roots.

Dr. Greenly compared the petrological characters of the several members of the succession in the Mona Complex with those found in Anglesey, showing that the correspondence, despite the distance, is singularly close. The Gwna Beds belong to the eastern facies. The fact that, despite the cover of Drifts and of frequent decomposition, the Acid Gneisses had been detected, was due to the minute mapping of Dr. Matley.

This region of the Complex does not appear to correspond to any of the region of Anglesey, and its prolongation is more likely to be buried beneath the Palæozoic formations between Bangor and the mountains.

The theory of recumbent folding has justified itself by furnishing consistent explanations of a number of anomalies, but ought not to be regarded as more than a good working hypothesis. The complexities of the visible structure are astonishing; and the speaker often wondered whether the key to these wonderful regions of crystalline schists might, after all, prove to be some principle whereof we have at present no idea whatever.

[*The Editors do not hold themselves responsible for the views expressed by their correspondents.*]

FIG. 1.

α β γ δ

FIG. 2.

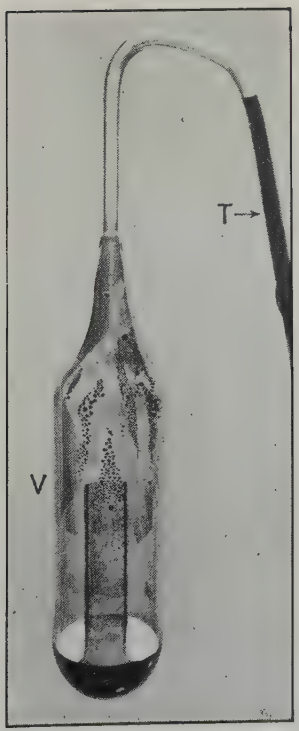

θ_1

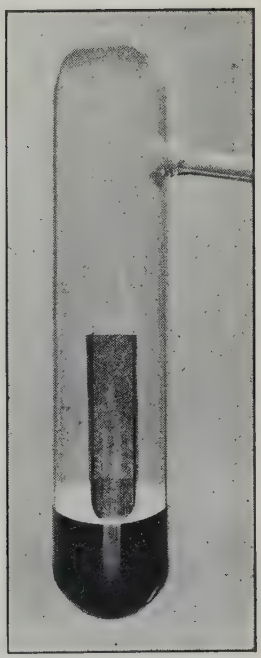

θ_2

FIG. 3.

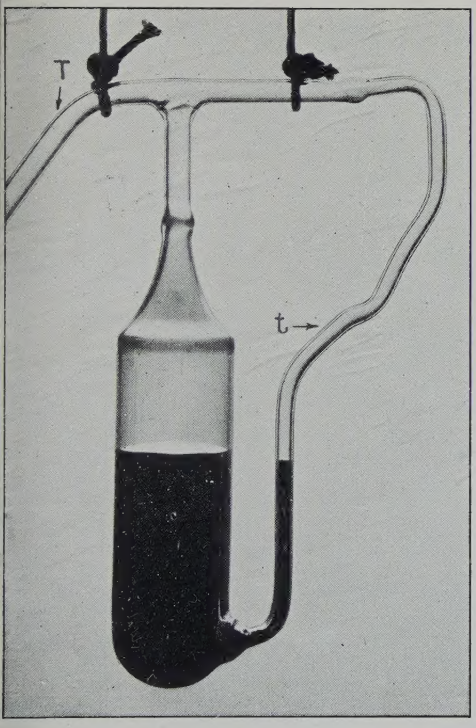

λ_1

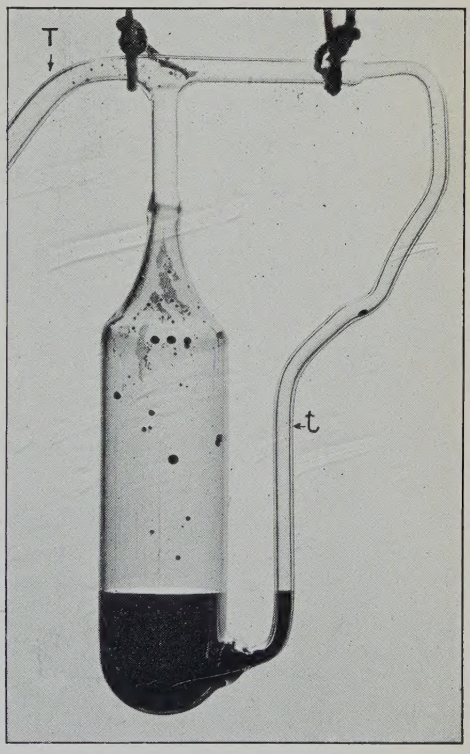

λ_2
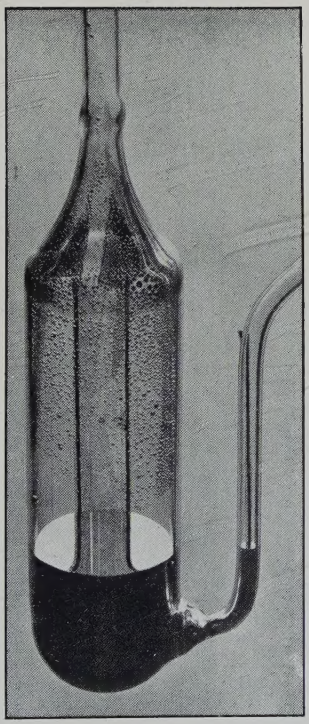
FIG. 4.